A functional m 6 A-RNA methylation pathway in the oyster Crassostrea gigas assumes epitranscriptomic regulation of lophotrochozoan development

Lorane Le Franc, Benoit Bernay, Bruno Petton, Marc Since, Pascal Favrel, Guillaume Rivière

The FEBS Journal

FEBS PRESS
science publishing by scientists

A functional m^{6}A-RNA methylation pathway in the oyster Crassostrea gigas assumes epitranscriptomic regulation of lophotrochozoan development

Journal:	*The FEBS Journal*
Manuscript ID	FJ-20-0151.R1
Manuscript Type:	Regular Paper
Date Submitted by the Author:	n/a
Complete List of Authors:	Le Franc, Lorane; University of Caen Normandy, FRE 2030 BOREA MNHN SU UNICAEN UA CNRS IRD Bernay, Benoit; University of Caen Normandy, SF ICORE Proteogen Petton, Bruno; Ifremer, UMR 6539 LEMAR Since, Marc; University of Caen Normandy, SF ICORE PRISMM Comprehensive Cancer Center F Baclesse Favrel, Pascal; University of Caen Normandy, FRE 2030 BOREA MNHN SU UNICAEN UA CNRS IRD Rivière, Guillaume; University of Caen Normandy, FRE 2030 BOREA MNHN SU UNICAEN UA CNRS IRD
Key Words:	

A functional m^{6}A-RNA methylation pathway in the oyster *Crassostrea gigas* assumes epitranscriptomic regulation of lophotrochozoan development

Authors

Lorane LE FRANC[1], Benoit BERNAY[2], Bruno PETTON[3], Marc SINCE[4], Pascal FAVREL[1] and Guillaume RIVIERE[1]

Addresses

[1]Normandie Univ, UNICAEN, CNRS, BOREA, 14000 Caen, France.

Laboratoire Biologie des organismes et Ecosystèmes aquatiques (BOREA), Muséum d'Histoire naturelle, Sorbonne Université, Université de Caen Normandie, Université des Antilles, CNRS, IRD, Esplanade de la paix, 14032 Caen, France.

[2]Normandie Univ, UNICAEN, SF ICORE, PROTEOGEN core facility, 14000 Caen, France

[3]Ifremer, Laboratoire des Sciences de l'Environnement Marin, UMR 6539 CNRS/UBO/IRD/Ifremer, Centre Bretagne, 29280, Plouzané, France

[4] Normandie Univ, UNICAEN, Comprehensive Cancer Center F. Baclesse, SF ICORE, PRISMM core facility, 14000 Caen, France.

Corresponding author

Guillaume Rivière (0033231565113 ; guillaume.riviere@unicaen.fr) , Normandie Univ, UNICAEN, CNRS, BOREA, 14000 Caen, France (https://borea.mnhn.fr/). Tel :

Running title

m^{6}A-RNA methylation pathway in oyster development

Abbreviations

N^6-methyladenosine (m^{6}A), Methyltransferase like (METTL), Wilms' tumor 1-associated protein (WTAP), RNA-binding motif 15 (RBM15), Ring finger E3 ubiquitin ligase (HAKAI), Zinc finger CCCH-type containing 13 (ZC3H13), AlkB homologue 5 (ALKBH5), Fat mass and obesity associated protein (FTO), YTH domain family protein (YTHDF), YTH domain containing protein (YTHDC), Heterogeneous nuclear ribonucleoproreins A2 B1 (HNRNPA2B1), Proline rich coiled-coil 2a (Prrc2a), Eukaryotic initiation factor 3 (eIF3), Sterile sea water (SSW), Oocytes (E), Fertilized oocytes (F E), Two to eight cell embryos (2/8 C), Hours post fertilization (hpf), Morula (M), Blastula (B), Gastrula (G), D larvae (D), solid-phase reversible immobilization (SPRI), TPM (Transcripts Per Million), Gene ontology (GO), oyster m^{6}A-interacting protein (Cg-m^{6}A-BPs), S-adenosyl-methionine (SAM), maternal-to-zygotic transition (MZT), acetonitrile (ACN)

Keywords

RNA, methylation, epitranscriptomics, oyster, development.

Conflicts of interest

The authors declare they have no competing conflict of interest

Abstract

N^6-methyladenosine (m^{6}A) is a prevalent epitranscriptomic mark in eukaryotic RNA, with crucial roles for mammalian and ecdysozoan development. Indeed, m^{6}A-RNA and the related protein machinery are important for splicing, translation, maternal-to-zygotic transition and cell differentiation. However, to date, the presence of an m^{6}A-RNA pathway remains unknown in more distant animals, questioning the evolution and significance of the epitranscriptomic regulation. Therefore, we investigated the m^{6}A-RNA pathway in the oyster *Crassostrea gigas*, a lophotrochozoan model whose development was demonstrated under strong epigenetic influence.

Using mass spectrometry and dot blot assays, we demonstrated that m^{6}A-RNA is actually present in the oyster and displays variations throughout early oyster development, with the lowest levels at the end of cleavage. In parallel, by *in silico* analyses, we were able to characterize at the molecular level a complete and conserved putative m^{6}A-machinery. The expression levels of the identified putative m^{6}A writers, erasers and readers were strongly regulated across oyster development. Finally, RNA pull-down coupled to LC-MS/MS allowed us to prove the actual presence of readers able to bind m^{6}A-RNA and exhibiting specific developmental patterns.

Altogether, our results demonstrate the conservation of a complete m^{6}A-RNA pathway in the oyster and strongly suggest its implication in early developmental processes including MZT. This first demonstration and characterization of an epitranscriptomic regulation in a lophotrochozoan model, potentially involved in the embryogenesis, brings new insights into our understanding of developmental epigenetic processes and their evolution.

Introduction

The *N*^{6}-methyladenosine (m^{6}A) is the prevalent chemical RNA modification in all eukaryotic coding and non-coding RNAs [1]. Messenger RNAs are the most heavily m^{6}A methylated RNAs, with m^{6}A bases lying mostly in their 3' UTRs, at the vicinity of their stop codon [2–4] and also in 5' UTRs and long internal exons [4,5]. *N*^{6}-methylation of RNA adenosines is responsible for RNA processing and, like DNA methylation or histone modifications, contributes to the regulation of gene expression without changing the DNA or mRNA sequence. Therefore m^{6}A constitutes a new layer of post-transcriptional gene regulation, which is emerging or has been proven critical in various biological processes, and referred to as epitranscriptomic [2].

The dynamics and biological outcomes of m^{6}A levels are the results of the activity of a complex protein machinery comprising writers, erasers and readers. The addition of a methyl group to the 6th nitrogen of RNA adenosines is catalysed by m^{6}A writers with distinct properties. Methyltransferase like 16 (METTL16) is a 'stand-alone' class I methyltransferase that recognizes the UACA*GAGAA consensus sequence (with * indicating the target adenosine) [6]. By contrast, METTL3 transfers methyl groups to adenosines within the RRA*CH motif [2,3,7]. METTL3 is only active within a tripartite 'core complex' [8] comprising METTL3, METTL14 which enhances the methyltransferase activity supported by the MTA-70 domain of METTL3 [9,10] and the regulator protein Wilms' tumor 1-associated protein (WTAP) [4,9,11]. This core complex can interact with Virilizer-like (or KIAA1429) [12], ring finger E3 ubiquitin

ligase (HAKAI) [12,13], zinc finger CCCH-type containing 13 (ZC3H13) [12,14], RNA-binding motif 15 (RBM15) and RBM15B [7,15] which are suspected to intervene in the core complex activity and target specificity. The demethylation of adenosines has been demonstrated to be an active process catalysed by eraser enzymes belonging to the Fe(II)/2-oxoglutarate dioxygenase family: AlkB homologue 5 (ALKBH5) [16,17] and the fat mass and obesity associated protein (FTO) [17,18].

A growing number of reader proteins which recognize the m^{6}A-RNA mark is being described. They may be divided into two classes depending on the presence of a YT521 B Homology (YTH) domain in their primary sequence. The YTH protein family includes YTH domain family protein 1-3 (YTHDF1-3) and YTH domain containing protein 2 (YTHDC2), which are cytosolic m^{6}A readers involved in m^{6}A-RNA stability and translation [19–22]. The fifth YTH member is YTHDC1, which is present in the nucleus and controls splicing [23] and nuclear export [24] of m^{6}A-RNA. The second class of readers comprises proteins without YTH domain which are involved in several molecular mechanisms. For example, the heterogeneous nuclear ribonucleoprotein A2 B1 (HNRNPA2B1) is important for miRNA processing [25]. Insulin-like growth factor 2 mRNA binding protein 1-3 (IGF2BP 1-3) [26] and proline-rich coiled-coil 2a (Prrc2a) [27] participate in RNA stability while eukaryotic initiation factor 3 (eIF3) guides cap-independent translation [5].

The m^{6}A epitranscriptomes underlie important biological functions, most of which being related to developmental processes, including the control of cell differentiation [27–32], maternal to zygotic transition (MZT) [33], sex determination [7,34] and gametogenesis [16,21,35,36]. Such

critical epitransriptomic outcomes are conserved in the animal evolution and were characterized in both vertebrates and ecdysozoans, i.e. mammals and drosophila.

However, such conserved biological significance originates in diverse epitranscriptomic mechanisms. Indeed, not all ecdysozoans bear a complete m^{6}A-RNA machinery, such as *C. elegans* whose genome is devoid of the related protein machinery with the exception of a putative orthologue of METTL16 [37,38]. In addition, no m^{6}A eraser has been described to date in non-vertebrate models, and especially ecdysozoans such as the drosophila or *C. elegans* [38–40], where it cannot be excluded that m^{6}A-RNA methylation could be removed by the activity of characterised 6mA-DNA demethylases [41,42]. This situation may illustrate a growing complexity of epitranscriptomic mechanisms during the animal phylogeny and raises fundamental questions about its evolution and its presence in organisms distant from mammals and ecdysozoans. However, to date, no data about a possible epitranscriptomic regulation is available to our knowledge in lophotrochozoans, the understudied sister group of ecdysozoans within protostomes, although representing an important range of metazoan biodiversity.

The Pacific oyster *Crassostrea gigas* (i.e. *Magallana gigas*) is a bivalve mollusc whose great ecological an economical significance allowed its emergence as a model species within lophotrochozoan organisms. As such, an important amount of genetic, transcriptomic and epigenetic data have been generated in this model. Interestingly, the embryolarval development of *C. gigas* is described to be under the strong epigenetic influence of DNA methylation [43–47] and histone marks [48–50]. Besides, oyster development occurs exposed to external environmental conditions, and in other models the m^{6}A methylation of RNA and/or

the expression of its machinery can be induced by heat stress, UV exposure or endocrine disruptors [5,51–54], questioning the presence of an m^{6}A pathway in *C. gigas* and its significance in oyster early development.

To investigate this, we measured m^{6}A levels in RNA across the entire embryolarval life of the oyster using mass spectrometry and dot-blot. We also searched the available *in silico* resources for putative conserved m^{6}A-related proteins in *C. gigas* genomic data as well as their cognate expression kinetics using RNAseq assembly analyses. We also performed RNA-pulldown with a synthetic m^{6}A-RNA oligonucleotide coupled to liquid chromatography and mass spectrometry (LC-MS/MS) to characterize potential oyster m^{6}A-binding proteins. To our knowledge, this study is the first report unravelling epitranscriptomic mechanisms outside vertebrate and ecdyzosoan animal models.

Results:

m^{6}A is present in oyster RNA, differentially affects distinct RNA populations and displays variations during embryonic life.

Mass spectrometry measurements revealed that m^{6}A is present in oyster RNA, with global m^{6}A/A levels of ca. 0.3%, a value comparable to what has been found in the human and the fruit fly (Figure 1A). Immunoblot assays indicate that total and polyA+ RNA present variable amounts of m^{6}A during oyster development and that these variations display distinct profiles suggesting specific methylation patterns between RNA populations. Indeed, *N*^{6}A-methylation in total RNA is the highest in the early stages (oocytes and fertilized oocytes) then gradually

decreases until the morula stage before gradually increasing again up to the trochophore stage when it recovers its maximum (Figure 1B). In contrast, m^{6}A levels in polyA+ RNA are hardly detected in early stages but display a peak in the gastrula and trochophore stages (Figure 1C).

m^{6}A machinery is conserved at the molecular level in the oyster.

In silico analyses led to the identification of oyster sequences encoding putative orthologues of m^{6}A writers, erasers and readers that are present in the human and/or in the human and the fruit fly.

All the eight m^{6}A-RNA writers characterized in the human and/or drosophila at the time of the study, namely METTL3, METTL14, WTAP, Virilizer-like, HAKAI, ZC3H13, RBM15/15B and METTL16, were present in the oyster at the gene level. The encoded protein primary sequences all display the specific domains required for enzymatic activity and/or binding. They include MT-A70 and AdoMetMtases SF domains for METTL3, METTL14 and METTL16, respectively, that bear the methyltransferase activity. Oyster WTAP and Virilizer-like orthologues exhibit WTAP and VIR_N domains, respectively, that are required in their human counterparts to bind and activate the catalytic subunit of the m^{6}A-RNA methyltransferase complex. Oyster Hakai and RBM15/15B present RHHL, RHF-Zn-BS and specific RRM domains, respectively, similar to human and fruit fly orthologues. Besides, the oyster ZC3H13 bears the Rho SF domain present in the human, but not in the fruit fly orthologue (Figure 2A). *C. gigas* also presents a putative m^{6}A-RNA eraser, ALKBH5, which is present in the human but has not been characterized in drosophila. The oyster ALKBH5 exhibits a 2OG-FeII_Oxy domain suggestive of a presumably conserved catalytic functionality through fe2+-dependent

oxoglutarate oxidation. Of note, no orthologue of the human FTO eraser could be identified in the oyster genomic or transcriptomic databases available to date (Figure 2B).

Many m^{6}A reader orthologues have also been found in the oyster, including proteins containing a YTH domain, such as YTHDF, YTHDC1 and YTHDC2. An oyster Prrc2a-like protein produces homology with the human Prrc2a, especially within the m^{6}A-binding GRE-rich domain. Oyster readers also include a heterogeneous nuclear ribonucleoprotein-coding gene, hnRNPA2B1 with greater sequence similarity with the drosophila counterpart than with the human orthologue. Similarly, the IGF2BP-coding sequence has also been found in *C. gigas* (Figure 2C). Five oyster sequences display homologies with eIF3a which is able to bind m^{6}A-RNA [5] but it was not possible to discriminate whether a unique oyster predicted protein was an eIF3a orthologue.

Overall, these results indicate the conservation of a complete m^{6}A-RNA machinery in the oyster. The complete list of the identified genes encoding the conserved m^{6}A machinery actors and their isoforms, as well as the related information is given in the supplementary data (Data S1).

Oyster putative m^{6}A actors display expression level variations across development.

RNAseq data analyses showed that all the oyster m^{6}A-related genes were expressed during the early life (Figure 3). Their expression level displayed gene-specific profiles, most of them being variable throughout oyster development.

The expression of writers belonging to the core methylation complex is weak overall. METTL3 and WTAP share similar profiles with little expression increasing up to the gastrulation and

remaining stable afterwards. In contrast METTL14 displays a weak expression level across the embryo larval life. The expression profile of Virilizer-like resembles WTAP, while HAKAI, RBM15/15B and METTL16 seem to have mRNA levels which decrease after cleavage, whereas those of ZC3H13 transcript variants seem to drop at the D larva stage. Interestingly, METTL16 mRNA levels display an opposite developmental profile when compared to METTL3 expression; with the highest values during cleavage which decrease later on (Figure 3A).

ALKBH5 transcripts are weakly represented within oyster early embryos and the higher TPM values are found in gastrulas. However, maximum levels are observed after metamorphosis in juveniles (Figure 3B).

Regarding m^{6}A putative readers, the expression of YTH family genes during development showed different patterns. In fact, YTHDF is the most represented YTH-domain bearing actor and YTHDF TPM values are ca. 5-fold higher than all the other oyster YTH readers. YTHDF is strongly expressed at the beginning of development until a peak at the morula stage. Prrc2a is the most represented reader at the mRNA level in oyster embryos, and the sum of the TPM of the two Prrc2a oyster isoforms are at most ca. 20-fold higher than those of YTH family. However, Prrc2a and YTHDF transcript content profiles are similar across oyster development, and also remind of the IGF2BP mRNA levels.

By contrast, the two isoforms of YTHDC1 identified by *in silico* analysis, YTHDC1.1 and YTHDC1.2, display similar patterns together with YTHDC2, with a maximum representation in gastrulas. The expression of hnRNPA2B1 isoforms has likewise patterns except for a marked drop at the D larvae stage (Figure 3 C).

Oyster orthologues of m^{6}A-RNA interacting proteins bind m^{6}A RNA *in vitro*.

To determine whether oyster proteins can bind m^{6}A-RNA, we performed RNA-pulldown of cytoplasmic and nuclear embryonic cell extracts using a methylated versus a non-methylated oligonucleotide, followed by LC/MS-MS characterisation and identification of the captured proteins with the Mascot software.

In nuclear extracts, we detected 591 proteins able to bind both the methylated and unmethylated oligos. We identified 43 proteins specific to unmethylated RNA while 131 proteins specifically bind the m^{6}A-methylated oligo. In cytosolic extracts, there were respectively 646, 436 and 36 of such proteins, respectively. Regardless of the methylation status, more proteins in the cytoplasmic extracts can bind to the RNA oligonucleotides than in the nuclear extracts (1118 proteins vs. 765, respectively). However, more nuclear proteins are found exclusively bound to the m^{6}A-containing oligo than cytoplasmic proteins (131 vs. 36, i.e. 17 % vs. 3 %, respectively). In addition, many nuclear and cytoplasmic proteins can bind both the methylated and the non-methylated oligo (591 vs. 646, i.e. 77 % vs. 58 %). An important number of proteins in the cytoplasmic extract were found exclusively bound to the non-methylated oligo, whereas only a limited number of nuclear proteins display such a specificity (436 vs. 43, i.e. 39 % vs. 6 %). Among the 167 m^{6}A-specific proteins in oyster extracts, only 5 were found in both the nuclear and cytoplasmic extracts. These results show that oyster proteins can directly or indirectly bind m^{6}A-RNA, and suggest an important compartmentalization of m^{6}A-related processes.

Among the identified proteins in this assay, four of the putative oyster m^{6}A readers are found, YTHDC1, hnRNPA2B1, IGF2BP and eIF3. In the nuclear extracts YTHDC1 is uncovered as

m^{6}A-specific whereas hnRNPA2B1 and IGF2BP were present complexed with both the m^{6}A- and A-oligos. In the cytoplasmic extracts, YTHDC1 and eIF3a are m^{6}A-specific while hnRNPA2B1, IGF2BP were pulled down by both methylated and unmethylated oligos (Figure 4A).

These results demonstrate that some proteins in the oyster can specifically bind m^{6}A-RNA and that the putative m^{6}A reader orthologues in the oyster are conserved at the protein level and are able to interact with m^{6}A-RNA.

The m^{6}A-interacting protein-coding genes display clustered expression regulation and functional annotation during oyster development.

The mRNA expression level of the genes encoding the 162 oyster m^{6}A-interacting protein (Cg-m^{6}A-BPs) was examined using RNAseq databases. Most of them display a specific and regulated expression level across oyster developmental stages. However, three main expression clusters could be distinguished according to their developmental mRNA expression level profile. Cluster 1 includes genes that show high expression at the beginning of the embryo life (i.e. cleavage) and strongly decrease after gastrulation; the second cluster contains weakly expressed genes except in the latest examined larval phases, after gastrulation (i.e. Trochophore and D Larvae); cluster 3 groups genes that show an expression peak during gastrulation (Figure 4B).

The Gene Ontology annotation of the Cg-m^{6}A-BP genes reveal that the distinct clusters are related to distinct functional pathways as indicated by the little - if any - common GO terms between them (Figure 4C). However, the functional pathways of all three gene clusters point

out to their implication in translation and its regulation, although the terms enriched in each cluster illustrate different aspects of translation, such as translation initiation (cluster 1), splicing and nuclear export (cluster 2) and ribosomal and mitochondrial processes (cluster 3) respectively (Figure 4D).

Discussion

This work demonstrates that m^{6}A-RNA is present and variable during the embryo-larval life of the oyster, and that *C. gigas* exhibits putative conserved and functional m^{6}A-RNA writers, eraser and readers. The dynamics of such mark and of its actors strongly suggest a biological significance of the epitranscriptomic pathway in the control of development of a lophotrochozoan species, which has, to date, never been demonstrated to our knowledge.

m^{6}A-RNA levels vary across oyster development.

Using mass spectrometry and immunological measurements, we showed that oyster RNA is m^{6}A-methylated. The global proportion of *N*^{6}-methyladenosine in RNA in the developing oyster (0.28 %) is similar to those observed elsewhere in the animal kingdom, such as in the fruit fly (0.24 %) [34] or the human (0.11- 0.23 %) [55] (Figure 1A), despite those values are difficult to compare because they were not measured within the same developmental phase (adult flies and human cell lines vs. oyster embryos). However, the comparable magnitude of m^{6}A-RNA amounts between taxa, in contrast to DNA methylation [46], may indicate conserved biological significance of epitranscriptomic processes between groups. The amount of m^{6}A in total RNA displays a striking decrease during cleavage and then recovers its maximum levels at the end of the gastrulation (Figure 1B). Therefore, the m^{6}A decrease in total RNA during cleavage, i.e.

before the transcription of the zygotic genome starts, reflects a degradation of maternal m^{6}A-RNAs or their demethylation. However, all RNA populations do not exhibit the same pattern, indeed polyA+ RNAs are m^{6}A methylated only after cleavage. The extent of polyadenylation of oyster maternal messenger RNAs accumulating during vitellogenesis is unknown. Therefore, which maternal RNA population(s) is methylated in oyster oocytes is unclear. Nevertheless, the observation that m^{6}A-RNA levels are variable and affecting distinct RNA populations across embryonic stages strongly favours an important biological significance of m^{6}A-RNA in oyster development. We hypothesize that oyster maternal messenger RNAs are poorly polyadenylated, and that m^{6}A, aside polyadenylation, might play a role in the stability of quiescent maternal mRNAs. Alternatively, other maternal RNA populations such as snRNA, miRNA, rRNA or lncRNA might be methylated [6,15,25,56], which become demethylated or degraded up to the morula stage. The later increase in m^{6}A RNA after cleavage could therefore be the result of the methylation of the increasingly transcribed RNAs from the blastula stage, including polyadenylated mRNAs.

The m^{6}A-RNA machinery is conserved in the oyster and regulated during development.

The important regulation of m^{6}A levels during oyster development assumes the presence of a related protein machinery. We identified *in silico* cDNA sequences encoding conserved putatively functional orthologues of m^{6}A-RNA writers, eraser and readers in the oyster, with great confidence (homologies ranging from ca. 30 to 65 % with their human counterpart, see Data S1). The writers include all the members of the methylation complex (METTL3, METTL14, WTAP, Virilizer-like, Hakai, ZC3H13, RBM15/15B) identified to date in the human and the fruit fly [7,11,12,14,15,57]. We also identified an orthologue of the stand-alone METTL16 m^{6}A

methyltransferase. Each orthologue bears the conserved domain(s) demonstrated to be implicated in the catalytic and/or binding activity of their cognate counterpart in other species, such as the MT-A70 domain which transfers methyl groups from the S-adenosyl-methionine (SAM) to the N^6 nitrogen of RNA adenines [57]. Of the two proteins that can erase RNA methylation, only ALKBH5, which is important for mouse spermatogenesis [16], was identified at the cDNA level in the oyster. Indeed, no *C. gigas* sequence displayed significant homology with the mammalian FTO protein, whose functional significance remains controversial [17]. Most the characterized m^{6}A-RNA readers are also present at the molecular level in the oyster and are putatively able to bind m^{6}A regarding their primary sequence, such as the YTHDC and YTHDF family members [19,21,23,58], Prrc2A [27], HnRNPA2B1 [25] and IGF2BP [26]. Of note, some of these readers have not been characterized to date in *D. melanogaster* but display strong homologies between humans and oysters. In mammals, eIF3a has important functional outcomes in cap-independent translational stress response [5]. However, it was not possible to ascribe a single oyster sequence as a unique eIF3a orthologue (Data S1), although its presence was demonstrated by RNA pull down (see below) (see Data S2). Altogether, *in silico* results show the conservation of a complete m^{6}A-RNA machinery in the oyster. To date to our knowledge, this is the first demonstration in a lophotrochozoan organism of an epitranscriptomic pathway. Its presence suggests its ancestral origin, and questions its biological significance in oyster development.

To investigate this, we analysed the expression level of the m^{6}A machinery genes using RNA-seq data. Our results indicate that the core methylation complex (METTL3, METTL14 and WTAP) would not be active during cleavage because of the absence of METTL3 and little

WTAP expression. METTL16 catalyses the downregulation of SAM methyl donor availability in mammals [59]. If METTL16 function is conserved in the oyster as suggested by the high sequence homology, the peak in METTL16 expression, together with the weak expression of the core complex in 2/8 cell embryos is consistent with an absence of m^{6}A-RNA up to the blastula stage. Then, the core complex would likely be active as soon as the end of cleavage (i.e. since the blastula stage), in line with the increase in m^{6}A levels observed at the same time. The correlation between the increasing METTL3 expression and m^{6}A-RNA levels after cleavage strongly favours the conservation of the methyltransferase activity of the oyster MT-A70 domain. Interpreting the regulation of the m^{6}A activity by the other methyltransferase complex members (i.e. Virilizer-like, HAKAI, ZC3H13 and RBM15/15B) is difficult because how - or even if - oyster orthologues act within the complex is not known. Nevertheless, their specific expression profiles may reflect their implication in the regulation of distinct biological contexts. There might be little functional significance of active m^{6}A-RNA erasure during oyster development, consistent with the normal embryonic phenotype of ALKBH5 knockdown mice [16]. Overall, the m^{6}A readers display distinct developmental expression patterns. While YTHDF and Prrc2a peak during cleavage, YTHDC1, YTHDC2, IGF2BP and hnRNPA2B1 mRNA levels gradually increase up to the gastrulation and remain mostly highly expressed afterwards (except for hnRNPA2B1 and IGF2BP). These profiles evoke the mediation of distinct biological functions depending on the reader and the developmental phases. Therefore, we hypothesized that YTHDF and Prrc2a might participate in the blastulean transition in the oyster. Indeed, in the zebrafish, a YTHDF reader triggers the maternal-to-zygotic transition through the decay of the maternal m^{6}A RNAs during cleavage [33]. The role

in the axon myelination and specification of mouse oligodendrocytes [27] is unlikely conserved for Prrc2a because the oyster orthologue is expressed before the neurogenesis is detected in trochophore stages [60]. Alternatively, the early expression of Prrc2a suggests that it might rather compete with YTHDF for m^{6}A-RNA targets [27], thereby possibly acting in oyster MZT, bringing new perspectives into this process which remains poorly understood in lophotrochozoans. In mammals m^{6}A is implicated in the embryonic cell fate [30,31] notably via the regulation of cell differentiation by YTHDC2 [32] or hnRNPA2B1 [29]. In the oyster, YTHDC1, YTHDC2, IGF2BP and hnRNPA2B1 have their maximum expression during gastrulation correlated to the second m^{6}A peak, suggesting similar implications.

Putative oyster m^{6}A readers actually bind m^{6}A-RNA *in vitro*.

To better approach the developmental processes involving m^{6}A in the oyster, we characterized the proteins that can interact with m^{6}A-RNA using a methylated-RNA-pulldown / mass spectrometry assay. We identified 162 proteins able to specifically bind the m^{6}A-RNA oligo in embryonic cell extracts, demonstrating the actual presence of genuine m^{6}A-readers in the oyster. Most (ca. 75 %) of these proteins were found in nuclear extracts and only 5 were found in both the cytoplasmic and nuclear fractions, showing an important compartmentalization of the epitranscriptomic pathway. Regarding the little number of m^{6}A readers in other animals, and because the assay conditions do not discriminate between direct and indirect interactions, we hypothesize that most these proteins indirectly bind m^{6}A via a limited number of 'scaffold' m^{6}A readers. Such authentic readers that only bind the m^{6}A-RNA oligo in our assay likely include YTHDC1 and eIF3a, which have been demonstrated to directly bind m^{6}A in other species, demonstrating the conservation of the m^{6}A-binding capacity and specificity of the YTH

domain in the oyster. Besides, YTHDC1 is found in both cell fractions, suggesting its implication in the trafficking of m^{6}A-RNA across the nuclear envelope [24], and reinforcing the hypothesis that YTH proteins could participate in oyster MZT and cell differentiation. The presence of the oyster eiF3a in the cytoplasm is consistent with a conserved role in m^{6}A-mediated translation processes, such as cap-independent translation [5].

Possible functions of m^{6}A-RNA in oyster development.

We investigated the expression level and the functional annotation of the 162 genes encoding the m^{6}A-interacting proteins across oyster early life. These genes can be clustered into three successive expression phases corresponding to three distinct functional pathways, which are independent albeit all mostly related to translation regulation. The cluster 1 is mostly expressed during the cleavage and the associated GO terms are related to the initiation of translation, consistent with maternal RNA consumption before MZT is complete and the zygotic genome becomes fully activated. The genes within cluster 3 show an expression peak during gastrulation. Their ontology terms evoke ribosomal and mitochondrial processes, the latter being required for energy supply and signalling integration during gastrulation [61–64]. The cluster 2 contains genes that peak after gastrulation and which are related to splicing and nuclear export. Such functional annotations are in line with a fine regulation of transcript variant translation within the distinct cell lineages in the three cell layers of the late embryos.

Taken together, our findings bring to light a possible implication of m^{6}A in oyster development. First, during cleavage the decrease of m^{6}A-RNA, the weak expression of methyltransferase complex genes, the maximum of YTHDF gene expression and the expression of *Cg*-m^{6}A-BPs

related to the initiation of the translation strongly suggest the implication of m^{6}A in MZT in *C. gigas*. Second, the increasing m^{6}A level during gastrula stage is correlated to the increase of methyltransferase complex gene expression. In addition, the increased RNA level of readers putatively related to cell differentiation and the peak of gene expression of *Cg*-m^{6}A-BPs associated to ribosomal and mitochondrial processes, support the hypothesize of a m^{6}A implication in gastrulation. Finally, the highest m^{6}A level at the trochophore stage, the gene expression of the methyltransferase complex and of readers associated to cell differentiation, as well as high RNA level of Cg-m^{6}A-BPs related to splicing and nuclear export is correlated with the fine cell differentiation taking place at this stage. However, inferring the biological significance of m^{6}A in development from the indirect and incomplete functional annotation of the oyster genome is only limited. Characterization of the precise targets of m^{6}A and how their individual methylation is regulated across development, for example using high throughput sequencing of precipitated m^{6}A-RNA (MeRIP-seq), could be extremely relevant to better understand this issue. In addition, despite sequence conservation and binding ability of oyster actor orthologues strongly suggest functional conservation, future dedicated studies such as biochemical inhibition or gene inactivation could help demonstrate their genuine biological function. Besides, there seems to be an inverse correlation between m^{6}A-RNA and 5mC-DNA levels during the considered oyster developmental window [46]. This may suggest an interplay between epigenetic and epitranscriptomic marks, possibly reflecting competition for methyl-donor availability [59] or a link by histone epigenetic pathways [65,66].

Regarding the potential influence of the environment on m^{6}A and the accumulation of RNA in oocytes, we are at present investigating our hypothesis that m^{6}A may convey intergenerational

epitranscriptomic inheritance of maternal life traits in the oyster. On an evolutionary perspective, the presence of a putatively fully conserved epitranscriptomic pathway in the oyster suggests that it was already present in the bilaterian common ancestor thereby in favour of an important biological significance. Why *Drosophila* and *Caenorhabditis* seem to have lost specific m^{6}A-RNA erasers could be related to a sub-functionalization of the DMAD [41] and NMAD-1 [42] *N*^{6}-methyladenine DNA demethylase activity broadened towards RNA. However, more work in required to better understand the evo-devo implications of our results.

To conclude, in this work we report the discovery and characterisation of a putatively complete epitranscriptomic pathway in a lophotrochozoan organism, the oyster *Crassostrea gigas*. This pathway includes the m^{6}A mark in RNA and the actors of all the aspects of its regulation (writers, eraser, readers) which are conserved at the molecular level and putatively functional. We show that m^{6}A levels are variable across oyster development and that m^{6}A differentially affects distinct RNA populations. Expression levels of the related enzymatic machinery is consistent with the observed m^{6}A level variations. We demonstrate the m^{6}A binding capacity and specificity of putative oyster m^{6}A readers in the cytoplasm and nucleus of embryolarval cells. These readers mediate distinct putative biological outcomes depending on the development stage considered. From these results we hypothesize that early decay of maternal m^{6}A RNA participates in maternal-to-zygotic transition during cleavage and that later *de novo* zygotic m6A methylation contributes to gastrulation and cell differentiation. This first characterisation of an m^{6}A-epitranscriptomic pathway in a lophotrochozoan organism, together with its potential implication in development, opens new perspectives on the evolution of

epigenetic mechanisms and on the potential epitranscriptomic inheritance of environmentally-induced life traits.

Methods:

Animals:

Broodstock oysters [67] and oyster embryos [46] were obtained at the IFREMER marine facilities (Argenton, France) as previously described. Briefly, gametes of mature broodstock oysters were obtained by stripping the gonads and filtering the recovered material on a 60 µm mesh to remove large debris. Oocytes were collected as the remaining fraction on a 20 µm mesh and spermatozoa as the passing fraction on a 20 µm mesh. Oocytes were pre-incubated in 5 L of UV-treated and 1 µm filtered sterile sea water (SSW) at 21 °C until germinal vesicle breakdown. Fertilization was triggered by the addition of ca.10 spermatozoids per oocyte. After the expulsion of the second polar body was assessed by light microscopy, embryos were transferred in 150 L tanks of oxygenated SSW at 21 °C. The development stages were determined by light microscopy observation. The stages collected were oocytes (E, immediately before sperm addition), fertilized oocytes (F E, immediately before transfer to 150L tanks), two to eight cell embryos (2/8 C, ca. 1.5 hours post fertilization (hpf)), morula (M, ca. 4 hpf), blastula (B, ca. 6 hpf), gastrula (G, ca. 10 hpf), trochophore (T, ca 16 hpf) and D larvae (D, ca. 24 hpf). For each development stage, 3 million embryos were collected as the remaining fraction on a 20 µm mesh and centrifuged at 123 g for 5min at room temperature.

Supernatant was discarded and samples of 1 million embryos were then snap-frozen in liquid nitrogen directly of after resuspension in Tri-Reagent (Sigma-Aldrich, St Louis, MO, USA) (1 mL/10^6 embryos) and stored at -80 °C. Three distinct experiments were realized (February to May 2019) using the gametes of 126 to 140 broodstock animals, respectively.

RNA extraction:

- total RNA extraction

RNA was extracted using phenol-chloroform followed by affinity chromatography as previously described [68]. Briefly, embryos were ground in Tri-Reagent (Sigma-Aldrich) and RNA was purified using affinity chromatography (Nucleospin RNA II kit, Macherey-Nagel, Duren, Germany). Potential contaminating DNA was removed by digestion with rDNase (Macherey-Nagel) according to the manufacturer's instructions for 15 min at 37 °C then RNA was purified using Beckman Coulter's solid-phase reversible immobilization (SPRI) paramagnetic beads (AgencourtAMPure XP, Beckman Coulter, Brea, CA, USA) according to the manufacturer's instructions. Briefly, paramagnetic beads and RNAs were mixed slowly and incubated 5 min at room temperature followed by 2 min on a magnetic rack. Cleared supernatant was removed, and beads were washed three times with 70 % ethanol. After 4 min of drying at room temperature, RNAs were mixed slowly with RNase free water and incubated for 1 min at room temperature on the magnetic rack. Eluted total RNA was stored at -80 °C.

- PolyA RNA enrichment

Poly-A RNA was extracted from total RNA by oligo-dT affinity chromatography (NucleoTrap mRNA kit, Macherey-Nagel) according to the manufacturer's instructions. Briefly, up to 130 µg

of total RNAs were mixed with oligo-dT latex beads and incubated for 5 min at 68 °C then 10 min at room temperature. After centrifugation (2,000 g then 11,000 g), the pellets were washed three times on the microfilter and dried by centrifugation at 11,000 g for 1 min. Finally, polyA+ RNA was incubated with RNAse-free water for 7 min at 68 °C then centrifuged at 11,000 g for 1 min. Eluted polyA+ RNA was stored at -80 °C until needed.

Total and polyA-enriched RNA purity and concentrations were assayed by spectrophotometry (Nanodrop, Thermo Scientific, Waltham, MA, USA).

m^{6}A quantification by LC-MS/MS:

- RNA hydrolysis

To generate nucleosides for quantification against standard curves, 5 µg of total RNA were denatured for 10 min at 70 °C followed by 10 min on ice, and hydrolyzed with 100 U Nuclease S1 (50 U/µL, Promega, Madison, WI, USA) in Nuclease S1 buffer (Promega) in a final reaction volume of 25 µL for 2 h at 37 °C under gentle shaking. Samples were then incubated with alkaline phosphatase buffer (Promega) for 5 min at room temperature, before 10 U alkaline phosphatase (Promega) were added and incubated further for 2 h at 37 °C under gentle shaking. Ten extra units of alkaline phosphatase were added after 1 hour of incubation to complete the reaction. Finally, samples were centrifuged at 13,000 rpm for 10 min at 4 °C and the supernatant containing digested total RNA was collected and kept at -20 °C before quantification.

- m^{6}A quantification:

The apparatus was composed of a NexeraX² UHPLC system coupled with LCMS8030 Plus (Shimadzu, Kyoto, Japan) mass spectrometer using an electrospray interface in positive mode. The column (1.7 µm, 100x3 mm) was a HILIC Aquity® Amide (Waters, Millford, MA, USA) maintained at 35 °C. The injection volume and run-to-run time were 3 µL and 10 min, respectively. The flow rate was set to 1 mL/min. Mobile phase was initially composed of a mixture of ammonium formate solution (10 mM) containing 0.2 % (v/v) formic acid and 95 % acetonitrile (ACN) and it was maintained for 1 min. Then, a linear gradient was applied to reach 83 % ACN for 6 min. The composition returned to the initial conditions and the column was equilibrated for 3 min.

The mass spectrometer was running in the Multiple Reaction Monitoring (MRM) acquisition mode. LabSolutions 5.86 SP1 software was used to process the data. The desolvatation temperature was 230 °C, source temperature was 400 °C and nitrogen flows were 2.5 L/min for the cone and 15 L/min for the desolvatation. The capillary voltage was +4.5 kV. For each compound, two transitions were monitored from the fragmentation of the $[M+H]^+$ ion. The first transition (A in Table S1) was used for quantification and the second one (B in Table S1) for confirmation of the compound according to European Commission Decision 2002/657/EC (Table S1).

Blank plasma samples were analysed to check specificity. Calibrators were prepared using diluted solutions of A (Toronto Research Chemical, Toronto, Canada) and m^6A (Carbosynth, Berkshire, UK) in water at 1, 2, 5, 10, 20 50, 100 ng/mL The calibration curves were drawn by plotting the ratio of the peak area of A and m^6A. For both nucleosides, a quadratic regression with 1/C weighting resulted in standard curves with $R^2>0.998$ and more than 75% of standards

with back-calculated concentrations within 15% of their nominal values as recommended for by the European medicines agency for bioanalytical methods [69]. The limits of quantifications for both compounds were considered as the lowest concentrations of the calibration curve. m^{6}A/A ratios were calculated for each single sample using the determined concentrations. Final results are the average of three technical replicates.

m^{6}A quantification by immunoblotting:

Immunological quantification of m^{6}A was performed by dot-blot using total and polyA+ RNAs. Dogfish total RNA (Dr. A. Gautier, personal communication) and a synthetic unmethylated RNA oligo (Eurogentec, Liege, Belgium) were used as positive and negative controls, respectively. RNA samples were denatured for 15 min at 55 °C with gentle shaking in denaturing solution (2.2 M formaldehyde, 50 % formamide, 0.5X MOPS, DEPC water) followed by 2 min on ice. Blotting was performed on a vacuum manifold as follows: a nylon membrane (Amersham Hybond-N+, GE Healthcare life Sciences, Chicago, IL, USA) was pre-hydrated in DEPC water for 5 min, then each well was washed twice with 10X SSC (Sigma-Aldrich) before RNA was spotted onto the membrane and incubated for 15 min at room temperature. Then, vacuum aspiration was applied and each well was washed twice with 10X SSC. After heat crosslinking for 2 h at 70 °C, the membrane was rehydrated with DEPC water for 5 min, washed with PBS then PBST (PBS, 0.1 % Tween-20) for 5 min each and blocked with two 5 min incubations with blocking buffer (PBS, 0.1 % Tween-20, 10 % dry milk, 1 % BSA) at room temperature. The blocked membrane was incubated overnight at 4 °C under gentle shaking with the anti-m^{6}A primary antibody (Total RNA: Millipore (Burlington, MA, USA) ABE572, 1 :

1,000 dilution in blocking buffer; polyA+ RNA: Diagenode (Liege, Belgium) C15200082, 1 : 500 dilution in blocking buffer) followed by four washes of PBST for 5 min. The secondary antibody (Total RNA: Dako (Santa Clara, CA, USA) P0447 goat anti-mouse HRP antibody, 1 : 10,000 dilution; polyA+ RNA: Invitrogen (Carlsbad, CA, USA) A21202 donkey anti-mouse Alexa 488, 1 : 250 dilution) was diluted in PBST supplemented with 5 % dry milk and added onto the membrane for 1 h 30 (total RNA) or 1 h (polyA+ RNA) at room temperature under gentle shaking. Membranes were extensively washed in PBST (at least 4 washes of 5 min for total RNA and 5 min then 1 h for polyA+ RNA) then total and polyA+ RNA immunoblots were visualized using chemiluminescence (ECL kit, Promega) or fluorescence scanning at 480-530 nm (Pro Xpress, Perkin-Elmer, Waltham, MA, USA), respectively. The amount of m^{6}A was inferred from dot intensity measurements using ImageJ (v.1.49). Signal intensities were determined as 'integrated densities as a percentage of the total' which corresponds to the area under the curve of the signal of each dot after membrane background and negative control signal subtraction.

***In silico* analyses:**

All protein and RNA sequences of the m^{6}A machinery of *Homo sapiens* and *Drosophila melanogaster* (Data S1) were recovered by their published designation (i.e., 'METTL3' or 'YTHDF' etc.) and their identified protein sequence (ie. RefSeq accession number NP…) collected from NCBI and used as query sequences to search for putative homologue sequences in *Crassostrea gigas* databases. The presence of oyster orthologue RNA and protein sequences were investigated by reciprocal

BLAST(https://blast.ncbi.nlm.nih.gov/Blast.cgi) on the *Crassostrea gigas* GigaTON [70] and NCBI databases and results were compared between the two oyster databases. Domain prediction was performed with CD-search software (https://www.ncbi.nlm.nih.gov/Structure/cdd/wrpsb.cgi) with default settings on protein sequences of *Homo sapiens*, *Drosophila melanogaster* and *Crassostrea gigas*. The GRE-rich domain identified in vertebrate Prrc2a sequence [27] was performed with ProtParam (https://web.expasy.org/cgi-bin/protparam/protparam).

Protein machinery mRNA expression analyses:

The transcriptome data of the different development stages are available on the GigaTON database [70,71]. The correspondence between development stages in our study, and the GigaTON database were assessed using light microscopy based on the morphological description by Zhang et al., 2012 [71] (Table S2). Expression data was expressed in TPM (Transcripts Per Million) [72] to provide a normalized comparison of gene expression between all samples. The actual presence of some transcripts that display unclear or chimeric sequences within available oyster databases was assessed using RT-PCR (Data S1).

Protein m^{6}A RNA pull down:

- Protein extraction and RNA affinity chromatography

Protein extraction and RNA affinity chromatography were performed as described previously [27] with some modifications as follows. Equal amounts (1 million individuals) of each developmental stage (oocyte to D larvae) were pooled together then homogenized in 3.5

volumes of buffer A (10 mM KCl, 1.5 mM MgCl2, 10 mM HEPES, pH 7.9, DEPC water, 1X Protease inhibitor cocktail, DTT 0.5 mM) by extensive pipetting (ca. 30 times) and incubated 10 min at 4 °C. Embryos were ground with 10 slow 23G-needle syringe strokes and centrifuged at 2,000 rpm for 10 min at 4 °C. The supernatant was diluted in 0.11 volume of buffer B (1.4 M KCl, 0.03 M MgCl2, HEPES 0.3 M, pH 7.9, DEPC water), centrifuged at 10,000 g for 1 h at 4 °C and the supernatant containing cytosolic proteins was stored at -80 °C. The pellet of the first centrifugation, containing nuclei, was re-suspended in two volumes of buffer C (0.42 M NaCl, 1.5 mM MgCl2, 0.2 mM EDTA, 25 % glycerol, 20 mM HEPES, pH 7.9, 0.5 mM PMSF, 0.5 mM DTT, water DEPC). Nuclei were then lysed with a 23 G needle (10 vigorous syringe strokes) followed by centrifugation at 30,000 rpm for 30 min at 4 °C and the supernatant containing nuclear proteins was stored at -80 °C.

To identify putative proteins able to bind m^{6}A-RNA, the cytosolic and nuclear fractions were submitted to affinity chromatography using 5'-biotin-labelled RNA oligonucleotides either bearing *N*^{6}-methylated adenosines or not. The methylated adenosines were designed to lie within RRACH motifs, according to the conserved methylated consensus sequence in other organisms [2,3,7,33,73] (oligo-m^{6}A: 5'Biotin-AGAAAAGACAACCAACGAGRR-m^{6}A-CWCAUCAU-3', oligo-A: 5'Biotin-AGAAAAGACAACCAACGAGRRACWCAUCAU-3', R = A or G, W = A or U, Eurogentec).

For RNA pull down, streptavidin-conjugated magnetic beads (Dynabeads Myone Streptavidin, Invitrogen) were pre-blocked with 0.2 mg/mL tRNA (Sigma-Aldrich) and 0.2 mg/mL BSA for 1 h at 4 °C under gentle rotation followed by three washes with 0.1 M NaCl. To avoid the identification of non-target proteins, cytosolic and nuclear protein extracts were cleared with

pre-blocked magnetic beads in binding buffer (50 mM Tris-HCl, 250 mM NaCl, 0.4 mM EDTA, 0.1 % NP-40, DEPC water, 1 mM DTT, 0.4 U/μL RNAsin) for 1 h at 4 °C under gentle rotation. After incubation on magnetic rack, the supernatants containing putative target proteins were collected and mixed with pre-blocked magnetic beads and oligo-m^{6}A or oligo-A for 2 h at 4 °C under gentle rotation. The beads binding putative target proteins were washed three times with binding buffer and diluted in 50 mM ammonium bicarbonate.

- Identification of m^{6}A-binding proteins by LC-MS/MS:

Protein samples were first reduced, alkylated and digested with trypsin then desalted and concentrated onto a μC18 Omix (Agilent, Santa Clara, CA, USA) before analysis.

The chromatography step was performed on a NanoElute (Bruker Daltonics, Billerica, MA, USA) ultra-high pressure nano flow chromatography system. Peptides were concentrated onto a C18 pepmap 100 (5 mm x 300 μm i.d.) precolumn (Thermo Scientific) and separated at 50 °C onto a reversed phase Reprosil column (25 cm x 75 μm i.d.) packed with 1.6 μm C18 coated porous silica beads (Ionopticks, Parkville, Victoria, Australia). Mobile phases consisted of 0.1 % formic acid, 99.9 % water (v/v) (A) and 0.1 % formic acid in 99.9 % ACN (v/v) (B). The nanoflow rate was set at 400 nL/min, and the gradient profile was as follows: from 2 to 15 % B within 60 min, followed by an increase to 25 % B within 30 min and further to 37 % within 10 min, followed by a washing step at 95 % B and re-equilibration.

MS experiments were carried out on an TIMS-TOF pro mass spectrometer (Bruker Daltonics) with a modified nano-electrospray ion source (CaptiveSpray, Bruker Daltonics). The system was calibrated each week and mass precision was better than 1 ppm. A 1600 spray voltage with a capillary temperature of 180 °C was typically employed for ionizing. MS spectra were

acquired in the positive mode in the mass range from 100 to 1700 m/z. In the experiments described here, the mass spectrometer was operated in PASEF mode with exclusion of single charged peptides. A number of 10 PASEF MS/MS scans was performed during 1.16 seconds from charge range 2-5.

The fragmentation pattern was used to determine the sequence of the peptide. Database searching was performed using the Mascot 2.6.1 program (Matrix Science) with a *Crassostrea gigas* Uniprot database (including 25,982 entries). The variable modifications allowed were as follows: C-Carbamidomethyl, K-acetylation, methionine oxidation, and Deamidation (NQ). The 'Trypsin' parameter was set to 'Semispecific'. Mass accuracy was set to 30 ppm and 0.05 Da for MS and MS/MS mode respectively. Mascot data were then transferred to Proline validation software (http://www.profiproteomics.fr/proline/) for data filtering according to a significance threshold of <0.05 and the elimination of protein redundancy on the basis of proteins being evidenced by the same set or a subset of peptides (Data S2).

- Gene ontology analysis:

The mRNA sequences of the characterized m^6A-binding proteins were identified using tBlastn [74–76] against the GigaTON database [70] with default settings. Gene ontology (GO) analyses were carried out with the GO annotations obtained from GigaTON database gene universe [70]. GO term-enrichment tests were performed using the goseq (V1.22.0) R package [77] with p-values calculated by the Wallenius method and filtered using REVIGO [78]. GO terms with a p-value < 0.05 were considered significantly enriched (Data S3).

Statistical analyses and graph production:

Results are given as the mean ± SD of three independent experiments unless otherwise stated. They were analysed using one-way ANOVA or Kruskall-wallis tests when required, depending on the normality of result distribution. The normality was tested using the Shapiro-Wilk's test and homoscedasticity of variances with Bartlett's tests. Statistics and graphics were computed with Prism v.6 (Graphpad), R (v.3.6.1) and RStudio (v.1.0.153) softwares. The R packages *eulerr* [79] and *Complexheatmap* [80] were used for production of specific figures.

Author contribution

Experiment design: GR, LLF.

Benchwork and bioinformatics: LLF, GR, BB, BP, MS.

Data analysis: LLF, GR, BB, MS.

Manuscript writing and editing: LLF, GR, PF, BB, MS, BP.

Acknowledgements

The authors would like to acknowledge PRISMM core facility collaborators R. Delepée and S. Lagadu for their expertise in m^6A/A UHPLC-MS/MS quantification. We also thank J. Pontin for technical assistance and J. Le Grand for help with sampling.

Funding sources and disclosure of conflicts of interest

This work was supported by the French National program CNRS EC2CO (Ecosphère Continentale et Côtière 'HERITAGe' to G. Rivière) and the council of the Normandy Region (RIN ECUME to P. Favrel). The authors declare they have no conflict of interest.

References:

1 Saletore Y, Meyer K, Korlach J, Vilfan ID, Jaffrey S & Mason CE (2012) The birth of the Epitranscriptome: deciphering the function of RNA modifications. *Genome Biol.* **13**, 175.

2 Meyer KD, Saletore Y, Zumbo P, Elemento O, Mason CE & Jaffrey SR (2012) Comprehensive analysis of mRNA methylation reveals enrichment in 3′ UTRs and near stop codons. *Cell* **149**, 1635–1646.

3 Dominissini D, Moshitch-moshkovitz S, Schwartz S, Salmon-Divon M, Ungar L, Osenberg S, Cesarkas K, Jacob-hirsch J, Amariglio N, Kupiee M, Sorek R & Rechavi G (2012) Topology of the human and mouse m 6 A RNAmethylomes revealed bym6A-seq. *Nature* **485**, 201–206.

4 Ke S, Alemu EA, Mertens C, Gantman EC, Fak JJ, Mele A, Haripal B, Zucker-Scharff I, Moore MJ, Park CY, Vågbø CB, Kusśnierczyk A, Klungland A, Darnell JE, Darnell RB, Kuśnierczyk A, Klungland A, Darnell JE, Darnell RB, Kusśnierczyk A, Klungland A, Darnell JE & Darnell RB (2015) A majority of m 6 A residues are in the last exons, allowing the potential for 3′ UTR regulation. *Genes Dev.* **29**, 2037–2053.

5 Meyer KD, Patil DP, Zhou J, Zinoviev A, Skabkin MA, Elemento O, Pestova T V., Qian SB & Jaffrey SR (2015) 5′ UTR m6A Promotes Cap-Independent Translation. *Cell* **163**, 999–1010.

6 Pendleton KE, Chen B, Liu K, Hunter O V., Xie Y, Tu BP & Conrad NK (2017) The U6 snRNA m6A Methyltransferase METTL16 Regulates SAM Synthetase Intron Retention. *Cell* **169**, 824-835.e14.

7 Lence T, Akhtar J, Bayer M, Schmid K, Spindler L, Ho CH, Kreim N, Andrade-Navarro MA, Poeck B, Helm M & Roignant JY (2016) M6A modulates neuronal functions and sex determination in Drosophila. *Nature* **540**, 242–247.

8 Bokar JA, Shambaugh ME, Polayes D, Matera AG & Rottman FM (1997) Purification and cDNA cloning of the AdoMet-binding subunit of the human mRNA (N6-adenosine)-methyltransferase. *RNA* **3**, 1233–47.

9 Liu J, Yue Y, Han D, Wang X, Fu YY, Zhang L, Jia G, Yu M, Lu Z, Deng X, Dai Q, Chen W & He C (2013) A METTL3–METTL14 complex mediates mammalian nuclear RNA N6-adenosine methylation. *Nat. Chem. Biol.* **10**, 93–95.

10 Wang X, Feng J, Xue Y, Guan Z, Zhang D, Liu Z, Gong Z, Wang Q, Huang J, Tang C, Zou T & Yin P (2016) Structural basis of N6-adenosine methylation by the METTL3-METTL14 complex. *Nature* **534**, 575–578.

11 Ping X-LL, Sun B-FF, Wang L, Xiao W, Yang X, Wang W-JJ, Adhikari S, Shi Y, Lv Y, Chen Y-SS, Zhao X, Li A, Yang YGYY-G, Dahal U, Lou X-MM, Liu X, Huang J, Yuan W-PP, Zhu X-FF, Cheng T, Zhao Y-LL, Wang X, Danielsen JMRR, Liu F & Yang YGYY-G (2014) Mammalian WTAP is a regulatory subunit of the RNA N6-methyladenosine methyltransferase. *Cell Res.* **24**, 177–189.

12 Yue Y, Liu J, Cui X, Cao J, Luo G, Zhang Z, Cheng T, Gao M, Shu X, Ma H, Wang F, Wang X, Shen B, Wang Y, Feng X, He C & Liu J (2018) VIRMA mediates preferential m6A mRNA methylation in 3′UTR and near stop codon and associates with alternative polyadenylation. *Cell Discov.* **4**, 10.

13 Růžička K, Zhang M, Campilho A, Bodi Z, Kashif M, Saleh M, Eeckhout D, El-Showk S, Li H, Zhong S, Jaeger G De, Mongan NP, Hejátko J, Helariutta Y & Fray RG (2017) Identification of factors required for m6A mRNA methylation in Arabidopsis reveals a

role for the conserved E3 ubiquitin ligase HAKAI. *New Phytol.* **215**, 157–172.

14 Knuckles P, Lence T, Haussmann IU, Jacob D, Kreim N, Carl SH, Masiello I, Hares T, Villaseñor R, Hess D, Andrade-Navarro MA, Biggiogera M, Helm M, Soller M, Bühler M & Roignant J-YY (2018) Zc3h13/Flacc is required for adenosine methylation by bridging the mRNA-binding factor Rbm15/Spenito to the m 6 A machinery component Wtap/Fl(2)d. *Genes Dev.* **32**, 1–15.

15 Patil DP, Chen CK, Pickering BF, Chow A, Jackson C, Guttman M & Jaffrey SR (2016) m6A RNA methylation promotes XIST-mediated transcriptional repression. *Nature* **537**, 369–373.

16 Zheng G, Dahl JA, Niu Y, Fedorcsak P, Huang CM, Li CJ, Vågbø CB, Shi Y, Wang WL, Song SH, Lu Z, Bosmans RPG, Dai Q, Hao YJ, Yang X, Zhao WM, Tong WM, Wang XJ, Bogdan F, Furu K, Fu Y, Jia G, Zhao X, Liu J, Krokan HE, Klungland A, Yang YG & He C (2013) ALKBH5 Is a Mammalian RNA Demethylase that Impacts RNA Metabolism and Mouse Fertility. *Mol. Cell* **49**, 18–29.

17 Mauer J, Luo X, Blanjoie A, Jiao X, Grozhik A V, Patil DP, Linder B, Pickering BF, Vasseur J-J, Chen Q, Gross SS, Elemento O, Debart F, Kiledjian M & Jaffrey SR (2017) Reversible methylation of m6Am in the 5′ cap controls mRNA stability. *Nature* **541**, 371–375.

18 Jia G, Fu Y, Zhao X, Dai Q, Zheng G, Yang YGYY-GGYY-G, Yi C, Lindahl T, Pan T, Yang YGYY-GGYY-G & He C (2011) N6-Methyladenosine in nuclear RNA is a major substrate of the obesity-associated FTO. *Nat. Chem. Biol.* **7**, 885–887.

19 Wang X, Lu Z, Gomez A, Hon GC, Yue Y, Han D, Fu Y, Parisien M, Dai Q, Jia G, Ren B, Pan T, He C, Zhike L, Gomez A, Hon GC, Yue Y, Han D, Fu Y, Ärisien M, Dai Q, Jia G, Ren B, Pan T & He C (2014) N6-methyladenosine-dependent regulation of messenger RNA stability. *Nature* **505**, 117–120.

20 Wang X, Zhao BS, Roundtree IA, Lu Z, Han D, Ma H, Weng X, Chen K, Shi H & He C (2015) N6-methyladenosine modulates messenger RNA translation efficiency. *Cell* **161**, 1388–1399.

21 Hsu PJ, Zhu Y, Ma H, Guo Y, Shi X, Liu Y, Qi M, Lu Z, Shi H, Wang J, Cheng Y, Luo G, Dai Q, Liu M, Guo X, Sha J, Shen B & He C (2017) Ythdc2 is an N6-methyladenosine binding protein that regulates mammalian spermatogenesis. *Cell Res.* **27**, 1115–1127.

22 Shi H, Wang X, Lu Z, Zhao BS, Ma H, Hsu PJ, Liu C & He C (2017) YTHDF3 facilitates translation and decay of N 6-methyladenosine-modified RNA. *Cell Res.* **27**, 315–328.

23 Xiao W, Adhikari S, Dahal U, Chen Y-S, Hao Y-J, Sun B-F, Sun H-Y, Li A, Ping X-L, Lai W-Y, Wang XX-J, Ma H-L, Huang C-M, Yang YY-G, Huang N, Jiang G-B, Wang H-L, Zhou Q, Wang XX-J, Zhao Y-L & Yang YY-G (2016) Nuclear m 6 A Reader YTHDC1 Regulates mRNA Splicing. *Mol. Cell* **61**, 507–519.

24 Roundtree IA, Luo G-ZZ, Zhang Z, Wang X, Zhou T, Cui Y, Sha J, Huang X, Guerrero L, Xie P, He E, Shen B & He C (2017) YTHDC1 mediates nuclear export of N6-methyladenosine methylated mRNAs. *Elife* **6**, 1–28.

25 Alarcón CR, Goodarzi H, Lee H, Liu X, Tavazoie SFSSF & Tavazoie SFSSF (2015) HNRNPA2B1 Is a Mediator of m6A-Dependent Nuclear RNA Processing Events. *Cell* **162**, 1299–1308.

26 Huang H, Weng H, Sun W, Qin X, Shi H, Wu H, Zhao BS, Mesquita A, Liu C, Yuan CL, Hu YC, Hüttelmaier S, Skibbe JR, Su R, Deng X, Dong L, Sun M, Li C, Nachtergaele S,

Wang Y, Hu C, Ferchen K, Greis KD, Jiang X, Wei M, Qu L, Guan JL, He C, Yang J & Chen J (2018) Recognition of RNA N6-methyladenosine by IGF2BP proteins enhances mRNA stability and translation. *Nat. Cell Biol.* **20**, 285–295.

27 Wu R, Li A, Sun B, Sun J-GG, Zhang J, Zhang T, Chen Y, Xiao Y, Gao Y, Zhang Q, Ma J, Yang X, Liao Y, Lai W-YY, Qi X, Wang S, Shu Y, Wang H-LL, Wang F, Yang Y-GG & Yuan Z (2018) A novel m6A reader Prrc2a controls oligodendroglial specification and myelination. *Cell Res.* **29**, 23–41.

28 Bertero A, Brown S, Madrigal P, Osnato A, Ortmann D, Yiangou L, Kadiwala J, Hubner NC, De Los Mozos IR, Sadee C, Lenaerts A-SS, Nakanoh S, Grandy R, Farnell E, Ule J, Stunnenberg HG, Mendjan S, Vallier L, Sadée C, Lenaerts A-SS, Nakanoh S, Grandy R, Farnell E, Ule J, Stunnenberg HG, Mendjan S & Vallier L (2018) The SMAD2/3 interactome reveals that TGFβ controls m 6 A mRNA methylation in pluripotency. *Nature* **555**, 256–259.

29 Kwon J, Jo YJ, Namgoong S & Kim NH (2019) Functional roles of hnRNPA2/B1 regulated by METTL3 in mammalian embryonic development. *Sci. Rep.* **9**, 8640.

30 Geula S, Moshitch-Moshkovitz S, Dominissini D, Mansour AAF, Kol N, Salmon-Divon M, Hershkovitz V, Peer E, Mor N, Manor YS, Ben-Haim MS, Eyal E, Yunger S, Pinto Y, Jaitin DA, Viukov S, Rais Y, Krupalnik V, Chomsky E, Zerbib M, Maza I, Rechavi Y, Massarwa R, Hanna S, Amit I, Levanon EY, Amariglio N, Stern-Ginossar N, Novershtern N, Rechavi G & Hanna JH (2015) m6A mRNA methylation facilitates resolution of naïve pluripotency toward differentiation. *Science (80-.).* **347**, 1002–1006.

31 Batista PJ, Molinie B, Wang J, Qu K, Zhang J, Li L, Bouley DM, Lujan E, Haddad B, Daneshvar K, Carter AC, Flynn RA, Zhou C, Lim KS, Dedon P, Wernig M, Mullen AC, Xing Y, Giallourakis CC, Chang HY, Howard Y, Batista PJ, Molinie B, Wang J, Qu K, Zhang J, Li L, Bouley DM, Dedon P, Wernig M, Mullen AC, Xing Y, Giallourakis CC & Chang HY (2014) M^{6}A RNA modification controls cell fate transition in mammalian embryonic stem cells. *Cell Stem Cell* **15**, 707–719.

32 Wojtas MN, Pandey RR, Mendel M, Homolka D, Sachidanandam R & Pillai RS (2017) Regulation of m6A Transcripts by the 3'→5' RNA Helicase YTHDC2 Is Essential for a Successful Meiotic Program in the Mammalian Germline. *Mol. Cell* **68**, 374-387.e12.

33 Zhao BS, Wang X, Beadell A V., Lu Z, Shi H, Kuuspalu A, Ho RK & He C (2017) M6A-dependent maternal mRNA clearance facilitates zebrafish maternal-to-zygotic transition. *Nature* **542**, 475–478.

34 Kan L, Grozhik A V., Vedanayagam J, Patil DP, Pang N, Lim K-S, Huang Y-C, Joseph B, Lin C-J, Despic V, Guo J, Yan D, Kondo S, Deng W-M, Dedon PC, Jaffrey SR & Lai EC (2017) The m6A pathway facilitates sex determination in Drosophila. *Nat. Commun.* **8**, 15737.

35 Kasowitz SD, Ma J, Anderson SJ, Leu NA, Xu Y, Gregory BD, Schultz RM & Wang PJ (2018) Nuclear m 6 A reader YTHDC1 regulates alternative polyadenylation and splicing during mouse oocyte development. *PLoS Genet.* **14**, 1–28.

36 Ivanova I, Much C, Di Giacomo M, Azzi C, Morgan M, Moreira PN, Monahan J, Carrieri C, Enright AJ, O'Carroll D, Giacomo M Di, Azzi C, Morgan M, Moreira PN, Monahan J, Carrieri C, Enright AJ, O'carroll D, Di Giacomo M, Azzi C, Morgan M, Moreira PN, Monahan J, Carrieri C, Enright AJ & O'carroll D (2017) The RNA m 6 A Reader YTHDF2 Is Essential for the Post-transcriptional Regulation of the Maternal Transcriptome and Oocyte Competence. *Mol. Cell* **67**, 1059-1067.e4.

37 Lence T, Paolantoni C, Worpenberg L & Roignant JY (2019) Mechanistic insights into m 6 A RNA enzymes. *Biochim. Biophys. Acta - Gene Regul. Mech.* **1862**, 222–229.

38 Balacco DL & Soller M (2018) The m ^{6} A writer: Rise of a machine for growing tasks. *Biochemistry* **58**, acs.biochem.8b01166.

39 Lence T, Soller M & Roignant JY (2017) A fly view on the roles and mechanisms of the m6A mRNA modification and its players. *RNA Biol.* **14**, 1232–1240.

40 Robbens S, Rouzé P, Cock JM, Spring J, Worden AZ & Van De Peer Y (2008) The FTO gene, implicated in human obesity, is found only in vertebrates and marine algae. *J. Mol. Evol.* **66**, 80–84.

41 Zhang G, Huang H, Liu D, Cheng Y, Liu X, Zhang W, Yin R, Zhang D, Zhang P, Liu J, Li C, Liu B, Luo Y, Zhu Y, Zhang N, He S, He C, Wang H & Chen D (2015) N6-methyladenine DNA modification in Drosophila. *Cell* **161**, 893–906.

42 Greer EL, Blanco MA, Gu L, Sendinc E, Liu J, Aristizábal-Corrales D, Hsu CH, Aravind L, He C & Shi Y (2015) DNA methylation on N6-adenine in C. elegans. *Cell* **161**, 868–878.

43 Riviere G, He Y, Tecchio S, Crowell E, Sourdaine P, Guo X & Favrel P (2017) Dynamics of DNA methylomes underlie oyster development. *PLOS Genet.* **13**, 1–16.

44 Sussarellu R, Lebreton M, Rouxel J, Akcha F, Riviere G & Rivière G (2018) Copper induces expression and methylation changes of early development genes in Crassostrea gigas embryos. *Aquat. Toxicol.* **196**, submitted.

45 Rondon R, Grunau C, Fallet M, Charlemagne N, Sussarellu R, Chaparro C, Montagnani C, Mitta G, Bachère E, Akcha F & Cosseau C (2017) Effects of a parental exposure to diuron on Pacific oyster spat methylome. *Environ. Epigenetics* **3**, 1–13.

46 Riviere G, Wu G-CC, Fellous A, Goux D, Sourdaine P & Favrel P (2013) DNA Methylation Is Crucial for the Early Development in the Oyster C . gigas. *Mar. Biotechnol.* **15**, 1–15.

47 Saint-Carlier E & Riviere G (2015) Regulation of Hox orthologues in the oyster Crassostrea gigas evidences a functional role for promoter DNA methylation in an invertebrate. *FEBS Lett.* **589**, 1459–1466.

48 Fellous A, Favrel P & Riviere G (2015) Temperature influences histone methylation and mRNA expression of the Jmj-C histone-demethylase orthologues during the early development of the oyster Crassostrea gigas. *Mar. Genomics* **19**, 23–30.

49 Fellous A, Favrel P, Guo X & Riviere G (2014) The Jumonji gene family in Crassostrea gigas suggests evolutionary conservation of Jmj-C histone demethylases orthologues in the oyster gametogenesis and development. *Gene* **538**, 164–175.

50 Fellous A, Le Franc L, Jouaux A, Goux D, Favrel P & Rivière G (2019) Histone Methylation Participates in Gene Expression Control during the Early Development of the Pacific Oyster Crassostrea gigas. *Genes (Basel).* **10**, 695.

51 Zhou J, Wan J, Gao X, Zhang X, Jaffrey SR & Qian S-B (2015) Dynamic m6A mRNA methylation directs translational control of heat shock response. *Nature* **526**, 591–594.

52 Lu Z, Ma Y, Li Q, Liu E, Jin M, Zhang L & Wei C (2019) The role of N6-methyladenosine RNA methylation in the heat stress response of sheep (Ovis aries). *Cell Stress Chaperones* **24**, 333–342.

53 Xiang Y, Laurent B, Hsu C, Nachtergaele S, Lu Z, Sheng W, Xu C, Chen H, Ouyang J,

Wang S, Ling D, Hsu P, Zou L, Jambhekar A & He C (2017) m6A RNA methylation regulates the UV-induced DNA damage response. *Nature* **543**, 573–576.

54 Cayir A, Barrow TM, Guo L & Byun HM (2019) Exposure to environmental toxicants reduces global N6-methyladenosine RNA methylation and alters expression of RNA methylation modulator genes. *Environ. Res.* **175**, 228–234.

55 Liu J, Li K, Cai J, Zhang M, Zhang X, Xiong X, Meng H, Xu X, Huang Z, Fan J & Yi C (2019) Landscape and Regulation of M ^{6}A and M ^{6}Am Methylome Across Human and Mouse Tissues. *SSRN Electron. J.*, 1–56.

56 Ren W, Lu J, Huang M, Gao L, Li D, Greg Wang G & Song J (2019) Structure and regulation of ZCCHC4 in m6A-methylation of 28S rRNA. *Nat. Commun.* **10**, 5042.

57 Bokar JA, Shambaugh ME, Polayes D, Matera AG & Rottman FM (1997) Purification and cDNA cloning of the AdoMet-binding subunit of the human mRNA (N6-adenosine)-methyltransferase. *RNA* **3**, 1233–1247.

58 Theler D, Dominguez C, Blatter M, Boudet J & Allain FHT (2014) Solution structure of the YTH domain in complex with N6-methyladenosine RNA: A reader of methylated RNA. *Nucleic Acids Res.* **42**, 13911–13919.

59 Shima H, Matsumoto M, Ishigami Y, Ebina M, Muto A, Sato Y, Kumagai S, Ochiai K, Suzuki T & Igarashi K (2017) S-Adenosylmethionine Synthesis Is Regulated by Selective N6-Adenosine Methylation and mRNA Degradation Involving METTL16 and YTHDC1. *Cell Rep.* **21**, 3354–3363.

60 Yurchenko O V., Skiteva OI, Voronezhskaya EE & Dyachuk VA (2018) Nervous system development in the Pacific oyster , Crassostrea gigas (Mollusca : Bivalvia). *Front. Zool.* **15**, 1–21.

61 Ratnaparkhi A (2013) Signaling by folded gastrulation is modulated by mitochondrial fusion and fission. *J. Cell Sci.* **126**, 5369–5376.

62 Ren L, Zhang C, Tao L, Hao J, Tan K, Miao K, Yu Y, Sui L, Wu Z, Tian J & An L (2017) High-resolution profiles of gene expression and DNA methylation highlight mitochondrial modifications during early embryonic development. *J. Reprod. Dev.* **63**, 247–261.

63 Prudent J, Popgeorgiev N, Bonneau B, Thibaut J, Gadet R, Lopez J, Gonzalo P, Rimokh R, Manon S, Houart C, Herbomel P, Aouacheria A & Gillet G (2013) Bcl-wav and the mitochondrial calcium uniporter drive gastrula morphogenesis in zebrafish. *Nat. Commun.* **4**.

64 Dumollard R, Duchen M & Carroll J (2007) The Role of Mitochondrial Function in the Oocyte and Embryo. *Curr. Top. Dev. Biol.* **77**, 21–49.

65 Huang H, Weng H, Zhou K, Wu T, Zhao BS, Sun MM, Chen Z, Deng X, Xiao G, Auer F, Klemm L, Wu H, Zuo Z, Qin X, Dong Y, Zhou Y, Qin H, Tao S, Du J, Liu J, Lu Z, Yin H, Mesquita A, Yuan CL, Hu Y-CC, Sun W, Su R, Dong L, Shen C, Li C, Qing Y, Jiang X, Wu X, Sun MM, Guan J-LL, Qu L, Wei M, Müschen M, Huang G, He C, Yang J & Chen J (2019) Histone H3 trimethylation at lysine 36 guides m6A RNA modification co-transcriptionally. *Nature* **567**, 414–419.

66 Wang Y, Li Y, Yue M, Wang J, Kumar S, Wechsler-Reya RJ, Zhang Z, Ogawa Y, Kellis M, Duester G & Zhao JC (2018) N 6-methyladenosine RNA modification regulates embryonic neural stem cell self-renewal through histone modifications. *Nat. Neurosci.* **21**, 195–206.

67 Petton B, Pernet F, Robert R & Boudry P (2013) Temperature influence on pathogen transmission and subsequent mortalities in juvenile pacific oysters Crassostrea gigas. *Aquac. Environ. Interact.* **3**, 257–273.

68 Riviere G, Fellous A, Franco A, Bernay B & Favrel P (2011) A crucial role in fertility for the oyster angiotensin-converting enzyme orthologue CgACE. *PLoS One* **6**.

69 EMA (2011) *Guideline on bioanalytical method validation. EMEA/CHMP/EWP/192217/2009*.

70 Riviere G, Klopp C, Ibouniyamine N, Huvet A, Boudry P & Favrel P (2015) GigaTON: An extensive publicly searchable database providing a new reference transcriptome in the pacific oyster Crassostrea gigas. *BMC Bioinformatics* **16**, 1–12.

71 Zhang G, Fang X, Guo X, Li L, Luo R, Xu F, Yang P, Zhang L, Wu F, Chen Y, Wang J, Peng C, Meng J, Yang L, Liu J, Wen B, Zhang N & Huang Z (2012) The oyster genome reveals stress adaptation and complexity of shell formation. *Nature* **490**, 49–54.

72 Li B, Ruotti V, Stewart RM, Thomson JA & Dewey CN (2010) RNA-Seq gene expression estimation with read mapping uncertainty. *Bioinformatics* **26**, 493–500.

73 Qi ST, Ma JY, Wang ZB, Guo L, Hou Y & Sun QY (2016) N6 -methyladenosine sequencing highlights the involvement of mRNA methylation in oocyte meiotic maturation and embryo development by regulating translation in xenopus laevis. *J. Biol. Chem.* **291**, 23020–23026.

74 Altschul SF, Madden TL, Schäffer AA, Zhang J, Zhang Z, Miller W & Lipman DJ (1997) Gapped BLAST and PSI-BLAST: a new generation of protein database search programs. *Nucleic Acids Res.* **25**, 3389–3402.

75 Cock PJA, Chilton JM, Grüning B, Johnson JE & Soranzo N (2015) NCBI BLAST+ integrated into Galaxy. *Gigascience* **4**, 0–6.

76 Camacho C, Coulouris G, Avagyan V, Ma N, Papadopoulos J, Bealer K & Madden TL (2009) BLAST+: Architecture and applications. *BMC Bioinformatics* **10**, 1–9.

77 Young MD, Wakefield MJ, Smyth GK & Oshlack A (2010) Gene ontology analysis for RNA-seq: accounting for selection bias. *Genome Biol.* **11**, R14.

78 Supek F, Bošnjak M, Škunca N & Šmuc T (2011) Revigo summarizes and visualizes long lists of gene ontology terms. *PLoS One* **6**.

79 Larsson J (2019) eulerr: Area-Proportional Euler and Venn Diagrams with Ellipses. .

80 Gu Z, Eils R & Schlesner M (2016) Complex heatmaps reveal patterns and correlations in multidimensional genomic data. *Bioinformatics* **32**, 2847–2849.

Figure legends

Figure 1: m^{6}A levels across oyster development.

A. m^{6}A level quantified by LC-MS/MS in *Crassostrea gigas* embryo-larval stages pooled from oocytes to D-larvae (n= 3) is compared to the m^{6}A level in *Homo sapiens* and *Drosophila melanogaster*; **B.** Dot blot quantification of m^{6}A in total RNA throughout oyster development (n=3); **C.** Dot blot quantification of m^{6}A in polyA+ RNAs throughout oyster development (n=3) Kruskal-Wallis test, $\alpha < 0{,}05$. E: Egg, F E: fertilized egg, 2/8C: two to eight cell embryos, M: Morula, B: Blastula, G: Gastrula, T: Trochophore, D: D larvae. Chemiluminescence (B) and fluorescence (C) are measured as a ratio between dot intensity of development stages and their respective controls for each amount of RNA (120ng, 60ng and 30ng).

Figure 2: The putative conserved m^{6}A machinery in *Crassostrea gigas*.

Domain architecture of actors of the m^{6}A machinery identified by *in silico* analyses in the oyster compared to the fruit fly and human, **A.** Writer proteins; **B.** Eraser protein; **C.** Reader proteins. Putative domains involved in m^{6}A processes are coloured (writers, green; eraser, red; readers, blue). Other domains identified but not involved in m^{6}A processes are indicated in grey. Only one isoform is represented for each protein and each species for clarity (see supplementary figure S2 for other isoforms).

Figure 3: Gene expression of the putative m^{6}A machinery throughout oyster development

Expression levels of writers (**A**), eraser (**B**) and readers (**C**) identified by *in silico* analysis at each development stage were inferred from the GigaTON database. Expression levels are given in Transcripts Per kilobases per Million Reads (TPM) as the mean of the GigaTON values according to the table S2. E: Egg, 2/8C: two to eight cell, M: Morula, B: Blastula, G: Gastrula, T: Trochophore, D: D larvae, S: Spat, J: Juvenile.

Figure 4: Characterization of m^{6}A-RNA binding proteins in oyster development.

A. Venn diagrams representation of proteins bound to the A- and/or m^{6}A- oligos in nuclear and cytosolic fractions of oyster embryo-larval stages. The number of proteins identified is indicated. Some actors characterized in this study are highlighted: eIF3, YTHC1, hnRNPA2B1 and IGF2BP. **B.** Heatmap of gene expression levels of the proteins that bind specifically to the m^{6}A-oligo throughout oyster development. The expression level is normalized regarding the maximum value for each gene according to the GigaTON database. **C.** GO term distribution among the three expression clusters in B. **D**. Examples of GO term enrichment within the expression clusters of the m^{6}A-bound proteins. The –log10(p-value) associated to each term is given. E: Egg, 2/8C: two to eight cells, M: Morula, B: Blastula, G: Gastrula, T: Trochophore, D: D larvae, S: Spat, J: Juvenile.

Supporting information:

Data S1: Complete list of *in silico* identified putative m^{6}A machinery proteins and their respective BLAST results

Data S2: Identified proteins by RNA pull down coupled with mass spectrometry with m^{6}A or A-oligo, in nuclear or cytosolic protein extracts

Data S3: Complete list of GO terms of clustered genes of m^{6}A interacting proteins (p-value<0,05)

Table S1: Transitions used for each compound. A: first transition, B: second transition

Table S2: Table of correspondence between development stages in our study, and the GigaTON database.

A functional m^{6}A-RNA methylation pathway in the oyster *Crassostrea gigas* assumes epitranscriptomic regulation of lophotrochozoan development

Authors

Lorane LE FRANC[1], Benoit BERNAY[2], Bruno PETTON[3], Marc SINCE[4], Pascal FAVREL[1] and Guillaume RIVIERE[1]

Addresses

[1]Normandie Univ, UNICAEN, CNRS, BOREA, 14000 Caen, France.

Laboratoire Biologie des organismes et Ecosystèmes aquatiques (BOREA), Muséum d'Histoire naturelle, Sorbonne Université, Université de Caen Normandie, Université des Antilles, CNRS, IRD, Esplanade de la paix, 14032 Caen, France.

[2]Normandie Univ, UNICAEN, SF ICORE, PROTEOGEN core facility, 14000 Caen, France

[3]Ifremer, Laboratoire des Sciences de l'Environnement Marin, UMR 6539 CNRS/UBO/IRD/Ifremer, Centre Bretagne, 29280, Plouzané, France

[4] Normandie Univ, UNICAEN, Comprehensive Cancer Center F. Baclesse, SF ICORE, PRISMM core facility, 14000 Caen, France.

Corresponding author

Guillaume Rivière (0033231565113 ; guillaume.riviere@unicaen.fr) , Normandie Univ, UNICAEN, CNRS, BOREA, 14000 Caen, France (https://borea.mnhn.fr/). Tel :

Running title

m^{6}A-RNA methylation pathway in oyster development

Abbreviations

N^6-methyladenosine (m^{6}A), Methyltransferase like (METTL), Wilms' tumor 1-associated protein (WTAP), RNA-binding motif 15 (RBM15), Ring finger E3 ubiquitin ligase (HAKAI), Zinc finger CCCH-type containing 13 (ZC3H13), AlkB homologue 5 (ALKBH5), Fat mass and obesity associated protein (FTO), YTH domain family protein (YTHDF), YTH domain containing protein (YTHDC), Heterogeneous nuclear ribonucleoproreins A2 B1 (HNRNPA2B1), Proline rich coiled-coil 2a (Prrc2a), Eukaryotic initiation factor 3 (eIF3), Sterile sea water (SSW), Oocytes (E), Fertilized oocytes (F E), Two to eight cell embryos (2/8 C), Hours post fertilization (hpf), Morula (M), Blastula (B), Gastrula (G), D larvae (D), solid-phase reversible immobilization (SPRI), TPM (Transcripts Per Million), Gene ontology (GO), oyster m^{6}A-interacting protein (Cg-m^{6}A-BPs), S-adenosyl-methionine (SAM), maternal-to-zygotic transition (MZT), acetonitrile (ACN)

Keywords

RNA, methylation, epitranscriptomics, oyster, development.

Conflicts of interest

The authors declare they have no competing conflict of interest

Abstract

N^6-methyladenosine (m^6A) is a prevalent epitranscriptomic mark in eukaryotic RNA, with crucial roles for mammalian and ecdysozoan development. Indeed, m^6A-RNA and the related protein machinery are important for splicing, translation, maternal-to-zygotic transition and cell differentiation. However, to date, the presence of an m^6A-RNA pathway remains unknown in more distant animals, questioning the evolution and significance of the epitranscriptomic regulation. Therefore, we investigated the m^6A-RNA pathway in the oyster *Crassostrea gigas*, a lophotrochozoan model whose development was demonstrated under strong epigenetic influence.

Using mass spectrometry and dot blot assays, we demonstrated that m^6A-RNA is actually present in the oyster and displays variations throughout early oyster development, with the lowest levels at the end of cleavage. In parallel, by *in silico* analyses, we were able to characterize at the molecular level a complete and conserved putative m^6A-machinery. The expression levels of the identified putative m^6A writers, erasers and readers were strongly regulated across oyster development. Finally, RNA pull-down coupled to LC-MS/MS allowed us to prove the actual presence of readers able to bind m^6A-RNA and exhibiting specific developmental patterns.

Altogether, our results demonstrate the conservation of a complete m^6A-RNA pathway in the oyster and strongly suggest its implication in early developmental processes including MZT. This first demonstration and characterization of an epitranscriptomic regulation in a lophotrochozoan model, potentially involved in the embryogenesis, brings new insights into our understanding of developmental epigenetic processes and their evolution.

Introduction

The *N*^{6}-methyladenosine (m^{6}A) is the prevalent chemical RNA modification in all eukaryotic coding and non-coding RNAs [1]. Messenger RNAs are the most heavily m^{6}A methylated RNAs, with m^{6}A bases lying mostly in their 3' UTRs, at the vicinity of their stop codon [2–4] and also in 5' UTRs and long internal exons [4,5]. *N*^{6}-methylation of RNA adenosines is responsible for RNA processing and, like DNA methylation or histone modifications, contributes to the regulation of gene expression without changing the DNA or mRNA sequence. Therefore m^{6}A constitutes a new layer of post-transcriptional gene regulation, which is emerging or has been proven critical in various biological processes, and referred to as epitranscriptomic [2].

The dynamics and biological outcomes of m^{6}A levels are the results of the activity of a complex protein machinery comprising writers, erasers and readers. The addition of a methyl group to the 6th nitrogen of RNA adenosines is catalysed by m^{6}A writers with distinct properties. Methyltransferase like 16 (METTL16) is a 'stand-alone' class I methyltransferase that recognizes the UACA*GAGAA consensus sequence (with * indicating the target adenosine) [6]. By contrast, METTL3 transfers methyl groups to adenosines within the RRA*CH motif [2,3,7]. METTL3 is only active within a tripartite 'core complex' [8] comprising METTL3, METTL14 which enhances the methyltransferase activity supported by the MTA-70 domain of METTL3 [9,10] and the regulator protein Wilms' tumor 1-associated protein (WTAP) [4,9,11]. This core complex can interact with Virilizer-like (or KIAA1429) [12], ring finger E3 ubiquitin

ligase (HAKAI) [12,13], zinc finger CCCH-type containing 13 (ZC3H13) [12,14], RNA-binding motif 15 (RBM15) and RBM15B [7,15] which are suspected to intervene in the core complex activity and target specificity. The demethylation of adenosines has been demonstrated to be an active process catalysed by eraser enzymes belonging to the Fe(II)/2-oxoglutarate dioxygenase family: AlkB homologue 5 (ALKBH5) [16,17] and the fat mass and obesity associated protein (FTO) [17,18].

A growing number of reader proteins which recognize the m^{6}A-RNA mark is being described. They may be divided into two classes depending on the presence of a YT521 B Homology (YTH) domain in their primary sequence. The YTH protein family includes YTH domain family protein 1-3 (YTHDF1-3) and YTH domain containing protein 2 (YTHDC2), which are cytosolic m^{6}A readers involved in m^{6}A-RNA stability and translation [19–22]. The fifth YTH member is YTHDC1, which is present in the nucleus and controls splicing [23] and nuclear export [24] of m^{6}A-RNA. The second class of readers comprises proteins without YTH domain which are involved in several molecular mechanisms. For example, the heterogeneous nuclear ribonucleoprotein A2 B1 (HNRNPA2B1) is important for miRNA processing [25]. Insulin-like growth factor 2 mRNA binding protein 1-3 (IGF2BP 1-3) [26] and proline-rich coiled-coil 2a (Prrc2a) [27] participate in RNA stability while eukaryotic initiation factor 3 (eIF3) guides cap-independent translation [5].

The m^{6}A epitranscriptomes underlie important biological functions, most of which being related to developmental processes, including the control of cell differentiation [27–32], maternal to zygotic transition (MZT) [33], sex determination [7,34] and gametogenesis [16,21,35,36]. Such

critical epitransriptomic outcomes are conserved in the animal evolution and were characterized in both vertebrates and ecdysozoans, i.e. mammals and drosophila.

However, such conserved biological significance originates in diverse epitranscriptomic mechanisms. Indeed, not all ecdysozoans bear a complete m^{6}A-RNA machinery, such as *C. elegans* whose genome is devoid of the related protein machinery with the exception of a putative orthologue of METTL16 [37,38]. In addition, no m^{6}A eraser has been described to date in non-vertebrate models, and especially ecdysozoans such as the drosophila or *C. elegans* [38–40], where it cannot be excluded that m^{6}A-RNA methylation could be removed by the activity of characterised 6mA-DNA demethylases [41,42]. This situation may illustrate a growing complexity of epitranscriptomic mechanisms during the animal phylogeny and raises fundamental questions about its evolution and its presence in organisms distant from mammals and ecdysozoans. However, to date, no data about a possible epitranscriptomic regulation is available to our knowledge in lophotrochozoans, the understudied sister group of ecdysozoans within protostomes, although representing an important range of metazoan biodiversity.

The Pacific oyster *Crassostrea gigas* (i.e. *Magallana gigas*) is a bivalve mollusc whose great ecological an economical significance allowed its emergence as a model species within lophotrochozoan organisms. As such, an important amount of genetic, transcriptomic and epigenetic data have been generated in this model. Interestingly, the embryolarval development of *C. gigas* is described to be under the strong epigenetic influence of DNA methylation [43–47] and histone marks [48–50]. Besides, oyster development occurs exposed to external environmental conditions, and in other models the m^{6}A methylation of RNA and/or

the expression of its machinery can be induced by heat stress, UV exposure or endocrine disruptors [5,51–54], questioning the presence of an m^{6}A pathway in *C. gigas* and its significance in oyster early development.

To investigate this, we measured m^{6}A levels in RNA across the entire embryolarval life of the oyster using mass spectrometry and dot-blot. We also searched the available *in silico* resources for putative conserved m^{6}A-related proteins in *C. gigas* genomic data as well as their cognate expression kinetics using RNAseq assembly analyses. We also performed RNA-pulldown with a synthetic m^{6}A-RNA oligonucleotide coupled to liquid chromatography and mass spectrometry (LC-MS/MS) to characterize potential oyster m^{6}A-binding proteins. To our knowledge, this study is the first report unravelling epitranscriptomic mechanisms outside vertebrate and ecdyzosoan animal models.

Results:

m^{6}A is present in oyster RNA, differentially affects distinct RNA populations and displays variations during embryonic life.

Mass spectrometry measurements revealed that m^{6}A is present in oyster RNA, with global m^{6}A/A levels of ca. 0.3%, a value comparable to what has been found in the human and the fruit fly (Figure 1A). Immunoblot assays indicate that total and polyA+ RNA present variable amounts of m^{6}A during oyster development and that these variations display distinct profiles suggesting specific methylation patterns between RNA populations. Indeed, *N*^{6}A-methylation in total RNA is the highest in the early stages (oocytes and fertilized oocytes) then gradually

decreases until the morula stage before gradually increasing again up to the trochophore stage when it recovers its maximum (Figure 1B). In contrast, m^{6}A levels in polyA+ RNA are hardly detected in early stages but display a peak in the gastrula and trochophore stages (Figure 1C).

m^{6}A machinery is conserved at the molecular level in the oyster.

In silico analyses led to the identification of oyster sequences encoding putative orthologues of m^{6}A writers, erasers and readers that are present in the human and/or in the human and the fruit fly.

All the eight m^{6}A-RNA writers characterized in the human and/or drosophila at the time of the study, namely METTL3, METTL14, WTAP, Virilizer-like, HAKAI, ZC3H13, RBM15/15B and METTL16, were present in the oyster at the gene level. The encoded protein primary sequences all display the specific domains required for enzymatic activity and/or binding. They include MT-A70 and AdoMetMtases SF domains for METTL3, METTL14 and METTL16, respectively, that bear the methyltransferase activity. Oyster WTAP and Virilizer-like orthologues exhibit WTAP and VIR_N domains, respectively, that are required in their human counterparts to bind and activate the catalytic subunit of the m^{6}A-RNA methyltransferase complex. Oyster Hakai and RBM15/15B present RHHL, RHF-Zn-BS and specific RRM domains, respectively, similar to human and fruit fly orthologues. Besides, the oyster ZC3H13 bears the Rho SF domain present in the human, but not in the fruit fly orthologue (Figure 2A). *C. gigas* also presents a putative m^{6}A-RNA eraser, ALKBH5, which is present in the human but has not been characterized in drosophila. The oyster ALKBH5 exhibits a 2OG-FeII_Oxy domain suggestive of a presumably conserved catalytic functionality through fe2+-dependent

oxoglutarate oxidation. Of note, no orthologue of the human FTO eraser could be identified in the oyster genomic or transcriptomic databases available to date (Figure 2B).

Many m^{6}A reader orthologues have also been found in the oyster, including proteins containing a YTH domain, such as YTHDF, YTHDC1 and YTHDC2. An oyster Prrc2a-like protein produces homology with the human Prrc2a, especially within the m^{6}A-binding GRE-rich domain. Oyster readers also include a heterogeneous nuclear ribonucleoprotein-coding gene, hnRNPA2B1 with greater sequence similarity with the drosophila counterpart than with the human orthologue. Similarly, the IGF2BP-coding sequence has also been found in *C. gigas* (Figure 2C). Five oyster sequences display homologies with eIF3a which is able to bind m^{6}A-RNA [5] but it was not possible to discriminate whether a unique oyster predicted protein was an eIF3a orthologue.

Overall, these results indicate the conservation of a complete m^{6}A-RNA machinery in the oyster. The complete list of the identified genes encoding the conserved m^{6}A machinery actors and their isoforms, as well as the related information is given in the supplementary data (Data S1).

Oyster putative m^{6}A actors display expression level variations across development.

RNAseq data analyses showed that all the oyster m^{6}A-related genes were expressed during the early life (Figure 3). Their expression level displayed gene-specific profiles, most of them being variable throughout oyster development.

The expression of writers belonging to the core methylation complex is weak overall. METTL3 and WTAP share similar profiles with little expression increasing up to the gastrulation and

remaining stable afterwards. In contrast METTL14 displays a weak expression level across the embryo larval life. The expression profile of Virilizer-like resembles WTAP, while HAKAI, RBM15/15B and METTL16 seem to have mRNA levels which decrease after cleavage, whereas those of ZC3H13 transcript variants seem to drop at the D larva stage. Interestingly, METTL16 mRNA levels display an opposite developmental profile when compared to METTL3 expression; with the highest values during cleavage which decrease later on (Figure 3A).

ALKBH5 transcripts are weakly represented within oyster early embryos and the higher TPM values are found in gastrulas. However, maximum levels are observed after metamorphosis in juveniles (Figure 3B).

Regarding m^{6}A putative readers, the expression of YTH family genes during development showed different patterns. In fact, YTHDF is the most represented YTH-domain bearing actor and YTHDF TPM values are ca. 5-fold higher than all the other oyster YTH readers. YTHDF is strongly expressed at the beginning of development until a peak at the morula stage. Prrc2a is the most represented reader at the mRNA level in oyster embryos, and the sum of the TPM of the two Prrc2a oyster isoforms are at most ca. 20-fold higher than those of YTH family. However, Prrc2a and YTHDF transcript content profiles are similar across oyster development, and also remind of the IGF2BP mRNA levels.

By contrast, the two isoforms of YTHDC1 identified by *in silico* analysis, YTHDC1.1 and YTHDC1.2, display similar patterns together with YTHDC2, with a maximum representation in gastrulas. The expression of hnRNPA2B1 isoforms has likewise patterns except for a marked drop at the D larvae stage (Figure 3 C).

Oyster orthologues of m^{6}A-RNA interacting proteins bind m^{6}A RNA *in vitro*.

To determine whether oyster proteins can bind m^{6}A-RNA, we performed RNA-pulldown of cytoplasmic and nuclear embryonic cell extracts using a methylated versus a non-methylated oligonucleotide, followed by LC/MS-MS characterisation and identification of the captured proteins with the Mascot software.

In nuclear extracts, we detected 591 proteins able to bind both the methylated and unmethylated oligos. We identified 43 proteins specific to unmethylated RNA while 131 proteins specifically bind the m^{6}A-methylated oligo. In cytosolic extracts, there were respectively 646, 436 and 36 of such proteins, respectively. Regardless of the methylation status, more proteins in the cytoplasmic extracts can bind to the RNA oligonucleotides than in the nuclear extracts (1118 proteins vs. 765, respectively). However, more nuclear proteins are found exclusively bound to the m^{6}A-containing oligo than cytoplasmic proteins (131 vs. 36, i.e. 17 % vs. 3 %, respectively). In addition, many nuclear and cytoplasmic proteins can bind both the methylated and the non-methylated oligo (591 vs. 646, i.e. 77 % vs. 58 %). An important number of proteins in the cytoplasmic extract were found exclusively bound to the non-methylated oligo, whereas only a limited number of nuclear proteins display such a specificity (436 vs. 43, i.e. 39 % vs. 6 %). Among the 167 m^{6}A-specific proteins in oyster extracts, only 5 were found in both the nuclear and cytoplasmic extracts. These results show that oyster proteins can directly or indirectly bind m^{6}A-RNA, and suggest an important compartmentalization of m^{6}A-related processes.

Among the identified proteins in this assay, four of the putative oyster m^{6}A readers are found, YTHDC1, hnRNPA2B1, IGF2BP and eIF3. In the nuclear extracts YTHDC1 is uncovered as

m^{6}A-specific whereas hnRNPA2B1 and IGF2BP were present complexed with both the m^{6}A- and A-oligos. In the cytoplasmic extracts, YTHDC1 and eIF3a are m^{6}A-specific while hnRNPA2B1, IGF2BP were pulled down by both methylated and unmethylated oligos (Figure 4A).

These results demonstrate that some proteins in the oyster can specifically bind m^{6}A-RNA and that the putative m^{6}A reader orthologues in the oyster are conserved at the protein level and are able to interact with m^{6}A-RNA.

The m^{6}A-interacting protein-coding genes display clustered expression regulation and functional annotation during oyster development.

The mRNA expression level of the genes encoding the 162 oyster m^{6}A-interacting protein (Cg-m^{6}A-BPs) was examined using RNAseq databases. Most of them display a specific and regulated expression level across oyster developmental stages. However, three main expression clusters could be distinguished according to their developmental mRNA expression level profile. Cluster 1 includes genes that show high expression at the beginning of the embryo life (i.e. cleavage) and strongly decrease after gastrulation; the second cluster contains weakly expressed genes except in the latest examined larval phases, after gastrulation (i.e. Trochophore and D Larvae); cluster 3 groups genes that show an expression peak during gastrulation (Figure 4B).

The Gene Ontology annotation of the Cg-m^{6}A-BP genes reveal that the distinct clusters are related to distinct functional pathways as indicated by the little - if any - common GO terms between them (Figure 4C). However, the functional pathways of all three gene clusters point

out to their implication in translation and its regulation, although the terms enriched in each cluster illustrate different aspects of translation, such as translation initiation (cluster 1), splicing and nuclear export (cluster 2) and ribosomal and mitochondrial processes (cluster 3) respectively (Figure 4D).

Discussion

This work demonstrates that m^{6}A-RNA is present and variable during the embryo-larval life of the oyster, and that *C. gigas* exhibits putative conserved and functional m^{6}A-RNA writers, eraser and readers. The dynamics of such mark and of its actors strongly suggest a biological significance of the epitranscriptomic pathway in the control of development of a lophotrochozoan species, which has, to date, never been demonstrated to our knowledge.

m^{6}A-RNA levels vary across oyster development.

Using mass spectrometry and immunological measurements, we showed that oyster RNA is m^{6}A-methylated. The global proportion of *N*^{6}-methyladenosine in RNA in the developing oyster (0.28 %) is similar to those observed elsewhere in the animal kingdom, such as in the fruit fly (0.24 %) [34] or the human (0.11- 0.23 %) [55] (Figure 1A), despite those values are difficult to compare because they were not measured within the same developmental phase (adult flies and human cell lines vs. oyster embryos). However, the comparable magnitude of m^{6}A-RNA amounts between taxa, in contrast to DNA methylation [46], may indicate conserved biological significance of epitranscriptomic processes between groups. The amount of m^{6}A in total RNA displays a striking decrease during cleavage and then recovers its maximum levels at the end of the gastrulation (Figure 1B). Therefore, the m^{6}A decrease in total RNA during cleavage, i.e.

before the transcription of the zygotic genome starts, reflects a degradation of maternal m^{6}A-RNAs or their demethylation. However, all RNA populations do not exhibit the same pattern, indeed polyA+ RNAs are m^{6}A methylated only after cleavage. The extent of polyadenylation of oyster maternal messenger RNAs accumulating during vitellogenesis is unknown. Therefore, which maternal RNA population(s) is methylated in oyster oocytes is unclear. Nevertheless, the observation that m^{6}A-RNA levels are variable and affecting distinct RNA populations across embryonic stages strongly favours an important biological significance of m^{6}A-RNA in oyster development. We hypothesize that oyster maternal messenger RNAs are poorly polyadenylated, and that m^{6}A, aside polyadenylation, might play a role in the stability of quiescent maternal mRNAs. Alternatively, other maternal RNA populations such as snRNA, miRNA, rRNA or lncRNA might be methylated [6,15,25,56], which become demethylated or degraded up to the morula stage. The later increase in m^{6}A RNA after cleavage could therefore be the result of the methylation of the increasingly transcribed RNAs from the blastula stage, including polyadenylated mRNAs.

The m^{6}A-RNA machinery is conserved in the oyster and regulated during development. The important regulation of m^{6}A levels during oyster development assumes the presence of a related protein machinery. We identified *in silico* cDNA sequences encoding conserved putatively functional orthologues of m^{6}A-RNA writers, eraser and readers in the oyster, with great confidence (homologies ranging from ca. 30 to 65 % with their human counterpart, see Data S1). The writers include all the members of the methylation complex (METTL3, METTL14, WTAP, Virilizer-like, Hakai, ZC3H13, RBM15/15B) identified to date in the human and the fruit fly [7,11,12,14,15,57]. We also identified an orthologue of the stand-alone METTL16 m^{6}A

methyltransferase. Each orthologue bears the conserved domain(s) demonstrated to be implicated in the catalytic and/or binding activity of their cognate counterpart in other species, such as the MT-A70 domain which transfers methyl groups from the S-adenosyl-methionine (SAM) to the N^6 nitrogen of RNA adenines [57]. Of the two proteins that can erase RNA methylation, only ALKBH5, which is important for mouse spermatogenesis [16], was identified at the cDNA level in the oyster. Indeed, no *C. gigas* sequence displayed significant homology with the mammalian FTO protein, whose functional significance remains controversial [17]. Most the characterized m^{6}A-RNA readers are also present at the molecular level in the oyster and are putatively able to bind m^{6}A regarding their primary sequence, such as the YTHDC and YTHDF family members [19,21,23,58], Prrc2A [27], HnRNPA2B1 [25] and IGF2BP [26]. Of note, some of these readers have not been characterized to date in *D. melanogaster* but display strong homologies between humans and oysters. In mammals, eIF3a has important functional outcomes in cap-independent translational stress response [5]. However, it was not possible to ascribe a single oyster sequence as a unique eIF3a orthologue (Data S1), although its presence was demonstrated by RNA pull down (see below) (see Data S2). Altogether, *in silico* results show the conservation of a complete m^{6}A-RNA machinery in the oyster. To date to our knowledge, this is the first demonstration in a lophotrochozoan organism of an epitranscriptomic pathway. Its presence suggests its ancestral origin, and questions its biological significance in oyster development.

To investigate this, we analysed the expression level of the m^{6}A machinery genes using RNA-seq data. Our results indicate that the core methylation complex (METTL3, METTL14 and WTAP) would not be active during cleavage because of the absence of METTL3 and little

WTAP expression. METTL16 catalyses the downregulation of SAM methyl donor availability in mammals [59]. If METTL16 function is conserved in the oyster as suggested by the high sequence homology, the peak in METTL16 expression, together with the weak expression of the core complex in 2/8 cell embryos is consistent with an absence of m^{6}A-RNA up to the blastula stage. Then, the core complex would likely be active as soon as the end of cleavage (i.e. since the blastula stage), in line with the increase in m^{6}A levels observed at the same time. The correlation between the increasing METTL3 expression and m^{6}A-RNA levels after cleavage strongly favours the conservation of the methyltransferase activity of the oyster MT-A70 domain. Interpreting the regulation of the m^{6}A activity by the other methyltransferase complex members (i.e. Virilizer-like, HAKAI, ZC3H13 and RBM15/15B) is difficult because how - or even if - oyster orthologues act within the complex is not known. Nevertheless, their specific expression profiles may reflect their implication in the regulation of distinct biological contexts. There might be little functional significance of active m^{6}A-RNA erasure during oyster development, consistent with the normal embryonic phenotype of ALKBH5 knockdown mice [16]. Overall, the m^{6}A readers display distinct developmental expression patterns. While YTHDF and Prrc2a peak during cleavage, YTHDC1, YTHDC2, IGF2BP and hnRNPA2B1 mRNA levels gradually increase up to the gastrulation and remain mostly highly expressed afterwards (except for hnRNPA2B1 and IGF2BP). These profiles evoke the mediation of distinct biological functions depending on the reader and the developmental phases. Therefore, we hypothesized that YTHDF and Prrc2a might participate in the blastulean transition in the oyster. Indeed, in the zebrafish, a YTHDF reader triggers the maternal-to-zygotic transition through the decay of the maternal m^{6}A RNAs during cleavage [33]. The role

in the axon myelination and specification of mouse oligodendrocytes [27] is unlikely conserved for Prrc2a because the oyster orthologue is expressed before the neurogenesis is detected in trochophore stages [60]. Alternatively, the early expression of Prrc2a suggests that it might rather compete with YTHDF for m^{6}A-RNA targets [27], thereby possibly acting in oyster MZT, bringing new perspectives into this process which remains poorly understood in lophotrochozoans. In mammals m^{6}A is implicated in the embryonic cell fate [30,31] notably via the regulation of cell differentiation by YTHDC2 [32] or hnRNPA2B1 [29]. In the oyster, YTHDC1, YTHDC2, IGF2BP and hnRNPA2B1 have their maximum expression during gastrulation correlated to the second m^{6}A peak, suggesting similar implications.

Putative oyster m^{6}A readers actually bind m^{6}A-RNA *in vitro*.

To better approach the developmental processes involving m^{6}A in the oyster, we characterized the proteins that can interact with m^{6}A-RNA using a methylated-RNA-pulldown / mass spectrometry assay. We identified 162 proteins able to specifically bind the m^{6}A-RNA oligo in embryonic cell extracts, demonstrating the actual presence of genuine m^{6}A-readers in the oyster. Most (ca. 75 %) of these proteins were found in nuclear extracts and only 5 were found in both the cytoplasmic and nuclear fractions, showing an important compartmentalization of the epitranscriptomic pathway. Regarding the little number of m^{6}A readers in other animals, and because the assay conditions do not discriminate between direct and indirect interactions, we hypothesize that most these proteins indirectly bind m^{6}A via a limited number of 'scaffold' m^{6}A readers. Such authentic readers that only bind the m^{6}A-RNA oligo in our assay likely include YTHDC1 and eIF3a, which have been demonstrated to directly bind m^{6}A in other species, demonstrating the conservation of the m^{6}A-binding capacity and specificity of the YTH

domain in the oyster. Besides, YTHDC1 is found in both cell fractions, suggesting its implication in the trafficking of m^{6}A-RNA across the nuclear envelope [24], and reinforcing the hypothesis that YTH proteins could participate in oyster MZT and cell differentiation. The presence of the oyster eiF3a in the cytoplasm is consistent with a conserved role in m^{6}A-mediated translation processes, such as cap-independent translation [5].

Possible functions of m^{6}A-RNA in oyster development.

We investigated the expression level and the functional annotation of the 162 genes encoding the m^{6}A-interacting proteins across oyster early life. These genes can be clustered into three successive expression phases corresponding to three distinct functional pathways, which are independent albeit all mostly related to translation regulation. The cluster 1 is mostly expressed during the cleavage and the associated GO terms are related to the initiation of translation, consistent with maternal RNA consumption before MZT is complete and the zygotic genome becomes fully activated. The genes within cluster 3 show an expression peak during gastrulation. Their ontology terms evoke ribosomal and mitochondrial processes, the latter being required for energy supply and signalling integration during gastrulation [61–64]. The cluster 2 contains genes that peak after gastrulation and which are related to splicing and nuclear export. Such functional annotations are in line with a fine regulation of transcript variant translation within the distinct cell lineages in the three cell layers of the late embryos.

Taken together, our findings bring to light a possible implication of m^{6}A in oyster development. First, during cleavage the decrease of m^{6}A-RNA, the weak expression of methyltransferase complex genes, the maximum of YTHDF gene expression and the expression of *Cg*-m^{6}A-BPs

related to the initiation of the translation strongly suggest the implication of m^{6}A in MZT in *C. gigas*. Second, the increasing m^{6}A level during gastrula stage is correlated to the increase of methyltransferase complex gene expression. In addition, the increased RNA level of readers putatively related to cell differentiation and the peak of gene expression of *Cg*-m^{6}A-BPs associated to ribosomal and mitochondrial processes, support the hypothesize of a m^{6}A implication in gastrulation. Finally, the highest m^{6}A level at the trochophore stage, the gene expression of the methyltransferase complex and of readers associated to cell differentiation, as well as high RNA level of Cg-m^{6}A-BPs related to splicing and nuclear export is correlated with the fine cell differentiation taking place at this stage. However, inferring the biological significance of m^{6}A in development from the indirect and incomplete functional annotation of the oyster genome is only limited. Characterization of the precise targets of m^{6}A and how their individual methylation is regulated across development, for example using high throughput sequencing of precipitated m^{6}A-RNA (MeRIP-seq), could be extremely relevant to better understand this issue. In addition, despite sequence conservation and binding ability of oyster actor orthologues strongly suggest functional conservation, future dedicated studies such as biochemical inhibition or gene inactivation could help demonstrate their genuine biological function. Besides, there seems to be an inverse correlation between m^{6}A-RNA and 5mC-DNA levels during the considered oyster developmental window [46]. This may suggest an interplay between epigenetic and epitranscriptomic marks, possibly reflecting competition for methyl-donor availability [59] or a link by histone epigenetic pathways [65,66].

Regarding the potential influence of the environment on m^{6}A and the accumulation of RNA in oocytes, we are at present investigating our hypothesis that m^{6}A may convey intergenerational

epitranscriptomic inheritance of maternal life traits in the oyster. On an evolutionary perspective, the presence of a putatively fully conserved epitranscriptomic pathway in the oyster suggests that it was already present in the bilaterian common ancestor thereby in favour of an important biological significance. Why *Drosophila* and *Caenorhabditis* seem to have lost specific m^{6}A-RNA erasers could be related to a sub-functionalization of the DMAD [41] and NMAD-1 [42] *N*^{6}-methyladenine DNA demethylase activity broadened towards RNA. However, more work in required to better understand the evo-devo implications of our results.

To conclude, in this work we report the discovery and characterisation of a putatively complete epitranscriptomic pathway in a lophotrochozoan organism, the oyster *Crassostrea gigas*. This pathway includes the m^{6}A mark in RNA and the actors of all the aspects of its regulation (writers, eraser, readers) which are conserved at the molecular level and putatively functional. We show that m^{6}A levels are variable across oyster development and that m^{6}A differentially affects distinct RNA populations. Expression levels of the related enzymatic machinery is consistent with the observed m^{6}A level variations. We demonstrate the m^{6}A binding capacity and specificity of putative oyster m^{6}A readers in the cytoplasm and nucleus of embryolarval cells. These readers mediate distinct putative biological outcomes depending on the development stage considered. From these results we hypothesize that early decay of maternal m^{6}A RNA participates in maternal-to-zygotic transition during cleavage and that later *de novo* zygotic m6A methylation contributes to gastrulation and cell differentiation. This first characterisation of an m^{6}A-epitranscriptomic pathway in a lophotrochozoan organism, together with its potential implication in development, opens new perspectives on the evolution of

epigenetic mechanisms and on the potential epitranscriptomic inheritance of environmentally-induced life traits.

Methods:

Animals:

Broodstock oysters [67] and oyster embryos [46] were obtained at the IFREMER marine facilities (Argenton, France) as previously described. Briefly, gametes of mature broodstock oysters were obtained by stripping the gonads and filtering the recovered material on a 60 µm mesh to remove large debris. Oocytes were collected as the remaining fraction on a 20 µm mesh and spermatozoa as the passing fraction on a 20 µm mesh. Oocytes were pre-incubated in 5 L of UV-treated and 1 µm filtered sterile sea water (SSW) at 21 °C until germinal vesicle breakdown. Fertilization was triggered by the addition of ca.10 spermatozoids per oocyte. After the expulsion of the second polar body was assessed by light microscopy, embryos were transferred in 150 L tanks of oxygenated SSW at 21 °C. The development stages were determined by light microscopy observation. The stages collected were oocytes (E, immediately before sperm addition), fertilized oocytes (F E, immediately before transfer to 150L tanks), two to eight cell embryos (2/8 C, ca. 1.5 hours post fertilization (hpf)), morula (M, ca. 4 hpf), blastula (B, ca. 6 hpf), gastrula (G, ca. 10 hpf), trochophore (T, ca 16 hpf) and D larvae (D, ca. 24 hpf). For each development stage, 3 million embryos were collected as the remaining fraction on a 20 µm mesh and centrifuged at 123 g for 5min at room temperature.

Supernatant was discarded and samples of 1 million embryos were then snap-frozen in liquid nitrogen directly of after resuspension in Tri-Reagent (Sigma-Aldrich, St Louis, MO, USA) (1 mL/10^6 embryos) and stored at -80 °C. Three distinct experiments were realized (February to May 2019) using the gametes of 126 to 140 broodstock animals, respectively.

RNA extraction:

- total RNA extraction

RNA was extracted using phenol-chloroform followed by affinity chromatography as previously described [68]. Briefly, embryos were ground in Tri-Reagent (Sigma-Aldrich) and RNA was purified using affinity chromatography (Nucleospin RNA II kit, Macherey-Nagel, Duren, Germany). Potential contaminating DNA was removed by digestion with rDNase (Macherey-Nagel) according to the manufacturer's instructions for 15 min at 37 °C then RNA was purified using Beckman Coulter's solid-phase reversible immobilization (SPRI) paramagnetic beads (AgencourtAMPure XP, Beckman Coulter, Brea, CA, USA) according to the manufacturer's instructions. Briefly, paramagnetic beads and RNAs were mixed slowly and incubated 5 min at room temperature followed by 2 min on a magnetic rack. Cleared supernatant was removed, and beads were washed three times with 70 % ethanol. After 4 min of drying at room temperature, RNAs were mixed slowly with RNase free water and incubated for 1 min at room temperature on the magnetic rack. Eluted total RNA was stored at -80 °C.

- PolyA RNA enrichment

Poly-A RNA was extracted from total RNA by oligo-dT affinity chromatography (NucleoTrap mRNA kit, Macherey-Nagel) according to the manufacturer's instructions. Briefly, up to 130 µg

of total RNAs were mixed with oligo-dT latex beads and incubated for 5 min at 68 °C then 10 min at room temperature. After centrifugation (2,000 g then 11,000 g), the pellets were washed three times on the microfilter and dried by centrifugation at 11,000 g for 1 min. Finally, polyA+ RNA was incubated with RNAse-free water for 7 min at 68 °C then centrifuged at 11,000 g for 1 min. Eluted polyA+ RNA was stored at -80 °C until needed.

Total and polyA-enriched RNA purity and concentrations were assayed by spectrophotometry (Nanodrop, Thermo Scientific, Waltham, MA, USA).

m^{6}A quantification by LC-MS/MS:

- RNA hydrolysis

To generate nucleosides for quantification against standard curves, 5 µg of total RNA were denatured for 10 min at 70 °C followed by 10 min on ice, and hydrolyzed with 100 U Nuclease S1 (50 U/µL, Promega, Madison, WI, USA) in Nuclease S1 buffer (Promega) in a final reaction volume of 25 µL for 2 h at 37 °C under gentle shaking. Samples were then incubated with alkaline phosphatase buffer (Promega) for 5 min at room temperature, before 10 U alkaline phosphatase (Promega) were added and incubated further for 2 h at 37 °C under gentle shaking. Ten extra units of alkaline phosphatase were added after 1 hour of incubation to complete the reaction. Finally, samples were centrifuged at 13,000 rpm for 10 min at 4 °C and the supernatant containing digested total RNA was collected and kept at -20 °C before quantification.

- m^{6}A quantification:

The apparatus was composed of a NexeraX² UHPLC system coupled with LCMS8030 Plus (Shimadzu, Kyoto, Japan) mass spectrometer using an electrospray interface in positive mode. The column (1.7 µm, 100x3 mm) was a HILIC Aquity® Amide (Waters, Millford, MA, USA) maintained at 35 °C. The injection volume and run-to-run time were 3 µL and 10 min, respectively. The flow rate was set to 1 mL/min. Mobile phase was initially composed of a mixture of ammonium formate solution (10 mM) containing 0.2 % (v/v) formic acid and 95 % acetonitrile (ACN) and it was maintained for 1 min. Then, a linear gradient was applied to reach 83 % ACN for 6 min. The composition returned to the initial conditions and the column was equilibrated for 3 min.

The mass spectrometer was running in the Multiple Reaction Monitoring (MRM) acquisition mode. LabSolutions 5.86 SP1 software was used to process the data. The desolvatation temperature was 230 °C, source temperature was 400 °C and nitrogen flows were 2.5 L/min for the cone and 15 L/min for the desolvatation. The capillary voltage was +4.5 kV. For each compound, two transitions were monitored from the fragmentation of the $[M+H]^+$ ion. The first transition (A in Table S1) was used for quantification and the second one (B in Table S1) for confirmation of the compound according to European Commission Decision 2002/657/EC (Table S1).

Blank plasma samples were analysed to check specificity. Calibrators were prepared using diluted solutions of A (Toronto Research Chemical, Toronto, Canada) and m^6A (Carbosynth, Berkshire, UK) in water at 1, 2, 5, 10, 20 50, 100 ng/mL The calibration curves were drawn by plotting the ratio of the peak area of A and m^6A. For both nucleosides, a quadratic regression with 1/C weighting resulted in standard curves with $R^2>0.998$ and more than 75% of standards

with back-calculated concentrations within 15% of their nominal values as recommended for by the European medicines agency for bioanalytical methods [69]. The limits of quantifications for both compounds were considered as the lowest concentrations of the calibration curve. m^6A/A ratios were calculated for each single sample using the determined concentrations. Final results are the average of three technical replicates.

m^6A quantification by immunoblotting:

Immunological quantification of m^6A was performed by dot-blot using total and polyA+ RNAs. Dogfish total RNA (Dr. A. Gautier, personal communication) and a synthetic unmethylated RNA oligo (Eurogentec, Liege, Belgium) were used as positive and negative controls, respectively. RNA samples were denatured for 15 min at 55 °C with gentle shaking in denaturing solution (2.2 M formaldehyde, 50 % formamide, 0.5X MOPS, DEPC water) followed by 2 min on ice. Blotting was performed on a vacuum manifold as follows: a nylon membrane (Amersham Hybond-N+, GE Healthcare life Sciences, Chicago, IL, USA) was pre-hydrated in DEPC water for 5 min, then each well was washed twice with 10X SSC (Sigma-Aldrich) before RNA was spotted onto the membrane and incubated for 15 min at room temperature. Then, vacuum aspiration was applied and each well was washed twice with 10X SSC. After heat crosslinking for 2 h at 70 °C, the membrane was rehydrated with DEPC water for 5 min, washed with PBS then PBST (PBS, 0.1 % Tween-20) for 5 min each and blocked with two 5 min incubations with blocking buffer (PBS, 0.1 % Tween-20, 10 % dry milk, 1 % BSA) at room temperature. The blocked membrane was incubated overnight at 4 °C under gentle shaking with the anti-m^6A primary antibody (Total RNA: Millipore (Burlington, MA, USA) ABE572, 1 :

1,000 dilution in blocking buffer; polyA+ RNA: Diagenode (Liege, Belgium) C15200082, 1 : 500 dilution in blocking buffer) followed by four washes of PBST for 5 min. The secondary antibody (Total RNA: Dako (Santa Clara, CA, USA) P0447 goat anti-mouse HRP antibody, 1 : 10,000 dilution; polyA+ RNA: Invitrogen (Carlsbad, CA, USA) A21202 donkey anti-mouse Alexa 488, 1 : 250 dilution) was diluted in PBST supplemented with 5 % dry milk and added onto the membrane for 1 h 30 (total RNA) or 1 h (polyA+ RNA) at room temperature under gentle shaking. Membranes were extensively washed in PBST (at least 4 washes of 5 min for total RNA and 5 min then 1 h for polyA+ RNA) then total and polyA+ RNA immunoblots were visualized using chemiluminescence (ECL kit, Promega) or fluorescence scanning at 480-530 nm (Pro Xpress, Perkin-Elmer, Waltham, MA, USA), respectively. The amount of m^{6}A was inferred from dot intensity measurements using ImageJ (v.1.49). Signal intensities were determined as 'integrated densities as a percentage of the total' which corresponds to the area under the curve of the signal of each dot after membrane background and negative control signal subtraction.

***In silico* analyses:**

All protein and RNA sequences of the m^{6}A machinery of *Homo sapiens* and *Drosophila melanogaster* (Data S1) were recovered by their published designation (i.e., 'METTL3' or 'YTHDF' etc.) and their identified protein sequence (ie. RefSeq accession number NP…) collected from NCBI and used as query sequences to search for putative homologue sequences in *Crassostrea gigas* databases. The presence of oyster orthologue RNA and protein sequences were investigated by reciprocal

BLAST(https://blast.ncbi.nlm.nih.gov/Blast.cgi) on the *Crassostrea gigas* GigaTON [70] and NCBI databases and results were compared between the two oyster databases. Domain prediction was performed with CD-search software (https://www.ncbi.nlm.nih.gov/Structure/cdd/wrpsb.cgi) with default settings on protein sequences of *Homo sapiens*, *Drosophila melanogaster* and *Crassostrea gigas*. The GRE-rich domain identified in vertebrate Prrc2a sequence [27] was performed with ProtParam (https://web.expasy.org/cgi-bin/protparam/protparam).

Protein machinery mRNA expression analyses:

The transcriptome data of the different development stages are available on the GigaTON database [70,71]. The correspondence between development stages in our study, and the GigaTON database were assessed using light microscopy based on the morphological description by Zhang et al., 2012 [71] (Table S2). Expression data was expressed in TPM (Transcripts Per Million) [72] to provide a normalized comparison of gene expression between all samples. The actual presence of some transcripts that display unclear or chimeric sequences within available oyster databases was assessed using RT-PCR (Data S1).

Protein m^{6}A RNA pull down:

- Protein extraction and RNA affinity chromatography

Protein extraction and RNA affinity chromatography were performed as described previously [27] with some modifications as follows. Equal amounts (1 million individuals) of each developmental stage (oocyte to D larvae) were pooled together then homogenized in 3.5

volumes of buffer A (10 mM KCl, 1.5 mM MgCl2, 10 mM HEPES, pH 7.9, DEPC water, 1X Protease inhibitor cocktail, DTT 0.5 mM) by extensive pipetting (ca. 30 times) and incubated 10 min at 4 °C. Embryos were ground with 10 slow 23G-needle syringe strokes and centrifuged at 2,000 rpm for 10 min at 4 °C. The supernatant was diluted in 0.11 volume of buffer B (1.4 M KCl, 0.03 M MgCl2, HEPES 0.3 M, pH 7.9, DEPC water), centrifuged at 10,000 g for 1 h at 4 °C and the supernatant containing cytosolic proteins was stored at -80 °C. The pellet of the first centrifugation, containing nuclei, was re-suspended in two volumes of buffer C (0.42 M NaCl, 1.5 mM MgCl2, 0.2 mM EDTA, 25 % glycerol, 20 mM HEPES, pH 7.9, 0.5 mM PMSF, 0.5 mM DTT, water DEPC). Nuclei were then lysed with a 23 G needle (10 vigorous syringe strokes) followed by centrifugation at 30,000 rpm for 30 min at 4 °C and the supernatant containing nuclear proteins was stored at -80 °C.

To identify putative proteins able to bind m^{6}A-RNA, the cytosolic and nuclear fractions were submitted to affinity chromatography using 5'-biotin-labelled RNA oligonucleotides either bearing *N*^{6}-methylated adenosines or not. The methylated adenosines were designed to lie within RRACH motifs, according to the conserved methylated consensus sequence in other organisms [2,3,7,33,73] (oligo-m^{6}A: 5'Biotin-AGAAAAGACAACCAACGAGRR-m^{6}A-CWCAUCAU-3', oligo-A: 5'Biotin-AGAAAAGACAACCAACGAGRRACWCAUCAU-3', R = A or G, W = A or U, Eurogentec).

For RNA pull down, streptavidin-conjugated magnetic beads (Dynabeads Myone Streptavidin, Invitrogen) were pre-blocked with 0.2 mg/mL tRNA (Sigma-Aldrich) and 0.2 mg/mL BSA for 1 h at 4 °C under gentle rotation followed by three washes with 0.1 M NaCl. To avoid the identification of non-target proteins, cytosolic and nuclear protein extracts were cleared with

pre-blocked magnetic beads in binding buffer (50 mM Tris-HCl, 250 mM NaCl, 0.4 mM EDTA, 0.1 % NP-40, DEPC water, 1 mM DTT, 0.4 U/μL RNAsin) for 1 h at 4 °C under gentle rotation. After incubation on magnetic rack, the supernatants containing putative target proteins were collected and mixed with pre-blocked magnetic beads and oligo-m^{6}A or oligo-A for 2 h at 4 °C under gentle rotation. The beads binding putative target proteins were washed three times with binding buffer and diluted in 50 mM ammonium bicarbonate.

- Identification of m^{6}A-binding proteins by LC-MS/MS:

Protein samples were first reduced, alkylated and digested with trypsin then desalted and concentrated onto a μC18 Omix (Agilent, Santa Clara, CA, USA) before analysis.

The chromatography step was performed on a NanoElute (Bruker Daltonics, Billerica, MA, USA) ultra-high pressure nano flow chromatography system. Peptides were concentrated onto a C18 pepmap 100 (5 mm x 300 μm i.d.) precolumn (Thermo Scientific) and separated at 50 °C onto a reversed phase Reprosil column (25 cm x 75 μm i.d.) packed with 1.6 μm C18 coated porous silica beads (Ionopticks, Parkville, Victoria, Australia). Mobile phases consisted of 0.1 % formic acid, 99.9 % water (v/v) (A) and 0.1 % formic acid in 99.9 % ACN (v/v) (B). The nanoflow rate was set at 400 nL/min, and the gradient profile was as follows: from 2 to 15 % B within 60 min, followed by an increase to 25 % B within 30 min and further to 37 % within 10 min, followed by a washing step at 95 % B and re-equilibration.

MS experiments were carried out on an TIMS-TOF pro mass spectrometer (Bruker Daltonics) with a modified nano-electrospray ion source (CaptiveSpray, Bruker Daltonics). The system was calibrated each week and mass precision was better than 1 ppm. A 1600 spray voltage with a capillary temperature of 180 °C was typically employed for ionizing. MS spectra were

acquired in the positive mode in the mass range from 100 to 1700 m/z. In the experiments described here, the mass spectrometer was operated in PASEF mode with exclusion of single charged peptides. A number of 10 PASEF MS/MS scans was performed during 1.16 seconds from charge range 2-5.

The fragmentation pattern was used to determine the sequence of the peptide. Database searching was performed using the Mascot 2.6.1 program (Matrix Science) with a *Crassostrea gigas* Uniprot database (including 25,982 entries). The variable modifications allowed were as follows: C-Carbamidomethyl, K-acetylation, methionine oxidation, and Deamidation (NQ). The 'Trypsin' parameter was set to 'Semispecific'. Mass accuracy was set to 30 ppm and 0.05 Da for MS and MS/MS mode respectively. Mascot data were then transferred to Proline validation software (http://www.profiproteomics.fr/proline/) for data filtering according to a significance threshold of <0.05 and the elimination of protein redundancy on the basis of proteins being evidenced by the same set or a subset of peptides (Data S2).

- Gene ontology analysis:

The mRNA sequences of the characterized m^6A-binding proteins were identified using tBlastn [74–76] against the GigaTON database [70] with default settings. Gene ontology (GO) analyses were carried out with the GO annotations obtained from GigaTON database gene universe [70]. GO term-enrichment tests were performed using the goseq (V1.22.0) R package [77] with p-values calculated by the Wallenius method and filtered using REVIGO [78]. GO terms with a p-value < 0.05 were considered significantly enriched (Data S3).

Statistical analyses and graph production:

Results are given as the mean ± SD of three independent experiments unless otherwise stated. They were analysed using one-way ANOVA or Kruskall-wallis tests when required, depending on the normality of result distribution. The normality was tested using the Shapiro-Wilk's test and homoscedasticity of variances with Bartlett's tests. Statistics and graphics were computed with Prism v.6 (Graphpad), R (v.3.6.1) and RStudio (v.1.0.153) softwares. The R packages *eulerr* [79] and *Complexheatmap* [80] were used for production of specific figures.

Author contribution

Experiment design: GR, LLF.

Benchwork and bioinformatics: LLF, GR, BB, BP, MS.

Data analysis: LLF, GR, BB, MS.

Manuscript writing and editing: LLF, GR, PF, BB, MS, BP.

Acknowledgements

The authors would like to acknowledge PRISMM core facility collaborators R. Delepée and S. Lagadu for their expertise in m^6A/A UHPLC-MS/MS quantification. We also thank J. Pontin for technical assistance and J. Le Grand for help with sampling.

Funding sources and disclosure of conflicts of interest

This work was supported by the French National program CNRS EC2CO (Ecosphère Continentale et Côtière 'HERITAGe' to G. Rivière) and the council of the Normandy Region (RIN ECUME to P. Favrel). The authors declare they have no conflict of interest.

References:

1 Saletore Y, Meyer K, Korlach J, Vilfan ID, Jaffrey S & Mason CE (2012) The birth of the Epitranscriptome: deciphering the function of RNA modifications. *Genome Biol.* **13**, 175.

2 Meyer KD, Saletore Y, Zumbo P, Elemento O, Mason CE & Jaffrey SR (2012) Comprehensive analysis of mRNA methylation reveals enrichment in 3′ UTRs and near stop codons. *Cell* **149**, 1635–1646.

3 Dominissini D, Moshitch-moshkovitz S, Schwartz S, Salmon-Divon M, Ungar L, Osenberg S, Cesarkas K, Jacob-hirsch J, Amariglio N, Kupiee M, Sorek R & Rechavi G (2012) Topology of the human and mouse m 6 A RNAmethylomes revealed bym6A-seq. *Nature* **485**, 201–206.

4 Ke S, Alemu EA, Mertens C, Gantman EC, Fak JJ, Mele A, Haripal B, Zucker-Scharff I, Moore MJ, Park CY, Vågbø CB, Kusśnierczyk A, Klungland A, Darnell JE, Darnell RB, Kuśnierczyk A, Klungland A, Darnell JE, Darnell RB, Kusśnierczyk A, Klungland A, Darnell JE & Darnell RB (2015) A majority of m 6 A residues are in the last exons, allowing the potential for 3′ UTR regulation. *Genes Dev.* **29**, 2037–2053.

5 Meyer KD, Patil DP, Zhou J, Zinoviev A, Skabkin MA, Elemento O, Pestova T V., Qian SB & Jaffrey SR (2015) 5′ UTR m6A Promotes Cap-Independent Translation. *Cell* **163**, 999–1010.

6 Pendleton KE, Chen B, Liu K, Hunter O V., Xie Y, Tu BP & Conrad NK (2017) The U6 snRNA m6A Methyltransferase METTL16 Regulates SAM Synthetase Intron Retention. *Cell* **169**, 824-835.e14.

7 Lence T, Akhtar J, Bayer M, Schmid K, Spindler L, Ho CH, Kreim N, Andrade-Navarro MA, Poeck B, Helm M & Roignant JY (2016) M6A modulates neuronal functions and sex determination in Drosophila. *Nature* **540**, 242–247.

8 Bokar JA, Shambaugh ME, Polayes D, Matera AG & Rottman FM (1997) Purification and cDNA cloning of the AdoMet-binding subunit of the human mRNA (N6-adenosine)-methyltransferase. *RNA* **3**, 1233–47.

9 Liu J, Yue Y, Han D, Wang X, Fu YY, Zhang L, Jia G, Yu M, Lu Z, Deng X, Dai Q, Chen W & He C (2013) A METTL3–METTL14 complex mediates mammalian nuclear RNA N6-adenosine methylation. *Nat. Chem. Biol.* **10**, 93–95.

10 Wang X, Feng J, Xue Y, Guan Z, Zhang D, Liu Z, Gong Z, Wang Q, Huang J, Tang C, Zou T & Yin P (2016) Structural basis of N6-adenosine methylation by the METTL3-METTL14 complex. *Nature* **534**, 575–578.

11 Ping X-LL, Sun B-FF, Wang L, Xiao W, Yang X, Wang W-JJ, Adhikari S, Shi Y, Lv Y, Chen Y-SS, Zhao X, Li A, Yang YGYY-G, Dahal U, Lou X-MM, Liu X, Huang J, Yuan W-PP, Zhu X-FF, Cheng T, Zhao Y-LL, Wang X, Danielsen JMRR, Liu F & Yang YGYY-G (2014) Mammalian WTAP is a regulatory subunit of the RNA N6-methyladenosine methyltransferase. *Cell Res.* **24**, 177–189.

12 Yue Y, Liu J, Cui X, Cao J, Luo G, Zhang Z, Cheng T, Gao M, Shu X, Ma H, Wang F, Wang X, Shen B, Wang Y, Feng X, He C & Liu J (2018) VIRMA mediates preferential m6A mRNA methylation in 3′UTR and near stop codon and associates with alternative polyadenylation. *Cell Discov.* **4**, 10.

13 Růžička K, Zhang M, Campilho A, Bodi Z, Kashif M, Saleh M, Eeckhout D, El-Showk S, Li H, Zhong S, Jaeger G De, Mongan NP, Hejátko J, Helariutta Y & Fray RG (2017) Identification of factors required for m6A mRNA methylation in Arabidopsis reveals a

role for the conserved E3 ubiquitin ligase HAKAI. *New Phytol.* **215**, 157–172.

14 Knuckles P, Lence T, Haussmann IU, Jacob D, Kreim N, Carl SH, Masiello I, Hares T, Villaseñor R, Hess D, Andrade-Navarro MA, Biggiogera M, Helm M, Soller M, Bühler M & Roignant J-YY (2018) Zc3h13/Flacc is required for adenosine methylation by bridging the mRNA-binding factor Rbm15/Spenito to the m 6 A machinery component Wtap/Fl(2)d. *Genes Dev.* **32**, 1–15.

15 Patil DP, Chen CK, Pickering BF, Chow A, Jackson C, Guttman M & Jaffrey SR (2016) m6A RNA methylation promotes XIST-mediated transcriptional repression. *Nature* **537**, 369–373.

16 Zheng G, Dahl JA, Niu Y, Fedorcsak P, Huang CM, Li CJ, Vågbø CB, Shi Y, Wang WL, Song SH, Lu Z, Bosmans RPG, Dai Q, Hao YJ, Yang X, Zhao WM, Tong WM, Wang XJ, Bogdan F, Furu K, Fu Y, Jia G, Zhao X, Liu J, Krokan HE, Klungland A, Yang YG & He C (2013) ALKBH5 Is a Mammalian RNA Demethylase that Impacts RNA Metabolism and Mouse Fertility. *Mol. Cell* **49**, 18–29.

17 Mauer J, Luo X, Blanjoie A, Jiao X, Grozhik A V, Patil DP, Linder B, Pickering BF, Vasseur J-J, Chen Q, Gross SS, Elemento O, Debart F, Kiledjian M & Jaffrey SR (2017) Reversible methylation of m6Am in the 5′ cap controls mRNA stability. *Nature* **541**, 371–375.

18 Jia G, Fu Y, Zhao X, Dai Q, Zheng G, Yang YGYY-GGYY-G, Yi C, Lindahl T, Pan T, Yang YGYY-GGYY-G & He C (2011) N6-Methyladenosine in nuclear RNA is a major substrate of the obesity-associated FTO. *Nat. Chem. Biol.* **7**, 885–887.

19 Wang X, Lu Z, Gomez A, Hon GC, Yue Y, Han D, Fu Y, Parisien M, Dai Q, Jia G, Ren B, Pan T, He C, Zhike L, Gomez A, Hon GC, Yue Y, Han D, Fu Y, Ärisien M, Dai Q, Jia G, Ren B, Pan T & He C (2014) N6-methyladenosine-dependent regulation of messenger RNA stability. *Nature* **505**, 117–120.

20 Wang X, Zhao BS, Roundtree IA, Lu Z, Han D, Ma H, Weng X, Chen K, Shi H & He C (2015) N6-methyladenosine modulates messenger RNA translation efficiency. *Cell* **161**, 1388–1399.

21 Hsu PJ, Zhu Y, Ma H, Guo Y, Shi X, Liu Y, Qi M, Lu Z, Shi H, Wang J, Cheng Y, Luo G, Dai Q, Liu M, Guo X, Sha J, Shen B & He C (2017) Ythdc2 is an N6-methyladenosine binding protein that regulates mammalian spermatogenesis. *Cell Res.* **27**, 1115–1127.

22 Shi H, Wang X, Lu Z, Zhao BS, Ma H, Hsu PJ, Liu C & He C (2017) YTHDF3 facilitates translation and decay of N 6-methyladenosine-modified RNA. *Cell Res.* **27**, 315–328.

23 Xiao W, Adhikari S, Dahal U, Chen Y-S, Hao Y-J, Sun B-F, Sun H-Y, Li A, Ping X-L, Lai W-Y, Wang XX-J, Ma H-L, Huang C-M, Yang YY-G, Huang N, Jiang G-B, Wang H-L, Zhou Q, Wang XX-J, Zhao Y-L & Yang YY-G (2016) Nuclear m 6 A Reader YTHDC1 Regulates mRNA Splicing. *Mol. Cell* **61**, 507–519.

24 Roundtree IA, Luo G-ZZ, Zhang Z, Wang X, Zhou T, Cui Y, Sha J, Huang X, Guerrero L, Xie P, He E, Shen B & He C (2017) YTHDC1 mediates nuclear export of N6-methyladenosine methylated mRNAs. *Elife* **6**, 1–28.

25 Alarcón CR, Goodarzi H, Lee H, Liu X, Tavazoie SFSSF & Tavazoie SFSSF (2015) HNRNPA2B1 Is a Mediator of m6A-Dependent Nuclear RNA Processing Events. *Cell* **162**, 1299–1308.

26 Huang H, Weng H, Sun W, Qin X, Shi H, Wu H, Zhao BS, Mesquita A, Liu C, Yuan CL, Hu YC, Hüttelmaier S, Skibbe JR, Su R, Deng X, Dong L, Sun M, Li C, Nachtergaele S,

Wang Y, Hu C, Ferchen K, Greis KD, Jiang X, Wei M, Qu L, Guan JL, He C, Yang J & Chen J (2018) Recognition of RNA N6-methyladenosine by IGF2BP proteins enhances mRNA stability and translation. *Nat. Cell Biol.* **20**, 285–295.

27 Wu R, Li A, Sun B, Sun J-GG, Zhang J, Zhang T, Chen Y, Xiao Y, Gao Y, Zhang Q, Ma J, Yang X, Liao Y, Lai W-YY, Qi X, Wang S, Shu Y, Wang H-LL, Wang F, Yang Y-GG & Yuan Z (2018) A novel m6A reader Prrc2a controls oligodendroglial specification and myelination. *Cell Res.* **29**, 23–41.

28 Bertero A, Brown S, Madrigal P, Osnato A, Ortmann D, Yiangou L, Kadiwala J, Hubner NC, De Los Mozos IR, Sadee C, Lenaerts A-SS, Nakanoh S, Grandy R, Farnell E, Ule J, Stunnenberg HG, Mendjan S, Vallier L, Sadée C, Lenaerts A-SS, Nakanoh S, Grandy R, Farnell E, Ule J, Stunnenberg HG, Mendjan S & Vallier L (2018) The SMAD2/3 interactome reveals that TGFβ controls m 6 A mRNA methylation in pluripotency. *Nature* **555**, 256–259.

29 Kwon J, Jo YJ, Namgoong S & Kim NH (2019) Functional roles of hnRNPA2/B1 regulated by METTL3 in mammalian embryonic development. *Sci. Rep.* **9**, 8640.

30 Geula S, Moshitch-Moshkovitz S, Dominissini D, Mansour AAF, Kol N, Salmon-Divon M, Hershkovitz V, Peer E, Mor N, Manor YS, Ben-Haim MS, Eyal E, Yunger S, Pinto Y, Jaitin DA, Viukov S, Rais Y, Krupalnik V, Chomsky E, Zerbib M, Maza I, Rechavi Y, Massarwa R, Hanna S, Amit I, Levanon EY, Amariglio N, Stern-Ginossar N, Novershtern N, Rechavi G & Hanna JH (2015) m6A mRNA methylation facilitates resolution of naïve pluripotency toward differentiation. *Science (80-.).* **347**, 1002–1006.

31 Batista PJ, Molinie B, Wang J, Qu K, Zhang J, Li L, Bouley DM, Lujan E, Haddad B, Daneshvar K, Carter AC, Flynn RA, Zhou C, Lim KS, Dedon P, Wernig M, Mullen AC, Xing Y, Giallourakis CC, Chang HY, Howard Y, Batista PJ, Molinie B, Wang J, Qu K, Zhang J, Li L, Bouley DM, Dedon P, Wernig M, Mullen AC, Xing Y, Giallourakis CC & Chang HY (2014) M^{6}A RNA modification controls cell fate transition in mammalian embryonic stem cells. *Cell Stem Cell* **15**, 707–719.

32 Wojtas MN, Pandey RR, Mendel M, Homolka D, Sachidanandam R & Pillai RS (2017) Regulation of m6A Transcripts by the 3'→5' RNA Helicase YTHDC2 Is Essential for a Successful Meiotic Program in the Mammalian Germline. *Mol. Cell* **68**, 374-387.e12.

33 Zhao BS, Wang X, Beadell A V., Lu Z, Shi H, Kuuspalu A, Ho RK & He C (2017) M6A-dependent maternal mRNA clearance facilitates zebrafish maternal-to-zygotic transition. *Nature* **542**, 475–478.

34 Kan L, Grozhik A V., Vedanayagam J, Patil DP, Pang N, Lim K-S, Huang Y-C, Joseph B, Lin C-J, Despic V, Guo J, Yan D, Kondo S, Deng W-M, Dedon PC, Jaffrey SR & Lai EC (2017) The m6A pathway facilitates sex determination in Drosophila. *Nat. Commun.* **8**, 15737.

35 Kasowitz SD, Ma J, Anderson SJ, Leu NA, Xu Y, Gregory BD, Schultz RM & Wang PJ (2018) Nuclear m 6 A reader YTHDC1 regulates alternative polyadenylation and splicing during mouse oocyte development. *PLoS Genet.* **14**, 1–28.

36 Ivanova I, Much C, Di Giacomo M, Azzi C, Morgan M, Moreira PN, Monahan J, Carrieri C, Enright AJ, O'Carroll D, Giacomo M Di, Azzi C, Morgan M, Moreira PN, Monahan J, Carrieri C, Enright AJ, O'carroll D, Di Giacomo M, Azzi C, Morgan M, Moreira PN, Monahan J, Carrieri C, Enright AJ & O'carroll D (2017) The RNA m 6 A Reader YTHDF2 Is Essential for the Post-transcriptional Regulation of the Maternal Transcriptome and Oocyte Competence. *Mol. Cell* **67**, 1059-1067.e4.

37 Lence T, Paolantoni C, Worpenberg L & Roignant JY (2019) Mechanistic insights into m 6 A RNA enzymes. *Biochim. Biophys. Acta - Gene Regul. Mech.* **1862**, 222–229.

38 Balacco DL & Soller M (2018) The m ^{6} A writer: Rise of a machine for growing tasks. *Biochemistry* **58**, acs.biochem.8b01166.

39 Lence T, Soller M & Roignant JY (2017) A fly view on the roles and mechanisms of the m6A mRNA modification and its players. *RNA Biol.* **14**, 1232–1240.

40 Robbens S, Rouzé P, Cock JM, Spring J, Worden AZ & Van De Peer Y (2008) The FTO gene, implicated in human obesity, is found only in vertebrates and marine algae. *J. Mol. Evol.* **66**, 80–84.

41 Zhang G, Huang H, Liu D, Cheng Y, Liu X, Zhang W, Yin R, Zhang D, Zhang P, Liu J, Li C, Liu B, Luo Y, Zhu Y, Zhang N, He S, He C, Wang H & Chen D (2015) N6-methyladenine DNA modification in Drosophila. *Cell* **161**, 893–906.

42 Greer EL, Blanco MA, Gu L, Sendinc E, Liu J, Aristizábal-Corrales D, Hsu CH, Aravind L, He C & Shi Y (2015) DNA methylation on N6-adenine in C. elegans. *Cell* **161**, 868–878.

43 Riviere G, He Y, Tecchio S, Crowell E, Sourdaine P, Guo X & Favrel P (2017) Dynamics of DNA methylomes underlie oyster development. *PLOS Genet.* **13**, 1–16.

44 Sussarellu R, Lebreton M, Rouxel J, Akcha F, Riviere G & Rivière G (2018) Copper induces expression and methylation changes of early development genes in Crassostrea gigas embryos. *Aquat. Toxicol.* **196**, submitted.

45 Rondon R, Grunau C, Fallet M, Charlemagne N, Sussarellu R, Chaparro C, Montagnani C, Mitta G, Bachère E, Akcha F & Cosseau C (2017) Effects of a parental exposure to diuron on Pacific oyster spat methylome. *Environ. Epigenetics* **3**, 1–13.

46 Riviere G, Wu G-CC, Fellous A, Goux D, Sourdaine P & Favrel P (2013) DNA Methylation Is Crucial for the Early Development in the Oyster C . gigas. *Mar. Biotechnol.* **15**, 1–15.

47 Saint-Carlier E & Riviere G (2015) Regulation of Hox orthologues in the oyster Crassostrea gigas evidences a functional role for promoter DNA methylation in an invertebrate. *FEBS Lett.* **589**, 1459–1466.

48 Fellous A, Favrel P & Riviere G (2015) Temperature influences histone methylation and mRNA expression of the Jmj-C histone-demethylase orthologues during the early development of the oyster Crassostrea gigas. *Mar. Genomics* **19**, 23–30.

49 Fellous A, Favrel P, Guo X & Riviere G (2014) The Jumonji gene family in Crassostrea gigas suggests evolutionary conservation of Jmj-C histone demethylases orthologues in the oyster gametogenesis and development. *Gene* **538**, 164–175.

50 Fellous A, Le Franc L, Jouaux A, Goux D, Favrel P & Rivière G (2019) Histone Methylation Participates in Gene Expression Control during the Early Development of the Pacific Oyster Crassostrea gigas. *Genes (Basel).* **10**, 695.

51 Zhou J, Wan J, Gao X, Zhang X, Jaffrey SR & Qian S-B (2015) Dynamic m6A mRNA methylation directs translational control of heat shock response. *Nature* **526**, 591–594.

52 Lu Z, Ma Y, Li Q, Liu E, Jin M, Zhang L & Wei C (2019) The role of N6-methyladenosine RNA methylation in the heat stress response of sheep (Ovis aries). *Cell Stress Chaperones* **24**, 333–342.

53 Xiang Y, Laurent B, Hsu C, Nachtergaele S, Lu Z, Sheng W, Xu C, Chen H, Ouyang J,

Wang S, Ling D, Hsu P, Zou L, Jambhekar A & He C (2017) m6A RNA methylation regulates the UV-induced DNA damage response. *Nature* **543**, 573–576.

54 Cayir A, Barrow TM, Guo L & Byun HM (2019) Exposure to environmental toxicants reduces global N6-methyladenosine RNA methylation and alters expression of RNA methylation modulator genes. *Environ. Res.* **175**, 228–234.

55 Liu J, Li K, Cai J, Zhang M, Zhang X, Xiong X, Meng H, Xu X, Huang Z, Fan J & Yi C (2019) Landscape and Regulation of M ^{6}A and M ^{6}Am Methylome Across Human and Mouse Tissues. *SSRN Electron. J.*, 1–56.

56 Ren W, Lu J, Huang M, Gao L, Li D, Greg Wang G & Song J (2019) Structure and regulation of ZCCHC4 in m6A-methylation of 28S rRNA. *Nat. Commun.* **10**, 5042.

57 Bokar JA, Shambaugh ME, Polayes D, Matera AG & Rottman FM (1997) Purification and cDNA cloning of the AdoMet-binding subunit of the human mRNA (N6-adenosine)-methyltransferase. *RNA* **3**, 1233–1247.

58 Theler D, Dominguez C, Blatter M, Boudet J & Allain FHT (2014) Solution structure of the YTH domain in complex with N6-methyladenosine RNA: A reader of methylated RNA. *Nucleic Acids Res.* **42**, 13911–13919.

59 Shima H, Matsumoto M, Ishigami Y, Ebina M, Muto A, Sato Y, Kumagai S, Ochiai K, Suzuki T & Igarashi K (2017) S-Adenosylmethionine Synthesis Is Regulated by Selective N6-Adenosine Methylation and mRNA Degradation Involving METTL16 and YTHDC1. *Cell Rep.* **21**, 3354–3363.

60 Yurchenko O V., Skiteva OI, Voronezhskaya EE & Dyachuk VA (2018) Nervous system development in the Pacific oyster , Crassostrea gigas (Mollusca : Bivalvia). *Front. Zool.* **15**, 1–21.

61 Ratnaparkhi A (2013) Signaling by folded gastrulation is modulated by mitochondrial fusion and fission. *J. Cell Sci.* **126**, 5369–5376.

62 Ren L, Zhang C, Tao L, Hao J, Tan K, Miao K, Yu Y, Sui L, Wu Z, Tian J & An L (2017) High-resolution profiles of gene expression and DNA methylation highlight mitochondrial modifications during early embryonic development. *J. Reprod. Dev.* **63**, 247–261.

63 Prudent J, Popgeorgiev N, Bonneau B, Thibaut J, Gadet R, Lopez J, Gonzalo P, Rimokh R, Manon S, Houart C, Herbomel P, Aouacheria A & Gillet G (2013) Bcl-wav and the mitochondrial calcium uniporter drive gastrula morphogenesis in zebrafish. *Nat. Commun.* **4**.

64 Dumollard R, Duchen M & Carroll J (2007) The Role of Mitochondrial Function in the Oocyte and Embryo. *Curr. Top. Dev. Biol.* **77**, 21–49.

65 Huang H, Weng H, Zhou K, Wu T, Zhao BS, Sun MM, Chen Z, Deng X, Xiao G, Auer F, Klemm L, Wu H, Zuo Z, Qin X, Dong Y, Zhou Y, Qin H, Tao S, Du J, Liu J, Lu Z, Yin H, Mesquita A, Yuan CL, Hu Y-CC, Sun W, Su R, Dong L, Shen C, Li C, Qing Y, Jiang X, Wu X, Sun MM, Guan J-LL, Qu L, Wei M, Müschen M, Huang G, He C, Yang J & Chen J (2019) Histone H3 trimethylation at lysine 36 guides m6A RNA modification co-transcriptionally. *Nature* **567**, 414–419.

66 Wang Y, Li Y, Yue M, Wang J, Kumar S, Wechsler-Reya RJ, Zhang Z, Ogawa Y, Kellis M, Duester G & Zhao JC (2018) N 6-methyladenosine RNA modification regulates embryonic neural stem cell self-renewal through histone modifications. *Nat. Neurosci.* **21**, 195–206.

67 Petton B, Pernet F, Robert R & Boudry P (2013) Temperature influence on pathogen transmission and subsequent mortalities in juvenile pacific oysters Crassostrea gigas. *Aquac. Environ. Interact.* **3**, 257–273.

68 Riviere G, Fellous A, Franco A, Bernay B & Favrel P (2011) A crucial role in fertility for the oyster angiotensin-converting enzyme orthologue CgACE. *PLoS One* **6**.

69 EMA (2011) *Guideline on bioanalytical method validation. EMEA/CHMP/EWP/192217/2009*.

70 Riviere G, Klopp C, Ibouniyamine N, Huvet A, Boudry P & Favrel P (2015) GigaTON: An extensive publicly searchable database providing a new reference transcriptome in the pacific oyster Crassostrea gigas. *BMC Bioinformatics* **16**, 1–12.

71 Zhang G, Fang X, Guo X, Li L, Luo R, Xu F, Yang P, Zhang L, Wu F, Chen Y, Wang J, Peng C, Meng J, Yang L, Liu J, Wen B, Zhang N & Huang Z (2012) The oyster genome reveals stress adaptation and complexity of shell formation. *Nature* **490**, 49–54.

72 Li B, Ruotti V, Stewart RM, Thomson JA & Dewey CN (2010) RNA-Seq gene expression estimation with read mapping uncertainty. *Bioinformatics* **26**, 493–500.

73 Qi ST, Ma JY, Wang ZB, Guo L, Hou Y & Sun QY (2016) N6 -methyladenosine sequencing highlights the involvement of mRNA methylation in oocyte meiotic maturation and embryo development by regulating translation in xenopus laevis. *J. Biol. Chem.* **291**, 23020–23026.

74 Altschul SF, Madden TL, Schäffer AA, Zhang J, Zhang Z, Miller W & Lipman DJ (1997) Gapped BLAST and PSI-BLAST: a new generation of protein database search programs. *Nucleic Acids Res.* **25**, 3389–3402.

75 Cock PJA, Chilton JM, Grüning B, Johnson JE & Soranzo N (2015) NCBI BLAST+ integrated into Galaxy. *Gigascience* **4**, 0–6.

76 Camacho C, Coulouris G, Avagyan V, Ma N, Papadopoulos J, Bealer K & Madden TL (2009) BLAST+: Architecture and applications. *BMC Bioinformatics* **10**, 1–9.

77 Young MD, Wakefield MJ, Smyth GK & Oshlack A (2010) Gene ontology analysis for RNA-seq: accounting for selection bias. *Genome Biol.* **11**, R14.

78 Supek F, Bošnjak M, Škunca N & Šmuc T (2011) Revigo summarizes and visualizes long lists of gene ontology terms. *PLoS One* **6**.

79 Larsson J (2019) eulerr: Area-Proportional Euler and Venn Diagrams with Ellipses. .

80 Gu Z, Eils R & Schlesner M (2016) Complex heatmaps reveal patterns and correlations in multidimensional genomic data. *Bioinformatics* **32**, 2847–2849.

Figure legends

Figure 1: m^{6}A levels across oyster development.

A. m^{6}A level quantified by LC-MS/MS in *Crassostrea gigas* embryo-larval stages pooled from oocytes to D-larvae (n= 3) is compared to the m^{6}A level in *Homo sapiens* and *Drosophila melanogaster*; **B.** Dot blot quantification of m^{6}A in total RNA throughout oyster development (n=3); **C.** Dot blot quantification of m^{6}A in polyA+ RNAs throughout oyster development (n=3) Kruskal-Wallis test, $\alpha < 0{,}05$. E: Egg, F E: fertilized egg, 2/8C: two to eight cell embryos, M: Morula, B: Blastula, G: Gastrula, T: Trochophore, D: D larvae. Chemiluminescence (B) and fluorescence (C) are measured as a ratio between dot intensity of development stages and their respective controls for each amount of RNA (120ng, 60ng and 30ng).

Figure 2: The putative conserved m^{6}A machinery in *Crassostrea gigas*.

Domain architecture of actors of the m^{6}A machinery identified by *in silico* analyses in the oyster compared to the fruit fly and human, **A.** Writer proteins; **B.** Eraser protein; **C.** Reader proteins. Putative domains involved in m^{6}A processes are coloured (writers, green; eraser, red; readers, blue). Other domains identified but not involved in m^{6}A processes are indicated in grey. Only one isoform is represented for each protein and each species for clarity (see supplementary figure S2 for other isoforms).

Figure 3: Gene expression of the putative m^{6}A machinery throughout oyster development

Expression levels of writers (**A**), eraser (**B**) and readers (**C**) identified by *in silico* analysis at each development stage were inferred from the GigaTON database. Expression levels are given in Transcripts Per kilobases per Million Reads (TPM) as the mean of the GigaTON values according to the table S2. E: Egg, 2/8C: two to eight cell, M: Morula, B: Blastula, G: Gastrula, T: Trochophore, D: D larvae, S: Spat, J: Juvenile.

Figure 4: Characterization of m^{6}A-RNA binding proteins in oyster development.

A. Venn diagrams representation of proteins bound to the A- and/or m^{6}A- oligos in nuclear and cytosolic fractions of oyster embryo-larval stages. The number of proteins identified is indicated. Some actors characterized in this study are highlighted: eIF3, YTHC1, hnRNPA2B1 and IGF2BP. **B.** Heatmap of gene expression levels of the proteins that bind specifically to the m^{6}A-oligo throughout oyster development. The expression level is normalized regarding the maximum value for each gene according to the GigaTON database. **C.** GO term distribution among the three expression clusters in B. **D**. Examples of GO term enrichment within the expression clusters of the m^{6}A-bound proteins. The –log10(p-value) associated to each term is given. E: Egg, 2/8C: two to eight cells, M: Morula, B: Blastula, G: Gastrula, T: Trochophore, D: D larvae, S: Spat, J: Juvenile.

Supporting information:

Data S1: Complete list of *in silico* identified putative m^{6}A machinery proteins and their respective BLAST results

Data S2: Identified proteins by RNA pull down coupled with mass spectrometry with m^{6}A or A-oligo, in nuclear or cytosolic protein extracts

Data S3: Complete list of GO terms of clustered genes of m^6A interacting proteins (p-value<0,05)

Table S1: Transitions used for each compound. A: first transition, B: second transition

Table S2: Table of correspondence between development stages in our study, and the GigaTON database.

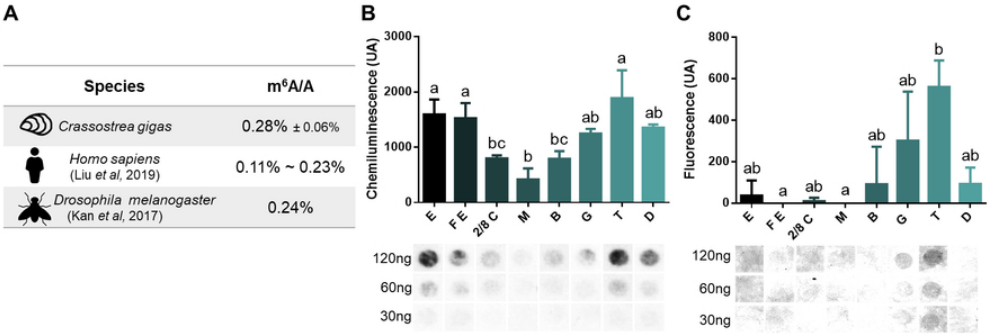

Figure 1: m6A levels across oyster development.
A. m6A level quantified by LC-MS/MS in Crassostrea gigas embryo-larval stages pooled from oocytes to D-larvae (n= 3) is compared to the m6A level in Homo sapiens and Drosophila melanogaster; B. Dot blot quantification of m6A in total RNA throughout oyster development (n=3); C. Dot blot quantification of m6A in polyA+ RNAs throughout oyster development (n=3) Kruskal-Wallis test, α < 0,05. E: Egg, F E: fertilized egg, 2/8C: two to eight cell embryos, M: Morula, B: Blastula, G: Gastrula, T: Trochophore, D: D larvae. Chemiluminescence (B) and fluorescence (C) are measured as a ratio between dot intensity of development stages and their respective controls for each amount of RNA (120ng, 60ng and 30ng).

75x25mm (300 x 300 DPI)

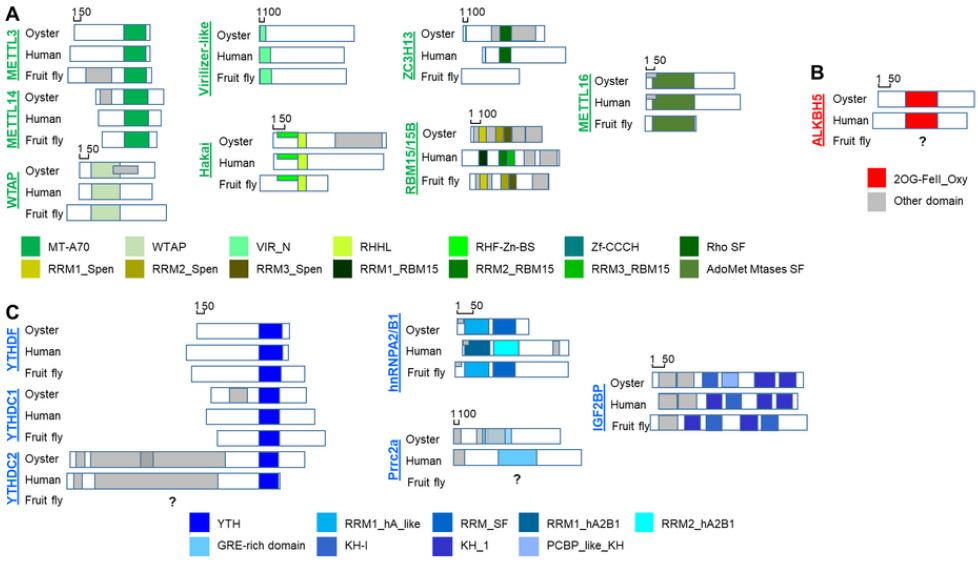

Figure 2: The putative conserved m6A machinery in Crassostrea gigas.
Domain architecture of actors of the m6A machinery identified by in silico analyses in the oyster compared to the fruit fly and human, A. Writer proteins; B. Eraser protein; C. Reader proteins. Putative domains involved in m6A processes are coloured (writers, green; eraser, red; readers, blue). Other domains identified but not involved in m6A processes are indicated in grey. Only one isoform is represented for each protein and each species for clarity (see supplementary figure S2 for other isoforms).

80x47mm (300 x 300 DPI)

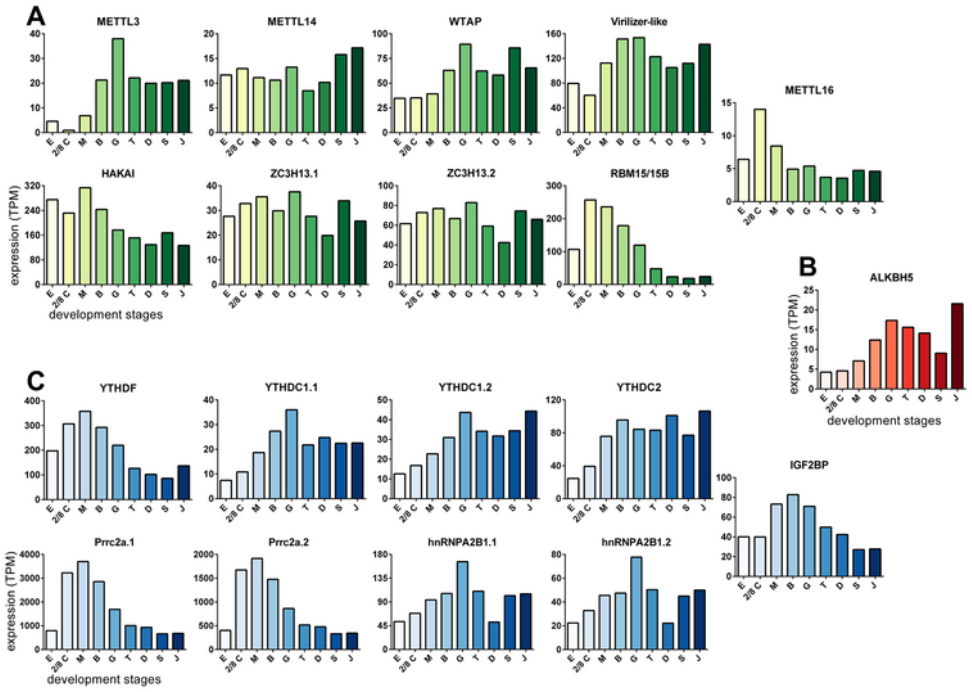

Figure 3: Gene expression of the putative m6A machinery throughout oyster development
Expression levels of writers (A), eraser (B) and readers (C) identified by in silico analysis at each development stage were inferred from the GigaTON database. Expression levels are given in Transcripts Per kilobases per Million Reads (TPM) as the mean of the GigaTON values according to the table S2. E: Egg, 2/8C: two to eight cell, M: Morula, B: Blastula, G: Gastrula, T: Trochophore, D: D larvae, S: Spat, J: Juvenile.

65x46mm (300 x 300 DPI)

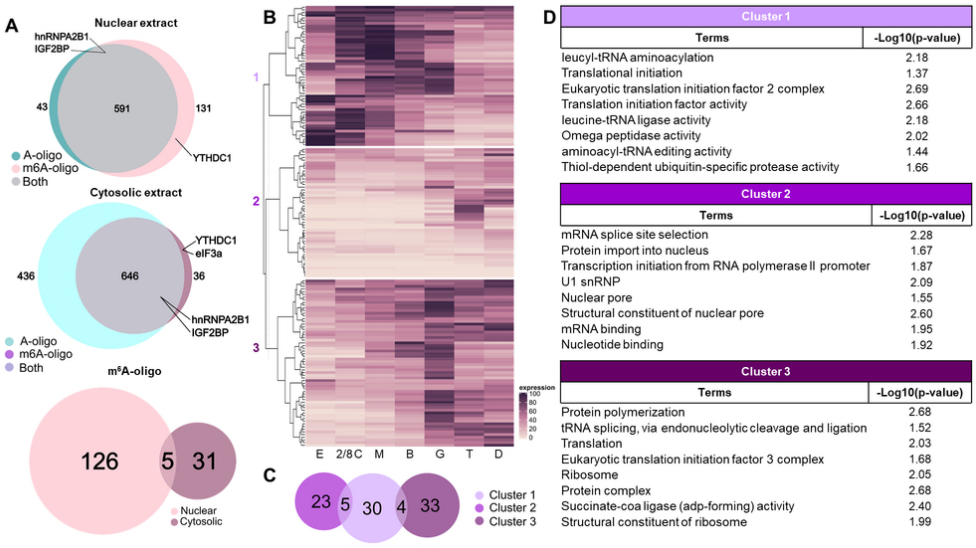

Figure 4: Characterization of m6A-RNA binding proteins in oyster development.
A. Venn diagrams representation of proteins bound to the A- and/or m6A- oligos in nuclear and cytosolic fractions of oyster embryo-larval stages. The number of proteins identified is indicated. Some actors characterized in this study are highlighted: eIF3, YTHC1, hnRNPA2B1 and IGF2BP. B. Heatmap of gene expression levels of the proteins that bind specifically to the m6A-oligo throughout oyster development. The expression level is normalized regarding the maximum value for each gene according to the GigaTON database. C. GO term distribution among the three expression clusters in B. D. Examples of GO term enrichment within the expression clusters of the m6A-bound proteins. The –log10(p-value) associated to each term is given. E: Egg, 2/8C: two to eight cells, M: Morula, B: Blastula, G: Gastrula, T: Trochophore, D: D larvae, S: Spat, J: Juvenile.

85x49mm (300 x 300 DPI)

Data S1: Complete list of in silico identified putative m6A machinery proteins and their respective BLAST results

Probable assembly artefact highlighted in grey

Specie	database	sequence accession number	length	conserved domain
METTL3				
Homo sapiens	NCBI	**gi|21361827 (NP_062826.2)**	580	MT-A70
Drosophila melanogaster (IME4)	NCBI	**gi|21355141 (NP_651204.1)**	608	MT-A70 MDN1
Crassostrea gigas	GIGATON	**CHOYP_PHUM_PHUM423190.1.1**	554	MT-A70
	NCBI	gi|762092209 (XP_011428532.1)	555	MT-A70
METTL14				
Homo sapiens	NCBI	**gi|24308265 (NP_066012.1)**	456	MT-A70
Drosophila melanogaster (CG7818)	NCBI	**gi|19920926 (NP_609205.1)**	397	MT-A70
Crassostrea gigas	GIGATON	**CHOYP_MET14.1.1**	495	MT-A70 MttA_Hfc106
		CHOYP_LOC100743733.1.1	723	MT-A70 7tmA_NPR-like_invertebrate
	NCBI	gi|762082967 (XP_011424173.1)	470	MT-A70 MttA_Hfc106
WTAP				
Homo sapiens	NCBI	**gi|395455090 (NP_001257460.1)**	396	WTAP
		gi|23199974 (NP_690596.1)	151	WTAP
		gi|395455092 (NP_001257461.1)	170	WTAP
Drosophila melanogaster (FL(2)D)	NCBI	**gi|24653459 (NP_523732.2)**	536	WTAP
		gi|24653461 (NP_725327.1)	412	WTAP
Crassostrea gigas	GIGATON	**CHOYP_FL2D.1.1**	406	WTAP IncA
		CHOYP_SODM.1.2	252	WTAP IncA
		CHOYP_LOC100121674.1.1	290	WTAP IncA
	NCBI	gi|762078268 (XP_011453082.1)	406	WTAP IncA

VIRILIZER-LIKE

Homo sapiens (Virilizer-like, VIRMA)	NCBI	**gi|33946282 (NP_056311.2)**	1812	VIR_ N
		gi|33946280 (NP_892121.1)	1147	VIR_ N
Drosophila melanogaster (Virilizer)	NCBI	**gi|17864576 (NP_524900.1)**	1854	VIR_ N
Crassostrea gigas	GIGATON	**CHOYP_VIR.1.1**	2021	VIR_ N
	NCBI	gi|762120202 (XP_011443024.1)	2023	VIR_ N
		gi|762120200 (XP_011443023.1)	2023	VIR_ N
		gi|1139822239 (XP_019927346.1)	2022	VIR_ N
		gi|1139822241 (XP_019927347.1)	2021	VIR_ N
		gi|1139822243 (XP_019927348.1)	1717	VIR_ N PTZ00249 super family

HAKAI

Homo sapiens	NCBI	**gi|209180481 (NP_079090.2)**	491	RHF-Zn-BS RHHL
		gi|546230945 (NP_001271220.1)	490	RHF-Zn-BS RHHL
Drosophila melanogaster	NCBI	**gi|19921556 (NP_609993.1)**	302	RHF-Zn-BS RHHL
		gi|24585301 (NP_724217.1)	311	RHF-Zn-BS RHHL
		gi|442628448 (NP_788075.2)	464	RHF-Zn-BS RHHL
		gi|442628450 (NP_001260593.1)	473	RHF-Zn-BS RHHL
Crassostrea gigas	GIGATON	**CHOYP_LOC100864501.1.1**	504	RHF-Zn-BS RHHL PHA03247 super family
	NCBI	gi|762140345 (XP_011453340.1)	498	RHF-Zn-BS RHHL PHA03247 super family
		gi|762140347 (XP_011453341.1)	497	RHF-Zn-BS RHHL PHA03247 super family

ZC3H13

Homo sapiens	NCBI	**gi|1060099240 (NP_001317493.1)**	1669	Zf-CCCH Rho SF
		gi|1060099108 (NP_001317496.1)	1668	Zf-CCCH Rho SF

		gi|116008442 (NP_055885.3)	1564	Zf-CCCH Rho SF
Drosophila melanogaster (CG7358)	NCBI	**gi|24643154 (NP_573339.1)**	1150	
		gi|665392303 (NP_001285418.1)	1139	
		gi|665392305 (NP_001285419.1)	842	
Crassostrea gigas	GIGATON	**CHOYP_BRAFLDRAFT_120702.1.1**	1631	Zf-CCCH Rho SF dnaA super family PTZ00121
		CHOYP_LOC100568158.1.1	1611	Zf-CCCH Rho SF dnaA super family PTZ00121
	NCBI	gi|762096734 (XP_011430912.1)	1400	Rho SF dnaA super family PTZ00121
		gi|762096736 (XP_011430913.1)	1400	Rho SF dnaA super family PTZ00121
		gi|762096738 (XP_011430914.1)	1380	Rho SF PHA03307 PTZ00121
		gi|762096740 (XP_011430915.1)	1329	Rho SF PTZ00121

RBM15/15B

Homo sapiens	NCBI	**gi|47933339 (NP_073605)**	977	RRM1_RBM15 RRM2_RBM15 RRM3_RBM15 SF-CC1 SPOC
		gi|319996623 (NP_001188474)	969	RRM1_RBM15 RRM2_RBM15 RRM3_RBM15 SF-CC1 SPOC
		gi|54607124 (NP_037418)	890	RRM1_RBM15 RRM2_RBM15 RRM3_RBM15 U2AF_Ig SF SPOC
Drosophila melanogaster (SPENITO/NITO)	NCBI	**gi|24586450 (NP_724633)**	793	RRM1_Spen RRM2_Spen RRM3_Spen RRM SPOC
		gi|19921778 (NP_610339)	793	RRM1_Spen RRM2_Spen RRM3_Spen RRM SPOC
		gi|665399388 (NP_001286174)	793	RRM1_Spen RRM2_Spen RRM3_Spen RRM SPOC
Crassostrea gigas	GIGATON	**CHOYP_LOC663518.1.1**	717	RRM1_Spen RRM2_Spen RRM3_Spen RRM SPOC PTZ00449 SF
	NCBI	gi|762129377 (XP_011447812)	717	RRM1_Spen RRM2_Spen RRM3_Spen RRM SPOC PTZ00449 SF

METTL16

Homo sapiens	NCBI	**gi|122114654 (NP_076991.3)**	562	AdoMet Mtases SF S-adenosylmethionine binding site
Drosophila melanogaster (CG7544)	NCBI	**gi|19922302 (NP_611015.1)**	305	AdoMet Mtases SF
	GIGATON	**CHOYP_LOC100561572.1.1**	527	AdoMet Mtases SF S-adenosylmethionine binding site

Crassostrea gigas	NCBI	gi|762141911 (XP_011454156.1)	538	AdoMet Mtases SF · S-adenosylmethionine binding site
		gi|762141913 (XP_011454157.1)	527	AdoMet Mtases SF · S-adenosylmethionine binding site

ALKBH5

Homo sapiens	NCBI	**gi|148539642 (NP_060228.3)**	394	2OG-FeII_Oxy
Drosophila melanogaster				
Crassostrea gigas	GIGATON	**CHOYP_BRAFLDRAFT_126925.1.1**	403	2OG-FeII_Oxy
	NCBI	gi|762097205 (XP_011431161.1)	374	2OG-FeII_Oxy

YTHDC1

Homo sapiens	NCBI	**gi|72534750 (NP_001026902.1)**	727	YTH
		gi|94536805 (NP_588611.2)	709	YTH
		gi|1061213987 (NP_001317627.1)	735	YTH
Drosophila melanogaster (YT521)	NCBI	**gi|24656811 (NP_647811.2)**	721	YTH
		gi|24656816 (NP_728876.1)	710	YTH
Crassostrea gigas	GIGATON	**CHOYP_YTDC1.2.2**	636	YTH · CDC27
		CHOYP_LOC586835.1.1	545	YTH · CDC27
	NCBI	gi|762070401 (XP_011447601.1)	636	YTH · CDC27

YTHDC2

Homo sapiens	NCBI	**gi|269847874 (NP_073739.3)**	1430	YTH · HrpA · R3H_DEXH_helicase · DEXHc_YTHDC2 · OB_NTP_bind
		gi|1066536696 (NP_001332904.1)	1268	YTH · HrpA · DEXHc_YTHDC2 · OB_NTP_bind
		gi|1066546270 (NP_001332905.1)	1130	YTH · HrpA · DEAD-like_helicase_N SF · ANKYR · OB_NTP_bind
Drosophila melanogaster				
Crassostrea gigas	GIGATON	**CHOYP_YTDC2.1.1**	1572	YTH · HrpA · R3H super family · Ank_2
	NCBI	gi|762086858 (XP_011425711.1)	1572	YTH · HrpA · R3H super family · Ank_2

YTHDF

Homo sapiens	NCBI	gi|29791407 (AAH50284.1)	559	YTH RPA_2b-aaRSs_OBF_like PHA03247 super family
		gi| 12803469 (AAH02559.1)	579	YTH
		gi|31419299 (AAH52970.1)	585	YTH
Drosophila melanogaster (CG6422)		**gi|21356147 (NP_651322.1)**	700	YTH
		gi|24649883 (NP_733067.1)	699	YTH
		gi|161078590 (NP_001097905.1)	694	YTH
Crassostrea gigas	GIGATON	CHOYP_COX1.6.15	532	YTH
		CHOYP_LOC100371022.1.1	531	YTH
	NCBI	gi|762146089 (XP_011456337.1)	522	YTH

hnRNPA2B1

Homo sapiens	NCBI	**gi|4504447 (NP_002128.1)**	341	RRM1_hA2B1 RRM2_hA2B1 Putative DNA binding site hnRNPA1
		gi|14043072 (NP_112533.1)	353	RRM1_hA2B1 RRM2_hA2B1 Putative DNA binding site hnRNPA1
Drosophila melanogaster (hrb98DE)	NCBI	**gi|24650831 (NP_733249.1)**	364	RRM1_hA_like RRM_SF Putative DNA binding site
		gi|17738267 (NP_524543.1)	365	RRM1_hA_like RRM_SF Putative DNA binding site
		gi|24650838 (NP_733252.1)	361	RRM1_hA_like RRM_SF Putative DNA binding site
		gi|24650833 (NP_733250.1)	360	RRM1_hA_like RRM_SF Putative DNA binding site
Crassostrea gigas	GIGATON	CHOYP_LOC100748395.1.7	229	RRM1_hA_like RRM_SF Putative DNA binding site
		CHOYP_LOC100748395.2.7	394	RRM1_hA_like RRM_SF Putative DNA binding site
		CHOYP_LOC100748395.3.7	315	RRM1_hA_like RRM_SF Putative DNA binding site
		CHOYP_LOC100748395.4.7	372	RRM1_hA_like RRM_SF Putative DNA binding site
		CHOYP_LOC100748395.6.7	315	RRM1_hA_like RRM_SF Putative DNA binding site
		CHOYP_AGAP_AGAP002374.1.1	236	RRM_SF

		CHOYP_LOC100748395.5.7	205	RRM_SF
	NCBI	gi|762104361 (XP_011434715.1)	370	RRM1_hA_like RRM_SF Putative DNA binding site
		gi|762104364 (XP_011434716.1)	369	RRM1_hA_like RRM_SF Putative DNA binding site
		gi|762104366 (XP_011434717.1)	363	RRM1_hA_like RRM_SF Putative DNA binding site
		gi|762104368 (XP_011434718.1)	353	RRM1_hA_like RRM_SF Putative DNA binding site

Prrc2a

Homo sapiens	NCBI	**gi|314122241 (NP_004629.3)**	2157	GRE-rich domain BAT2_N
Drosophila melanogaster				
Crassostrea gigas	GIGATON	**CHOYP_LOC100559941.1.2**	2578	GRE-rich domain BAT2_N PTZ00121 PTZ00449
		CHOYP_LOC100559941.2.2	2554	GRE-rich domain BAT2_N PTZ00121 PTZ00449
		gi|1139830093 (XP_019928978.1)	2922	GRE-rich domain BAT2_N PTZ00121 PTZ00449

IGF2BP

Homo sapiens	NCBI	**gi|56237027 (NP_006537.3)**	577	KH-I KH-1 RRM1_IGF2BP1 RRM2_IGF2BP1
		gi|238624257 (NP_001153895.1)	438	KH-I KH-1 RRM1_IGF2BP1 RRM_SF super family
		gi|64085377 (NP_006539.3)	599	KH-I KH-1 PCBP_like_KH RRM1_IGF2BP2 RRM2_IGF2BP2
		gi|56118219 (NP_001007226.1)	556	KH-I KH-1 PCBP_like_KH RRM1_IGF2BP2 RRM2_IGF2BP2
		gi|631226390 (NP_001278798.1)	605	KH-I KH-1 PCBP_like_KH RRM1_IGF2BP2 RRM_SF super family
		gi|631226392 (NP_001278801.1)	542	KH-I KH-1 PCBP_like_KH RRM_SF super family
		gi|631226396 (NP_001278802.1)	536	KH-I KH-1 PCBP_like_KH RRM2_IGF2BP2
		gi|631226394 (NP_001278803.1)	493	KH-I KH-1 PCBP_like_KH RRM2_IGF2BP2
		gi|631226398 (NP_001278804.1)	463	KH-I KH-1 PCBP_like_KH RRM_SF super family
		gi|30795212 (NP_006538.2)	579	KH-I KH-1 PCBP_like_KH RRM1_IGF2BP3 RRM2_IGF2BP3
		gi|386764188 (NP_001036268.2)	631	KH-I KH-1 RRM2_VICKZ

Drosophila melanogaster (IGF-II binding protein)	NCBI	gi|386764191 (NP_001245616.1)	638	KH-I KH-1 RRM2_VICKZ
		gi|17530887 (NP_511111.1)	566	KH-I KH-1
		gi|24641097 (NP_727451.1)	573	KH-I KH-1
		gi|281360685 (NP_001162717.1)	580	KH-I KH-1
Crassostrea gigas	GIGATON	**CHOYP_LOC100114171.1.1**	607	KH-I KH-1 PCBP_like_KH RRM1_VICKZ RRM_SF super family
	NCBI	gi|762079091 (XP_011412002.1)	611	KH-I KH-1 PCBP_like_KH RRM1_VICKZ RRM_SF super family
		gi|762079093 (XP_011412008.1)	607	KH-I KH-1 PCBP_like_KH RRM1_VICKZ RRM_SF super family
		gi|762079095 (XP_011412017.1)	590	KH-I KH-1 PCBP_like_KH RRM1_VICKZ RRM_SF super family

eIF3a

Homo sapiens	NCBI	gi|4503509(NP_003741.1)	1382	PINT Smc super family U2AF_Ig super family dnaA super family Rho SF
Drosophila melanogaster (IGF-II binding protein)	NCBI	gi|665393171 (NP_730838.3)	1140	PINT DUF5401 Rho SF
		gi|24643988 (NP_649470.2)	1140	PINT DUF5401 Rho SF
Crassostrea gigas	GIGATON	CHOYP_BRAFLDRAFT_75590.1.1	155	
		CHOYP_UBP47.2.2	1253	PAM DUF5401
		CHOYP_MROH1.1.1	1046	PAM DUF5401
	NCBI	gi|762160635 (XP_011418535.1)	759	PAM DUF5401
		gi|762122193 (XP_011444042.1)	1252	PAM DUF5401

Data S1: Complete list of in silico identified putative m6A machinery proteins and their respective BLAST results

	Crassostrea gigas	*Homo sapiens*									*Drosophila melanogaster*			
METTL3	CHOYP_PHUM_PHUM423190.1.1 gi|762092209 (XP_011428532.1)	gi|21361827 (NP_062826.2) 52.3% 52.81%									gi|21355141 (NP_651204.1) 73.26% 73.96%			
METTL14	CHOYP_MET14.1.1 CHOYP_LOC100743733.1.1 gi|762082967 (XP_011424173.1)	gi|24308265 (NP_066012.1) 62.03% 60.88% 61.58%									gi|19920926 (NP_609205.1) 58.05% 57.76% 58.05%			
WTAP	CHOYP_FL2D.1.1 CHOYP_SODM.1.2 CHOYP_LOC100121674.1.1 gi|762078268 (XP_011453082.1)	gi|395455090 (NP_001257460.1) 52.68% 47.55% 52.68% 51.06%	gi|23199974 (NP_690596.1) 47.55% 47.92% 47.55% 47.55%	gi|395455092 (NP_001257461.1) 47.55% 47.65% 47.55% 47.55%							gi|24653459 (NP_523732.2) 56.16% 60.40% 56.16% 53.49%	gi|24653461 (NP_725327.1) 58.42% 60.40% 58.42% 58.42%		
VIRILIZER-like	CHOYP_VIR.1.1 gi|762120202 (XP_011443024.1) gi|762120200 (XP_011443023.1) gi|1139822239 (XP_019927346.1) gi|1139822241 (XP_019927347.1) gi|1139822243 (XP_019927348.1)	gi|33946282 (NP_056311.2) 30.70% 30.85% 30.85% 30.89% 30.95% 30.62%	gi|33946280 (NP_892121.1) 29.59% 30.17% 30.17% 30.17% 30.24% 30.35%								gi|17864576 (NP_524900.1) 25.49% 25.49% 25.49% 25.49% 25.49% 26.04%			
HAKAI	CHOYP_LOC100864501.1.1 gi|762140345 (XP_011453340.1) gi|762140347 (XP_011453341.1)	gi|209180481 (NP_079090.2) 43.27% 29.43% 29.28%	gi|546230945 (NP_001271220.1) 43.96% 29.68% 29.68%								gi|19921556 (NP_609993.1) 60.45% 56.29% 57.14%	gi|24585301 (NP_724217.1) 60.45% 60.45% 60.45%	gi|442628448 (NP_788075.2) 60.45% 56.29% 57.14%	gi|442628450 (NP_001260593.1) 60.45% 60.45% 60.45%
ZC3H13	CHOYP_BRAFLDRAFT_120702.1.1 CHOYP_LOC100568158.1.1 gi|762096734 (XP_011430912.1) gi|762096736 (XP_011430913.1) gi|762096738 (XP_011430914.1) gi|762096740 (XP_011430915.1)	gi|1060099240 (NP_001317493.1) 37.11% 37.11% 31.48% 31.48% 31.48% 31.68%	gi|1060099108 (NP_001317496.1) 37.11% 37.11% 31.48% 31.48% 31.48% 31.68%	gi|116008442 (NP_055885.3) 37.11% 37.11% 40.00% 40.00% 40.00% 40.58%							gi|24643154 (NP_573339.1) N/A N/A N/A N/A N/A N/A	gi|665392303 (NP_001285418.1) N/A N/A N/A N/A N/A N/A	gi|665392305 (NP_001285419.1) N/A N/A N/A N/A N/A N/A	
RBM15/15B	CHOYP_LOC663518.1.1 gi|762129377 (XP_011447812)	gi|47933339 (NP_073605) 56.73% 41.64%	gi|319996623 (NP_001188474) 56.73% 41.64%	gi|54607124 (NP_037418) 61.59% 34.94%							gi|24586450 (NP_724633) 59.22% 42.75%	gi|19921778 (NP_610339) 59.22% 42.75%	gi|665399388 (NP_001286174) 59.22% 42.75%	
METTL16	CHOYP_LOC100561572.1.1 gi|762141911 (XP_011454156.1) gi|762141913 (XP_011454157.1)	gi|122114654 (NP_076991.3) 38.05% 37.68% 37.68%									gi|19922302 (NP_611015.1) 38.81% 39.16% 39.16%			
ALKBH5	CHOYP_BRAFLDRAFT_126925.1.1 gi|762097205 (XP_011431161.1)	gi|148539642 (NP_060228.3) 72.43% 72.43%												
YTHDC1	CHOYP_YTDC1.2.2 CHOYP_LOC580835.1.1 gi|762070401 (XP_011447601.1)	gi|72534750 (NP_001026902.1) 46.61% 51.52% 43.92%	gi|94536805 (NP_588611.2) 46.61% 51.52% 44.52%	gi|1061213987 (NP_001317627.1) 45.30% 52.27% 42.86%							gi|24656811 (NP_647811.2) 57.74% 57.74% 46.53%	gi|24656816 (NP_728876.1) 57.74% 57.74% 46.53%		
YTHDC2	CHOYP_YTDC2.1.1 gi|762086858 (XP_011425711.1)	gi|269847874 (NP_073739.3) 52.99% 53.09%	gi|1066536696 (NP_001332904.1) 53.66% 53.77%	gi|1066546270 (NP_001332905.1) 51.83% 52.05%										
YTHDF	CHOYP_COX1.6.15 CHOYP_LOC100371022.1.1 gi|762146089 (XP_011456337.1)	gi|29791407 (AAH50284.1) 53.09% 53.09% 43.49%	gi| 12803469 (AAH02559.1) 53.77% 53.77% 71.21%	gi|31419299 (AAH52970.1) 52.05% 52.05% 71.72%							gi|21356147 (NP_651322.1) 71.51% 71.51% 71.20%	gi|24649883 (NP_733067.1) 71.51% 71.51% 71.20%	gi|161078590 (NP_001097905.1) 71.51% 71.51% 71.20%	
hnRNPA2B1	CHOYP_LOC100748395.1.7 CHOYP_LOC100748395.2.7 CHOYP_LOC100748395.3.7 CHOYP_LOC100748395.4.7 CHOYP_LOC100748395.6.7 CHOYP_AGAP_AGAP002374.1.1 CHOYP_LOC100748395.5.7 gi|762104361 (XP_011434715.1) gi|762104364 (XP_011434716.1) gi|762104366 (XP_011434717.1) gi|762104368 (XP_011434718.1)	gi|4504447 (NP_002128.1) 55.37% 55.37% 55.37% 55.37% 55.37% 54.24% 55.37% 55.37% 54.80% 55.37% 55.37%	gi|14043072 (NP_112533.1) 54.71% 54.71% 54.71% 54.71% 54.71% 53.53% 54.71% 55.37% 54.80% 55.37% 55.37%								gi|24650831 (NP_733249.1) 58.14% 58.14% 58.14% 58.14% 58.14% 58.72% 58.14% 58.14% 58.72% 58.14% 50.63%	gi|17738267 (NP_524543.1) 58.14% 58.14% 57.71% 58.14% 57.71% 58.29% 58.14% 58.14% 58.72% 58.14% 50.63%	gi|24650838 (NP_733252.1) 58.14% 58.14% 58.14% 58.14% 58.14% 58.29% 58.14% 58.14% 58.72% 58.14% 50.63%	gi|24650833 (NP_733250.1) 58.14% 58.14% 58.14% 58.14% 58.14% 56.83% 58.14% 58.14% 58.72% 58.14% 50.63%
Prrc2a	CHOYP_LOC100559941.1.2 CHOYP_LOC100559941.2.2 gi|1139830093 (XP_019928978.1)	gi|314122241 (NP_004629.3) 46.02% 46.02% 34.66%												
IGF2BP	CHOYP_LOC100114171.1.1 gi|762070091 (XP_011412002.1) gi|762079093 (XP_011412008.1) gi|762079095 (XP_011412017.1)	gi|56237027 (NP_006537.3) 34.87% 34.80% 35.04% 34.80%	gi|238624257 (NP_001153895.1) 35.71% 36.39% 36.39% 36.39%	gi|64085377 (NP_006539.3) 35.86% 35.96% 36.20% 35.96%	gi|56118219 (NP_001007226.1) N/A 36.52% 36.77% 36.52%	gi|631226390 (NP_001278798.1) 35.50% 35.61% 36.11% 35.88%	gi|631226392 (NP_001278801.1) 34.93% 35.53% 35.83% 35.53%	gi|631226396 (NP_001278802.1) 35.34% 35.93% 35.93% 36.24%	gi|631226394 (NP_001278803.1) 35.85% 36.38% 36.38% 36.38%	gi|631226398 (NP_001278804.1) 38.61% 39.76% 39.76% 39.76%	gi|30795212 (NP_006538.2) 33.16% 33.78% 34.01% 33.78%	gi|386764188 (NP_001036268.2) 42.72% 42.83% 42.77% 42.83%	gi|386764191 (NP_001245616.1) 42.26% 42.83% 42.45% 42.83%	gi|17530887 (NP_511111.1) 44.89% 45.07% 45.07% 45.07%	gi|24641097 (NP_727451.1) 44.89% 45.07% 45.07% 45.07%	gi|281360685 (NP_001162717.1) 44.20% 44.37% 44.52% 44.37%
eIF3a	CHOYP_BRAFLDRAFT_75590.1.1 CHOYP_UBP47.2.2 CHOYP_MROH1.1.1 gi|762160635 (XP_011418535.1) gi|762122193 (XP_011444042.1)	gi|4503509(NP_003741.1) 40.86% 63.83% 63.71% 54.20% 58.13%									gi|665393171 (NP_730838.3) 45.97% 50.89% 50.89% 44.99% 48.45%	gi|24643988 (NP_649470.2) 45.97% 50.89% 50.89% 44.99% 48.45%		

Data S2: Identified proteins by RNA pull down coupled with mass spectrometry with m6A or A-oligo, in nuclear or cytosolic protein extracts

Proteins identified in nuclear extracts

Oligo	Accession	Description
m6A	K1PTY5_CRAGI	Protocadherin Fat 4
m6A	K1QNA2_CRAGI	Vitellogenin-6
m6A	K1QBR5_CRAGI	Uncharacterized protein
m6A	K1PFG1_CRAGI	Uncharacterized protein
m6A	K1P9A4_CRAGI	Beta-1,3-glucan-binding protein
m6A	K1QHI5_CRAGI	Pyruvate carboxylase, mitochondrial
m6A	K1QQ94_CRAGI	Uncharacterized protein
m6A	K1R5B4_CRAGI	Proteasome activator complex subunit 4
m6A	K1R164_CRAGI	Galectin-4
m6A	K1PNI6_CRAGI	Heterogeneous nuclear ribonucleoprotein A/B
m6A	K1QMX5_CRAGI	Uncharacterized protein
m6A	K1PQP2_CRAGI	Nucleolin
m6A	K1QXR4_CRAGI	Pancreatic lipase-related protein 2
m6A	K1R7V7_CRAGI	Tubulin beta chain
m6A	K1RGT5_CRAGI	Metalloendopeptidase
m6A	K1QSX8_CRAGI	ATPase family AAA domain-containing protein 2B
m6A	K1R9B6_CRAGI	H/ACA ribonucleoprotein complex subunit 4
m6A	K1RWS2_CRAGI	Transcriptional activator protein Pur-alpha
m6A	K1RLF8_CRAGI	Splicing factor 3B subunit 3
m6A	K1R3U2_CRAGI	Uncharacterized protein
m6A	K1QQ68_CRAGI	Tubulin alpha chain
m6A	K1QVJ8_CRAGI	Piwi-like protein 1
m6A	K1PVA1_CRAGI	Transitional endoplasmic reticulum ATPase
m6A	K1QKB5_CRAGI	Uncharacterized protein
m6A	K1QHM2_CRAGI	Dolichyl-diphosphooligosaccharide--protein glycosyltransferase subunit 2
m6A	K1QII6_CRAGI	Tubulin alpha chain
m6A	K1QSQ9_CRAGI	Putative ATP-dependent RNA helicase an3
m6A	K1QQ27_CRAGI	Pancreatic lipase-related protein 2
m6A	K1QMA4_CRAGI	RRP5-like protein
m6A	K1PEP0_CRAGI	40S ribosomal protein S8
m6A	K1QXX7_CRAGI	Myosin heavy chain, non-muscle (Fragment)
m6A	K1QK56_CRAGI	Uncharacterized protein
m6A	K1PNR3_CRAGI	Clathrin heavy chain
m6A	K1PN21_CRAGI	Tubulin beta chain
m6A	K1RG73_CRAGI	Acetyl-CoA carboxylase
m6A	K1RD58_CRAGI	Uncharacterized protein
m6A	K1QU53_CRAGI	NAD(P) transhydrogenase, mitochondrial
m6A	K1R473_CRAGI	Tubulin alpha chain
m6A	K1PH76_CRAGI	Y-box factor-like protein (Fragment)
m6A	K1PE00_CRAGI	Tubulin alpha chain
m6A	K1PJC1_CRAGI	Adipophilin
m6A	K1R6Z7_CRAGI	ATP synthase subunit alpha
m6A	K1R545_CRAGI	Pre-mRNA-processing-splicing factor 8 (Fragment)
m6A	K1RI55_CRAGI	Insulin-like growth factor 2 mRNA-binding protein 3
m6A	K1QGS8_CRAGI	Elongation factor 1-alpha
m6A	K1QFM6_CRAGI	Vitellogenin
m6A	K1R6Q7_CRAGI	DNA topoisomerase I
m6A	K1Q988_CRAGI	Band 4.1-like protein 3
m6A	K1QLS3_CRAGI	Cytochrome b-c1 complex subunit 2, mitochondrial
m6A	K1RWW5_CRAGI	ATP synthase subunit beta
m6A	K1S2N7_CRAGI	Innexin
m6A	K1P421_CRAGI	Histone H2A
m6A	K1RK12_CRAGI	40S ribosomal protein S23
m6A	K1QKD6_CRAGI	Uncharacterized protein
m6A	K1QWZ6_CRAGI	Dolichyl-diphosphooligosaccharide--protein glycosyltransferase subunit 1
m6A	K1QFN2_CRAGI	Uncharacterized protein
m6A	K1PHW2_CRAGI	Uncharacterized protein

m6A	K1PJ06_CRAGI	Importin subunit alpha-1
m6A	K1QA13_CRAGI	Calcium-transporting ATPase
m6A	K1R0L4_CRAGI	Sodium/potassium-transporting ATPase subunit alpha
m6A	K1R115_CRAGI	Succinate dehydrogenase [ubiquinone] flavoprotein subunit, mitochondrial
m6A	K1QB61_CRAGI	Protocadherin Fat 4
m6A	K1Q4H2_CRAGI	Nodal modulator 3
m6A	K1QWK2_CRAGI	MAM domain-containing glycosylphosphatidylinositol anchor protein 2
m6A	K1R466_CRAGI	T-complex protein 1 subunit gamma
m6A	K1QFW9_CRAGI	Uncharacterized protein
m6A	K1R5U4_CRAGI	Acetyl-CoA carboxylase 1
m6A	A5LGH1_CRAGI	Voltage-dependent anion channel
m6A	K1S4Q2_CRAGI	T-complex protein 1 subunit delta (Fragment)
m6A	K1REG6_CRAGI	DNA helicase
m6A	K1PUL2_CRAGI	Long-chain-fatty-acid--CoA ligase 1
m6A	K1R294_CRAGI	T-complex protein 1 subunit beta
m6A	K1PMT6_CRAGI	Heterogeneous nuclear ribonucleoprotein U-like protein 1
m6A	K1RGB7_CRAGI	Epidermal retinal dehydrogenase 2
m6A	K1R435_CRAGI	Splicing factor, arginine/serine-rich 4
m6A	K1R252_CRAGI	Putative methylmalonate-semialdehyde dehydrogenase [acylating], mitochondrial
m6A	K1QAE5_CRAGI	Uncharacterized protein
m6A	K1QIR8_CRAGI	78 kDa glucose-regulated protein
m6A	K1QYB3_CRAGI	Ig-like and fibronectin type-III domain-containing protein C25G4.10
m6A	K1QI14_CRAGI	40S ribosomal protein S3a
m6A	K1PNQ5_CRAGI	Heat shock protein HSP 90-alpha 1
m6A	K1S1S1_CRAGI	Insulin-like growth factor 2 mRNA-binding protein 1
m6A	K1QM19_CRAGI	Uncharacterized protein
m6A	K1R420_CRAGI	Non-specific serine/threonine protein kinase
m6A	K1R4R9_CRAGI	Mitotic apparatus protein p62
m6A	K1R0S3_CRAGI	T-complex protein 1 subunit theta
m6A	K1RAJ1_CRAGI	T-complex protein 1 subunit alpha
m6A	K1QH74_CRAGI	Splicing factor, arginine/serine-rich 1
m6A	K1QRL6_CRAGI	Methenyltetrahydrofolate synthetase domain-containing protein
m6A	K1QUC6_CRAGI	Uncharacterized protein
m6A	K1RIT6_CRAGI	NADH-ubiquinone oxidoreductase 75 kDa subunit, mitochondrial
m6A	K1RBF6_CRAGI	Uncharacterized protein yfeX
m6A	K1PCS4_CRAGI	Eukaryotic translation initiation factor 2 subunit 3, Y-linked
m6A	K1Q620_CRAGI	Uncharacterized protein
m6A	K1QWX2_CRAGI	60S acidic ribosomal protein P0
m6A	K1PD57_CRAGI	Constitutive coactivator of PPAR-gamma-like protein 1-like protein
m6A	K1Q4S5_CRAGI	Cadherin-87A
m6A	K1RQA0_CRAGI	Dolichyl-diphosphooligosaccharide--protein glycosyltransferase subunit 2
m6A	K1QMX8_CRAGI	DNA replication licensing factor MCM7
m6A	K1QPX8_CRAGI	Alkyl/aryl-sulfatase BDS1
m6A	K1QZW0_CRAGI	Polyadenylate-binding protein 2
m6A	K1RWX7_CRAGI	Metabotropic glutamate receptor 3
m6A	K1RFT1_CRAGI	Band 4.1-like protein 3
m6A	K1RNB5_CRAGI	Propionyl-CoA carboxylase beta chain, mitochondrial
m6A	K1QBK6_CRAGI	Splicing factor 3B subunit 1
m6A	K1Q0Z3_CRAGI	Estradiol 17-beta-dehydrogenase 11
m6A	K1R953_CRAGI	Acetyl-CoA carboxylase
m6A	K1QNN9_CRAGI	MICOS complex subunit MIC60
m6A	K1QXS6_CRAGI	Heterogeneous nuclear ribonucleoprotein A2-like protein 1
m6A	K1RJH5_CRAGI	Polyadenylate-binding protein
m6A	K1R0Y9_CRAGI	ADP,ATP carrier protein
m6A	K1R4D4_CRAGI	40S ribosomal protein SA
m6A	K1QWT8_CRAGI	Uncharacterized protein
m6A	K1Q0L1_CRAGI	60S ribosomal protein L23a
m6A	K1Q260_CRAGI	Nucleolar protein 58
m6A	K1QT04_CRAGI	Uncharacterized protein
m6A	K1Q9K6_CRAGI	Histone H3

m6A	K1QT21_CRAGI	Putative ATP-dependent RNA helicase DDX5
m6A	K1QBN0_CRAGI	Methylcrotonoyl-CoA carboxylase beta chain, mitochondrial
m6A	K1PLY1_CRAGI	DNA polymerase
m6A	K1QBH0_CRAGI	Uncharacterized protein
m6A	K1Q923_CRAGI	Putative ATP-dependent RNA helicase DDX4
m6A	K1QG58_CRAGI	Actin
m6A	K1QQB6_CRAGI	40S ribosomal protein S14
m6A	K1QDX9_CRAGI	Ribosome biogenesis protein BMS1-like protein
m6A	K1QF01_CRAGI	40S ribosomal protein S4
m6A	K1RLC5_CRAGI	T-complex protein 1 subunit epsilon
m6A	K1QY12_CRAGI	Dynamin-1-like protein
m6A	K1R0W4_CRAGI	Signal recognition particle subunit SRP72
m6A	K1QX26_CRAGI	Endoplasmin
m6A	K1QHS8_CRAGI	Ribonucleoside-diphosphate reductase
m6A	K1QQ05_CRAGI	Insulin-like growth factor-binding protein complex acid labile chain
m6A	K1QFP5_CRAGI	NADH dehydrogenase [ubiquinone] flavoprotein 1, mitochondrial
m6A	K1QP17_CRAGI	Caprin-1
m6A	K1R7A2_CRAGI	Uncharacterized protein
m6A	K1R4L8_CRAGI	Electron transfer flavoprotein-ubiquinone oxidoreductase, mitochondrial
m6A	K1R591_CRAGI	Inter-alpha-trypsin inhibitor heavy chain H4
m6A	K1R7I9_CRAGI	Heterogeneous nuclear ribonucleoprotein Q
m6A	K1QBW8_CRAGI	Uncharacterized protein
m6A	K1RSZ6_CRAGI	40S ribosomal protein S7
m6A	K1QDZ5_CRAGI	Cytochrome c1, heme protein, mitochondrial
m6A	K1PGW7_CRAGI	Transmembrane protein 2
m6A	K1QMB9_CRAGI	Eukaryotic translation initiation factor 3 subunit A
m6A	K1RNZ6_CRAGI	Eukaryotic translation initiation factor 3 subunit D
m6A	K1Q9W5_CRAGI	T-complex protein 1 subunit eta
m6A	K1Q404_CRAGI	DNA topoisomerase 2
m6A	K1R7J6_CRAGI	Putative sodium/potassium-transporting ATPase subunit beta-2
m6A	K1P8W6_CRAGI	60S ribosomal protein L4
m6A	K1RSA6_CRAGI	Methylcrotonoyl-CoA carboxylase subunit alpha, mitochondrial
m6A	K1RW85_CRAGI	Adenosylhomocysteinase
m6A	K1PS27_CRAGI	DNA helicase
m6A	K1RH18_CRAGI	Sarcalumenin
m6A	K1Q5H6_CRAGI	FACT complex subunit SSRP1
m6A	K1PH66_CRAGI	Fibrinolytic enzyme, isozyme C
m6A	K1PF10_CRAGI	PAN2-PAN3 deadenylation complex catalytic subunit PAN2
m6A	K1Q358_CRAGI	60S acidic ribosomal protein P2
m6A	K1PXH5_CRAGI	Putative saccharopine dehydrogenase
m6A	K1Q8S0_CRAGI	Nucleolar complex protein 3 homolog
m6A	K1QYB6_CRAGI	Delta-1-pyrroline-5-carboxylate synthetase
m6A	K1PV79_CRAGI	Importin subunit alpha
m6A	K1PV49_CRAGI	RuvB-like helicase
m6A	K1PRL4_CRAGI	60S ribosomal protein L38 (Fragment)
m6A	K1QL67_CRAGI	60S ribosomal protein L7a
m6A	K1PAY7_CRAGI	Propionyl-CoA carboxylase alpha chain, mitochondrial
m6A	K1R6L5_CRAGI	NADH-cytochrome b5 reductase
m6A	K1R1B1_CRAGI	35 kDa SR repressor protein
m6A	K1QHQ6_CRAGI	Acyl-CoA dehydrogenase family member 9, mitochondrial
m6A	K1QZU8_CRAGI	Calcium-transporting ATPase
m6A	K1RN77_CRAGI	Nuclear autoantigenic sperm protein
m6A	K1PZ23_CRAGI	DnaJ-like protein subfamily C member 3
m6A	K1R005_CRAGI	Filamin-C (Fragment)
m6A	K1RA35_CRAGI	Splicing factor, arginine/serine-rich 7
m6A	K1R2V1_CRAGI	Importin subunit beta-1
m6A	K1QAH9_CRAGI	H/ACA ribonucleoprotein complex subunit
m6A	K1QET2_CRAGI	Coatomer subunit alpha
m6A	K1RAB9_CRAGI	Epoxide hydrolase 4
m6A	K1QGK2_CRAGI	Coatomer subunit beta

m6A	K1PXN5_CRAGI	T-complex protein 1 subunit zeta
m6A	K1QHX2_CRAGI	La-related protein 7
m6A	K1PZ08_CRAGI	Ras-related protein Rab-7a
m6A	K1RK68_CRAGI	Uncharacterized protein
m6A	K1Q0R4_CRAGI	ATP-binding cassette sub-family F member 2
m6A	K1QW72_CRAGI	Catalase
m6A	K1PPP8_CRAGI	Vigilin
m6A	K1QVW3_CRAGI	Alkylglycerone-phosphate synthase
m6A	K1PBZ4_CRAGI	Regulator of nonsense transcripts 1
m6A	K1Q6W5_CRAGI	FACT complex subunit spt16
m6A	K1R5F2_CRAGI	14-3-3 protein epsilon
m6A	K1RLT4_CRAGI	Signal recognition particle subunit SRP68
m6A	K1RSS3_CRAGI	Myosin heavy chain, striated muscle
m6A	K1RNN9_CRAGI	Cytoskeleton-associated protein 5
m6A	K1QN11_CRAGI	Pre-mRNA-processing-splicing factor 8
m6A	K1PA54_CRAGI	Replication factor C subunit 3
m6A	K1QC78_CRAGI	Ras-related protein Rab-14
m6A	K1QW36_CRAGI	60S ribosomal protein L6
m6A	K1Q9P5_CRAGI	Mitochondrial-processing peptidase subunit beta
m6A	K1Q253_CRAGI	Neutral and basic amino acid transport protein rBAT
m6A	K1QHK9_CRAGI	Dynein heavy chain, cytoplasmic
m6A	K1QFN1_CRAGI	60S ribosomal protein L23
m6A	K1P112_CRAGI	ATP synthase subunit gamma, mitochondrial
m6A	K1QE71_CRAGI	DNA helicase
m6A	K1PK85_CRAGI	Cullin-associated NEDD8-dissociated protein 1
m6A	K1QTD9_CRAGI	Nucleolar protein 56
m6A	K1P9N7_CRAGI	14-3-3 protein zeta
m6A	K1RG19_CRAGI	Protein FAM98A
m6A	K1PMP3_CRAGI	Protoporphyrinogen oxidase
m6A	K1QVN9_CRAGI	T-complex protein 1 subunit eta
m6A	K1QG65_CRAGI	rRNA 2'-O-methyltransferase fibrillarin
m6A	K1PM76_CRAGI	NADH dehydrogenase [ubiquinone] 1 alpha subcomplex subunit 9, mitochondrial
m6A	K1PM50_CRAGI	40S ribosomal protein S16
m6A	K1QEF9_CRAGI	Protein-glutamine gamma-glutamyltransferase K
m6A	K1RKC1_CRAGI	Far upstream element-binding protein 3
m6A	K1PY89_CRAGI	Extracellular superoxide dismutase [Cu-Zn]
m6A	K1RIZ3_CRAGI	Bone morphogenetic protein 7
m6A	K1RA95_CRAGI	Filamin-A
m6A	K1PWZ3_CRAGI	Guanine nucleotide-binding protein subunit beta
m6A	K1Q812_CRAGI	NADH dehydrogenase [ubiquinone] iron-sulfur protein 2, mitochondrial
m6A	K1PFS5_CRAGI	Elongation factor 1-gamma
m6A	K1PX23_CRAGI	Eukaryotic peptide chain release factor subunit 1
m6A	K1QSV1_CRAGI	Uncharacterized protein
m6A	K1Q6X5_CRAGI	Protein disulfide-isomerase
m6A	K1RAU3_CRAGI	DNA ligase
m6A	K1PXG6_CRAGI	Serine/threonine-protein phosphatase
m6A	K1RIG6_CRAGI	LSM14-like protein A
m6A	K1QWK6_CRAGI	Metalloendopeptidase
m6A	K1RCW3_CRAGI	Elongation factor 1-beta
m6A	K1QK18_CRAGI	Cytochrome b5
m6A	K1Q056_CRAGI	Calpain-A
m6A	K1Q9M7_CRAGI	Histone H1-delta
m6A	K1P7L5_CRAGI	Transmembrane 9 superfamily member
m6A	K1QSU3_CRAGI	Protein l(2)37Cc
m6A	K1PLF9_CRAGI	Arginine kinase
m6A	K1Q1F4_CRAGI	60S ribosomal protein L3 (Fragment)
m6A	K1R1T8_CRAGI	Nucleolar protein 56
m6A	K1QGB4_CRAGI	40S ribosomal protein S17
m6A	K1QJ08_CRAGI	60S ribosomal protein L26
m6A	K1Q4Y8_CRAGI	Histone H1oo

m6A	K1PKF5_CRAGI	Protein-glutamine gamma-glutamyltransferase 4
m6A	K1QYT5_CRAGI	Phosphate carrier protein, mitochondrial
m6A	K1RHB2_CRAGI	Nucleolar RNA helicase 2
m6A	K1RJJ7_CRAGI	Histone H5
m6A	K1PS84_CRAGI	Alpha-crystallin B chain
m6A	K1R2N0_CRAGI	Histone H4
m6A	K1PZP6_CRAGI	Coatomer subunit gamma
m6A	K1RGJ7_CRAGI	Neogenin
m6A	K1R9P5_CRAGI	Mitochondrial import receptor subunit TOM70
m6A	K1RUM2_CRAGI	Uncharacterized protein
m6A	K1RJ97_CRAGI	Multifunctional protein ADE2
m6A	K1RJS5_CRAGI	Uncharacterized protein
m6A	K1QW41_CRAGI	Leucine-zipper-like transcriptional regulator 1
m6A	K1R834_CRAGI	60S ribosomal protein L9
m6A	K1QLK8_CRAGI	GTP-binding protein SAR1b
m6A	K1QDH9_CRAGI	Myosin-11
m6A	K1QEF2_CRAGI	ADP-ribosylation factor-like protein 15
m6A	K1PUX5_CRAGI	Casein kinase II subunit alpha
m6A	K1QLU6_CRAGI	Poly [ADP-ribose] polymerase
m6A	K1QUK3_CRAGI	Putative ATP-dependent RNA helicase DDX41
m6A	K1S2S8_CRAGI	Signal recognition particle 54 kDa protein
m6A	K1PY73_CRAGI	Basic leucine zipper and W2 domain-containing protein 1
m6A	K1S6V7_CRAGI	Serine/threonine-protein phosphatase 2A 65 kDa regulatory subunit A alpha isoform
m6A	K1QPC6_CRAGI	Nucleolar complex protein 2-like protein
m6A	K1QPP2_CRAGI	Elongation factor Tu, mitochondrial
m6A	K1QDN1_CRAGI	Heat shock protein 75 kDa, mitochondrial (Fragment)
m6A	K1R996_CRAGI	Long-chain-fatty-acid--CoA ligase 4
m6A	K1RDW8_CRAGI	Golgi apparatus protein 1
m6A	K1S3G2_CRAGI	HMGB1
m6A	K1QR48_CRAGI	Calcium-binding mitochondrial carrier protein SCaMC-2
m6A	K1P5V7_CRAGI	Eukaryotic translation initiation factor 3 subunit C
m6A	K1PV86_CRAGI	Phosphoglycerate mutase family member 5
m6A	K1QWC3_CRAGI	40S ribosomal protein S3
m6A	K1PZ70_CRAGI	NADH dehydrogenase [ubiquinone] iron-sulfur protein 6, mitochondrial
m6A	K1PTL4_CRAGI	Odr-4-like protein
m6A	K1QRM1_CRAGI	Nuclear pore protein
m6A	K1PVD7_CRAGI	Cytochrome c oxidase subunit 5A, mitochondrial
m6A	K1QFR2_CRAGI	Calnexin
m6A	K1Q273_CRAGI	60S ribosomal protein L14
m6A	K1R0M2_CRAGI	Uncharacterized protein
m6A	K1R5W3_CRAGI	Uncharacterized protein
m6A	K1QXQ8_CRAGI	DNA helicase
m6A	K1QPY8_CRAGI	Extracellular superoxide dismutase [Cu-Zn]
m6A	K1Q6V6_CRAGI	Replication factor C subunit 4
m6A	K1QMS2_CRAGI	Cadherin EGF LAG seven-pass G-type receptor 3
m6A	K1Q7T5_CRAGI	Protein disulfide-isomerase
m6A	K1QRZ3_CRAGI	40S ribosomal protein S13
m6A	K1R4Z3_CRAGI	Malate dehydrogenase, mitochondrial
m6A	K1PJ85_CRAGI	26S protease regulatory subunit 6A
m6A	K1PB87_CRAGI	Uncharacterized protein
m6A	K1PXU6_CRAGI	60S ribosomal protein L24
m6A	K1R6S5_CRAGI	40S ribosomal protein S9
m6A	K1PVH5_CRAGI	Centromere/kinetochore protein zw10-like protein
m6A	K1R512_CRAGI	Uncharacterized protein
m6A	K1QK68_CRAGI	Myosin-2 essential light chain
m6A	K1PUV4_CRAGI	40S ribosomal protein S24
m6A	K1R5U8_CRAGI	UBX domain-containing protein 4
m6A	K1PW39_CRAGI	Glycerol-3-phosphate dehydrogenase, mitochondrial
m6A	K1R790_CRAGI	Retinol dehydrogenase 13
m6A	K1QT61_CRAGI	NADH dehydrogenase [ubiquinone] flavoprotein 2, mitochondrial (Fragment)

m6A	K1RG28_CRAGI	Kinase C and casein kinase substrate in neurons protein 2
m6A	K1QKV1_CRAGI	Cytochrome b-c1 complex subunit 6
m6A	K1P9S7_CRAGI	Brix domain-containing protein 2
m6A	K1QN79_CRAGI	40S ribosomal protein S11
m6A	K1QEJ0_CRAGI	Ras GTPase-activating protein-binding protein 2
m6A	K1S1X3_CRAGI	SWI/SNF-related matrix-associated actin-dependent regulator of chromatin subfamily A member 5
m6A	K1R9T2_CRAGI	Eukaryotic translation initiation factor 3 subunit B
m6A	K1QED7_CRAGI	Replication protein A subunit
m6A	K1QQK5_CRAGI	Metabotropic glutamate receptor 2
m6A	K1RN97_CRAGI	Hemagglutinin/amebocyte aggregation factor
m6A	K1PJS7_CRAGI	Poly [ADP-ribose] polymerase
m6A	K1R6F5_CRAGI	Putative ATP-dependent RNA helicase DDX23
m6A	K1R8R6_CRAGI	Fructose-bisphosphate aldolase
m6A	K1QY85_CRAGI	Transport protein Sec31A
m6A	K1QF31_CRAGI	Serine/threonine-protein kinase PLK
m6A	K1Q5J7_CRAGI	Uncharacterized protein
m6A	K1QPF0_CRAGI	Uncharacterized protein
m6A	K1P6Y1_CRAGI	Uncharacterized protein
m6A	K1QJM1_CRAGI	60S ribosomal protein L30
m6A	K1PXD4_CRAGI	Putative ATP-dependent RNA helicase DDX6
m6A	K1PH31_CRAGI	Protein arginine N-methyltransferase 1
m6A	K1PAM6_CRAGI	Uncharacterized protein
m6A	K1RFU6_CRAGI	Proteasome activator complex subunit 3
m6A	K1Q324_CRAGI	Heterogeneous nuclear ribonucleoprotein K
m6A	K1QRG9_CRAGI	Uncharacterized protein
m6A	K1S6H7_CRAGI	Vacuolar protein sorting-associated protein 13C
m6A	K1QE94_CRAGI	Alpha-galactosidase
m6A	K1Q7Q2_CRAGI	CCAAT/enhancer-binding protein zeta
m6A	K1Q7G8_CRAGI	Fatty acid synthase
m6A	K1QXH3_CRAGI	Translational activator GCN1
m6A	K1P8G1_CRAGI	Heterogeneous nuclear ribonucleoprotein H
m6A	K1QKQ8_CRAGI	THO complex subunit 4-A
m6A	K1RA63_CRAGI	Transmembrane protein 2
m6A	K1QAA2_CRAGI	Uncharacterized protein
m6A	K1PLA7_CRAGI	Eukaryotic initiation factor 4A-II (Fragment)
m6A	K1QIV3_CRAGI	Uncharacterized protein
m6A	K1RAH2_CRAGI	Superoxide dismutase [Cu-Zn]
m6A	K1QXA9_CRAGI	Sortilin-related receptor
m6A	K1QSD9_CRAGI	Uncharacterized protein
m6A	K1Q3W3_CRAGI	NADH dehydrogenase [ubiquinone] iron-sulfur protein 3, mitochondrial
m6A	K1R3T3_CRAGI	Transcription factor BTF3
m6A	K1QMH5_CRAGI	Small nuclear ribonucleoprotein Sm D1
m6A	K1R1R9_CRAGI	Pre-mRNA-processing factor 6
m6A	K1PM66_CRAGI	60S ribosomal protein L12
m6A	K1Q3W9_CRAGI	FAS-associated factor 2-B
m6A	K1P9D0_CRAGI	Stress-70 protein, mitochondrial
m6A	K1R4F7_CRAGI	Ras-related protein Rab-6B
m6A	K1QGP7_CRAGI	Uncharacterized protein
m6A	K1REY2_CRAGI	Dysferlin
m6A	K1QSB2_CRAGI	26S protease regulatory subunit 6B
m6A	K1RAU8_CRAGI	Eukaryotic translation initiation factor 3 subunit E
m6A	K1QAB1_CRAGI	AP-2 complex subunit alpha
m6A	K1RFU8_CRAGI	High mobility group protein DSP1
m6A	K1QAA8_CRAGI	CAAX prenyl protease 1-like protein
m6A	K1PXS8_CRAGI	Calreticulin
m6A	K1RV41_CRAGI	Guanine nucleotide-binding protein subunit beta-2-like 1
m6A	K1Q5Z6_CRAGI	Eukaryotic translation initiation factor 2 subunit 2
m6A	K1QYQ9_CRAGI	Uncharacterized protein
m6A	K1RCL2_CRAGI	Mitochondrial import inner membrane translocase subunit Tim13-B
m6A	K1PI50_CRAGI	40S ribosomal protein S26

m6A	K1QGP1_CRAGI	Replication factor C subunit 2
m6A	K1P541_CRAGI	Alpha-soluble NSF attachment protein
m6A	K1Q667_CRAGI	tRNA-splicing ligase RtcB homolog
m6A	K1QBM3_CRAGI	Ras-related protein Rab-2
m6A	K1R7L4_CRAGI	Neural cell adhesion molecule 1
m6A	K1PH13_CRAGI	Dolichyl-diphosphooligosaccharide--protein glycosyltransferase subunit STT3B
m6A	K1QAI2_CRAGI	Ufm1-specific protease 2
m6A	K1RJW8_CRAGI	Protein DEK
m6A	K1QKG8_CRAGI	Upstream activation factor subunit spp27
m6A	K1R150_CRAGI	Ras-related protein Rab-1A
m6A	K1PI40_CRAGI	Uncharacterized protein
m6A	K1PZT2_CRAGI	Cytochrome c oxidase subunit 5B, mitochondrial
m6A	K1PJB0_CRAGI	Heat shock protein 70 B2
m6A	K1PR25_CRAGI	Regulator of differentiation 1
m6A	K1QMV5_CRAGI	Annexin
m6A	K1Q0N6_CRAGI	Dolichyl-diphosphooligosaccharide--protein glycosyltransferase subunit STT3A
m6A	K1QY58_CRAGI	Eukaryotic translation initiation factor 3 subunit I (Fragment)
m6A	K1RIJ1_CRAGI	Synaptobrevin (Fragment)
m6A	K1PNC7_CRAGI	AFG3-like protein 2
m6A	K1QQR1_CRAGI	Major vault protein
m6A	K1R5V4_CRAGI	GTP-binding nuclear protein
m6A	K1QGA7_CRAGI	Kynurenine formamidase
m6A	K1PTV1_CRAGI	Splicing factor 3B subunit 4
m6A	K1P3Q5_CRAGI	Programmed cell death 6-interacting protein
m6A	K1R2G9_CRAGI	SEC13-like protein
m6A	K1PF96_CRAGI	Spliceosome RNA helicase BAT1
m6A	K1R1F0_CRAGI	ATP-dependent DNA helicase 2 subunit 1
m6A	K1Q5Z1_CRAGI	Uncharacterized protein
m6A	K1Q880_CRAGI	Transportin-1
m6A	K1PDF8_CRAGI	Splicing factor, arginine/serine-rich 6
m6A	K1PMY9_CRAGI	Calmodulin
m6A	K1PPW8_CRAGI	Coatomer subunit beta
m6A	K1QZQ8_CRAGI	Low-density lipoprotein receptor-related protein 8
m6A	K1QE43_CRAGI	Uncharacterized protein
m6A	K1RDS1_CRAGI	Splicing factor, arginine/serine-rich 2
m6A	K1RAI3_CRAGI	Annexin
m6A	K1PCR5_CRAGI	KH domain-containing, RNA-binding, signal transduction-associated protein 2
m6A	K1QWP1_CRAGI	Nucleoporin seh1
m6A	K1QAL1_CRAGI	Transmembrane emp24 domain-containing protein 7
m6A	K1Q2H5_CRAGI	Uncharacterized protein
m6A	K1REP0_CRAGI	Uncharacterized protein
m6A	K1PKI9_CRAGI	Uncharacterized protein
m6A	K1RG79_CRAGI	Neuronal acetylcholine receptor subunit alpha-6
m6A	K1Q1L4_CRAGI	Uncharacterized protein
m6A	K1QTP6_CRAGI	Cation-transporting ATPase
m6A	K1Q615_CRAGI	Peroxiredoxin-1
m6A	K1QIZ7_CRAGI	Programmed cell death protein 6
m6A	K1R0D7_CRAGI	Eukaryotic translation initiation factor 3 subunit M (Fragment)
m6A	K1QTW3_CRAGI	Murinoglobulin-2
m6A	K1PDL3_CRAGI	Ribosomal protein L19
m6A	K1QW21_CRAGI	39S ribosomal protein L40, mitochondrial
m6A	K1Q317_CRAGI	Serine/threonine-protein kinase SRPK1
m6A	K1QKG9_CRAGI	Cysteine desulfurase, mitochondrial
m6A	K1PS77_CRAGI	Prostaglandin G/H synthase 1
m6A	K1QJW6_CRAGI	Translocon-associated protein subunit gamma
m6A	K1QTV1_CRAGI	Uncharacterized protein
m6A	K1QTW6_CRAGI	Eukaryotic translation initiation factor 3 subunit F
m6A	K1PNY5_CRAGI	Splicing factor, proline-and glutamine-rich
m6A	K1R100_CRAGI	Metaxin-2
m6A	K1R8L1_CRAGI	Exportin-2

m6A	K1QZ64_CRAGI	Nuclear pore complex protein Nup98-Nup96
m6A	K1QWZ8_CRAGI	Catenin beta
m6A	K1QAT9_CRAGI	ATP-dependent RNA helicase DDX1
m6A	K1P8Y9_CRAGI	Cytochrome b-c1 complex subunit 7
m6A	K1PIC5_CRAGI	Transmembrane protein 85
m6A	K1QMV7_CRAGI	V-type proton ATPase subunit D
m6A	K1RC37_CRAGI	Uncharacterized protein
m6A	K1PEY4_CRAGI	26S proteasome non-ATPase regulatory subunit 2
m6A	K1RG04_CRAGI	ALK tyrosine kinase receptor
m6A	K1QG72_CRAGI	Hemagglutinin/amebocyte aggregation factor
m6A	K1RK83_CRAGI	Tyrosine-protein kinase BAZ1B
m6A	K1QMT1_CRAGI	DnaJ-like protein subfamily B member 4
m6A	K1P8I1_CRAGI	Pleckstrin-like protein domain-containing family F member 2 (Fragment)
m6A	K1R3I6_CRAGI	Nucleolar complex protein 2-like protein (Fragment)
m6A	K1QDB9_CRAGI	Transport protein Sec61 subunit alpha isoform 2 (Fragment)
m6A	K1QMJ8_CRAGI	Transcription initiation factor IIA subunit 1
m6A	K1R5G4_CRAGI	60S ribosomal protein L31
m6A	K1R1W9_CRAGI	Nicalin-1
m6A	K1QDA7_CRAGI	Uracil phosphoribosyltransferase
m6A	K1QI02_CRAGI	Vesicle-trafficking protein SEC22b
m6A	K1QFZ8_CRAGI	Ceramide kinase-like protein
m6A	K1Q151_CRAGI	60S ribosomal protein L32
m6A	K1QNS4_CRAGI	DnaJ-like protein subfamily C member 9
m6A	K1REQ4_CRAGI	Cytochrome c oxidase subunit 6B
m6A	K1R4B8_CRAGI	Plexin domain-containing protein 2
m6A	K1QC10_CRAGI	GTP-binding protein 1
m6A	K1PJY2_CRAGI	Inositol polyphosphate 1-phosphatase
m6A	K1R983_CRAGI	Protein transport protein SEC23
m6A	K1Q5Y3_CRAGI	Annexin
m6A	K1Q1N1_CRAGI	Alpha-mannosidase
m6A	K1QNU0_CRAGI	Non-specific serine/threonine protein kinase
m6A	K1R1Q8_CRAGI	Ras-related protein Rab-5C
m6A	K1RH95_CRAGI	Myosin-IIIB
m6A	K1QWE5_CRAGI	Ras-related protein Rab-18-B
m6A	K1QCB0_CRAGI	40S ribosomal protein S5
m6A	K1Q0I8_CRAGI	Putative splicing factor, arginine/serine-rich 7
m6A	K1QXF5_CRAGI	Calcyphosin-like protein
m6A	K1R8C6_CRAGI	40S ribosomal protein S12
m6A	K1QFA9_CRAGI	Low-density lipoprotein receptor-related protein 2
m6A	K1QYF5_CRAGI	Apoptosis-inducing factor 1, mitochondrial
m6A	K1QA50_CRAGI	V-type proton ATPase subunit H
m6A	K1PY39_CRAGI	Protocadherin Fat 4
m6A	K1Q330_CRAGI	Dihydrolipoyl dehydrogenase
m6A	K1Q350_CRAGI	Glyceraldehyde-3-phosphate dehydrogenase
m6A	K1Q6U7_CRAGI	78 kDa glucose-regulated protein
m6A	K1RBI9_CRAGI	Small nuclear ribonucleoprotein Sm D2
m6A	K1P0H0_CRAGI	Aspartyl/asparaginyl beta-hydroxylase
m6A	K1QSR2_CRAGI	Apoptosis inhibitor 5
m6A	K1RDV7_CRAGI	Cell division control protein 2-like protein (Fragment)
m6A	K1PD30_CRAGI	Putative histone-binding protein Caf1
m6A	K1P7K8_CRAGI	Vesicle-fusing ATPase 1
m6A	K1PVZ3_CRAGI	Cold shock domain-containing protein E1
m6A	K1RKZ5_CRAGI	DNA damage-binding protein 1
m6A	K1R0Z4_CRAGI	Uncharacterized protein
m6A	K1Q947_CRAGI	Dynein light chain
m6A	K1PU46_CRAGI	Lethal(2) giant larvae-like protein 1
m6A	K1Q8K9_CRAGI	KRR1 small subunit processome component-like protein
m6A	K1PQZ3_CRAGI	Armadillo repeat-containing protein 4
m6A	K1QL00_CRAGI	Microsomal glutathione S-transferase 1
m6A	K1RDM2_CRAGI	60S ribosomal protein L18a

m6A	K1Q3V9_CRAGI	Mitochondrial carnitine/acylcarnitine carrier protein
m6A	K1QN55_CRAGI	60S acidic ribosomal protein P1
m6A	K1R3G0_CRAGI	Transformer-2-like protein beta
m6A	K1PWM3_CRAGI	MICOS complex subunit MIC13
m6A	K1QKL8_CRAGI	V-type proton ATPase subunit a
m6A	K1S6T6_CRAGI	UPF0480 protein C15orf24-like protein
m6A	K1R0W0_CRAGI	Ferritin
m6A	K1PGK7_CRAGI	Uncharacterized protein
m6A	K1QY71_CRAGI	Histone H2B
m6A	K1QNT7_CRAGI	Aldehyde dehydrogenase, mitochondrial
m6A	K1RJ96_CRAGI	Sphere organelles protein SPH-1
m6A	K1RZE2_CRAGI	Isocitrate dehydrogenase [NADP]
m6A	K1PPV1_CRAGI	Atlastin-2
m6A	K1P9F1_CRAGI	Insulin-like growth factor-binding protein complex acid labile chain
m6A	K1QVU0_CRAGI	Synaptojanin-2-binding protein
m6A	K1QX44_CRAGI	Ras-related protein Rab-11B
m6A	K1QKU6_CRAGI	mRNA export factor
m6A	K1QDV6_CRAGI	Protein argonaute-2
m6A	K1R5B9_CRAGI	DNA-directed RNA polymerase, mitochondrial
m6A	K1RCT2_CRAGI	Translocon-associated protein subunit delta
m6A	K1PKD4_CRAGI	40S ribosomal protein S30
m6A	K1PP50_CRAGI	Golgi integral membrane protein 4
m6A	K1PG60_CRAGI	60S ribosomal protein L17
m6A	K1QWJ4_CRAGI	Splicing factor 3B subunit 5
m6A	K1RB91_CRAGI	Neutral alpha-glucosidase AB
m6A	K1RD12_CRAGI	Uncharacterized protein
m6A	K1PQE3_CRAGI	RNA-binding protein Raly
m6A	K1Q2Y1_CRAGI	40S ribosomal protein S15
m6A	K1PQF1_CRAGI	Neural cell adhesion molecule L1
m6A	K1QKJ0_CRAGI	Aldehyde dehydrogenase family 3 member B1
m6A	K1PUQ5_CRAGI	Histone H2B
m6A	K1Q2W7_CRAGI	Uncharacterized protein
m6A	K1Q412_CRAGI	Uncharacterized protein
m6A	K1RNH1_CRAGI	60S ribosomal protein L18 (Fragment)
m6A	K1QNT4_CRAGI	Anoctamin
m6A	K1P8B7_CRAGI	Ubiquitin-conjugating enzyme E2-17 kDa (Fragment)
m6A	K1Q1D7_CRAGI	Putative rRNA-processing protein EBP2
m6A	K1PY30_CRAGI	Septin-2
m6A	K1Q1R1_CRAGI	Exostosin-3
m6A	K1RHP3_CRAGI	Proliferation-associated protein 2G4
m6A	K1PZI3_CRAGI	SWI/SNF complex subunit SMARCC2
m6A	K1QT97_CRAGI	N(G),N(G)-dimethylarginine dimethylaminohydrolase 1
m6A	K1QQQ5_CRAGI	Replication factor C subunit 5
m6A	K1PA61_CRAGI	Actin-like protein 6A
m6A	K1PNL0_CRAGI	Microtubule-associated protein futsch
m6A	K1QI28_CRAGI	V-type proton ATPase subunit B
m6A	K1PYL5_CRAGI	Uncharacterized protein
m6A	K1PJ65_CRAGI	Dual specificity mitogen-activated protein kinase kinase 7
m6A	K1QMD8_CRAGI	Proteasome subunit alpha type
m6A	K1Q2L4_CRAGI	Transmembrane emp24 domain-containing protein 9
m6A	K1Q8C1_CRAGI	Putative RNA-binding protein Luc7-like 2
m6A	K1PS71_CRAGI	Uncharacterized protein
m6A	K1Q900_CRAGI	Galectin
m6A	K1RKR8_CRAGI	Pumilio-like protein 2
m6A	K1RKE5_CRAGI	IQ and AAA domain-containing protein 1
m6A	K1QRL4_CRAGI	Importin-5
m6A	K1PGN0_CRAGI	Fatty-acid amide hydrolase 2
m6A	K1RD83_CRAGI	Serine hydroxymethyltransferase
m6A	K1RFA3_CRAGI	Lamin Dm0
m6A	K1QAG7_CRAGI	Phosphatidylinositide phosphatase SAC1

m6A	K1PJP7_CRAGI	Surfeit locus protein 4
m6A	K1PG07_CRAGI	Lupus La-like protein
m6A	K1QVS0_CRAGI	Ras-like GTP-binding protein Rho1
m6A	K1PWC3_CRAGI	Tetratricopeptide repeat protein 35
m6A	K1QZK9_CRAGI	Uncharacterized protein
m6A	K1QAG9_CRAGI	Ferritin
m6A	K1QHW8_CRAGI	Ferritin
m6A	K1PZF2_CRAGI	Exportin-7
m6A	K1RCF4_CRAGI	Translocon-associated protein subunit alpha
m6A	K1QVI0_CRAGI	Isocitrate dehydrogenase [NAD] subunit, mitochondrial
m6A	K1PX47_CRAGI	Ubiquitin carboxyl-terminal hydrolase
m6A	K1P8G6_CRAGI	Vesicular integral-membrane protein VIP36
m6A	K1PNZ8_CRAGI	Ribosomal protein L37
m6A	K1Q373_CRAGI	Splicing factor, arginine/serine-rich 7
m6A	K1R0U6_CRAGI	Uncharacterized protein
m6A	K1QAV0_CRAGI	Guanine nucleotide-binding protein G(Q) subunit alpha
m6A	K1R8Y1_CRAGI	Obg-like ATPase 1
m6A	K1QBY6_CRAGI	Transmembrane protein Tmp21
m6A	K1QZ58_CRAGI	Splicing factor U2AF 26 kDa subunit
m6A	K1RAE9_CRAGI	ADP-ribosylation factor-like protein 8A
m6A	K1RCW5_CRAGI	Eukaryotic translation initiation factor 4 gamma 3
m6A	K1PZ89_CRAGI	Mannosyl-oligosaccharide glucosidase
m6A	K1PBG6_CRAGI	Uncharacterized protein
m6A	K1QPS1_CRAGI	Poly [ADP-ribose] polymerase
m6A	K1R1C5_CRAGI	Signal recognition particle receptor subunit beta
m6A	K1PVG0_CRAGI	Long-chain fatty acid transport protein 4
m6A	K1QXA1_CRAGI	Retinol dehydrogenase 12
m6A	K1R481_CRAGI	Epimerase family protein SDR39U1
m6A	K1QVP6_CRAGI	Developmentally-regulated GTP-binding protein 1
m6A	K1PWB7_CRAGI	Uncharacterized protein
m6A	K1PNQ1_CRAGI	Ankyrin repeat domain-containing protein 5
m6A	K1Q8C5_CRAGI	Putative ATP-dependent RNA helicase DDX47
m6A	K1PR38_CRAGI	TAR DNA-binding protein 43
m6A	K1P7Q6_CRAGI	40S ribosomal protein S19
m6A	K1RFD2_CRAGI	Adenylate kinase
m6A	K1PQJ9_CRAGI	ATP synthase subunit delta, mitochondrial
m6A	K1Q4U7_CRAGI	AP-3 complex subunit delta-1
m6A	K1QM06_CRAGI	Prohibitin
m6A	K1QUW5_CRAGI	U2 snRNP auxiliary factor large subunit
m6A	K1PD36_CRAGI	Ubiquitin
m6A	K1PBL2_CRAGI	Eukaryotic initiation factor 4A-III
m6A	K1R3V8_CRAGI	COP9 signalosome complex subunit 4
m6A	K1PII4_CRAGI	YTH domain-containing protein 1
m6A	K1PZL0_CRAGI	B-box type zinc finger protein ncl-1
m6A	K1REW8_CRAGI	Ribosomal protein L15
m6A	K1R9V5_CRAGI	Tetraspanin
m6A	K1QPX1_CRAGI	ATPase family AAA domain-containing protein 3
m6A	K1QHI2_CRAGI	Heterogeneous nuclear ribonucleoprotein L
m6A	K1QZ95_CRAGI	Nuclear pore complex protein
m6A	K1R401_CRAGI	Spectrin alpha chain
m6A	K1PSA1_CRAGI	Transmembrane 9 superfamily member
m6A	K1Q486_CRAGI	Uncharacterized protein
m6A	K1PYA0_CRAGI	Cytoplasmic dynein 2 heavy chain 1
m6A	K1QLC6_CRAGI	JmjC domain-containing protein 8
m6A	K1RDG4_CRAGI	DNA helicase
m6A	K1PQY0_CRAGI	Protein quiver
m6A	K1QTD5_CRAGI	Low-density lipoprotein receptor-related protein 12
m6A	K1PSP7_CRAGI	Uncharacterized protein
m6A	K1QAL3_CRAGI	RNA-binding protein 28
m6A	K1QND2_CRAGI	Septin-2

m6A	K1RMM6_CRAGI	Centromere protein J
m6A	K1R1K6_CRAGI	Heat shock protein beta-1
m6A	K1R3Z4_CRAGI	5'-3' exoribonuclease 1
m6A	K1RB56_CRAGI	Ferritin
m6A	K1RIZ9_CRAGI	Band 4.1-like protein 5
m6A	K1RFB1_CRAGI	Stomatin-like protein 2 (Fragment)
m6A	K1RNI9_CRAGI	Leucine-rich repeat-containing protein 59
m6A	K1Q7U7_CRAGI	Basigin
m6A	K1RNX0_CRAGI	Small nuclear ribonucleoprotein E
m6A	K1P5F7_CRAGI	Metastasis-associated protein MTA1
m6A	K1PVG9_CRAGI	Malectin
m6A	K1R247_CRAGI	Condensin complex subunit 1
m6A	K1PSN0_CRAGI	Pre-mRNA-processing factor 40-like protein A
m6A	K1PZV3_CRAGI	Guanine nucleotide-binding protein-like 3-like protein (Fragment)
m6A	K1RWP3_CRAGI	Peptidyl-tRNA hydrolase 2, mitochondrial
m6A	K1Q7E4_CRAGI	Ubiquitin-conjugating enzyme E2 N
m6A	K1RK33_CRAGI	Exportin-1
m6A	K1RPP1_CRAGI	Synaptophysin
m6A	K1Q5P0_CRAGI	60S ribosomal protein L17
m6A	K1PND7_CRAGI	Fatty acid synthase
m6A	K1R0R7_CRAGI	Putative ATP-dependent RNA helicase DHX36
m6A	K1QJL6_CRAGI	Microtubule-associated protein RP/EB family member 3
m6A	K1QKZ6_CRAGI	Inosine-5'-monophosphate dehydrogenase
m6A	Q70MT4_CRAGI	40S ribosomal protein S10
m6A	K1RP91_CRAGI	Putative RNA exonuclease NEF-sp
m6A	K1PKK7_CRAGI	AP-2 complex subunit mu-1
m6A	K1PLR8_CRAGI	Chromosome transmission fidelity protein 18-like protein (Fragment)
m6A	K1PH10_CRAGI	Polyadenylate-binding protein-interacting protein 1
m6A	K1P2G0_CRAGI	Strawberry notch-like protein 1
m6A	K1PNU2_CRAGI	Histone-arginine methyltransferase CARM1
m6A	K1QZJ6_CRAGI	Uncharacterized protein (Fragment)
m6A	K1PXB6_CRAGI	Cadherin-23
m6A	K1QCK4_CRAGI	CLIP-associating protein 1
m6A	K1PPH0_CRAGI	Gamma-tubulin complex component
m6A	K1Q105_CRAGI	Ferrochelatase
m6A	K1QF52_CRAGI	Uncharacterized protein
m6A	K1Q2Z5_CRAGI	Putative ATP-dependent RNA helicase DDX46
m6A	K1PXI0_CRAGI	Angiopoietin-4
m6A	K1RPF7_CRAGI	60S ribosomal protein L5
m6A	K1QV25_CRAGI	Transcription elongation factor B polypeptide 2
m6A	K1PUJ1_CRAGI	Radixin
m6A	K1QHT0_CRAGI	Deoxyuridine 5'-triphosphate nucleotidohydrolase, mitochondrial
m6A	K1QMK5_CRAGI	Kinesin-associated protein 3
m6A	K1QQ16_CRAGI	AP complex subunit beta
m6A	K1QZ49_CRAGI	Adipocyte plasma membrane-associated protein
m6A	K1QIB2_CRAGI	Mitogen-activated protein kinase
m6A	K1QXH7_CRAGI	DNA replication licensing factor mcm4-B
m6A	K1QQV0_CRAGI	Histone H1.2
m6A	K1QG61_CRAGI	Acetolactate synthase-like protein
m6A	K1R5R4_CRAGI	Dynein heavy chain 10, axonemal
m6A	K1R4J0_CRAGI	MAGUK p55 subfamily member 2
m6A	K1RR98_CRAGI	NADH dehydrogenase [ubiquinone] 1 alpha subcomplex subunit 4-like 2
m6A	K1Q5E0_CRAGI	Dual specificity protein kinase CLK2
m6A	K1R275_CRAGI	Putative ATP-dependent RNA helicase DDX52
m6A	K1RFV5_CRAGI	ATP-dependent RNA helicase DDX1
m6A	K1QNZ7_CRAGI	Ubiquilin-1
m6A	K1QZ50_CRAGI	RNA-dependent RNA polymerase
m6A	K1QHX4_CRAGI	Uncharacterized protein
m6A	K1Q455_CRAGI	Netrin-3
m6A	K1QQL6_CRAGI	Leucyl-tRNA synthetase, cytoplasmic

m6A	K1RZM3_CRAGI	Cartilage acidic protein 1
m6A	K1R065_CRAGI	Golgi membrane protein 1
m6A	K1RD19_CRAGI	RNA-binding protein 4
m6A	K1R969_CRAGI	Uncharacterized protein
m6A	K1RE19_CRAGI	V-type proton ATPase subunit S1
m6A	K1QGW5_CRAGI	WD repeat and SOF domain-containing protein 1
m6A	K1QKI1_CRAGI	Tudor domain-containing protein 1
m6A	K1PSH2_CRAGI	28S ribosomal protein S12, mitochondrial
m6A	K1QMT2_CRAGI	Signal peptidase complex catalytic subunit SEC11
m6A	K1QDI0_CRAGI	Transmembrane protein 49
m6A	K1Q8T3_CRAGI	Importin subunit alpha
m6A	K1Q525_CRAGI	Mechanosensory protein 2 (Fragment)
m6A	K1Q5G6_CRAGI	60 kDa heat shock protein, mitochondrial
m6A	K1QHF0_CRAGI	40S ribosomal protein S27
m6A	K1Q7X3_CRAGI	Pre-mRNA-splicing factor SYF1
m6A	K1RRH1_CRAGI	Chromodomain-helicase-DNA-binding protein Mi-2-like protein
m6A	K1Q435_CRAGI	Eukaryotic translation initiation factor 2 subunit 1
m6A	K1RNS1_CRAGI	NADH dehydrogenase [ubiquinone] 1 alpha subcomplex subunit 8
m6A	K1QGF9_CRAGI	Rootletin
m6A	K1QJ36_CRAGI	Muscle, skeletal receptor tyrosine protein kinase
m6A	K1RNU5_CRAGI	Pre-mRNA-splicing factor RBM22
m6A	K1R916_CRAGI	Structural maintenance of chromosomes protein
m6A	K1RUC9_CRAGI	Uncharacterized protein
m6A	K1QR54_CRAGI	Zinc finger RNA-binding protein
m6A	K1P9Q2_CRAGI	Signal peptidase complex subunit 3
m6A	K1RTR1_CRAGI	ATP-citrate synthase
m6A	K1Q050_CRAGI	Centrin-3
m6A	K1QPA5_CRAGI	Uncharacterized protein C16orf61-like protein
m6A	K1PSY2_CRAGI	Fragile X mental retardation syndrome-related protein 1
m6A	K1R7G0_CRAGI	Chromobox-like protein 5
m6A	K1QFG2_CRAGI	Telomere-associated protein RIF1
m6A	K1QYV5_CRAGI	Cytoplasmic polyadenylation element-binding protein 1-B
m6A	K1R1I2_CRAGI	Cation-independent mannose-6-phosphate receptor
m6A	K1R255_CRAGI	Heterogeneous nuclear ribonucleoprotein L
m6A	K1RB07_CRAGI	60S ribosomal protein L27a
m6A	K1RYF2_CRAGI	Enoyl-CoA hydratase domain-containing protein 3, mitochondrial
m6A	K1RJ53_CRAGI	Tetratricopeptide repeat protein 12
m6A	K1QW73_CRAGI	Glycoprotein 3-alpha-L-fucosyltransferase A
m6A	K1RBC9_CRAGI	Transketolase-like protein 2
m6A	K1QJ46_CRAGI	Putative methylcrotonoyl-CoA carboxylase beta chain, mitochondrial
m6A	K1Q9V2_CRAGI	Antigen KI-67
m6A	K1PWQ2_CRAGI	60 kDa neurofilament protein
m6A	K1QGF1_CRAGI	Splicing factor 3B subunit 2
m6A	K1QTE0_CRAGI	Epidermal retinal dehydrogenase 2
m6A	K1PPQ1_CRAGI	14-3-3 protein gamma
m6A	K1Q7A7_CRAGI	Putative tyrosinase-like protein tyr-3
m6A	K1QHA2_CRAGI	Spectrin beta chain, brain 4
m6A	K1Q6U0_CRAGI	Coatomer subunit zeta-1
m6A	K1QU16_CRAGI	Protein polybromo-1
m6A	K1P7W5_CRAGI	Histone H1-delta
m6A	K1QBL6_CRAGI	Tudor domain-containing protein 1
m6A	K1QVS1_CRAGI	ER membrane protein complex subunit 3
m6A	K1Q1L9_CRAGI	Interferon-induced protein 44-like protein
m6A	K1Q109_CRAGI	Neurexin-4
m6A	K1PJN7_CRAGI	PC3-like endoprotease variant A
m6A	K1RAH1_CRAGI	Uncharacterized protein
m6A	K1R472_CRAGI	Synaptobrevin-like protein YKT6
m6A	K1QMY9_CRAGI	Uncharacterized protein
m6A	K1QBT8_CRAGI	Uncharacterized protein
m6A	K1Q1R2_CRAGI	Caprin-2

m6A	K1R8V1_CRAGI	Puratrophin-1
m6A	K1PUF0_CRAGI	G-protein coupled receptor moody
m6A	K1Q4R2_CRAGI	Zinc finger protein 26
m6A	K1QXP9_CRAGI	Uncharacterized protein
m6A	K1P6M6_CRAGI	Cerebellin-1
A	K1QNA2_CRAGI	Vitellogenin-6
A	K1PTY5_CRAGI	Protocadherin Fat 4
A	K1QBR5_CRAGI	Uncharacterized protein
A	K1PFG1_CRAGI	Uncharacterized protein
A	K1P9A4_CRAGI	Beta-1,3-glucan-binding protein
A	K1QHI5_CRAGI	Pyruvate carboxylase, mitochondrial
A	K1R5B4_CRAGI	Proteasome activator complex subunit 4
A	K1QQ94_CRAGI	Uncharacterized protein
A	K1QXR4_CRAGI	Pancreatic lipase-related protein 2
A	K1RWS2_CRAGI	Transcriptional activator protein Pur-alpha
A	K1PNI6_CRAGI	Heterogeneous nuclear ribonucleoprotein A/B
A	K1R3U2_CRAGI	Uncharacterized protein
A	K1R7V7_CRAGI	Tubulin beta chain
A	K1QMX5_CRAGI	Uncharacterized protein
A	K1R9B6_CRAGI	H/ACA ribonucleoprotein complex subunit 4
A	K1QQ68_CRAGI	Tubulin alpha chain
A	K1PQP2_CRAGI	Nucleolin
A	K1RLF8_CRAGI	Splicing factor 3B subunit 3
A	K1R164_CRAGI	Galectin-4
A	K1QVJ8_CRAGI	Piwi-like protein 1
A	K1RGT5_CRAGI	Metalloendopeptidase
A	K1PH76_CRAGI	Y-box factor-like protein (Fragment)
A	K1QII6_CRAGI	Tubulin alpha chain
A	K1QSX8_CRAGI	ATPase family AAA domain-containing protein 2B
A	K1QK56_CRAGI	Uncharacterized protein
A	K1QKB5_CRAGI	Uncharacterized protein
A	K1PE00_CRAGI	Tubulin alpha chain
A	K1QQ27_CRAGI	Pancreatic lipase-related protein 2
A	K1PVA1_CRAGI	Transitional endoplasmic reticulum ATPase
A	K1PEP0_CRAGI	40S ribosomal protein S8
A	K1QXX7_CRAGI	Myosin heavy chain, non-muscle (Fragment)
A	K1RK12_CRAGI	40S ribosomal protein S23
A	K1QSQ9_CRAGI	Putative ATP-dependent RNA helicase an3
A	K1PNR3_CRAGI	Clathrin heavy chain
A	K1QMA4_CRAGI	RRP5-like protein
A	K1QHM2_CRAGI	Dolichyl-diphosphooligosaccharide--protein glycosyltransferase subunit 2
A	K1QU53_CRAGI	NAD(P) transhydrogenase, mitochondrial
A	K1PJC1_CRAGI	Adipophilin
A	K1RG73_CRAGI	Acetyl-CoA carboxylase
A	K1QFM6_CRAGI	Vitellogenin
A	K1R6Q7_CRAGI	DNA topoisomerase I
A	K1R6Z7_CRAGI	ATP synthase subunit alpha
A	K1QGS8_CRAGI	Elongation factor 1-alpha
A	K1QWZ6_CRAGI	Dolichyl-diphosphooligosaccharide--protein glycosyltransferase subunit 1
A	K1RD58_CRAGI	Uncharacterized protein
A	K1QLS3_CRAGI	Cytochrome b-c1 complex subunit 2, mitochondrial
A	K1S1S1_CRAGI	Insulin-like growth factor 2 mRNA-binding protein 1
A	K1R0L4_CRAGI	Sodium/potassium-transporting ATPase subunit alpha
A	K1RWW5_CRAGI	ATP synthase subunit beta
A	K1QA13_CRAGI	Calcium-transporting ATPase
A	K1QFN2_CRAGI	Uncharacterized protein
A	K1R545_CRAGI	Pre-mRNA-processing-splicing factor 8 (Fragment)
A	K1R252_CRAGI	Putative methylmalonate-semialdehyde dehydrogenase [acylating], mitochondrial
A	K1PMT6_CRAGI	Heterogeneous nuclear ribonucleoprotein U-like protein 1
A	K1RGB7_CRAGI	Epidermal retinal dehydrogenase 2

A	K1R466_CRAGI	T-complex protein 1 subunit gamma
A	K1R294_CRAGI	T-complex protein 1 subunit beta
A	K1RIT6_CRAGI	NADH-ubiquinone oxidoreductase 75 kDa subunit, mitochondrial
A	K1QIR8_CRAGI	78 kDa glucose-regulated protein
A	K1RI55_CRAGI	Insulin-like growth factor 2 mRNA-binding protein 3
A	K1QH74_CRAGI	Splicing factor, arginine/serine-rich 1
A	K1S2N7_CRAGI	Innexin
A	K1R435_CRAGI	Splicing factor, arginine/serine-rich 4
A	K1R5U4_CRAGI	Acetyl-CoA carboxylase 1
A	K1QBK6_CRAGI	Splicing factor 3B subunit 1
A	K1Q988_CRAGI	Band 4.1-like protein 3
A	K1R420_CRAGI	Non-specific serine/threonine protein kinase
A	A5LGH1_CRAGI	Voltage-dependent anion channel
A	K1PHW2_CRAGI	Uncharacterized protein
A	K1REG6_CRAGI	DNA helicase
A	K1QAE5_CRAGI	Uncharacterized protein
A	K1QWT8_CRAGI	Uncharacterized protein
A	K1QRL6_CRAGI	Methenyltetrahydrofolate synthetase domain-containing protein
A	K1QYB3_CRAGI	Ig-like and fibronectin type-III domain-containing protein C25G4.10
A	K1QKD6_CRAGI	Uncharacterized protein
A	K1R115_CRAGI	Succinate dehydrogenase [ubiquinone] flavoprotein subunit, mitochondrial
A	K1S4Q2_CRAGI	T-complex protein 1 subunit delta (Fragment)
A	K1QWK2_CRAGI	MAM domain-containing glycosylphosphatidylinositol anchor protein 2
A	K1R0S3_CRAGI	T-complex protein 1 subunit theta
A	K1QFW9_CRAGI	Uncharacterized protein
A	K1Q0Z3_CRAGI	Estradiol 17-beta-dehydrogenase 11
A	K1PNQ5_CRAGI	Heat shock protein HSP 90-alpha 1
A	K1RBF6_CRAGI	Uncharacterized protein yfeX
A	K1R4D4_CRAGI	40S ribosomal protein SA
A	K1QI14_CRAGI	40S ribosomal protein S3a
A	K1PUL2_CRAGI	Long-chain-fatty-acid--CoA ligase 1
A	K1RFT1_CRAGI	Band 4.1-like protein 3
A	K1PJ06_CRAGI	Importin subunit alpha-1
A	K1QT21_CRAGI	Putative ATP-dependent RNA helicase DDX5
A	K1QM19_CRAGI	Uncharacterized protein
A	K1QXS6_CRAGI	Heterogeneous nuclear ribonucleoprotein A2-like protein 1
A	K1QMX8_CRAGI	DNA replication licensing factor MCM7
A	K1PD57_CRAGI	Constitutive coactivator of PPAR-gamma-like protein 1-like protein
A	K1R953_CRAGI	Acetyl-CoA carboxylase
A	K1RJH5_CRAGI	Polyadenylate-binding protein
A	K1RSZ6_CRAGI	40S ribosomal protein S7
A	K1R7A2_CRAGI	Uncharacterized protein
A	K1QUC6_CRAGI	Uncharacterized protein
A	K1QWX2_CRAGI	60S acidic ribosomal protein P0
A	K1RNB5_CRAGI	Propionyl-CoA carboxylase beta chain, mitochondrial
A	K1PCS4_CRAGI	Eukaryotic translation initiation factor 2 subunit 3, Y-linked
A	K1Q923_CRAGI	Putative ATP-dependent RNA helicase DDX4
A	K1QPX8_CRAGI	Alkyl/aryl-sulfatase BDS1
A	K1R4R9_CRAGI	Mitotic apparatus protein p62
A	K1RAJ1_CRAGI	T-complex protein 1 subunit alpha
A	K1Q0L1_CRAGI	60S ribosomal protein L23a
A	K1Q620_CRAGI	Uncharacterized protein
A	K1QG58_CRAGI	Actin
A	K1Q4H2_CRAGI	Nodal modulator 3
A	K1Q260_CRAGI	Nucleolar protein 58
A	K1QF01_CRAGI	40S ribosomal protein S4
A	K1PUM2_CRAGI	Histone H2A
A	K1QNN9_CRAGI	MICOS complex subunit MIC60
A	K1RQA0_CRAGI	Dolichyl-diphosphooligosaccharide--protein glycosyltransferase subunit 2
A	K1QZW0_CRAGI	Polyadenylate-binding protein 2

A	K1QBN0_CRAGI	Methylcrotonoyl-CoA carboxylase beta chain, mitochondrial
A	K1Q8S0_CRAGI	Nucleolar complex protein 3 homolog
A	K1RH18_CRAGI	Sarcalumenin
A	K1QQ05_CRAGI	Insulin-like growth factor-binding protein complex acid labile chain
A	K1QT04_CRAGI	Uncharacterized protein
A	K1RLC5_CRAGI	T-complex protein 1 subunit epsilon
A	K1Q9K6_CRAGI	Histone H3
A	K1QBW8_CRAGI	Uncharacterized protein
A	K1Q9W5_CRAGI	T-complex protein 1 subunit eta
A	K1R0Y9_CRAGI	ADP,ATP carrier protein
A	K1QP17_CRAGI	Caprin-1
A	K1QYB6_CRAGI	Delta-1-pyrroline-5-carboxylate synthetase
A	K1R7I9_CRAGI	Heterogeneous nuclear ribonucleoprotein Q
A	K1QMB9_CRAGI	Eukaryotic translation initiation factor 3 subunit A
A	K1PM50_CRAGI	40S ribosomal protein S16
A	K1P8W6_CRAGI	60S ribosomal protein L4
A	K1PXH5_CRAGI	Putative saccharopine dehydrogenase
A	K1PBZ4_CRAGI	Regulator of nonsense transcripts 1
A	K1R4L8_CRAGI	Electron transfer flavoprotein-ubiquinone oxidoreductase, mitochondrial
A	K1QFP5_CRAGI	NADH dehydrogenase [ubiquinone] flavoprotein 1, mitochondrial
A	K1RIG6_CRAGI	LSM14-like protein A
A	K1R591_CRAGI	Inter-alpha-trypsin inhibitor heavy chain H4
A	K1RSA6_CRAGI	Methylcrotonoyl-CoA carboxylase subunit alpha, mitochondrial
A	K1R1B1_CRAGI	35 kDa SR repressor protein
A	K1QZU8_CRAGI	Calcium-transporting ATPase
A	K1QX26_CRAGI	Endoplasmin
A	K1Q358_CRAGI	60S acidic ribosomal protein P2
A	K1P112_CRAGI	ATP synthase subunit gamma, mitochondrial
A	K1QHS8_CRAGI	Ribonucleoside-diphosphate reductase
A	K1PXN5_CRAGI	T-complex protein 1 subunit zeta
A	K1R7J6_CRAGI	Putative sodium/potassium-transporting ATPase subunit beta-2
A	K1Q5H6_CRAGI	FACT complex subunit SSRP1
A	K1QTD9_CRAGI	Nucleolar protein 56
A	K1QC78_CRAGI	Ras-related protein Rab-14
A	K1Q9M7_CRAGI	Histone H1-delta
A	K1RNZ6_CRAGI	Eukaryotic translation initiation factor 3 subunit D
A	K1QAH9_CRAGI	H/ACA ribonucleoprotein complex subunit
A	K1RLT4_CRAGI	Signal recognition particle subunit SRP68
A	K1RWX7_CRAGI	Metabotropic glutamate receptor 3
A	K1RA35_CRAGI	Splicing factor, arginine/serine-rich 7
A	K1QE71_CRAGI	DNA helicase
A	K1PS27_CRAGI	DNA helicase
A	K1Q4Y8_CRAGI	Histone H1oo
A	K1PGW7_CRAGI	Transmembrane protein 2
A	K1RAB9_CRAGI	Epoxide hydrolase 4
A	K1Q9P5_CRAGI	Mitochondrial-processing peptidase subunit beta
A	K1QL67_CRAGI	60S ribosomal protein L7a
A	K1PLY1_CRAGI	DNA polymerase
A	K1R996_CRAGI	Long-chain-fatty-acid--CoA ligase 4
A	K1Q404_CRAGI	DNA topoisomerase 2
A	K1QBH0_CRAGI	Uncharacterized protein
A	K1R0W4_CRAGI	Signal recognition particle subunit SRP72
A	K1RN77_CRAGI	Nuclear autoantigenic sperm protein
A	K1PA54_CRAGI	Replication factor C subunit 3
A	K1Q4S5_CRAGI	Cadherin-87A
A	K1QEF2_CRAGI	ADP-ribosylation factor-like protein 15
A	K1QYT5_CRAGI	Phosphate carrier protein, mitochondrial
A	K1QDX9_CRAGI	Ribosome biogenesis protein BMS1-like protein
A	K1QB61_CRAGI	Protocadherin Fat 4
A	K1R0D7_CRAGI	Eukaryotic translation initiation factor 3 subunit M (Fragment)

A	K1PM76_CRAGI	NADH dehydrogenase [ubiquinone] 1 alpha subcomplex subunit 9, mitochondrial
A	K1PRL4_CRAGI	60S ribosomal protein L38 (Fragment)
A	K1RW85_CRAGI	Adenosylhomocysteinase
A	K1PAY7_CRAGI	Propionyl-CoA carboxylase alpha chain, mitochondrial
A	K1PZ08_CRAGI	Ras-related protein Rab-7a
A	K1QY12_CRAGI	Dynamin-1-like protein
A	K1QFN1_CRAGI	60S ribosomal protein L23
A	K1RDW8_CRAGI	Golgi apparatus protein 1
A	K1RSS3_CRAGI	Myosin heavy chain, striated muscle
A	K1QGK2_CRAGI	Coatomer subunit beta
A	K1PV79_CRAGI	Importin subunit alpha
A	K1QN79_CRAGI	40S ribosomal protein S11
A	K1PV49_CRAGI	RuvB-like helicase
A	K1QG65_CRAGI	rRNA 2'-O-methyltransferase fibrillarin
A	K1PK85_CRAGI	Cullin-associated NEDD8-dissociated protein 1
A	K1QVN9_CRAGI	T-complex protein 1 subunit eta
A	K1QGB4_CRAGI	40S ribosomal protein S17
A	K1QK18_CRAGI	Cytochrome b5
A	K1QVW3_CRAGI	Alkylglycerone-phosphate synthase
A	K1QN11_CRAGI	Pre-mRNA-processing-splicing factor 8
A	K1RJS5_CRAGI	Uncharacterized protein
A	K1Q6W5_CRAGI	FACT complex subunit spt16
A	K1QQB6_CRAGI	40S ribosomal protein S14
A	K1PKF5_CRAGI	Protein-glutamine gamma-glutamyltransferase 4
A	K1PH66_CRAGI	Fibrinolytic enzyme, isozyme C
A	K1PY89_CRAGI	Extracellular superoxide dismutase [Cu-Zn]
A	K1QUK3_CRAGI	Putative ATP-dependent RNA helicase DDX41
A	K1R2V1_CRAGI	Importin subunit beta-1
A	K1PV86_CRAGI	Phosphoglycerate mutase family member 5
A	K1QJ08_CRAGI	60S ribosomal protein L26
A	K1QLU6_CRAGI	Poly [ADP-ribose] polymerase
A	K1QDN1_CRAGI	Heat shock protein 75 kDa, mitochondrial (Fragment)
A	K1QPP2_CRAGI	Elongation factor Tu, mitochondrial
A	K1R834_CRAGI	60S ribosomal protein L9
A	K1R005_CRAGI	Filamin-C (Fragment)
A	K1QET2_CRAGI	Coatomer subunit alpha
A	K1RKC1_CRAGI	Far upstream element-binding protein 3
A	K1RG19_CRAGI	Protein FAM98A
A	K1Q056_CRAGI	Calpain-A
A	K1QKJ0_CRAGI	Aldehyde dehydrogenase family 3 member B1
A	K1QDZ5_CRAGI	Cytochrome c1, heme protein, mitochondrial
A	K1PPP8_CRAGI	Vigilin
A	K1RHB2_CRAGI	Nucleolar RNA helicase 2
A	K1PH31_CRAGI	Protein arginine N-methyltransferase 1
A	K1Q6V6_CRAGI	Replication factor C subunit 4
A	K1PI50_CRAGI	40S ribosomal protein S26
A	K1PX23_CRAGI	Eukaryotic peptide chain release factor subunit 1
A	K1QFZ8_CRAGI	Ceramide kinase-like protein
A	K1S2S8_CRAGI	Signal recognition particle 54 kDa protein
A	K1R1T8_CRAGI	Nucleolar protein 56
A	K1QRZ3_CRAGI	40S ribosomal protein S13
A	K1PMP3_CRAGI	Protoporphyrinogen oxidase
A	K1P9N7_CRAGI	14-3-3 protein zeta
A	K1Q0R4_CRAGI	ATP-binding cassette sub-family F member 2
A	K1QWC3_CRAGI	40S ribosomal protein S3
A	K1Q812_CRAGI	NADH dehydrogenase [ubiquinone] iron-sulfur protein 2, mitochondrial
A	K1P5V7_CRAGI	Eukaryotic translation initiation factor 3 subunit C
A	K1R2N0_CRAGI	Histone H4
A	K1QLK8_CRAGI	GTP-binding protein SAR1b
A	K1QHX2_CRAGI	La-related protein 7

A	K1S6V7_CRAGI	Serine/threonine-protein phosphatase 2A 65 kDa regulatory subunit A alpha isoform
A	K1Q3W9_CRAGI	FAS-associated factor 2-B
A	K1QG72_CRAGI	Hemagglutinin/amebocyte aggregation factor
A	K1QHQ6_CRAGI	Acyl-CoA dehydrogenase family member 9, mitochondrial
A	K1QFR2_CRAGI	Calnexin
A	K1S1X3_CRAGI	SWI/SNF-related matrix-associated actin-dependent regulator of chromatin subfamily A member 5
A	K1PWZ3_CRAGI	Guanine nucleotide-binding protein subunit beta
A	K1QW41_CRAGI	Leucine-zipper-like transcriptional regulator 1
A	K1RK68_CRAGI	Uncharacterized protein
A	K1RA95_CRAGI	Filamin-A
A	K1QMV5_CRAGI	Annexin
A	K1QW72_CRAGI	Catalase
A	K1QXQ8_CRAGI	DNA helicase
A	K1P7L5_CRAGI	Transmembrane 9 superfamily member
A	K1P8G1_CRAGI	Heterogeneous nuclear ribonucleoprotein H
A	K1PZ23_CRAGI	DnaJ-like protein subfamily C member 3
A	K1RIZ3_CRAGI	Bone morphogenetic protein 7
A	K1RNN9_CRAGI	Cytoskeleton-associated protein 5
A	K1R6L5_CRAGI	NADH-cytochrome b5 reductase
A	K1R5F2_CRAGI	14-3-3 protein epsilon
A	K1P9D0_CRAGI	Stress-70 protein, mitochondrial
A	K1RGJ7_CRAGI	Neogenin
A	K1PZP6_CRAGI	Coatomer subunit gamma
A	K1RJ97_CRAGI	Multifunctional protein ADE2
A	K1R6F5_CRAGI	Putative ATP-dependent RNA helicase DDX23
A	K1PS84_CRAGI	Alpha-crystallin B chain
A	K1P9S7_CRAGI	Brix domain-containing protein 2
A	K1PI40_CRAGI	Uncharacterized protein
A	K1QAI2_CRAGI	Ufm1-specific protease 2
A	K1REP0_CRAGI	Uncharacterized protein
A	K1QJM1_CRAGI	60S ribosomal protein L30
A	K1S3G2_CRAGI	HMGB1
A	K1PXD4_CRAGI	Putative ATP-dependent RNA helicase DDX6
A	K1RJJ7_CRAGI	Histone H5
A	K1Q3W3_CRAGI	NADH dehydrogenase [ubiquinone] iron-sulfur protein 3, mitochondrial
A	K1RJW8_CRAGI	Protein DEK
A	K1RN97_CRAGI	Hemagglutinin/amebocyte aggregation factor
A	K1QW36_CRAGI	60S ribosomal protein L6
A	K1RA63_CRAGI	Transmembrane protein 2
A	K1R9T2_CRAGI	Eukaryotic translation initiation factor 3 subunit B
A	K1PM66_CRAGI	60S ribosomal protein L12
A	K1Q273_CRAGI	60S ribosomal protein L14
A	K1PXG6_CRAGI	Serine/threonine-protein phosphatase
A	K1QPC6_CRAGI	Nucleolar complex protein 2-like protein
A	K1RCW3_CRAGI	Elongation factor 1-beta
A	K1Q324_CRAGI	Heterogeneous nuclear ribonucleoprotein K
A	K1PLA7_CRAGI	Eukaryotic initiation factor 4A-II (Fragment)
A	K1RBI9_CRAGI	Small nuclear ribonucleoprotein Sm D2
A	K1RCL2_CRAGI	Mitochondrial import inner membrane translocase subunit Tim13-B
A	K1QKV1_CRAGI	Cytochrome b-c1 complex subunit 6
A	K1QVU0_CRAGI	Synaptojanin-2-binding protein
A	K1QRG9_CRAGI	Uncharacterized protein
A	K1PZ70_CRAGI	NADH dehydrogenase [ubiquinone] iron-sulfur protein 6, mitochondrial
A	K1Q350_CRAGI	Glyceraldehyde-3-phosphate dehydrogenase
A	K1PXU6_CRAGI	60S ribosomal protein L24
A	K1QZQ8_CRAGI	Low-density lipoprotein receptor-related protein 8
A	K1RUM2_CRAGI	Uncharacterized protein
A	K1REY2_CRAGI	Dysferlin
A	K1Q6X5_CRAGI	Protein disulfide-isomerase
A	K1QWK6_CRAGI	Metalloendopeptidase

A	K1QDH9_CRAGI	Myosin-11
A	K1QQR1_CRAGI	Major vault protein
A	K1RAH2_CRAGI	Superoxide dismutase [Cu-Zn]
A	K1PH13_CRAGI	Dolichyl-diphosphooligosaccharide--protein glycosyltransferase subunit STT3B
A	K1PY73_CRAGI	Basic leucine zipper and W2 domain-containing protein 1
A	K1Q7T5_CRAGI	Protein disulfide-isomerase
A	K1PFS5_CRAGI	Elongation factor 1-gamma
A	K1PW39_CRAGI	Glycerol-3-phosphate dehydrogenase, mitochondrial
A	K1R1C5_CRAGI	Signal recognition particle receptor subunit beta
A	K1Q1F4_CRAGI	60S ribosomal protein L3 (Fragment)
A	K1QNS4_CRAGI	DnaJ-like protein subfamily C member 9
A	K1QY85_CRAGI	Transport protein Sec31A
A	K1QWP1_CRAGI	Nucleoporin seh1
A	K1RAU3_CRAGI	DNA ligase
A	K1R5W3_CRAGI	Uncharacterized protein
A	K1QF31_CRAGI	Serine/threonine-protein kinase PLK
A	K1Q667_CRAGI	tRNA-splicing ligase RtcB homolog
A	K1QRM1_CRAGI	Nuclear pore protein
A	K1R790_CRAGI	Retinol dehydrogenase 13
A	K1R0M2_CRAGI	Uncharacterized protein
A	K1QNT7_CRAGI	Aldehyde dehydrogenase, mitochondrial
A	K1QIV3_CRAGI	Uncharacterized protein
A	K1QR48_CRAGI	Calcium-binding mitochondrial carrier protein SCaMC-2
A	K1R4F7_CRAGI	Ras-related protein Rab-6B
A	K1PIC5_CRAGI	Transmembrane protein 85
A	K1RKZ5_CRAGI	DNA damage-binding protein 1
A	K1QW21_CRAGI	39S ribosomal protein L40, mitochondrial
A	K1PB87_CRAGI	Uncharacterized protein
A	K1R150_CRAGI	Ras-related protein Rab-1A
A	K1PVZ3_CRAGI	Cold shock domain-containing protein E1
A	K1QSD9_CRAGI	Uncharacterized protein
A	K1PPW8_CRAGI	Coatomer subunit beta
A	K1QKG9_CRAGI	Cysteine desulfurase, mitochondrial
A	K1RK83_CRAGI	Tyrosine-protein kinase BAZ1B
A	K1QE94_CRAGI	Alpha-galactosidase
A	K1RIJ1_CRAGI	Synaptobrevin (Fragment)
A	K1PJB0_CRAGI	Heat shock protein 70 B2
A	K1R6S5_CRAGI	40S ribosomal protein S9
A	K1PAM6_CRAGI	Uncharacterized protein
A	K1QY71_CRAGI	Histone H2B
A	K1P6Y1_CRAGI	Uncharacterized protein
A	K1PNY5_CRAGI	Splicing factor, proline-and glutamine-rich
A	K1PDL3_CRAGI	Ribosomal protein L19
A	K1RDG4_CRAGI	DNA helicase
A	K1RV41_CRAGI	Guanine nucleotide-binding protein subunit beta-2-like 1
A	K1QMH5_CRAGI	Small nuclear ribonucleoprotein Sm D1
A	K1R4Z3_CRAGI	Malate dehydrogenase, mitochondrial
A	K1R3T3_CRAGI	Transcription factor BTF3
A	K1QAB1_CRAGI	AP-2 complex subunit alpha
A	K1QSU3_CRAGI	Protein l(2)37Cc
A	K1PEY4_CRAGI	26S proteasome non-ATPase regulatory subunit 2
A	K1PU46_CRAGI	Lethal(2) giant larvae-like protein 1
A	K1Q0N6_CRAGI	Dolichyl-diphosphooligosaccharide--protein glycosyltransferase subunit STT3A
A	K1QGP1_CRAGI	Replication factor C subunit 2
A	K1QDV6_CRAGI	Protein argonaute-2
A	K1S6H7_CRAGI	Vacuolar protein sorting-associated protein 13C
A	K1PF10_CRAGI	PAN2-PAN3 deadenylation complex catalytic subunit PAN2
A	K1Q1L4_CRAGI	Uncharacterized protein
A	K1PWC3_CRAGI	Tetratricopeptide repeat protein 35
A	K1QKL8_CRAGI	V-type proton ATPase subunit a

A	K1QT61_CRAGI	NADH dehydrogenase [ubiquinone] flavoprotein 2, mitochondrial (Fragment)
A	K1Q7G8_CRAGI	Fatty acid synthase
A	K1QX44_CRAGI	Ras-related protein Rab-11B
A	K1P7K8_CRAGI	Vesicle-fusing ATPase 1
A	K1QHK9_CRAGI	Dynein heavy chain, cytoplasmic
A	K1Q7Q2_CRAGI	CCAAT/enhancer-binding protein zeta
A	K1Q880_CRAGI	Transportin-1
A	K1Q253_CRAGI	Neutral and basic amino acid transport protein rBAT
A	K1QGA7_CRAGI	Kynurenine formamidase
A	K1QAL3_CRAGI	RNA-binding protein 28
A	K1PXS8_CRAGI	Calreticulin
A	K1QTP6_CRAGI	Cation-transporting ATPase
A	K1PR25_CRAGI	Regulator of differentiation 1
A	K1PA61_CRAGI	Actin-like protein 6A
A	K1QAA8_CRAGI	CAAX prenyl protease 1-like protein
A	K1PY30_CRAGI	Septin-2
A	K1R100_CRAGI	Metaxin-2
A	K1PTL4_CRAGI	Odr-4-like protein
A	K1QA50_CRAGI	V-type proton ATPase subunit H
A	K1PVH5_CRAGI	Centromere/kinetochore protein zw10-like protein
A	K1PUQ5_CRAGI	Histone H2B
A	K1RFB1_CRAGI	Stomatin-like protein 2 (Fragment)
A	K1QAA2_CRAGI	Uncharacterized protein
A	K1PNC7_CRAGI	AFG3-like protein 2
A	K1PJS7_CRAGI	Poly [ADP-ribose] polymerase
A	K1PLF9_CRAGI	Arginine kinase
A	K1RC37_CRAGI	Uncharacterized protein
A	K1PKD4_CRAGI	40S ribosomal protein S30
A	K1RDS1_CRAGI	Splicing factor, arginine/serine-rich 2
A	K1Q5Z1_CRAGI	Uncharacterized protein
A	K1PF96_CRAGI	Spliceosome RNA helicase BAT1
A	K1QTW6_CRAGI	Eukaryotic translation initiation factor 3 subunit F
A	K1RAU8_CRAGI	Eukaryotic translation initiation factor 3 subunit E
A	K1RAI3_CRAGI	Annexin
A	K1PUX5_CRAGI	Casein kinase II subunit alpha
A	K1PDF8_CRAGI	Splicing factor, arginine/serine-rich 6
A	K1QXH3_CRAGI	Translational activator GCN1
A	K1PQE3_CRAGI	RNA-binding protein Raly
A	K1QWE5_CRAGI	Ras-related protein Rab-18-B
A	K1R5G4_CRAGI	60S ribosomal protein L31
A	K1RCT2_CRAGI	Translocon-associated protein subunit delta
A	K1RFU6_CRAGI	Proteasome activator complex subunit 3
A	K1R0W0_CRAGI	Ferritin
A	K1Q5Z6_CRAGI	Eukaryotic translation initiation factor 2 subunit 2
A	K1RKE5_CRAGI	IQ and AAA domain-containing protein 1
A	K1P8G6_CRAGI	Vesicular integral-membrane protein VIP36
A	K1P3Q5_CRAGI	Programmed cell death 6-interacting protein
A	K1Q615_CRAGI	Peroxiredoxin-1
A	K1RG04_CRAGI	ALK tyrosine kinase receptor
A	K1QQK5_CRAGI	Metabotropic glutamate receptor 2
A	K1R3G0_CRAGI	Transformer-2-like protein beta
A	K1QCB0_CRAGI	40S ribosomal protein S5
A	K1REQ4_CRAGI	Cytochrome c oxidase subunit 6B
A	K1QHI2_CRAGI	Heterogeneous nuclear ribonucleoprotein L
A	K1PSH2_CRAGI	28S ribosomal protein S12, mitochondrial
A	K1R9P5_CRAGI	Mitochondrial import receptor subunit TOM70
A	K1PGK7_CRAGI	Uncharacterized protein
A	K1QPF0_CRAGI	Uncharacterized protein
A	K1QT00_CRAGI	ATP synthase subunit alpha, mitochondrial
A	K1RG28_CRAGI	Kinase C and casein kinase substrate in neurons protein 2

A	K1PMY9_CRAGI	Calmodulin
A	K1R1Q8_CRAGI	Ras-related protein Rab-5C
A	K1RPP1_CRAGI	Synaptophysin
A	K1RFU8_CRAGI	High mobility group protein DSP1
A	K1PJ85_CRAGI	26S protease regulatory subunit 6A
A	K1R2G9_CRAGI	SEC13-like protein
A	K1QJW6_CRAGI	Translocon-associated protein subunit gamma
A	K1R5B9_CRAGI	DNA-directed RNA polymerase, mitochondrial
A	K1R8C6_CRAGI	40S ribosomal protein S12
A	K1QSR2_CRAGI	Apoptosis inhibitor 5
A	K1Q5E0_CRAGI	Dual specificity protein kinase CLK2
A	K1QBM3_CRAGI	Ras-related protein Rab-2
A	K1Q8K9_CRAGI	KRR1 small subunit processome component-like protein
A	K1QNU0_CRAGI	Non-specific serine/threonine protein kinase
A	K1RDM2_CRAGI	60S ribosomal protein L18a
A	K1RD12_CRAGI	Uncharacterized protein
A	K1QGP7_CRAGI	Uncharacterized protein
A	K1PBL2_CRAGI	Eukaryotic initiation factor 4A-III
A	K1QAT9_CRAGI	ATP-dependent RNA helicase DDX1
A	K1QWJ4_CRAGI	Splicing factor 3B subunit 5
A	K1Q412_CRAGI	Uncharacterized protein
A	K1R8R6_CRAGI	Fructose-bisphosphate aldolase
A	K1RWP3_CRAGI	Peptidyl-tRNA hydrolase 2, mitochondrial
A	K1PGN0_CRAGI	Fatty-acid amide hydrolase 2
A	K1PUV4_CRAGI	40S ribosomal protein S24
A	K1PJY2_CRAGI	Inositol polyphosphate 1-phosphatase
A	K1QWZ8_CRAGI	Catenin beta
A	K1R1F0_CRAGI	ATP-dependent DNA helicase 2 subunit 1
A	K1PN47_CRAGI	Succinate dehydrogenase [ubiquinone] iron-sulfur subunit, mitochondrial
A	K1QYQ9_CRAGI	Uncharacterized protein
A	K1PNZ8_CRAGI	Ribosomal protein L37
A	K1PVD7_CRAGI	Cytochrome c oxidase subunit 5A, mitochondrial
A	K1QEJ0_CRAGI	Ras GTPase-activating protein-binding protein 2
A	K1PYL5_CRAGI	Uncharacterized protein
A	K1QQQ5_CRAGI	Replication factor C subunit 5
A	K1RFA3_CRAGI	Lamin Dm0
A	K1RRH1_CRAGI	Chromodomain-helicase-DNA-binding protein Mi-2-like protein
A	K1Q2Y1_CRAGI	40S ribosomal protein S15
A	K1RIZ9_CRAGI	Band 4.1-like protein 5
A	K1QVI0_CRAGI	Isocitrate dehydrogenase [NAD] subunit, mitochondrial
A	K1PS77_CRAGI	Prostaglandin G/H synthase 1
A	K1QZK9_CRAGI	Uncharacterized protein
A	K1R9V5_CRAGI	Tetraspanin
A	K1PPV1_CRAGI	Atlastin-2
A	K1R0Z4_CRAGI	Uncharacterized protein
A	K1R1R9_CRAGI	Pre-mRNA-processing factor 6
A	K1QKU6_CRAGI	mRNA export factor
A	K1PCR5_CRAGI	KH domain-containing, RNA-binding, signal transduction-associated protein 2
A	K1R7L4_CRAGI	Neural cell adhesion molecule 1
A	K1QAL1_CRAGI	Transmembrane emp24 domain-containing protein 7
A	K1QB65_CRAGI	Dolichyl-diphosphooligosaccharide--protein glycosyltransferase subunit 1
A	K1QVP6_CRAGI	Developmentally-regulated GTP-binding protein 1
A	K1QNT4_CRAGI	Anoctamin
A	K1QMT1_CRAGI	DnaJ-like protein subfamily B member 4
A	K1RCF4_CRAGI	Translocon-associated protein subunit alpha
A	K1QJL6_CRAGI	Microtubule-associated protein RP/EB family member 3
A	K1QPY8_CRAGI	Extracellular superoxide dismutase [Cu-Zn]
A	K1R5V4_CRAGI	GTP-binding nuclear protein
A	K1RNU5_CRAGI	Pre-mRNA-splicing factor RBM22
A	K1QK68_CRAGI	Myosin-2 essential light chain

A	K1QED7_CRAGI	Replication protein A subunit
A	K1QPS1_CRAGI	Poly [ADP-ribose] polymerase
A	K1PD36_CRAGI	Ubiquitin
A	K1R4B8_CRAGI	Plexin domain-containing protein 2
A	K1RHP3_CRAGI	Proliferation-associated protein 2G4
A	K1QE43_CRAGI	Uncharacterized protein
A	K1R3I6_CRAGI	Nucleolar complex protein 2-like protein (Fragment)
A	K1QMJ8_CRAGI	Transcription initiation factor IIA subunit 1
A	K1QXF5_CRAGI	Calcyphosin-like protein
A	K1R512_CRAGI	Uncharacterized protein
A	K1QM06_CRAGI	Prohibitin
A	K1R275_CRAGI	Putative ATP-dependent RNA helicase DDX52
A	K1QSB2_CRAGI	26S protease regulatory subunit 6B
A	K1QBW6_CRAGI	Tudor domain-containing protein 1
A	K1PZT2_CRAGI	Cytochrome c oxidase subunit 5B, mitochondrial
A	K1QIZ7_CRAGI	Programmed cell death protein 6
A	K1QDA7_CRAGI	Uracil phosphoribosyltransferase
A	K1R401_CRAGI	Spectrin alpha chain
A	K1P541_CRAGI	Alpha-soluble NSF attachment protein
A	K1PND7_CRAGI	Fatty acid synthase
A	K1R8L1_CRAGI	Exportin-2
A	K1QEF9_CRAGI	Protein-glutamine gamma-glutamyltransferase K
A	K1Q2W7_CRAGI	Uncharacterized protein
A	K1RYM7_CRAGI	LAG1 longevity assurance-like protein 6
A	K1PY09_CRAGI	Uncharacterized protein
A	K1Q105_CRAGI	Ferrochelatase
A	K1PD30_CRAGI	Putative histone-binding protein Caf1
A	K1QDB9_CRAGI	Transport protein Sec61 subunit alpha isoform 2 (Fragment)
A	K1QTW3_CRAGI	Murinoglobulin-2
A	K1PVG9_CRAGI	Malectin
A	K1Q3V9_CRAGI	Mitochondrial carnitine/acylcarnitine carrier protein
A	K1QVS0_CRAGI	Ras-like GTP-binding protein Rho1
A	K1PX68_CRAGI	Tyrosine-protein phosphatase non-receptor type 6
A	K1RPF7_CRAGI	60S ribosomal protein L5
A	K1QZ64_CRAGI	Nuclear pore complex protein Nup98-Nup96
A	K1QSV1_CRAGI	Uncharacterized protein
A	K1Q2L4_CRAGI	Transmembrane emp24 domain-containing protein 9
A	K1RMM6_CRAGI	Centromere protein J
A	K1QKK2_CRAGI	NADH dehydrogenase [ubiquinone] 1 beta subcomplex subunit 11, mitochondrial
A	K1PNV6_CRAGI	Dolichyl-diphosphooligosaccharide--protein glycosyltransferase subunit DAD1
A	K1PNQ1_CRAGI	Ankyrin repeat domain-containing protein 5
A	K1QKQ8_CRAGI	THO complex subunit 4-A
A	K1QAG9_CRAGI	Ferritin
A	K1QHW8_CRAGI	Ferritin
A	K1RFV5_CRAGI	ATP-dependent RNA helicase DDX1
A	K1RNH1_CRAGI	60S ribosomal protein L18 (Fragment)
A	K1PPQ1_CRAGI	14-3-3 protein gamma
A	K1QQV0_CRAGI	Histone H1.2
A	K1Q1R1_CRAGI	Exostosin-3
A	K1QYF5_CRAGI	Apoptosis-inducing factor 1, mitochondrial
A	K1RZE2_CRAGI	Isocitrate dehydrogenase [NADP]
A	K1QL00_CRAGI	Microsomal glutathione S-transferase 1
A	K1QTV1_CRAGI	Uncharacterized protein
A	K1RZM3_CRAGI	Cartilage acidic protein 1
A	K1Q0I8_CRAGI	Putative splicing factor, arginine/serine-rich 7
A	K1RP91_CRAGI	Putative RNA exonuclease NEF-sp
A	K1PG60_CRAGI	60S ribosomal protein L17
A	K1QTP4_CRAGI	5'-3' exoribonuclease
A	K1RG79_CRAGI	Neuronal acetylcholine receptor subunit alpha-6
A	K1Q947_CRAGI	Dynein light chain

A	K1RJ91_CRAGI	Ubiquitin-associated protein 2
A	K1Q2Z5_CRAGI	Putative ATP-dependent RNA helicase DDX46
A	K1PYA0_CRAGI	Cytoplasmic dynein 2 heavy chain 1
A	K1QAV0_CRAGI	Guanine nucleotide-binding protein G(Q) subunit alpha
A	K1RKR8_CRAGI	Pumilio-like protein 2
A	K1QZI3_CRAGI	Myosin-Ie
A	K1R5R4_CRAGI	Dynein heavy chain 10, axonemal
A	K1QKG8_CRAGI	Upstream activation factor subunit spp27
A	K1P8I1_CRAGI	Pleckstrin-like protein domain-containing family F member 2 (Fragment)
A	K1Q1N1_CRAGI	Alpha-mannosidase
A	K1PXB6_CRAGI	Cadherin-23
A	K1QXA9_CRAGI	Sortilin-related receptor
A	K1PVG0_CRAGI	Long-chain fatty acid transport protein 4
A	K1PBG6_CRAGI	Uncharacterized protein
A	K1PP50_CRAGI	Golgi integral membrane protein 4
A	K1QCQ5_CRAGI	Succinate--CoA ligase [ADP-forming] subunit beta, mitochondrial
A	K1PK87_CRAGI	Putative E3 ubiquitin-protein ligase TRIP12
A	K1Q373_CRAGI	Splicing factor, arginine/serine-rich 7
A	K1Q151_CRAGI	60S ribosomal protein L32
A	K1QZ95_CRAGI	Nuclear pore complex protein
A	K1PPH0_CRAGI	Gamma-tubulin complex component
A	K1R0R7_CRAGI	Putative ATP-dependent RNA helicase DHX36
A	K1R247_CRAGI	Condensin complex subunit 1
A	K1QIB2_CRAGI	Mitogen-activated protein kinase
A	K1QG61_CRAGI	Acetolactate synthase-like protein
A	K1RBC9_CRAGI	Transketolase-like protein 2
A	K1RCW5_CRAGI	Eukaryotic translation initiation factor 4 gamma 3
A	K1PQZ3_CRAGI	Armadillo repeat-containing protein 4
A	K1PYJ8_CRAGI	Uncharacterized protein
A	K1QQP1_CRAGI	Programmed cell death protein 4
A	K1PQY0_CRAGI	Protein quiver
A	K1PLC6_CRAGI	Nucleolar protein 14
A	K1QV25_CRAGI	Transcription elongation factor B polypeptide 2
A	K1QZ50_CRAGI	RNA-dependent RNA polymerase
A	K1QXH7_CRAGI	DNA replication licensing factor mcm4-B
A	K1PDE4_CRAGI	Protein arginine N-methyltransferase
A	K1QT36_CRAGI	Golgi resident protein GCP60
A	K1PZ89_CRAGI	Mannosyl-oligosaccharide glucosidase
A	K1Q7A7_CRAGI	Putative tyrosinase-like protein tyr-3
A	K1R481_CRAGI	Epimerase family protein SDR39U1
A	K1RJ35_CRAGI	All-trans-retinol 13,14-reductase
A	Q70MT4_CRAGI	40S ribosomal protein S10
A	K1REV3_CRAGI	DNA polymerase delta subunit 2
A	K1P9F1_CRAGI	Insulin-like growth factor-binding protein complex acid labile chain
A	K1PJ65_CRAGI	Dual specificity mitogen-activated protein kinase kinase 7
A	K1Q2T0_CRAGI	ADP-dependent glucokinase
A	K1PZI3_CRAGI	SWI/SNF complex subunit SMARCC2
A	K1Q8C5_CRAGI	Putative ATP-dependent RNA helicase DDX47
A	K1QZ58_CRAGI	Splicing factor U2AF 26 kDa subunit
A	K1RR98_CRAGI	NADH dehydrogenase [ubiquinone] 1 alpha subcomplex subunit 4-like 2
A	K1QMT2_CRAGI	Signal peptidase complex catalytic subunit SEC11
A	K1PWM3_CRAGI	MICOS complex subunit MIC13
A	K1QMM4_CRAGI	Leucine zipper transcription factor-like protein 1
A	K1QMV7_CRAGI	V-type proton ATPase subunit D
A	K1QKI1_CRAGI	Tudor domain-containing protein 1
A	K1P0H0_CRAGI	Aspartyl/asparaginyl beta-hydroxylase
A	K1PVQ8_CRAGI	Eukaryotic translation initiation factor 3 subunit K
A	K1Q5P0_CRAGI	60S ribosomal protein L17
A	K1QJ36_CRAGI	Muscle, skeletal receptor tyrosine protein kinase
A	K1PHS4_CRAGI	Ribosome-binding protein 1

A	K1QQB4_CRAGI	Long-chain-fatty-acid--CoA ligase 1
A	K1QYM4_CRAGI	D-beta-hydroxybutyrate dehydrogenase, mitochondrial
A	K1P2G0_CRAGI	Strawberry notch-like protein 1
A	K1QCT0_CRAGI	Sideroflexin
A	K1QFG2_CRAGI	Telomere-associated protein RIF1
A	K1Q5J7_CRAGI	Uncharacterized protein
A	K1QKA9_CRAGI	Piwi-like protein 2
A	K1P7Q6_CRAGI	40S ribosomal protein S19
A	K1QYV5_CRAGI	Cytoplasmic polyadenylation element-binding protein 1-B
A	K1QG84_CRAGI	THO complex subunit 2
A	K1R7G0_CRAGI	Chromobox-like protein 5
A	K1QHX4_CRAGI	Uncharacterized protein
A	K1QBY6_CRAGI	Transmembrane protein Tmp21
A	K1PKK7_CRAGI	AP-2 complex subunit mu-1
A	K1P9V5_CRAGI	General transcription factor IIF subunit 1
A	K1Q9V2_CRAGI	Antigen KI-67
A	K1PNU2_CRAGI	Histone-arginine methyltransferase CARM1
A	K1Q109_CRAGI	Neurexin-4
A	K1P9Q2_CRAGI	Signal peptidase complex subunit 3
A	K1QCN0_CRAGI	Signal recognition particle 9 kDa protein
A	K1Q7E4_CRAGI	Ubiquitin-conjugating enzyme E2 N
A	K1Q5G6_CRAGI	60 kDa heat shock protein, mitochondrial
A	K1RUW0_CRAGI	E3 SUMO-protein ligase RanBP2
A	K1RB91_CRAGI	Neutral alpha-glucosidase AB
A	K1QGF1_CRAGI	Splicing factor 3B subunit 2
A	K1Q525_CRAGI	Mechanosensory protein 2 (Fragment)
A	K1RDB3_CRAGI	F-box/WD repeat-containing protein 1A
A	K1QI28_CRAGI	V-type proton ATPase subunit B
A	K1R4J0_CRAGI	MAGUK p55 subfamily member 2
A	K1Q9T7_CRAGI	Afadin-and alpha-actinin-binding protein
A	K1RNH6_CRAGI	Toll-like receptor 3
A	K1PZC0_CRAGI	Structural maintenance of chromosomes protein
A	K1PT69_CRAGI	Uncharacterized protein
A	K1RE67_CRAGI	Methylated-DNA--protein-cysteine methyltransferase
A	K1QCX5_CRAGI	Cyclic AMP-dependent transcription factor ATF-2
A	K1QBT8_CRAGI	Uncharacterized protein
A	K1RFF1_CRAGI	Uncharacterized protein
A	K1RS40_CRAGI	Uncharacterized protein
A	K1R8V1_CRAGI	Puratrophin-1

Data S2: Identified proteins by RNA pull down coupled with mass spectrometry with m6A or A-oligo, in nuclear or cytosolic protein extracts

Proteins identified in cytosolic extracts

Oligo	Accession	Description
m6A	K1QNA2_CRAGI	Vitellogenin-6
m6A	K1QVJ8_CRAGI	Piwi-like protein 1
m6A	K1QQ94_CRAGI	Uncharacterized protein
m6A	K1QHK9_CRAGI	Dynein heavy chain, cytoplasmic
m6A	K1QQ68_CRAGI	Tubulin alpha chain
m6A	K1RLF8_CRAGI	Splicing factor 3B subunit 3
m6A	K1R473_CRAGI	Tubulin alpha chain
m6A	K1QII6_CRAGI	Tubulin alpha chain
m6A	K1PNR3_CRAGI	Clathrin heavy chain
m6A	K1R7V7_CRAGI	Tubulin beta chain
m6A	K1PNI6_CRAGI	Heterogeneous nuclear ribonucleoprotein A/B
m6A	K1QMX5_CRAGI	Uncharacterized protein
m6A	K1QHI5_CRAGI	Pyruvate carboxylase, mitochondrial
m6A	K1PE00_CRAGI	Tubulin alpha chain
m6A	K1R294_CRAGI	T-complex protein 1 subunit beta
m6A	K1S4Q2_CRAGI	T-complex protein 1 subunit delta (Fragment)
m6A	K1PQP2_CRAGI	Nucleolin
m6A	K1R466_CRAGI	T-complex protein 1 subunit gamma
m6A	K1PN21_CRAGI	Tubulin beta chain
m6A	K1R164_CRAGI	Galectin-4
m6A	K1S2N7_CRAGI	Innexin
m6A	K1R6Z7_CRAGI	ATP synthase subunit alpha
m6A	K1R5B4_CRAGI	Proteasome activator complex subunit 4
m6A	K1PVA1_CRAGI	Transitional endoplasmic reticulum ATPase
m6A	K1QFW9_CRAGI	Uncharacterized protein
m6A	K1R0S3_CRAGI	T-complex protein 1 subunit theta
m6A	K1QMA4_CRAGI	RRP5-like protein
m6A	K1R3U2_CRAGI	Uncharacterized protein
m6A	K1Q9W5_CRAGI	T-complex protein 1 subunit eta
m6A	K1QBK6_CRAGI	Splicing factor 3B subunit 1
m6A	K1R545_CRAGI	Pre-mRNA-processing-splicing factor 8 (Fragment)
m6A	K1RAJ1_CRAGI	T-complex protein 1 subunit alpha
m6A	K1RWS2_CRAGI	Transcriptional activator protein Pur-alpha
m6A	K1Q350_CRAGI	Glyceraldehyde-3-phosphate dehydrogenase
m6A	K1RGT5_CRAGI	Metalloendopeptidase
m6A	K1PJ85_CRAGI	26S protease regulatory subunit 6A
m6A	K1S6V7_CRAGI	Serine/threonine-protein phosphatase 2A 65 kDa regulatory subunit A alpha isoform
m6A	K1S1S1_CRAGI	Insulin-like growth factor 2 mRNA-binding protein 1
m6A	K1RZE2_CRAGI	Isocitrate dehydrogenase [NADP]
m6A	K1PNQ5_CRAGI	Heat shock protein HSP 90-alpha 1
m6A	K1R866_CRAGI	Puromycin-sensitive aminopeptidase
m6A	K1P9D0_CRAGI	Stress-70 protein, mitochondrial
m6A	K1QXX7_CRAGI	Myosin heavy chain, non-muscle (Fragment)
m6A	K1RG73_CRAGI	Acetyl-CoA carboxylase
m6A	K1R420_CRAGI	Non-specific serine/threonine protein kinase
m6A	K1PXN5_CRAGI	T-complex protein 1 subunit zeta
m6A	K1QGS8_CRAGI	Elongation factor 1-alpha
m6A	K1RLC5_CRAGI	T-complex protein 1 subunit epsilon
m6A	K1R6Q7_CRAGI	DNA topoisomerase I
m6A	K1RW85_CRAGI	Adenosylhomocysteinase
m6A	K1QSX8_CRAGI	ATPase family AAA domain-containing protein 2B
m6A	K1R4Z3_CRAGI	Malate dehydrogenase, mitochondrial
m6A	K1PEY4_CRAGI	26S proteasome non-ATPase regulatory subunit 2
m6A	K1RI55_CRAGI	Insulin-like growth factor 2 mRNA-binding protein 3
m6A	K1PK85_CRAGI	Cullin-associated NEDD8-dissociated protein 1
m6A	K1R9B6_CRAGI	H/ACA ribonucleoprotein complex subunit 4
m6A	K1R252_CRAGI	Putative methylmalonate-semialdehyde dehydrogenase [acylating], mitochondrial

m6A	K1RK12_CRAGI	40S ribosomal protein S23
m6A	K1QVN9_CRAGI	T-complex protein 1 subunit eta
m6A	K1PLF9_CRAGI	Arginine kinase
m6A	Q8TA69_CRAGI	Actin 2
m6A	K1QG58_CRAGI	Actin
m6A	K1QSB2_CRAGI	26S protease regulatory subunit 6B
m6A	K1R401_CRAGI	Spectrin alpha chain
m6A	K1Q1I2_CRAGI	26S protease regulatory subunit 7
m6A	K1Q4I9_CRAGI	D-3-phosphoglycerate dehydrogenase (Fragment)
m6A	K1RJH5_CRAGI	Polyadenylate-binding protein
m6A	K1RWD4_CRAGI	Actin, cytoplasmic
m6A	K1QI14_CRAGI	40S ribosomal protein S3a
m6A	K1RWW5_CRAGI	ATP synthase subunit beta
m6A	K1QET2_CRAGI	Coatomer subunit alpha
m6A	K1QVS3_CRAGI	Thimet oligopeptidase
m6A	K1QSQ9_CRAGI	Putative ATP-dependent RNA helicase an3
m6A	K1Q923_CRAGI	Putative ATP-dependent RNA helicase DDX4
m6A	K1QXR4_CRAGI	Pancreatic lipase-related protein 2
m6A	K1R512_CRAGI	Uncharacterized protein
m6A	K1R8L1_CRAGI	Exportin-2
m6A	K1PAG1_CRAGI	Dynein beta chain, ciliary
m6A	K1Q988_CRAGI	Band 4.1-like protein 3
m6A	K1PJ06_CRAGI	Importin subunit alpha-1
m6A	K1QWX2_CRAGI	60S acidic ribosomal protein P0
m6A	K1PH76_CRAGI	Y-box factor-like protein (Fragment)
m6A	K1PW06_CRAGI	Filamin-C
m6A	K1RNB5_CRAGI	Propionyl-CoA carboxylase beta chain, mitochondrial
m6A	K1QWT8_CRAGI	Uncharacterized protein
m6A	K1QNW9_CRAGI	Bifunctional aminoacyl-tRNA synthetase
m6A	K1QCC1_CRAGI	Phosphoglycerate kinase
m6A	K1QBN0_CRAGI	Methylcrotonoyl-CoA carboxylase beta chain, mitochondrial
m6A	K1Q3S7_CRAGI	Cytosolic carboxypeptidase 1
m6A	K1PMT6_CRAGI	Heterogeneous nuclear ribonucleoprotein U-like protein 1
m6A	K1Q9Z6_CRAGI	26S proteasome non-ATPase regulatory subunit 7
m6A	K1PH66_CRAGI	Fibrinolytic enzyme, isozyme C
m6A	K1R1M7_CRAGI	Ubiquitin-like modifier-activating enzyme 1
m6A	K1Q7G8_CRAGI	Fatty acid synthase
m6A	K1QEA6_CRAGI	Phosphoenolpyruvate carboxykinase [GTP]
m6A	K1QRL4_CRAGI	Importin-5
m6A	K1RFT1_CRAGI	Band 4.1-like protein 3
m6A	K1QR72_CRAGI	Dipeptidyl peptidase 3
m6A	K1R5R4_CRAGI	Dynein heavy chain 10, axonemal
m6A	K1QLK6_CRAGI	E3 ubiquitin-protein ligase HUWE1
m6A	K1R5U4_CRAGI	Acetyl-CoA carboxylase 1
m6A	K1QXS6_CRAGI	Heterogeneous nuclear ribonucleoprotein A2-like protein 1
m6A	K1R953_CRAGI	Acetyl-CoA carboxylase
m6A	K1PCS4_CRAGI	Eukaryotic translation initiation factor 2 subunit 3, Y-linked
m6A	K1QIR8_CRAGI	78 kDa glucose-regulated protein
m6A	K1RSA6_CRAGI	Methylcrotonoyl-CoA carboxylase subunit alpha, mitochondrial
m6A	K1R2V1_CRAGI	Importin subunit beta-1
m6A	K1QZW0_CRAGI	Polyadenylate-binding protein 2
m6A	K1R4R9_CRAGI	Mitotic apparatus protein p62
m6A	K1QWK2_CRAGI	MAM domain-containing glycosylphosphatidylinositol anchor protein 2
m6A	K1R2D6_CRAGI	Plastin-3
m6A	K1QB04_CRAGI	26S proteasome non-ATPase regulatory subunit 3
m6A	K1RH70_CRAGI	6-phosphogluconate dehydrogenase, decarboxylating
m6A	K1QGK2_CRAGI	Coatomer subunit beta
m6A	K1QUE6_CRAGI	26S proteasome non-ATPase regulatory subunit 6
m6A	K1R7I9_CRAGI	Heterogeneous nuclear ribonucleoprotein Q
m6A	K1PND7_CRAGI	Fatty acid synthase

m6A	K1QI28_CRAGI	V-type proton ATPase subunit B
m6A	K1Q2H5_CRAGI	Uncharacterized protein
m6A	K1QLT5_CRAGI	26S protease regulatory subunit 4
m6A	K1R4I2_CRAGI	26S proteasome non-ATPase regulatory subunit 3
m6A	K1QQR1_CRAGI	Major vault protein
m6A	K1RAU3_CRAGI	DNA ligase
m6A	K1PFG1_CRAGI	Uncharacterized protein
m6A	K1RBC9_CRAGI	Transketolase-like protein 2
m6A	K1QT21_CRAGI	Putative ATP-dependent RNA helicase DDX5
m6A	K1PKK7_CRAGI	AP-2 complex subunit mu-1
m6A	K1Q358_CRAGI	60S acidic ribosomal protein P2
m6A	K1PS71_CRAGI	Uncharacterized protein
m6A	K1QHA2_CRAGI	Spectrin beta chain, brain 4
m6A	K1REG6_CRAGI	DNA helicase
m6A	A7M7T7_CRAGI	Non-selenium glutathione peroxidase
m6A	K1QHX2_CRAGI	La-related protein 7
m6A	K1RJ97_CRAGI	Multifunctional protein ADE2
m6A	K1RNZ6_CRAGI	Eukaryotic translation initiation factor 3 subunit D
m6A	K1PAY7_CRAGI	Propionyl-CoA carboxylase alpha chain, mitochondrial
m6A	K1QQ27_CRAGI	Pancreatic lipase-related protein 2
m6A	K1Q9K6_CRAGI	Histone H3
m6A	K1R083_CRAGI	Aspartate aminotransferase, mitochondrial
m6A	K1PEP0_CRAGI	40S ribosomal protein S8
m6A	K1PU26_CRAGI	Malate dehydrogenase (Fragment)
m6A	K1QF01_CRAGI	40S ribosomal protein S4
m6A	K1QDN1_CRAGI	Heat shock protein 75 kDa, mitochondrial (Fragment)
m6A	K1QBH0_CRAGI	Uncharacterized protein
m6A	K1Q9V3_CRAGI	V-type proton ATPase catalytic subunit A
m6A	K1PJC1_CRAGI	Adipophilin
m6A	K1Q330_CRAGI	Dihydrolipoyl dehydrogenase
m6A	K1S3Y1_CRAGI	2-amino-3-ketobutyrate coenzyme A ligase, mitochondrial (Fragment)
m6A	K1R2Q9_CRAGI	Aspartate aminotransferase
m6A	K1QEF2_CRAGI	ADP-ribosylation factor-like protein 15
m6A	K1PVH5_CRAGI	Centromere/kinetochore protein zw10-like protein
m6A	K1PG07_CRAGI	Lupus La-like protein
m6A	K1QMX8_CRAGI	DNA replication licensing factor MCM7
m6A	K1P7K8_CRAGI	Vesicle-fusing ATPase 1
m6A	K1QQL6_CRAGI	Leucyl-tRNA synthetase, cytoplasmic
m6A	K1PY89_CRAGI	Extracellular superoxide dismutase [Cu-Zn]
m6A	K1QKA9_CRAGI	Piwi-like protein 2
m6A	K1QHI6_CRAGI	Dynein heavy chain 5, axonemal
m6A	K1QBF7_CRAGI	Hypoxia up-regulated protein 1
m6A	K1RTR1_CRAGI	ATP-citrate synthase
m6A	K1PZF2_CRAGI	Exportin-7
m6A	K1PPP8_CRAGI	Vigilin
m6A	K1RN77_CRAGI	Nuclear autoantigenic sperm protein
m6A	K1PV49_CRAGI	RuvB-like helicase
m6A	K1QXQ8_CRAGI	DNA helicase
m6A	K1P2G0_CRAGI	Strawberry notch-like protein 1
m6A	K1QRQ2_CRAGI	Glutamate dehydrogenase 1, mitochondrial
m6A	K1QHS8_CRAGI	Ribonucleoside-diphosphate reductase
m6A	K1QX26_CRAGI	Endoplasmin
m6A	K1QGB4_CRAGI	40S ribosomal protein S17
m6A	K1RJJ7_CRAGI	Histone H5
m6A	K1QY85_CRAGI	Transport protein Sec31A
m6A	K1Q6W3_CRAGI	Talin-1
m6A	K1R3V8_CRAGI	COP9 signalosome complex subunit 4
m6A	K1QY12_CRAGI	Dynamin-1-like protein
m6A	K1PYA0_CRAGI	Cytoplasmic dynein 2 heavy chain 1
m6A	K1PF10_CRAGI	PAN2-PAN3 deadenylation complex catalytic subunit PAN2

m6A	K1PNP4_CRAGI	26S proteasome non-ATPase regulatory subunit 11
m6A	K1QMB9_CRAGI	Eukaryotic translation initiation factor 3 subunit A
m6A	K1QC10_CRAGI	GTP-binding protein 1
m6A	K1QK56_CRAGI	Uncharacterized protein
m6A	K1PJP9_CRAGI	26S proteasome non-ATPase regulatory subunit 1
m6A	K1PUL2_CRAGI	Long-chain-fatty-acid--CoA ligase 1
m6A	K1Q7Q2_CRAGI	CCAAT/enhancer-binding protein zeta
m6A	K1QQK1_CRAGI	26S proteasome non-ATPase regulatory subunit 12
m6A	K1R3T3_CRAGI	Transcription factor BTF3
m6A	K1PK93_CRAGI	GDP-L-fucose synthetase
m6A	K1PF96_CRAGI	Spliceosome RNA helicase BAT1
m6A	K1PM50_CRAGI	40S ribosomal protein S16
m6A	K1PX47_CRAGI	Ubiquitin carboxyl-terminal hydrolase
m6A	K1QMV7_CRAGI	V-type proton ATPase subunit D
m6A	K1RAL0_CRAGI	Aspartate aminotransferase, cytoplasmic
m6A	K1P9N7_CRAGI	14-3-3 protein zeta
m6A	K1QBR5_CRAGI	Uncharacterized protein
m6A	K1PVW0_CRAGI	S-adenosylmethionine synthase
m6A	K1PY73_CRAGI	Basic leucine zipper and W2 domain-containing protein 1
m6A	K1QBL6_CRAGI	Tudor domain-containing protein 1
m6A	K1Q9M7_CRAGI	Histone H1-delta
m6A	K1S151_CRAGI	Rab GDP dissociation inhibitor
m6A	K1RM80_CRAGI	Citrate synthase
m6A	K1R115_CRAGI	Succinate dehydrogenase [ubiquinone] flavoprotein subunit, mitochondrial
m6A	K1R5D5_CRAGI	U3 small nucleolar RNA-associated protein 6-like protein
m6A	K1QSR2_CRAGI	Apoptosis inhibitor 5
m6A	K1P5D4_CRAGI	Cysteine synthase
m6A	K1PE57_CRAGI	Severin
m6A	K1P8I1_CRAGI	Pleckstrin-like protein domain-containing family F member 2 (Fragment)
m6A	K1Q5G9_CRAGI	SUMO-activating enzyme subunit 2
m6A	K1PVZ3_CRAGI	Cold shock domain-containing protein E1
m6A	K1R4D4_CRAGI	40S ribosomal protein SA
m6A	K1QXH3_CRAGI	Translational activator GCN1
m6A	K1PI02_CRAGI	Talin-1
m6A	K1P3Q5_CRAGI	Programmed cell death 6-interacting protein
m6A	K1PKF5_CRAGI	Protein-glutamine gamma-glutamyltransferase 4
m6A	K1QFZ8_CRAGI	Ceramide kinase-like protein
m6A	K1PJF4_CRAGI	Isoleucyl-tRNA synthetase, cytoplasmic
m6A	K1PV79_CRAGI	Importin subunit alpha
m6A	K1QMD3_CRAGI	Glycerol-3-phosphate dehydrogenase [NAD(+)]
m6A	K1RDV7_CRAGI	Cell division control protein 2-like protein (Fragment)
m6A	K1P8W6_CRAGI	60S ribosomal protein L4
m6A	K1P112_CRAGI	ATP synthase subunit gamma, mitochondrial
m6A	K1R5F2_CRAGI	14-3-3 protein epsilon
m6A	K1QBW8_CRAGI	Uncharacterized protein
m6A	K1PZP6_CRAGI	Coatomer subunit gamma
m6A	K1PAR4_CRAGI	Unc-45-like protein A
m6A	K1QRZ3_CRAGI	40S ribosomal protein S13
m6A	K1QQB6_CRAGI	40S ribosomal protein S14
m6A	K1QE71_CRAGI	DNA helicase
m6A	K1RJM8_CRAGI	SAGA-associated factor 11 homolog
m6A	K1RK33_CRAGI	Exportin-1
m6A	K1PPW8_CRAGI	Coatomer subunit beta
m6A	K1QRK9_CRAGI	Succinyl-CoA ligase [GDP-forming] subunit beta, mitochondrial
m6A	K1Q273_CRAGI	60S ribosomal protein L14
m6A	K1PLY1_CRAGI	DNA polymerase
m6A	K1PYR4_CRAGI	26S proteasome non-ATPase regulatory subunit 1
m6A	K1QPC6_CRAGI	Nucleolar complex protein 2-like protein
m6A	K1QP17_CRAGI	Caprin-1
m6A	K1R2N0_CRAGI	Histone H4

m6A	K1Q5G6_CRAGI	60 kDa heat shock protein, mitochondrial
m6A	K1RIG6_CRAGI	LSM14-like protein A
m6A	K1QY71_CRAGI	Histone H2B
m6A	K1QAB1_CRAGI	AP-2 complex subunit alpha
m6A	K1QAF3_CRAGI	Alanine aminotransferase 2
m6A	K1QI97_CRAGI	Adenylyl cyclase-associated protein
m6A	K1PD57_CRAGI	Constitutive coactivator of PPAR-gamma-like protein 1-like protein
m6A	K1Q0L1_CRAGI	60S ribosomal protein L23a
m6A	K1RGB7_CRAGI	Epidermal retinal dehydrogenase 2
m6A	K1R0Y9_CRAGI	ADP,ATP carrier protein
m6A	K1QXF5_CRAGI	Calcyphosin-like protein
m6A	K1PA54_CRAGI	Replication factor C subunit 3
m6A	K1PS27_CRAGI	DNA helicase
m6A	K1R8C6_CRAGI	40S ribosomal protein S12
m6A	K1Q880_CRAGI	Transportin-1
m6A	K1PXD4_CRAGI	Putative ATP-dependent RNA helicase DDX6
m6A	K1P421_CRAGI	Histone H2A
m6A	K1RL00_CRAGI	Proteasome-associated protein ECM29-like protein
m6A	K1PI50_CRAGI	40S ribosomal protein S26
m6A	K1RCW5_CRAGI	Eukaryotic translation initiation factor 4 gamma 3
m6A	K1R0W4_CRAGI	Signal recognition particle subunit SRP72
m6A	K1QN11_CRAGI	Pre-mRNA-processing-splicing factor 8
m6A	K1R8R6_CRAGI	Fructose-bisphosphate aldolase
m6A	K1QVE8_CRAGI	Phosphoacetylglucosamine mutase
m6A	K1R5B9_CRAGI	DNA-directed RNA polymerase, mitochondrial
m6A	K1QA50_CRAGI	V-type proton ATPase subunit H
m6A	K1Q9J5_CRAGI	Importin-4
m6A	K1R3V0_CRAGI	CAD protein
m6A	K1PFK8_CRAGI	Uncharacterized protein
m6A	K1PSN0_CRAGI	Pre-mRNA-processing factor 40-like protein A
m6A	K1QL67_CRAGI	60S ribosomal protein L7a
m6A	K1QE32_CRAGI	Very long-chain specific acyl-CoA dehydrogenase, mitochondrial
m6A	K1QQ16_CRAGI	AP complex subunit beta
m6A	K1QN79_CRAGI	40S ribosomal protein S11
m6A	K1P8B7_CRAGI	Ubiquitin-conjugating enzyme E2-17 kDa (Fragment)
m6A	K1RHB2_CRAGI	Nucleolar RNA helicase 2
m6A	K1QWC3_CRAGI	40S ribosomal protein S3
m6A	K1Q4E1_CRAGI	N-acetyl-D-glucosamine kinase
m6A	K1Q6F7_CRAGI	V-type proton ATPase subunit C
m6A	K1R3I6_CRAGI	Nucleolar complex protein 2-like protein (Fragment)
m6A	K1PFS5_CRAGI	Elongation factor 1-gamma
m6A	K1PBZ4_CRAGI	Regulator of nonsense transcripts 1
m6A	K1RV41_CRAGI	Guanine nucleotide-binding protein subunit beta-2-like 1
m6A	K1QKV1_CRAGI	Cytochrome b-c1 complex subunit 6
m6A	K1S2Y0_CRAGI	Uncharacterized protein
m6A	K1QKK5_CRAGI	Vacuolar protein sorting-associated protein 4B
m6A	K1Q8S0_CRAGI	Nucleolar complex protein 3 homolog
m6A	K1QWK6_CRAGI	Metalloendopeptidase
m6A	K1PH31_CRAGI	Protein arginine N-methyltransferase 1
m6A	K1R834_CRAGI	60S ribosomal protein L9
m6A	K1RDG4_CRAGI	DNA helicase
m6A	K1R591_CRAGI	Inter-alpha-trypsin inhibitor heavy chain H4
m6A	K1Q9P5_CRAGI	Mitochondrial-processing peptidase subunit beta
m6A	K1QLS3_CRAGI	Cytochrome b-c1 complex subunit 2, mitochondrial
m6A	K1QNT7_CRAGI	Aldehyde dehydrogenase, mitochondrial
m6A	K1QDX9_CRAGI	Ribosome biogenesis protein BMS1-like protein
m6A	K1S6G3_CRAGI	Ubiquitin-like modifier-activating enzyme 1
m6A	K1R8S7_CRAGI	Phospholipase A-2-activating protein
m6A	K1QFN1_CRAGI	60S ribosomal protein L23
m6A	K1Q5Z6_CRAGI	Eukaryotic translation initiation factor 2 subunit 2

m6A	K1R6C2_CRAGI	Peroxisomal 3,2-trans-enoyl-CoA isomerase
m6A	K1Q0R4_CRAGI	ATP-binding cassette sub-family F member 2
m6A	K1P5V7_CRAGI	Eukaryotic translation initiation factor 3 subunit C
m6A	K1PGW7_CRAGI	Transmembrane protein 2
m6A	K1RKC1_CRAGI	Far upstream element-binding protein 3
m6A	K1QHY1_CRAGI	Eosinophil peroxidase
m6A	K1QLK8_CRAGI	GTP-binding protein SAR1b
m6A	K1QRG9_CRAGI	Uncharacterized protein
m6A	K1QRW4_CRAGI	Coronin
m6A	K1QKI1_CRAGI	Tudor domain-containing protein 1
m6A	K1QRM1_CRAGI	Nuclear pore protein
m6A	K1RBZ5_CRAGI	Ran GTPase-activating protein 1
m6A	K1RLT4_CRAGI	Signal recognition particle subunit SRP68
m6A	K1R7N6_CRAGI	Eukaryotic translation initiation factor 6
m6A	K1P5F7_CRAGI	Metastasis-associated protein MTA1
m6A	K1RCW3_CRAGI	Elongation factor 1-beta
m6A	K1R2H9_CRAGI	WD repeat-containing protein 35
m6A	K1Q1K8_CRAGI	Elongation factor 1-beta
m6A	K1QTD9_CRAGI	Nucleolar protein 56
m6A	K1QBW6_CRAGI	Tudor domain-containing protein 1
m6A	K1QFR9_CRAGI	Spectrin beta chain
m6A	K1P9S7_CRAGI	Brix domain-containing protein 2
m6A	K1QEK7_CRAGI	Ubiquitin carboxyl-terminal hydrolase
m6A	K1PAM6_CRAGI	Uncharacterized protein
m6A	K1S3G2_CRAGI	HMGB1
m6A	K1QI11_CRAGI	Pyruvate dehydrogenase E1 component subunit alpha type II, mitochondrial
m6A	K1QF31_CRAGI	Serine/threonine-protein kinase PLK
m6A	K1QDA7_CRAGI	Uracil phosphoribosyltransferase
m6A	K1QKN4_CRAGI	Dynein heavy chain 6, axonemal
m6A	K1RNH1_CRAGI	60S ribosomal protein L18 (Fragment)
m6A	K1QK11_CRAGI	Dynein heavy chain 7, axonemal
m6A	K1QED7_CRAGI	Replication protein A subunit
m6A	K1PB82_CRAGI	Electron transfer flavoprotein subunit beta
m6A	K1PPQ1_CRAGI	14-3-3 protein gamma
m6A	K1R8T6_CRAGI	Cullin-1
m6A	K1Q7E4_CRAGI	Ubiquitin-conjugating enzyme E2 N
m6A	K1RSZ6_CRAGI	40S ribosomal protein S7
m6A	K1Q1S3_CRAGI	Myosin-VI
m6A	K1QH70_CRAGI	Leucine-rich repeat-containing protein 40
m6A	K1QZI3_CRAGI	Myosin-Ie
m6A	K1Q4Z4_CRAGI	Bifunctional purine biosynthesis protein PURH
m6A	K1Q5H6_CRAGI	FACT complex subunit SSRP1
m6A	K1PKL8_CRAGI	Serine/threonine-protein phosphatase 2A 56 kDa regulatory subunit alpha isoform
m6A	K1QUC6_CRAGI	Uncharacterized protein
m6A	K1QPP2_CRAGI	Elongation factor Tu, mitochondrial
m6A	K1QMH5_CRAGI	Small nuclear ribonucleoprotein Sm D1
m6A	K1PZD9_CRAGI	26S proteasome non-ATPase regulatory subunit 11
m6A	K1PBU0_CRAGI	L-fucose kinase
m6A	K1QYB6_CRAGI	Delta-1-pyrroline-5-carboxylate synthetase
m6A	K1PMP3_CRAGI	Protoporphyrinogen oxidase
m6A	K1Q2E0_CRAGI	AP-1 complex subunit mu-1
m6A	K1QEF9_CRAGI	Protein-glutamine gamma-glutamyltransferase K
m6A	K1QGE4_CRAGI	Proteasome endopeptidase complex (Fragment)
m6A	K1Q6V6_CRAGI	Replication factor C subunit 4
m6A	K1QYT7_CRAGI	COP9 signalosome complex subunit 7a
m6A	K1PWP4_CRAGI	Phenylalanyl-tRNA synthetase alpha chain
m6A	K1PWD9_CRAGI	Uncharacterized protein
m6A	K1QAH9_CRAGI	H/ACA ribonucleoprotein complex subunit
m6A	K1PS13_CRAGI	Coatomer subunit beta (Fragment)
m6A	K1QJ33_CRAGI	Aminoacyl tRNA synthetase complex-interacting multifunctional protein 2

m6A	K1QRL6_CRAGI	Methenyltetrahydrofolate synthetase domain-containing protein
m6A	K1PU46_CRAGI	Lethal(2) giant larvae-like protein 1
m6A	K1R7J6_CRAGI	Putative sodium/potassium-transporting ATPase subunit beta-2
m6A	K1QYV6_CRAGI	NMDA receptor-regulated protein 1
m6A	K1R6E9_CRAGI	Dihydrolipoamide acetyltransferase component of pyruvate dehydrogenase complex
m6A	K1P7L9_CRAGI	Nucleolar GTP-binding protein 1
m6A	K1PIB7_CRAGI	Phenylalanyl-tRNA synthetase beta chain
m6A	K1PX23_CRAGI	Eukaryotic peptide chain release factor subunit 1
m6A	K1QDV6_CRAGI	Protein argonaute-2
m6A	K1R5G4_CRAGI	60S ribosomal protein L31
m6A	K1R9T2_CRAGI	Eukaryotic translation initiation factor 3 subunit B
m6A	K1PW99_CRAGI	Protein OSCP1
m6A	K1R1F0_CRAGI	ATP-dependent DNA helicase 2 subunit 1
m6A	K1Q260_CRAGI	Nucleolar protein 58
m6A	K1QFS4_CRAGI	Actin-related protein 2
m6A	K1QLZ1_CRAGI	Actin-related protein 3
m6A	K1Q6X5_CRAGI	Protein disulfide-isomerase
m6A	K1PJB0_CRAGI	Heat shock protein 70 B2
m6A	K1Q8K2_CRAGI	Importin subunit alpha
m6A	K1PKF6_CRAGI	26S proteasome non-ATPase regulatory subunit 13
m6A	K1QGL9_CRAGI	Mannose-1-phosphate guanyltransferase beta
m6A	K1RGJ7_CRAGI	Neogenin
m6A	K1PUJ1_CRAGI	Radixin
m6A	K1Q811_CRAGI	Alpha-centractin
m6A	K1QWZ0_CRAGI	Tetratricopeptide repeat protein 38
m6A	K1PRL4_CRAGI	60S ribosomal protein L38 (Fragment)
m6A	K1Q9I1_CRAGI	TRAF2 and NCK-interacting protein kinase
m6A	K1QVR0_CRAGI	26S proteasome non-ATPase regulatory subunit 8
m6A	K1QK68_CRAGI	Myosin-2 essential light chain
m6A	K1QMH2_CRAGI	DNA polymerase
m6A	K1PD36_CRAGI	Ubiquitin
m6A	K1Q4V0_CRAGI	Myosin-VIIa
m6A	K1QBT2_CRAGI	Proteasome subunit beta
m6A	K1PXU6_CRAGI	60S ribosomal protein L24
m6A	K1Q329_CRAGI	Pyruvate dehydrogenase E1 component subunit beta, mitochondrial
m6A	K1QDH9_CRAGI	Myosin-11
m6A	K1QW36_CRAGI	60S ribosomal protein L6
m6A	K1Q4Y8_CRAGI	Histone H1oo
m6A	K1PM66_CRAGI	60S ribosomal protein L12
m6A	K1Q4U7_CRAGI	AP-3 complex subunit delta-1
m6A	K1QPY8_CRAGI	Extracellular superoxide dismutase [Cu-Zn]
m6A	K1QIP0_CRAGI	26S proteasome non-ATPase regulatory subunit 5
m6A	K1QW72_CRAGI	Catalase
m6A	K1QMD8_CRAGI	Proteasome subunit alpha type
m6A	K1PZC0_CRAGI	Structural maintenance of chromosomes protein
m6A	K1RBI9_CRAGI	Small nuclear ribonucleoprotein Sm D2
m6A	K1QCQ5_CRAGI	Succinate--CoA ligase [ADP-forming] subunit beta, mitochondrial
m6A	K1R0L4_CRAGI	Sodium/potassium-transporting ATPase subunit alpha
m6A	K1QKG9_CRAGI	Cysteine desulfurase, mitochondrial
m6A	K1PPK1_CRAGI	Actin-related protein 2/3 complex subunit 4
m6A	K1PUQ5_CRAGI	Histone H2B
m6A	K1RFU6_CRAGI	Proteasome activator complex subunit 3
m6A	K1Q615_CRAGI	Peroxiredoxin-1
m6A	K1RIT6_CRAGI	NADH-ubiquinone oxidoreductase 75 kDa subunit, mitochondrial
m6A	K1PQZ3_CRAGI	Armadillo repeat-containing protein 4
m6A	K1QW41_CRAGI	Leucine-zipper-like transcriptional regulator 1
m6A	K1PNS2_CRAGI	33 kDa inner dynein arm light chain, axonemal
m6A	K1QQP1_CRAGI	Programmed cell death protein 4
m6A	K1QQC1_CRAGI	Dynein light chain roadblock
m6A	K1P6F0_CRAGI	HEAT repeat-containing protein 2

m6A	K1QHM2_CRAGI	Dolichyl-diphosphooligosaccharide--protein glycosyltransferase subunit 2
m6A	K1QY58_CRAGI	Eukaryotic translation initiation factor 3 subunit I (Fragment)
m6A	K1PLA7_CRAGI	Eukaryotic initiation factor 4A-II (Fragment)
m6A	K1R8I8_CRAGI	Acetyltransferase component of pyruvate dehydrogenase complex
m6A	K1R2L7_CRAGI	Glutaminyl-tRNA synthetase (Fragment)
m6A	K1QSD9_CRAGI	Uncharacterized protein
m6A	K1R008_CRAGI	Proteasome subunit alpha type
m6A	K1QBL3_CRAGI	Putative phosphoglycerate mutase
m6A	K1R6S5_CRAGI	40S ribosomal protein S9
m6A	K1QNS4_CRAGI	DnaJ-like protein subfamily C member 9
m6A	K1Q7X3_CRAGI	Pre-mRNA-splicing factor SYF1
m6A	K1QG65_CRAGI	rRNA 2'-O-methyltransferase fibrillarin
m6A	K1QU53_CRAGI	NAD(P) transhydrogenase, mitochondrial
m6A	K1RU04_CRAGI	Actin, cytoplasmic
m6A	K1RAH6_CRAGI	Ubiquitin-conjugating enzyme E2-17 kDa
m6A	K1PTV1_CRAGI	Splicing factor 3B subunit 4
m6A	K1PCR5_CRAGI	KH domain-containing, RNA-binding, signal transduction-associated protein 2
m6A	K1QYH6_CRAGI	COP9 signalosome complex subunit 3
m6A	K1QH74_CRAGI	Splicing factor, arginine/serine-rich 1
m6A	K1PX83_CRAGI	Dynein heavy chain 5, axonemal
m6A	K1QJF7_CRAGI	Coronin
m6A	K1PNX0_CRAGI	Methionyl-tRNA synthetase, cytoplasmic
m6A	K1Q1L4_CRAGI	Uncharacterized protein
m6A	K1PH10_CRAGI	Polyadenylate-binding protein-interacting protein 1
m6A	K1QCL6_CRAGI	Proteasomal ubiquitin receptor ADRM1
m6A	K1Q1Q9_CRAGI	Alpha-aminoadipic semialdehyde synthase, mitochondrial
m6A	K1QVP6_CRAGI	Developmentally-regulated GTP-binding protein 1
m6A	K1QNU0_CRAGI	Non-specific serine/threonine protein kinase
m6A	K1Q6U0_CRAGI	Coatomer subunit zeta-1
m6A	K1S058_CRAGI	Transcription factor RFX3
m6A	K1R488_CRAGI	Actin-related protein 2/3 complex subunit
m6A	K1Q4G7_CRAGI	Tubulin gamma chain
m6A	K1PDL3_CRAGI	Ribosomal protein L19
m6A	K1PBL2_CRAGI	Eukaryotic initiation factor 4A-III
m6A	K1QE83_CRAGI	CCR4-NOT transcription complex subunit 1
m6A	K1R1Q8_CRAGI	Ras-related protein Rab-5C
m6A	K1R0P8_CRAGI	CTP synthase
m6A	K1QJ46_CRAGI	Putative methylcrotonoyl-CoA carboxylase beta chain, mitochondrial
m6A	K1QG70_CRAGI	Katanin p60 ATPase-containing subunit A1
m6A	K1RBF6_CRAGI	Uncharacterized protein yfeX
m6A	K1RZM3_CRAGI	Cartilage acidic protein 1
m6A	K1R5V4_CRAGI	GTP-binding nuclear protein
m6A	K1QZX9_CRAGI	Uncharacterized protein
m6A	K1Q6U7_CRAGI	78 kDa glucose-regulated protein
m6A	K1R195_CRAGI	Protein DJ-1
m6A	K1Q317_CRAGI	Serine/threonine-protein kinase SRPK1
m6A	K1QJE9_CRAGI	Uncharacterized protein
m6A	K1PD30_CRAGI	Putative histone-binding protein Caf1
m6A	K1QJM1_CRAGI	60S ribosomal protein L30
m6A	K1RHP3_CRAGI	Proliferation-associated protein 2G4
m6A	K1PMJ9_CRAGI	Cleavage stimulation factor 77 kDa subunit
m6A	K1RAU8_CRAGI	Eukaryotic translation initiation factor 3 subunit E
m6A	K1RIS2_CRAGI	3-oxoacyl-[acyl-carrier-protein] reductase
m6A	K1PLM3_CRAGI	Hydroxyacyl-coenzyme A dehydrogenase, mitochondrial
m6A	K1PWU5_CRAGI	Cytosolic carboxypeptidase 1
m6A	K1QFF0_CRAGI	Vacuolar protein sorting-associated protein 35 (Fragment)
m6A	K1P6C4_CRAGI	Poly [ADP-ribose] polymerase
m6A	K1RG19_CRAGI	Protein FAM98A
m6A	K1QCB0_CRAGI	40S ribosomal protein S5
m6A	K1PCH8_CRAGI	Nucleoporin p54

m6A	K1Q2Y1_CRAGI	40S ribosomal protein S15
m6A	K1QGW4_CRAGI	Density-regulated protein
m6A	K1R6H7_CRAGI	Uncharacterized protein
m6A	K1R0D7_CRAGI	Eukaryotic translation initiation factor 3 subunit M (Fragment)
m6A	K1PPI6_CRAGI	Synaptobrevin-like protein YKT6
m6A	K1RMW3_CRAGI	Protein kinase C
m6A	K1QV25_CRAGI	Transcription elongation factor B polypeptide 2
m6A	K1QC27_CRAGI	Hydroxysteroid dehydrogenase-like protein 2
m6A	K1RAT9_CRAGI	Tubulin-specific chaperone D
m6A	K1QWJ4_CRAGI	Splicing factor 3B subunit 5
m6A	K1PZ08_CRAGI	Ras-related protein Rab-7a
m6A	K1QMQ1_CRAGI	TBC1 domain family member 10B
m6A	K1R811_CRAGI	Ribonucleoside-diphosphate reductase small chain
m6A	K1P8G1_CRAGI	Heterogeneous nuclear ribonucleoprotein H
m6A	K1R983_CRAGI	Protein transport protein SEC23
m6A	K1QDI4_CRAGI	Superoxide dismutase [Cu-Zn]
m6A	K1RDM2_CRAGI	60S ribosomal protein L18a
m6A	K1QYI9_CRAGI	Arginyl-tRNA synthetase, cytoplasmic (Fragment)
m6A	K1QVS0_CRAGI	Ras-like GTP-binding protein Rho1
m6A	K1PJS7_CRAGI	Poly [ADP-ribose] polymerase
m6A	K1QRD0_CRAGI	Cytoplasmic dynein 1 light intermediate chain 1
m6A	K1R0R7_CRAGI	Putative ATP-dependent RNA helicase DHX36
m6A	K1Q1F1_CRAGI	Serine/threonine-protein kinase 31
m6A	K1QI32_CRAGI	Synaptotagmin-like protein 5
m6A	K1PMY9_CRAGI	Calmodulin
m6A	K1PXG6_CRAGI	Serine/threonine-protein phosphatase
m6A	K1QW61_CRAGI	WD repeat-containing protein 19
m6A	K1P2B8_CRAGI	GDP-mannose 4,6 dehydratase
m6A	K1QYT5_CRAGI	Phosphate carrier protein, mitochondrial
m6A	K1RIZ9_CRAGI	Band 4.1-like protein 5
m6A	K1QT97_CRAGI	N(G),N(G)-dimethylarginine dimethylaminohydrolase 1
m6A	K1QKF8_CRAGI	S-(hydroxymethyl)glutathione dehydrogenase
m6A	K1REJ2_CRAGI	Lon protease homolog, mitochondrial
m6A	K1R1B1_CRAGI	35 kDa SR repressor protein
m6A	K1PRK2_CRAGI	Small glutamine-rich tetratricopeptide repeat-containing protein beta
m6A	K1QAT9_CRAGI	ATP-dependent RNA helicase DDX1
m6A	K1PFV9_CRAGI	4-trimethylaminobutyraldehyde dehydrogenase
m6A	K1QLP5_CRAGI	Coatomer subunit delta
m6A	K1PIH2_CRAGI	V-type proton ATPase subunit E
m6A	K1RBU9_CRAGI	Non-specific serine/threonine protein kinase
m6A	K1QGP1_CRAGI	Replication factor C subunit 2
m6A	K1PJ96_CRAGI	Uncharacterized protein
m6A	K1QHH0_CRAGI	Protein henna
m6A	K1R0W0_CRAGI	Ferritin
m6A	K1Q6W5_CRAGI	FACT complex subunit spt16
m6A	K1QEZ5_CRAGI	MON2-like protein
m6A	K1RJW8_CRAGI	Protein DEK
m6A	K1P752_CRAGI	UPF0195 protein FAM96B
m6A	K1RP91_CRAGI	Putative RNA exonuclease NEF-sp
m6A	K1QSZ6_CRAGI	Uncharacterized protein
m6A	K1RD83_CRAGI	Serine hydroxymethyltransferase
m6A	K1R5W3_CRAGI	Uncharacterized protein
m6A	K1S211_CRAGI	Poly(A) RNA polymerase gld-2-like protein A
m6A	K1QTW6_CRAGI	Eukaryotic translation initiation factor 3 subunit F
m6A	K1QEJ0_CRAGI	Ras GTPase-activating protein-binding protein 2
m6A	K1R1R9_CRAGI	Pre-mRNA-processing factor 6
m6A	K1QJL2_CRAGI	CCR4-NOT transcription complex subunit 10
m6A	K1PUV4_CRAGI	40S ribosomal protein S24
m6A	K1RH58_CRAGI	Alpha-actinin, sarcomeric
m6A	K1PQI4_CRAGI	Enolase-phosphatase E1

m6A	K1R7D7_CRAGI	Poly(A)-specific ribonuclease PARN
m6A	K1PS84_CRAGI	Alpha-crystallin B chain
m6A	K1QQV0_CRAGI	Histone H1.2
m6A	K1QPJ9_CRAGI	Serine/threonine-protein phosphatase 2A 55 kDa regulatory subunit B
m6A	K1QZX3_CRAGI	Vacuolar protein sorting-associated protein VTA1-like protein
m6A	K1R517_CRAGI	Superkiller viralicidic activity 2-like 2
m6A	K1RJS5_CRAGI	Uncharacterized protein
m6A	K1S3Q9_CRAGI	MAK16-like protein (Fragment)
m6A	K1PKD4_CRAGI	40S ribosomal protein S30
m6A	K1PGZ0_CRAGI	Thyroid adenoma-associated protein
m6A	K1REV3_CRAGI	DNA polymerase delta subunit 2
m6A	K1QGF1_CRAGI	Splicing factor 3B subunit 2
m6A	K1R8B2_CRAGI	Isovaleryl-CoA dehydrogenase, mitochondrial
m6A	K1PR25_CRAGI	Regulator of differentiation 1
m6A	K1PZ23_CRAGI	DnaJ-like protein subfamily C member 3
m6A	K1PLG1_CRAGI	Putative ribosomal RNA methyltransferase NOP2
m6A	K1PNY5_CRAGI	Splicing factor, proline-and glutamine-rich
m6A	K1RG79_CRAGI	Neuronal acetylcholine receptor subunit alpha-6
m6A	K1PRB6_CRAGI	Apolipoprotein D
m6A	K1PTR3_CRAGI	Oxysterol-binding protein
m6A	K1Q1F4_CRAGI	60S ribosomal protein L3 (Fragment)
m6A	Q70MT4_CRAGI	40S ribosomal protein S10
m6A	K1Q662_CRAGI	Actin-interacting protein 1
m6A	K1R2G9_CRAGI	SEC13-like protein
m6A	K1PRV7_CRAGI	Profilin
m6A	K1QWZ6_CRAGI	Dolichyl-diphosphooligosaccharide--protein glycosyltransferase subunit 1
m6A	K1R9S5_CRAGI	Cytosolic Fe-S cluster assembly factor NUBP2 homolog
m6A	K1QUK0_CRAGI	NEDD8-activating enzyme E1 catalytic subunit
m6A	K1PTE3_CRAGI	Uncharacterized protein
m6A	K1Q6M6_CRAGI	6-phosphofructokinase
m6A	K1QZN3_CRAGI	Myosin-Id
m6A	K1PB94_CRAGI	ATP-binding cassette sub-family E member 1
m6A	K1RNN9_CRAGI	Cytoskeleton-associated protein 5
m6A	K1PZL0_CRAGI	B-box type zinc finger protein ncl-1
m6A	K1RKZ5_CRAGI	DNA damage-binding protein 1
m6A	K1R138_CRAGI	Nuclear pore glycoprotein p62
m6A	K1Q9D7_CRAGI	Sorting nexin-2
m6A	K1R6F1_CRAGI	Proteasome subunit alpha type
m6A	K1QKQ5_CRAGI	N-terminal acetyltransferase B complex subunit MDM20
m6A	K1PDC6_CRAGI	Proteasome subunit beta
m6A	A5LGH1_CRAGI	Voltage-dependent anion channel
m6A	K1PF60_CRAGI	3-ketoacyl-CoA thiolase, mitochondrial
m6A	K1R924_CRAGI	RNA-binding protein 45
m6A	K1RTQ6_CRAGI	Fructose-bisphosphate aldolase
m6A	K1Q888_CRAGI	Translin
m6A	K1R255_CRAGI	Heterogeneous nuclear ribonucleoprotein L
m6A	K1QIZ7_CRAGI	Programmed cell death protein 6
m6A	K1QI48_CRAGI	Inositol hexakisphosphate and diphosphoinositol-pentakisphosphate kinase
m6A	K1PWB9_CRAGI	EH domain-containing protein 1
m6A	K1QZ84_CRAGI	Thioredoxin domain-containing protein 3-like protein
m6A	K1PJY4_CRAGI	Calcium-binding protein 39
m6A	K1PBC0_CRAGI	Non-neuronal cytoplasmic intermediate filament protein
m6A	K1PRD5_CRAGI	Trifunctional purine biosynthetic protein adenosine-3
m6A	K1QXH7_CRAGI	DNA replication licensing factor mcm4-B
m6A	K1Q719_CRAGI	Serine/threonine-protein kinase OSR1
m6A	K1QV87_CRAGI	Catenin alpha-2
m6A	K1PBH3_CRAGI	Dynein heavy chain 3, axonemal
m6A	K1R4M7_CRAGI	Serine/threonine protein phosphatase 2A regulatory subunit
m6A	K1R3A0_CRAGI	Transcription initiation factor IIB
m6A	K1QQQ5_CRAGI	Replication factor C subunit 5

m6A	K1RJ70_CRAGI	Cytosolic non-specific dipeptidase
m6A	K1QNY7_CRAGI	Transport protein Sec24C
m6A	K1R481_CRAGI	Epimerase family protein SDR39U1
m6A	K1QRE1_CRAGI	COP9 signalosome complex subunit 6
m6A	K1RA63_CRAGI	Transmembrane protein 2
m6A	K1QHT0_CRAGI	Deoxyuridine 5'-triphosphate nucleotidohydrolase, mitochondrial
m6A	K1PQA3_CRAGI	Pseudouridylate synthase 7-like protein
m6A	K1PII4_CRAGI	YTH domain-containing protein 1
m6A	K1P8S5_CRAGI	Condensin complex subunit 3
m6A	K1QMT1_CRAGI	DnaJ-like protein subfamily B member 4
m6A	K1PN10_CRAGI	Intron-binding protein aquarius
m6A	K1PCR9_CRAGI	Proteasome endopeptidase complex
m6A	K1PZI3_CRAGI	SWI/SNF complex subunit SMARCC2
m6A	K1RIZ3_CRAGI	Bone morphogenetic protein 7
m6A	K1QMY1_CRAGI	Aconitate hydratase, mitochondrial
m6A	K1R3W9_CRAGI	Replication protein A 14 kDa subunit
m6A	K1PLD4_CRAGI	Dynein heavy chain 2, axonemal
m6A	K1QC78_CRAGI	Ras-related protein Rab-14
m6A	K1PTV5_CRAGI	Programmed cell death protein 10
m6A	K1RGG1_CRAGI	Alanyl-tRNA synthetase, cytoplasmic
m6A	K1R3R4_CRAGI	Cytosolic Fe-S cluster assembly factor NUBP1 homolog
m6A	K1R266_CRAGI	Retinal dehydrogenase 1
m6A	K1QGC9_CRAGI	Acetyl-coenzyme A synthetase
m6A	K1Q7T5_CRAGI	Protein disulfide-isomerase
m6A	K1QKQ8_CRAGI	THO complex subunit 4-A
m6A	K1QR54_CRAGI	Zinc finger RNA-binding protein
m6A	K1PEW1_CRAGI	Sorting nexin
m6A	K1PFL3_CRAGI	Dihydropteridine reductase
m6A	K1QC11_CRAGI	AP-1 complex subunit gamma
m6A	K1QQI3_CRAGI	Rab-like protein 5
m6A	K1R916_CRAGI	Structural maintenance of chromosomes protein
m6A	K1PF37_CRAGI	Thioredoxin domain-containing protein 9
m6A	K1PJW0_CRAGI	Talin-1
m6A	K1PUX5_CRAGI	Casein kinase II subunit alpha
m6A	K1QB86_CRAGI	Dynamin-1
m6A	K1QWX0_CRAGI	26S proteasome non-ATPase regulatory subunit 14
m6A	K1QBM3_CRAGI	Ras-related protein Rab-2
m6A	K1RG04_CRAGI	ALK tyrosine kinase receptor
m6A	K1PXH5_CRAGI	Putative saccharopine dehydrogenase
m6A	K1Q407_CRAGI	Ras GTPase-activating protein 1
m6A	K1PYK7_CRAGI	RNA-binding protein 39
m6A	K1PZR3_CRAGI	U2 small nuclear ribonucleoprotein A
m6A	K1RBJ3_CRAGI	DnaJ-like protein subfamily C member 13
m6A	K1Q324_CRAGI	Heterogeneous nuclear ribonucleoprotein K
m6A	K1PA61_CRAGI	Actin-like protein 6A
m6A	K1PWS8_CRAGI	Mitotic spindle assembly checkpoint protein MAD2A
m6A	K1PL64_CRAGI	Poly(A) polymerase gamma
m6A	K1RB97_CRAGI	Kinetochore-associated protein 1
m6A	K1R6S7_CRAGI	Mannose-1-phosphate guanyltransferase alpha-A
m6A	K1RK83_CRAGI	Tyrosine-protein kinase BAZ1B
m6A	K1QSA2_CRAGI	Short-chain specific acyl-CoA dehydrogenase, mitochondrial
m6A	K1RFU8_CRAGI	High mobility group protein DSP1
m6A	K1QV46_CRAGI	Tetratricopeptide repeat protein 21B
m6A	K1R8W3_CRAGI	S-phase kinase-associated protein 1
m6A	K1RFF7_CRAGI	Protein lethal(2)essential for life
m6A	K1R1T8_CRAGI	Nucleolar protein 56
m6A	K1PNG7_CRAGI	Sorting nexin-33
m6A	K1PCV0_CRAGI	Severin
m6A	K1QVX4_CRAGI	Glycogen synthase kinase-3 beta
m6A	K1P9V5_CRAGI	General transcription factor IIF subunit 1

m6A	K1Q904_CRAGI	PAN2-PAN3 deadenylation complex subunit PAN3
m6A	K1REC3_CRAGI	Exportin-5
m6A	K1P137_CRAGI	Actin-related protein 2/3 complex subunit 5
m6A	K1QBT8_CRAGI	Uncharacterized protein
m6A	K1PZN1_CRAGI	Calcium/calmodulin-dependent protein kinase type II delta chain
m6A	K1QVZ2_CRAGI	Uncharacterized protein
m6A	K1REP0_CRAGI	Uncharacterized protein
m6A	K1QHX0_CRAGI	Double-stranded RNA-specific editase 1
m6A	K1PVL5_CRAGI	tRNA 2'-phosphotransferase 1
m6A	K1Q6Y2_CRAGI	Uncharacterized protein
m6A	K1PMQ4_CRAGI	Microtubule-associated serine/threonine-protein kinase-like protein
m6A	K1PQR9_CRAGI	Squamous cell carcinoma antigen recognized by T-cells 3
m6A	K1R150_CRAGI	Ras-related protein Rab-1A
m6A	K1PNU2_CRAGI	Histone-arginine methyltransferase CARM1
m6A	K1PEX5_CRAGI	Protein hu-li tai shao
m6A	K1PDF0_CRAGI	Protein disulfide-isomerase A6
m6A	K1QC22_CRAGI	40S ribosomal protein S19
m6A	K1PUF0_CRAGI	G-protein coupled receptor moody
m6A	K1S422_CRAGI	Katanin p80 WD40 repeat-containing subunit B1
m6A	K1PI41_CRAGI	Flap endonuclease 1
m6A	K1R0N8_CRAGI	Flap endonuclease GEN-like protein 1
m6A	K1RXR4_CRAGI	Arrestin domain-containing protein 3
m6A	K1PXX6_CRAGI	Uncharacterized protein
m6A	K1QXP9_CRAGI	Uncharacterized protein
m6A	K1RJB4_CRAGI	Ubiquitin carboxyl-terminal hydrolase 1
A	K1QNA2_CRAGI	Vitellogenin-6
A	K1QHK9_CRAGI	Dynein heavy chain, cytoplasmic
A	K1PNR3_CRAGI	Clathrin heavy chain
A	K1QVJ8_CRAGI	Piwi-like protein 1
A	K1R7V7_CRAGI	Tubulin beta chain
A	K1QQ94_CRAGI	Uncharacterized protein
A	K1RLF8_CRAGI	Splicing factor 3B subunit 3
A	K1QQ68_CRAGI	Tubulin alpha chain
A	K1S2N7_CRAGI	Innexin
A	K1R164_CRAGI	Galectin-4
A	K1QMX5_CRAGI	Uncharacterized protein
A	K1QHI5_CRAGI	Pyruvate carboxylase, mitochondrial
A	K1PQP2_CRAGI	Nucleolin
A	K1PN21_CRAGI	Tubulin beta chain
A	K1PAG1_CRAGI	Dynein beta chain, ciliary
A	K1QII6_CRAGI	Tubulin alpha chain
A	K1R5B4_CRAGI	Proteasome activator complex subunit 4
A	K1QFW9_CRAGI	Uncharacterized protein
A	K1R473_CRAGI	Tubulin alpha chain
A	K1PK85_CRAGI	Cullin-associated NEDD8-dissociated protein 1
A	K1R294_CRAGI	T-complex protein 1 subunit beta
A	K1PE00_CRAGI	Tubulin alpha chain
A	K1PNI6_CRAGI	Heterogeneous nuclear ribonucleoprotein A/B
A	K1PYA0_CRAGI	Cytoplasmic dynein 2 heavy chain 1
A	K1R466_CRAGI	T-complex protein 1 subunit gamma
A	K1S4Q2_CRAGI	T-complex protein 1 subunit delta (Fragment)
A	K1QMA4_CRAGI	RRP5-like protein
A	K1R5R4_CRAGI	Dynein heavy chain 10, axonemal
A	K1RZE2_CRAGI	Isocitrate dehydrogenase [NADP]
A	K1QGS8_CRAGI	Elongation factor 1-alpha
A	K1QXX7_CRAGI	Myosin heavy chain, non-muscle (Fragment)
A	K1S6V7_CRAGI	Serine/threonine-protein phosphatase 2A 65 kDa regulatory subunit A alpha isoform
A	K1R866_CRAGI	Puromycin-sensitive aminopeptidase
A	K1QBK6_CRAGI	Splicing factor 3B subunit 1
A	K1R3U2_CRAGI	Uncharacterized protein

A	K1QNW9_CRAGI	Bifunctional aminoacyl-tRNA synthetase
A	K1R545_CRAGI	Pre-mRNA-processing-splicing factor 8 (Fragment)
A	K1R6Z7_CRAGI	ATP synthase subunit alpha
A	K1R6Q7_CRAGI	DNA topoisomerase I
A	K1R0S3_CRAGI	T-complex protein 1 subunit theta
A	K1RAJ1_CRAGI	T-complex protein 1 subunit alpha
A	K1PNQ5_CRAGI	Heat shock protein HSP 90-alpha 1
A	K1PVA1_CRAGI	Transitional endoplasmic reticulum ATPase
A	K1QHI6_CRAGI	Dynein heavy chain 5, axonemal
A	K1Q7G8_CRAGI	Fatty acid synthase
A	K1R401_CRAGI	Spectrin alpha chain
A	K1PND7_CRAGI	Fatty acid synthase
A	K1RGT5_CRAGI	Metalloendopeptidase
A	K1PLF9_CRAGI	Arginine kinase
A	K1QET2_CRAGI	Coatomer subunit alpha
A	K1QSB2_CRAGI	26S protease regulatory subunit 6B
A	K1R9B6_CRAGI	H/ACA ribonucleoprotein complex subunit 4
A	K1R512_CRAGI	Uncharacterized protein
A	K1RK12_CRAGI	40S ribosomal protein S23
A	K1QQR1_CRAGI	Major vault protein
A	K1R420_CRAGI	Non-specific serine/threonine protein kinase
A	K1Q9W5_CRAGI	T-complex protein 1 subunit eta
A	K1QSX8_CRAGI	ATPase family AAA domain-containing protein 2B
A	K1Q350_CRAGI	Glyceraldehyde-3-phosphate dehydrogenase
A	K1PJ85_CRAGI	26S protease regulatory subunit 6A
A	K1Q923_CRAGI	Putative ATP-dependent RNA helicase DDX4
A	K1PJ06_CRAGI	Importin subunit alpha-1
A	K1RLC5_CRAGI	T-complex protein 1 subunit epsilon
A	K1R278_CRAGI	Tubulin beta chain
A	K1R8L1_CRAGI	Exportin-2
A	K1PEY4_CRAGI	26S proteasome non-ATPase regulatory subunit 2
A	K1RWS2_CRAGI	Transcriptional activator protein Pur-alpha
A	K1RG73_CRAGI	Acetyl-CoA carboxylase
A	K1QLK6_CRAGI	E3 ubiquitin-protein ligase HUWE1
A	K1PXN5_CRAGI	T-complex protein 1 subunit zeta
A	K1P9D0_CRAGI	Stress-70 protein, mitochondrial
A	K1QR72_CRAGI	Dipeptidyl peptidase 3
A	K1R4Z3_CRAGI	Malate dehydrogenase, mitochondrial
A	K1Q988_CRAGI	Band 4.1-like protein 3
A	K1QB04_CRAGI	26S proteasome non-ATPase regulatory subunit 3
A	K1QRL4_CRAGI	Importin-5
A	K1Q1I2_CRAGI	26S protease regulatory subunit 7
A	K1QXR4_CRAGI	Pancreatic lipase-related protein 2
A	K1RH70_CRAGI	6-phosphogluconate dehydrogenase, decarboxylating
A	K1PH66_CRAGI	Fibrinolytic enzyme, isozyme C
A	K1PTY5_CRAGI	Protocadherin Fat 4
A	K1QI14_CRAGI	40S ribosomal protein S3a
A	K1QBN0_CRAGI	Methylcrotonoyl-CoA carboxylase beta chain, mitochondrial
A	K1QMD3_CRAGI	Glycerol-3-phosphate dehydrogenase [NAD(+)]
A	K1QVN9_CRAGI	T-complex protein 1 subunit eta
A	K1RN77_CRAGI	Nuclear autoantigenic sperm protein
A	K1QSQ9_CRAGI	Putative ATP-dependent RNA helicase an3
A	K1RI55_CRAGI	Insulin-like growth factor 2 mRNA-binding protein 3
A	K1S1S1_CRAGI	Insulin-like growth factor 2 mRNA-binding protein 1
A	K1PH76_CRAGI	Y-box factor-like protein (Fragment)
A	K1QWP8_CRAGI	Actin-2
A	K1R252_CRAGI	Putative methylmalonate-semialdehyde dehydrogenase [acylating], mitochondrial
A	K1QEA6_CRAGI	Phosphoenolpyruvate carboxykinase [GTP]
A	K1RNB5_CRAGI	Propionyl-CoA carboxylase beta chain, mitochondrial
A	K1RJH5_CRAGI	Polyadenylate-binding protein

A	K1PLY1_CRAGI	DNA polymerase
A	K1R5U4_CRAGI	Acetyl-CoA carboxylase 1
A	K1PF10_CRAGI	PAN2-PAN3 deadenylation complex catalytic subunit PAN2
A	K1QBR5_CRAGI	Uncharacterized protein
A	K1QVS3_CRAGI	Thimet oligopeptidase
A	K1RFT1_CRAGI	Band 4.1-like protein 3
A	K1R2V1_CRAGI	Importin subunit beta-1
A	K1RW85_CRAGI	Adenosylhomocysteinase
A	K1QWT8_CRAGI	Uncharacterized protein
A	K1PFG1_CRAGI	Uncharacterized protein
A	K1QWX2_CRAGI	60S acidic ribosomal protein P0
A	K1R1M7_CRAGI	Ubiquitin-like modifier-activating enzyme 1
A	K1QK11_CRAGI	Dynein heavy chain 7, axonemal
A	K1RWW5_CRAGI	ATP synthase subunit beta
A	K1RJ97_CRAGI	Multifunctional protein ADE2
A	K1RWD4_CRAGI	Actin, cytoplasmic
A	K1R3V0_CRAGI	CAD protein
A	K1QHA2_CRAGI	Spectrin beta chain, brain 4
A	K1REG6_CRAGI	DNA helicase
A	K1R4I2_CRAGI	26S proteasome non-ATPase regulatory subunit 3
A	K1RTR1_CRAGI	ATP-citrate synthase
A	K1QGK2_CRAGI	Coatomer subunit beta
A	K1Q9Z6_CRAGI	26S proteasome non-ATPase regulatory subunit 7
A	K1QQL6_CRAGI	Leucyl-tRNA synthetase, cytoplasmic
A	K1Q330_CRAGI	Dihydrolipoyl dehydrogenase
A	K1QUE6_CRAGI	26S proteasome non-ATPase regulatory subunit 6
A	K1QY12_CRAGI	Dynamin-1-like protein
A	K1Q3S7_CRAGI	Cytosolic carboxypeptidase 1
A	K1RSZ6_CRAGI	40S ribosomal protein S7
A	K1PJF4_CRAGI	Isoleucyl-tRNA synthetase, cytoplasmic
A	K1Q9V3_CRAGI	V-type proton ATPase catalytic subunit A
A	K1RBC9_CRAGI	Transketolase-like protein 2
A	K1PPP8_CRAGI	Vigilin
A	K1PX47_CRAGI	Ubiquitin carboxyl-terminal hydrolase
A	K1QX26_CRAGI	Endoplasmin
A	K1PZP6_CRAGI	Coatomer subunit gamma
A	K1QE71_CRAGI	DNA helicase
A	K1QBH0_CRAGI	Uncharacterized protein
A	K1QCC1_CRAGI	Phosphoglycerate kinase
A	K1PJP9_CRAGI	26S proteasome non-ATPase regulatory subunit 1
A	K1QIR8_CRAGI	78 kDa glucose-regulated protein
A	K1Q4I9_CRAGI	D-3-phosphoglycerate dehydrogenase (Fragment)
A	K1RNZ6_CRAGI	Eukaryotic translation initiation factor 3 subunit D
A	K1R3V8_CRAGI	COP9 signalosome complex subunit 4
A	K1PUL2_CRAGI	Long-chain-fatty-acid--CoA ligase 1
A	K1QHX2_CRAGI	La-related protein 7
A	K1QDN1_CRAGI	Heat shock protein 75 kDa, mitochondrial (Fragment)
A	K1PZF2_CRAGI	Exportin-7
A	K1PMT6_CRAGI	Heterogeneous nuclear ribonucleoprotein U-like protein 1
A	K1RCW5_CRAGI	Eukaryotic translation initiation factor 4 gamma 3
A	K1R7I9_CRAGI	Heterogeneous nuclear ribonucleoprotein Q
A	K1QYB6_CRAGI	Delta-1-pyrroline-5-carboxylate synthetase
A	K1P3Q5_CRAGI	Programmed cell death 6-interacting protein
A	K1Q2H5_CRAGI	Uncharacterized protein
A	K1QBF7_CRAGI	Hypoxia up-regulated protein 1
A	K1PW06_CRAGI	Filamin-C
A	K1QHS8_CRAGI	Ribonucleoside-diphosphate reductase
A	K1RL00_CRAGI	Proteasome-associated protein ECM29-like protein
A	K1QQ16_CRAGI	AP complex subunit beta
A	K1R4R9_CRAGI	Mitotic apparatus protein p62

A	K1QXH3_CRAGI	Translational activator GCN1
A	K1P5D4_CRAGI	Cysteine synthase
A	K1RM80_CRAGI	Citrate synthase
A	K1PVH5_CRAGI	Centromere/kinetochore protein zw10-like protein
A	K1QQ27_CRAGI	Pancreatic lipase-related protein 2
A	K1QMX8_CRAGI	DNA replication licensing factor MCM7
A	K1QK56_CRAGI	Uncharacterized protein
A	K1QMB9_CRAGI	Eukaryotic translation initiation factor 3 subunit A
A	K1R0W4_CRAGI	Signal recognition particle subunit SRP72
A	K1QLT5_CRAGI	26S protease regulatory subunit 4
A	K1QSR2_CRAGI	Apoptosis inhibitor 5
A	K1QKA9_CRAGI	Piwi-like protein 2
A	K1RJM8_CRAGI	SAGA-associated factor 11 homolog
A	K1QQB6_CRAGI	40S ribosomal protein S14
A	K1PE57_CRAGI	Severin
A	K1PKK7_CRAGI	AP-2 complex subunit mu-1
A	K1QXS6_CRAGI	Heterogeneous nuclear ribonucleoprotein A2-like protein 1
A	K1R5F2_CRAGI	14-3-3 protein epsilon
A	K1Q4V0_CRAGI	Myosin-VIIa
A	K1QA50_CRAGI	V-type proton ATPase subunit H
A	K1QWK2_CRAGI	MAM domain-containing glycosylphosphatidylinositol anchor protein 2
A	K1PV49_CRAGI	RuvB-like helicase
A	K1QAB1_CRAGI	AP-2 complex subunit alpha
A	K1RK33_CRAGI	Exportin-1
A	K1PCS4_CRAGI	Eukaryotic translation initiation factor 2 subunit 3, Y-linked
A	K1RSA6_CRAGI	Methylcrotonoyl-CoA carboxylase subunit alpha, mitochondrial
A	K1PI02_CRAGI	Talin-1
A	K1PNP4_CRAGI	26S proteasome non-ATPase regulatory subunit 11
A	K1RAL0_CRAGI	Aspartate aminotransferase, cytoplasmic
A	K1QXQ8_CRAGI	DNA helicase
A	K1QI28_CRAGI	V-type proton ATPase subunit B
A	K1Q9K6_CRAGI	Histone H3
A	K1S151_CRAGI	Rab GDP dissociation inhibitor
A	K1P2G0_CRAGI	Strawberry notch-like protein 1
A	K1QI97_CRAGI	Adenylyl cyclase-associated protein
A	K1QBW6_CRAGI	Tudor domain-containing protein 1
A	K1PEP0_CRAGI	40S ribosomal protein S8
A	K1QG84_CRAGI	THO complex subunit 2
A	K1PUM2_CRAGI	Histone H2A
A	K1PU26_CRAGI	Malate dehydrogenase (Fragment)
A	A7M7T7_CRAGI	Non-selenium glutathione peroxidase
A	K1PWW9_CRAGI	26S proteasome non-ATPase regulatory subunit 3
A	K1QF01_CRAGI	40S ribosomal protein S4
A	K1QZW0_CRAGI	Polyadenylate-binding protein 2
A	K1RAU3_CRAGI	DNA ligase
A	K1PVW0_CRAGI	S-adenosylmethionine synthase
A	K1QBL6_CRAGI	Tudor domain-containing protein 1
A	K1QE32_CRAGI	Very long-chain specific acyl-CoA dehydrogenase, mitochondrial
A	K1PY73_CRAGI	Basic leucine zipper and W2 domain-containing protein 1
A	K1S2Y0_CRAGI	Uncharacterized protein
A	K1QEF2_CRAGI	ADP-ribosylation factor-like protein 15
A	K1PV79_CRAGI	Importin subunit alpha
A	K1R083_CRAGI	Aspartate aminotransferase, mitochondrial
A	K1QMH2_CRAGI	DNA polymerase
A	K1QL67_CRAGI	60S ribosomal protein L7a
A	K1QDV6_CRAGI	Protein argonaute-2
A	K1QU53_CRAGI	NAD(P) transhydrogenase, mitochondrial
A	K1RIZ9_CRAGI	Band 4.1-like protein 5
A	K1R2Q9_CRAGI	Aspartate aminotransferase
A	K1Q4E1_CRAGI	N-acetyl-D-glucosamine kinase

A	K1R916_CRAGI	Structural maintenance of chromosomes protein
A	K1R2N0_CRAGI	Histone H4
A	K1P7K8_CRAGI	Vesicle-fusing ATPase 1
A	K1PJC1_CRAGI	Adipophilin
A	K1QVR0_CRAGI	26S proteasome non-ATPase regulatory subunit 8
A	K1Q6X5_CRAGI	Protein disulfide-isomerase
A	K1QGB4_CRAGI	40S ribosomal protein S17
A	K1QT21_CRAGI	Putative ATP-dependent RNA helicase DDX5
A	K1Q7Q2_CRAGI	CCAAT/enhancer-binding protein zeta
A	K1Q6W3_CRAGI	Talin-1
A	K1R4D4_CRAGI	40S ribosomal protein SA
A	K1QH70_CRAGI	Leucine-rich repeat-containing protein 40
A	K1Q880_CRAGI	Transportin-1
A	K1PS71_CRAGI	Uncharacterized protein
A	K1PAY7_CRAGI	Propionyl-CoA carboxylase alpha chain, mitochondrial
A	K1QPP2_CRAGI	Elongation factor Tu, mitochondrial
A	K1PX23_CRAGI	Eukaryotic peptide chain release factor subunit 1
A	K1QRG9_CRAGI	Uncharacterized protein
A	K1PIB7_CRAGI	Phenylalanyl-tRNA synthetase beta chain
A	K1R115_CRAGI	Succinate dehydrogenase [ubiquinone] flavoprotein subunit, mitochondrial
A	K1PF96_CRAGI	Spliceosome RNA helicase BAT1
A	K1QFN1_CRAGI	60S ribosomal protein L23
A	K1R0D7_CRAGI	Eukaryotic translation initiation factor 3 subunit M (Fragment)
A	K1PK93_CRAGI	GDP-L-fucose synthetase
A	K1R2D6_CRAGI	Plastin-3
A	K1Q358_CRAGI	60S acidic ribosomal protein P2
A	K1QMV7_CRAGI	V-type proton ATPase subunit D
A	K1R953_CRAGI	Acetyl-CoA carboxylase
A	K1PPQ1_CRAGI	14-3-3 protein gamma
A	K1QYV6_CRAGI	NMDA receptor-regulated protein 1
A	K1PH31_CRAGI	Protein arginine N-methyltransferase 1
A	K1RDV7_CRAGI	Cell division control protein 2-like protein (Fragment)
A	K1PBZ4_CRAGI	Regulator of nonsense transcripts 1
A	K1PD57_CRAGI	Constitutive coactivator of PPAR-gamma-like protein 1-like protein
A	K1PVZ3_CRAGI	Cold shock domain-containing protein E1
A	K1PLA7_CRAGI	Eukaryotic initiation factor 4A-II (Fragment)
A	K1Q1S3_CRAGI	Myosin-VI
A	K1QY85_CRAGI	Transport protein Sec31A
A	K1QH74_CRAGI	Splicing factor, arginine/serine-rich 1
A	K1RB97_CRAGI	Kinetochore-associated protein 1
A	K1REC3_CRAGI	Exportin-5
A	K1R3T3_CRAGI	Transcription factor BTF3
A	K1Q9J5_CRAGI	Importin-4
A	K1Q0R4_CRAGI	ATP-binding cassette sub-family F member 2
A	K1QD40_CRAGI	Importin-7
A	K1R5B9_CRAGI	DNA-directed RNA polymerase, mitochondrial
A	K1PD30_CRAGI	Putative histone-binding protein Caf1
A	K1QRW4_CRAGI	Coronin
A	K1RDG4_CRAGI	DNA helicase
A	K1QHY1_CRAGI	Eosinophil peroxidase
A	K1QLS3_CRAGI	Cytochrome b-c1 complex subunit 2, mitochondrial
A	K1Q5G9_CRAGI	SUMO-activating enzyme subunit 2
A	K1QED7_CRAGI	Replication protein A subunit
A	K1S3Y1_CRAGI	2-amino-3-ketobutyrate coenzyme A ligase, mitochondrial (Fragment)
A	K1PGW7_CRAGI	Transmembrane protein 2
A	K1R7N6_CRAGI	Eukaryotic translation initiation factor 6
A	K1QRL6_CRAGI	Methenyltetrahydrofolate synthetase domain-containing protein
A	K1PN10_CRAGI	Intron-binding protein aquarius
A	K1QNT7_CRAGI	Aldehyde dehydrogenase, mitochondrial
A	K1QLZ1_CRAGI	Actin-related protein 3

A	K1R9T2_CRAGI	Eukaryotic translation initiation factor 3 subunit B
A	K1PS27_CRAGI	DNA helicase
A	K1Q5G6_CRAGI	60 kDa heat shock protein, mitochondrial
A	K1QRM1_CRAGI	Nuclear pore protein
A	K1QGC9_CRAGI	Acetyl-coenzyme A synthetase
A	K1RLT4_CRAGI	Signal recognition particle subunit SRP68
A	K1PAR4_CRAGI	Unc-45-like protein A
A	K1QVE8_CRAGI	Phosphoacetylglucosamine mutase
A	K1Q4Z4_CRAGI	Bifunctional purine biosynthesis protein PURH
A	K1P8W6_CRAGI	60S ribosomal protein L4
A	K1QQK1_CRAGI	26S proteasome non-ATPase regulatory subunit 12
A	K1RIT6_CRAGI	NADH-ubiquinone oxidoreductase 75 kDa subunit, mitochondrial
A	K1R2L7_CRAGI	Glutaminyl-tRNA synthetase (Fragment)
A	K1QRQ2_CRAGI	Glutamate dehydrogenase 1, mitochondrial
A	K1RKZ5_CRAGI	DNA damage-binding protein 1
A	K1QC10_CRAGI	GTP-binding protein 1
A	K1PGZ0_CRAGI	Thyroid adenoma-associated protein
A	K1QUK0_CRAGI	NEDD8-activating enzyme E1 catalytic subunit
A	K1QQP1_CRAGI	Programmed cell death protein 4
A	K1PM50_CRAGI	40S ribosomal protein S16
A	K1PJS7_CRAGI	Poly [ADP-ribose] polymerase
A	K1QX37_CRAGI	Enolase
A	K1QCA7_CRAGI	Valyl-tRNA synthetase
A	K1Q811_CRAGI	Alpha-centractin
A	K1QRZ3_CRAGI	40S ribosomal protein S13
A	K1QG70_CRAGI	Katanin p60 ATPase-containing subunit A1
A	K1QW36_CRAGI	60S ribosomal protein L6
A	K1R8S7_CRAGI	Phospholipase A-2-activating protein
A	K1P9N7_CRAGI	14-3-3 protein zeta
A	K1PG07_CRAGI	Lupus La-like protein
A	K1QFZ8_CRAGI	Ceramide kinase-like protein
A	K1Q1Q9_CRAGI	Alpha-aminoadipic semialdehyde synthase, mitochondrial
A	K1PX83_CRAGI	Dynein heavy chain 5, axonemal
A	K1PCV0_CRAGI	Severin
A	K1QP17_CRAGI	Caprin-1
A	K1PS13_CRAGI	Coatomer subunit beta (Fragment)
A	K1Q273_CRAGI	60S ribosomal protein L14
A	K1PBU0_CRAGI	L-fucose kinase
A	K1QVV5_CRAGI	Periostin
A	K1P112_CRAGI	ATP synthase subunit gamma, mitochondrial
A	K1QKN4_CRAGI	Dynein heavy chain 6, axonemal
A	K1P2B8_CRAGI	GDP-mannose 4,6 dehydratase
A	K1QC11_CRAGI	AP-1 complex subunit gamma
A	K1QPD6_CRAGI	Ubiquitin conjugation factor E4 B
A	K1QWZ0_CRAGI	Tetratricopeptide repeat protein 38
A	K1QKF8_CRAGI	S-(hydroxymethyl)glutathione dehydrogenase
A	K1RD83_CRAGI	Serine hydroxymethyltransferase
A	K1R1F0_CRAGI	ATP-dependent DNA helicase 2 subunit 1
A	K1QMD8_CRAGI	Proteasome subunit alpha type
A	K1Q8S0_CRAGI	Nucleolar complex protein 3 homolog
A	K1PI50_CRAGI	40S ribosomal protein S26
A	K1R8T6_CRAGI	Cullin-1
A	K1P6F0_CRAGI	HEAT repeat-containing protein 2
A	K1PXG6_CRAGI	Serine/threonine-protein phosphatase
A	K1QG65_CRAGI	rRNA 2'-O-methyltransferase fibrillarin
A	K1R5W3_CRAGI	Uncharacterized protein
A	K1QB60_CRAGI	Uncharacterized protein
A	K1R5D5_CRAGI	U3 small nucleolar RNA-associated protein 6-like protein
A	K1REJ2_CRAGI	Lon protease homolog, mitochondrial
A	K1PLD4_CRAGI	Dynein heavy chain 2, axonemal

A	K1QPC6_CRAGI	Nucleolar complex protein 2-like protein
A	K1PQZ3_CRAGI	Armadillo repeat-containing protein 4
A	K1Q6F7_CRAGI	V-type proton ATPase subunit C
A	K1RPF7_CRAGI	60S ribosomal protein L5
A	K1QHQ6_CRAGI	Acyl-CoA dehydrogenase family member 9, mitochondrial
A	K1PFS5_CRAGI	Elongation factor 1-gamma
A	K1PPW8_CRAGI	Coatomer subunit beta
A	K1QGE4_CRAGI	Proteasome endopeptidase complex (Fragment)
A	K1QDX9_CRAGI	Ribosome biogenesis protein BMS1-like protein
A	K1Q8K2_CRAGI	Importin subunit alpha
A	K1QTW6_CRAGI	Eukaryotic translation initiation factor 3 subunit F
A	K1QBW8_CRAGI	Uncharacterized protein
A	K1QT97_CRAGI	N(G),N(G)-dimethylarginine dimethylaminohydrolase 1
A	K1QWK6_CRAGI	Metalloendopeptidase
A	K1QQ93_CRAGI	Adenosine kinase 1
A	K1PWD9_CRAGI	Uncharacterized protein
A	K1R6S5_CRAGI	40S ribosomal protein S9
A	K1QBL3_CRAGI	Putative phosphoglycerate mutase
A	K1RH58_CRAGI	Alpha-actinin, sarcomeric
A	K1R5V4_CRAGI	GTP-binding nuclear protein
A	K1P8I1_CRAGI	Pleckstrin-like protein domain-containing family F member 2 (Fragment)
A	K1PA54_CRAGI	Replication factor C subunit 3
A	K1QYI9_CRAGI	Arginyl-tRNA synthetase, cytoplasmic (Fragment)
A	K1PVV6_CRAGI	Putative aminopeptidase W07G4.4
A	K1RV41_CRAGI	Guanine nucleotide-binding protein subunit beta-2-like 1
A	K1PMP3_CRAGI	Protoporphyrinogen oxidase
A	K1PJ96_CRAGI	Uncharacterized protein
A	K1RG19_CRAGI	Protein FAM98A
A	K1QIP0_CRAGI	26S proteasome non-ATPase regulatory subunit 5
A	K1QXF5_CRAGI	Calcyphosin-like protein
A	K1Q6W5_CRAGI	FACT complex subunit spt16
A	K1QRK9_CRAGI	Succinyl-CoA ligase [GDP-forming] subunit beta, mitochondrial
A	K1R983_CRAGI	Protein transport protein SEC23
A	K1P5V7_CRAGI	Eukaryotic translation initiation factor 3 subunit C
A	K1RCW3_CRAGI	Elongation factor 1-beta
A	K1R8R6_CRAGI	Fructose-bisphosphate aldolase
A	K1QPY8_CRAGI	Extracellular superoxide dismutase [Cu-Zn]
A	K1PCQ2_CRAGI	E3 ubiquitin-protein ligase UBR4
A	K1Q7T5_CRAGI	Protein disulfide-isomerase
A	K1PLM3_CRAGI	Hydroxyacyl-coenzyme A dehydrogenase, mitochondrial
A	K1RAT9_CRAGI	Tubulin-specific chaperone D
A	K1QKK5_CRAGI	Vacuolar protein sorting-associated protein 4B
A	K1QJL6_CRAGI	Microtubule-associated protein RP/EB family member 3
A	K1QB86_CRAGI	Dynamin-1
A	K1QN11_CRAGI	Pre-mRNA-processing-splicing factor 8
A	K1QHH0_CRAGI	Protein henna
A	K1QVP6_CRAGI	Developmentally-regulated GTP-binding protein 1
A	K1PQI4_CRAGI	Enolase-phosphatase E1
A	K1R3I6_CRAGI	Nucleolar complex protein 2-like protein (Fragment)
A	K1QJF7_CRAGI	Coronin
A	K1PKF5_CRAGI	Protein-glutamine gamma-glutamyltransferase 4
A	K1R266_CRAGI	Retinal dehydrogenase 1
A	K1Q3F9_CRAGI	Armadillo repeat-containing protein 8
A	K1QSZ6_CRAGI	Uncharacterized protein
A	K1P8B7_CRAGI	Ubiquitin-conjugating enzyme E2-17 kDa (Fragment)
A	K1QLK8_CRAGI	GTP-binding protein SAR1b
A	K1QF31_CRAGI	Serine/threonine-protein kinase PLK
A	K1RKC1_CRAGI	Far upstream element-binding protein 3
A	K1PHE1_CRAGI	Putative ubiquitin carboxyl-terminal hydrolase FAF-X
A	K1Q0L1_CRAGI	60S ribosomal protein L23a

A	K1R008_CRAGI	Proteasome subunit alpha type
A	K1QBG8_CRAGI	Proteasome subunit beta type-4
A	K1R8B2_CRAGI	Isovaleryl-CoA dehydrogenase, mitochondrial
A	K1RNN9_CRAGI	Cytoskeleton-associated protein 5
A	K1QYG7_CRAGI	Glucosamine--fructose-6-phosphate aminotransferase [isomerizing] 1
A	K1PFK8_CRAGI	Uncharacterized protein
A	K1PRD5_CRAGI	Trifunctional purine biosynthetic protein adenosine-3
A	K1PBH3_CRAGI	Dynein heavy chain 3, axonemal
A	K1QVK0_CRAGI	Transaldolase
A	K1PAM6_CRAGI	Uncharacterized protein
A	K1Q948_CRAGI	Alpha-1,4 glucan phosphorylase
A	K1RGG1_CRAGI	Alanyl-tRNA synthetase, cytoplasmic
A	K1Q9P5_CRAGI	Mitochondrial-processing peptidase subunit beta
A	K1QTE3_CRAGI	ATP-binding cassette sub-family F member 1
A	K1PZ08_CRAGI	Ras-related protein Rab-7a
A	K1RGJ7_CRAGI	Neogenin
A	K1RK68_CRAGI	Uncharacterized protein
A	K1QEF9_CRAGI	Protein-glutamine gamma-glutamyltransferase K
A	K1RHB2_CRAGI	Nucleolar RNA helicase 2
A	K1QAF3_CRAGI	Alanine aminotransferase 2
A	K1PB94_CRAGI	ATP-binding cassette sub-family E member 1
A	K1R488_CRAGI	Actin-related protein 2/3 complex subunit
A	K1QC65_CRAGI	DNA polymerase alpha subunit B
A	K1PCR9_CRAGI	Proteasome endopeptidase complex
A	K1RFU6_CRAGI	Proteasome activator complex subunit 3
A	K1R9R5_CRAGI	Proteasome subunit alpha type
A	K1PRQ5_CRAGI	Ubiquitin-like modifier-activating enzyme 1
A	K1Q1L4_CRAGI	Uncharacterized protein
A	K1Q982_CRAGI	Malignant fibrous histiocytoma-amplified sequence 1
A	K1PKF6_CRAGI	26S proteasome non-ATPase regulatory subunit 13
A	K1QBT2_CRAGI	Proteasome subunit beta
A	K1P5Z3_CRAGI	Lysosomal aspartic protease
A	K1P7L9_CRAGI	Nucleolar GTP-binding protein 1
A	K1Q9M7_CRAGI	Histone H1-delta
A	K1PS84_CRAGI	Alpha-crystallin B chain
A	K1R6C2_CRAGI	Peroxisomal 3,2-trans-enoyl-CoA isomerase
A	K1PZC0_CRAGI	Structural maintenance of chromosomes protein
A	K1PMJ9_CRAGI	Cleavage stimulation factor 77 kDa subunit
A	K1R4M7_CRAGI	Serine/threonine protein phosphatase 2A regulatory subunit
A	K1S3G2_CRAGI	HMGB1
A	K1PB82_CRAGI	Electron transfer flavoprotein subunit beta
A	K1PWP4_CRAGI	Phenylalanyl-tRNA synthetase alpha chain
A	K1QNS4_CRAGI	DnaJ-like protein subfamily C member 9
A	K1Q7E4_CRAGI	Ubiquitin-conjugating enzyme E2 N
A	K1R6F1_CRAGI	Proteasome subunit alpha type
A	K1Q667_CRAGI	tRNA-splicing ligase RtcB homolog
A	K1QWC3_CRAGI	40S ribosomal protein S3
A	K1RAH6_CRAGI	Ubiquitin-conjugating enzyme E2-17 kDa
A	K1RIM7_CRAGI	Methionine aminopeptidase 2
A	K1PXS8_CRAGI	Calreticulin
A	K1RIG6_CRAGI	LSM14-like protein A
A	K1R168_CRAGI	Dynein heavy chain 2, axonemal
A	K1R591_CRAGI	Inter-alpha-trypsin inhibitor heavy chain H4
A	K1QKI1_CRAGI	Tudor domain-containing protein 1
A	K1RNB6_CRAGI	Alpha-aminoadipic semialdehyde dehydrogenase
A	K1R0Y9_CRAGI	ADP,ATP carrier protein
A	K1QE83_CRAGI	CCR4-NOT transcription complex subunit 1
A	K1QFR9_CRAGI	Spectrin beta chain
A	K1RAP8_CRAGI	Malic enzyme
A	K1PK49_CRAGI	Myosin-Ic

A	K1QAH9_CRAGI	H/ACA ribonucleoprotein complex subunit
A	K1PYR4_CRAGI	26S proteasome non-ATPase regulatory subunit 1
A	K1R8C6_CRAGI	40S ribosomal protein S12
A	K1PY89_CRAGI	Extracellular superoxide dismutase [Cu-Zn]
A	K1Q662_CRAGI	Actin-interacting protein 1
A	K1Q4G7_CRAGI	Tubulin gamma chain
A	K1R472_CRAGI	Synaptobrevin-like protein YKT6
A	K1PS69_CRAGI	Importin-9
A	K1QDU9_CRAGI	3-phosphoinositide-dependent protein kinase 1
A	K1PFU5_CRAGI	Ubiquitin-conjugating enzyme E2 C
A	K1QKG8_CRAGI	Upstream activation factor subunit spp27
A	K1R0P8_CRAGI	CTP synthase
A	K1QZX9_CRAGI	Uncharacterized protein
A	K1QTD9_CRAGI	Nucleolar protein 56
A	K1PIP8_CRAGI	Proteasome subunit beta
A	K1RBF6_CRAGI	Uncharacterized protein yfeX
A	K1PW99_CRAGI	Protein OSCP1
A	K1PWB9_CRAGI	EH domain-containing protein 1
A	K1PU46_CRAGI	Lethal(2) giant larvae-like protein 1
A	K1QYH6_CRAGI	COP9 signalosome complex subunit 3
A	K1Q6I1_CRAGI	Ubiquitin-conjugating enzyme E2 L3
A	K1PF60_CRAGI	3-ketoacyl-CoA thiolase, mitochondrial
A	K1PQD4_CRAGI	Phosphoglucomutase-1
A	K1PSN0_CRAGI	Pre-mRNA-processing factor 40-like protein A
A	K1R834_CRAGI	60S ribosomal protein L9
A	K1RBU9_CRAGI	Non-specific serine/threonine protein kinase
A	K1QHM2_CRAGI	Dolichyl-diphosphooligosaccharide--protein glycosyltransferase subunit 2
A	K1QW73_CRAGI	Glycoprotein 3-alpha-L-fucosyltransferase A
A	K1Q7X3_CRAGI	Pre-mRNA-splicing factor SYF1
A	K1PUJ1_CRAGI	Radixin
A	K1R8I8_CRAGI	Acetyltransferase component of pyruvate dehydrogenase complex
A	K1PRL4_CRAGI	60S ribosomal protein L38 (Fragment)
A	K1Q0G7_CRAGI	Developmentally-regulated GTP-binding protein 2
A	K1PBN1_CRAGI	Phospholipase
A	K1QJ33_CRAGI	Aminoacyl tRNA synthetase complex-interacting multifunctional protein 2
A	A5LGH1_CRAGI	Voltage-dependent anion channel
A	K1PUV4_CRAGI	40S ribosomal protein S24
A	K1QJE9_CRAGI	Uncharacterized protein
A	K1R005_CRAGI	Filamin-C (Fragment)
A	K1RGB7_CRAGI	Epidermal retinal dehydrogenase 2
A	K1PPJ6_CRAGI	Nicotinamide phosphoribosyltransferase
A	K1PEW1_CRAGI	Sorting nexin
A	K1QDH9_CRAGI	Myosin-11
A	K1QPJ9_CRAGI	Serine/threonine-protein phosphatase 2A 55 kDa regulatory subunit B
A	K1R9S5_CRAGI	Cytosolic Fe-S cluster assembly factor NUBP2 homolog
A	K1PTV1_CRAGI	Splicing factor 3B subunit 4
A	K1Q5H6_CRAGI	FACT complex subunit SSRP1
A	K1RN05_CRAGI	Transportin-3
A	K1PDE4_CRAGI	Protein arginine N-methyltransferase
A	K1Q9G3_CRAGI	Isocitrate dehydrogenase [NAD] subunit, mitochondrial
A	K1R2H9_CRAGI	WD repeat-containing protein 35
A	K1PA61_CRAGI	Actin-like protein 6A
A	K1QQT2_CRAGI	Uncharacterized protein y4xO
A	K1PJG8_CRAGI	Timeless-like protein
A	K1QJM1_CRAGI	60S ribosomal protein L30
A	K1QK68_CRAGI	Myosin-2 essential light chain
A	K1R517_CRAGI	Superkiller viralicidic activity 2-like 2
A	K1Q6V6_CRAGI	Replication factor C subunit 4
A	K1Q888_CRAGI	Translin
A	K1QQC1_CRAGI	Dynein light chain roadblock

A	K1Q1F4_CRAGI	60S ribosomal protein L3 (Fragment)
A	K1Q2E0_CRAGI	AP-1 complex subunit mu-1
A	K1Q155_CRAGI	THO complex subunit 1
A	K1R3M4_CRAGI	Ubiquitin-like modifier-activating enzyme 1
A	K1PML4_CRAGI	Pre-mRNA-processing factor 39
A	K1QEK7_CRAGI	Ubiquitin carboxyl-terminal hydrolase
A	K1QDI4_CRAGI	Superoxide dismutase [Cu-Zn]
A	K1Q1Z3_CRAGI	Seryl-tRNA synthetase, cytoplasmic
A	K1Q4X8_CRAGI	DNA mismatch repair protein Msh2
A	K1P5F7_CRAGI	Metastasis-associated protein MTA1
A	K1R7J6_CRAGI	Putative sodium/potassium-transporting ATPase subunit beta-2
A	K1QNY7_CRAGI	Transport protein Sec24C
A	K1QKQ5_CRAGI	N-terminal acetyltransferase B complex subunit MDM20
A	K1PH10_CRAGI	Polyadenylate-binding protein-interacting protein 1
A	K1Q329_CRAGI	Pyruvate dehydrogenase E1 component subunit beta, mitochondrial
A	K1QI08_CRAGI	Ribose-phosphate pyrophosphokinase 1
A	K1QV87_CRAGI	Catenin alpha-2
A	K1PXD4_CRAGI	Putative ATP-dependent RNA helicase DDX6
A	K1QCQ5_CRAGI	Succinate--CoA ligase [ADP-forming] subunit beta, mitochondrial
A	K1QCL6_CRAGI	Proteasomal ubiquitin receptor ADRM1
A	K1PFV9_CRAGI	4-trimethylaminobutyraldehyde dehydrogenase
A	K1PTR3_CRAGI	Oxysterol-binding protein
A	K1R1T8_CRAGI	Nucleolar protein 56
A	K1QUC6_CRAGI	Uncharacterized protein
A	K1QCM0_CRAGI	Rho GDP-dissociation inhibitor 1
A	K1QNZ3_CRAGI	Serine/threonine-protein phosphatase
A	K1QKG9_CRAGI	Cysteine desulfurase, mitochondrial
A	K1RUW0_CRAGI	E3 SUMO-protein ligase RanBP2
A	K1QPZ1_CRAGI	Actin-related protein 2/3 complex subunit 3
A	K1QHT0_CRAGI	Deoxyuridine 5'-triphosphate nucleotidohydrolase, mitochondrial
A	K1Q5I4_CRAGI	COP9 signalosome complex subunit 2
A	K1PLW6_CRAGI	Bifunctional purine biosynthesis protein PURH
A	K1PWU5_CRAGI	Cytosolic carboxypeptidase 1
A	K1P9S7_CRAGI	Brix domain-containing protein 2
A	K1Q260_CRAGI	Nucleolar protein 58
A	K1PKL8_CRAGI	Serine/threonine-protein phosphatase 2A 56 kDa regulatory subunit alpha isoform
A	K1S1X3_CRAGI	SWI/SNF-related matrix-associated actin-dependent regulator of chromatin subfamily A member 5
A	K1Q3F4_CRAGI	Inorganic pyrophosphatase
A	K1P7J8_CRAGI	6-phosphofructokinase
A	K1QXR6_CRAGI	Protein farnesyltransferase/geranylgeranyltransferase type-1 subunit alpha
A	K1Q4Q8_CRAGI	Pyruvate dehydrogenase E1 component subunit alpha, somatic form, mitochondrial
A	K1RA63_CRAGI	Transmembrane protein 2
A	K1Q8T3_CRAGI	Importin subunit alpha
A	K1QMT1_CRAGI	DnaJ-like protein subfamily B member 4
A	K1RBZ5_CRAGI	Ran GTPase-activating protein 1
A	K1PST9_CRAGI	Brefeldin A-inhibited guanine nucleotide-exchange protein 1
A	K1QWJ4_CRAGI	Splicing factor 3B subunit 5
A	K1QYT7_CRAGI	COP9 signalosome complex subunit 7a
A	K1R7D7_CRAGI	Poly(A)-specific ribonuclease PARN
A	K1QZI3_CRAGI	Myosin-Ie
A	K1PNX0_CRAGI	Methionyl-tRNA synthetase, cytoplasmic
A	K1Q324_CRAGI	Heterogeneous nuclear ribonucleoprotein K
A	K1QY71_CRAGI	Histone H2B
A	K1QDA7_CRAGI	Uracil phosphoribosyltransferase
A	K1RAU8_CRAGI	Eukaryotic translation initiation factor 3 subunit E
A	K1QRD0_CRAGI	Cytoplasmic dynein 1 light intermediate chain 1
A	K1Q719_CRAGI	Serine/threonine-protein kinase OSR1
A	K1RJJ7_CRAGI	Histone H5
A	K1P8Y3_CRAGI	Sulfotransferase 1C4
A	K1QMY1_CRAGI	Aconitate hydratase, mitochondrial

A	K1RBI9_CRAGI	Small nuclear ribonucleoprotein Sm D2
A	K1QEJ0_CRAGI	Ras GTPase-activating protein-binding protein 2
A	K1Q5Z6_CRAGI	Eukaryotic translation initiation factor 2 subunit 2
A	K1RGS1_CRAGI	WD repeat-containing protein 19
A	K1R195_CRAGI	Protein DJ-1
A	K1R8Y1_CRAGI	Obg-like ATPase 1
A	K1RRH1_CRAGI	Chromodomain-helicase-DNA-binding protein Mi-2-like protein
A	K1PM66_CRAGI	60S ribosomal protein L12
A	K1PKQ3_CRAGI	Uncharacterized protein
A	K1QIB2_CRAGI	Mitogen-activated protein kinase
A	K1PSN4_CRAGI	Tetratricopeptide repeat protein 39C
A	K1PT09_CRAGI	Uncharacterized protein
A	K1S0I4_CRAGI	Methylthioribose-1-phosphate isomerase
A	K1Q9I1_CRAGI	TRAF2 and NCK-interacting protein kinase
A	K1R5G4_CRAGI	60S ribosomal protein L31
A	K1R7F6_CRAGI	Cystathionine gamma-lyase
A	K1QGP1_CRAGI	Replication factor C subunit 2
A	K1Q4S7_CRAGI	Calreticulin
A	K1RTQ6_CRAGI	Fructose-bisphosphate aldolase
A	K1QN79_CRAGI	40S ribosomal protein S11
A	K1R6E9_CRAGI	Dihydrolipoamide acetyltransferase component of pyruvate dehydrogenase complex
A	K1PXU6_CRAGI	60S ribosomal protein L24
A	K1PVA0_CRAGI	Cullin-5
A	K1QSZ4_CRAGI	Serine--pyruvate aminotransferase
A	K1RNH1_CRAGI	60S ribosomal protein L18 (Fragment)
A	K1PIH2_CRAGI	V-type proton ATPase subunit E
A	K1QG08_CRAGI	Phosphatidylinositol-binding clathrin assembly protein LAP
A	K1RVR1_CRAGI	Telomerase protein component 1
A	K1Q9D7_CRAGI	Sorting nexin-2
A	K1PDC6_CRAGI	Proteasome subunit beta
A	K1R1E2_CRAGI	Arp2/3 complex 34 kDa subunit
A	K1PCR5_CRAGI	KH domain-containing, RNA-binding, signal transduction-associated protein 2
A	K1P8S5_CRAGI	Condensin complex subunit 3
A	K1PCH8_CRAGI	Nucleoporin p54
A	K1QY58_CRAGI	Eukaryotic translation initiation factor 3 subunit I (Fragment)
A	K1Q947_CRAGI	Dynein light chain
A	K1Q615_CRAGI	Peroxiredoxin-1
A	K1QC78_CRAGI	Ras-related protein Rab-14
A	K1QET6_CRAGI	Neurobeachin
A	K1PG48_CRAGI	Dynein-1-beta heavy chain, flagellar inner arm I1 complex
A	K1R9P5_CRAGI	Mitochondrial import receptor subunit TOM70
A	K1PGV8_CRAGI	Nucleoprotein TPR
A	K1PRV7_CRAGI	Profilin
A	K1QIZ7_CRAGI	Programmed cell death protein 6
A	K1Q4U7_CRAGI	AP-3 complex subunit delta-1
A	K1QGL9_CRAGI	Mannose-1-phosphate guanyltransferase beta
A	K1PBL2_CRAGI	Eukaryotic initiation factor 4A-III
A	K1R3A0_CRAGI	Transcription initiation factor IIB
A	K1P7Q2_CRAGI	Elongation factor 1-gamma
A	K1PNU2_CRAGI	Histone-arginine methyltransferase CARM1
A	K1PWP8_CRAGI	Echinoderm microtubule-associated protein-like 1
A	K1QV46_CRAGI	Tetratricopeptide repeat protein 21B
A	K1QKQ9_CRAGI	Dynein heavy chain 7, axonemal
A	K1PR47_CRAGI	Eukaryotic translation initiation factor 2A
A	K1S058_CRAGI	Transcription factor RFX3
A	K1QEG3_CRAGI	Heat shock 70 kDa protein 12B
A	K1R481_CRAGI	Epimerase family protein SDR39U1
A	K1QBF3_CRAGI	Trpc4-associated protein
A	K1PUX5_CRAGI	Casein kinase II subunit alpha
A	K1QK98_CRAGI	IST1-like protein

A	K1RDV2_CRAGI	Myotrophin-like protein
A	K1PDL3_CRAGI	Ribosomal protein L19
A	K1S2S8_CRAGI	Signal recognition particle 54 kDa protein
A	K1QZ11_CRAGI	Geranylgeranyl transferase type-2 subunit alpha
A	K1QU47_CRAGI	Dual oxidase 2
A	K1QXF9_CRAGI	Acyl-protein thioesterase 2
A	K1PL64_CRAGI	Poly(A) polymerase gamma
A	K1RQJ6_CRAGI	Enhancer of mRNA-decapping protein 4
A	K1QLP5_CRAGI	Coatomer subunit delta
A	K1PJB0_CRAGI	Heat shock protein 70 B2
A	K1Q404_CRAGI	DNA topoisomerase 2
A	K1QJA7_CRAGI	Histone chaperone asf1-B
A	K1RP91_CRAGI	Putative RNA exonuclease NEF-sp
A	K1PZD9_CRAGI	26S proteasome non-ATPase regulatory subunit 11
A	K1QI32_CRAGI	Synaptotagmin-like protein 5
A	K1RK83_CRAGI	Tyrosine-protein kinase BAZ1B
A	K1QQG2_CRAGI	ATP-dependent RNA helicase DHX8
A	K1PUQ5_CRAGI	Histone H2B
A	K1QW72_CRAGI	Catalase
A	K1R2U8_CRAGI	Universal stress protein A-like protein
A	K1PY30_CRAGI	Septin-2
A	K1Q8C5_CRAGI	Putative ATP-dependent RNA helicase DDX47
A	K1QNP9_CRAGI	Putative deoxyribose-phosphate aldolase
A	K1PDF0_CRAGI	Protein disulfide-isomerase A6
A	K1R1R9_CRAGI	Pre-mRNA-processing factor 6
A	K1Q3G8_CRAGI	Chaperone activity of bc1 complex-like, mitochondrial
A	K1QBH4_CRAGI	ATP-dependent RNA helicase DDX42
A	K1PEM0_CRAGI	Ubiquitin-like modifier-activating enzyme 5
A	K1QD23_CRAGI	Acetyl-CoA acetyltransferase B, mitochondrial
A	K1RJ96_CRAGI	Sphere organelles protein SPH-1
A	K1R1B1_CRAGI	35 kDa SR repressor protein
A	K1QCB0_CRAGI	40S ribosomal protein S5
A	K1RGZ8_CRAGI	Wings apart-like protein
A	K1Q107_CRAGI	Histidine triad nucleotide-binding protein 1
A	K1QYM1_CRAGI	Thymidylate synthase
A	K1QYT5_CRAGI	Phosphate carrier protein, mitochondrial
A	K1QJT3_CRAGI	COP9 signalosome complex subunit 1
A	K1QAU8_CRAGI	Peptidyl-prolyl cis-trans isomerase E
A	K1RG28_CRAGI	Kinase C and casein kinase substrate in neurons protein 2
A	K1R2S4_CRAGI	NEDD8-activating enzyme E1 regulatory subunit (Fragment)
A	K1Q4Y8_CRAGI	Histone H1oo
A	K1PYQ1_CRAGI	Protein phosphatase 1 regulatory subunit 7
A	K1RWE5_CRAGI	Thioredoxin-like protein 1
A	K1QJL2_CRAGI	CCR4-NOT transcription complex subunit 10
A	K1P6C4_CRAGI	Poly [ADP-ribose] polymerase
A	K1PNL0_CRAGI	Microtubule-associated protein futsch
A	K1QSA2_CRAGI	Short-chain specific acyl-CoA dehydrogenase, mitochondrial
A	K1QU30_CRAGI	MON2-like protein
A	K1Q317_CRAGI	Serine/threonine-protein kinase SRPK1
A	K1RGE2_CRAGI	Prostaglandin reductase 1
A	K1RIB1_CRAGI	Arginyl-tRNA synthetase, cytoplasmic
A	K1R0W0_CRAGI	Ferritin
A	K1P8T5_CRAGI	Glycerol-3-phosphate dehydrogenase [NAD(+)]
A	K1QQD8_CRAGI	Putative ATP-dependent RNA helicase DDX43
A	K1QMH5_CRAGI	Small nuclear ribonucleoprotein Sm D1
A	K1QS22_CRAGI	UPF0160 protein MYG1, mitochondrial (Fragment)
A	K1QHP8_CRAGI	Uncharacterized protein
A	K1PXM3_CRAGI	Chromatin assembly factor 1 subunit A
A	K1QF45_CRAGI	Alpha-tocopherol transfer-like protein
A	K1QC27_CRAGI	Hydroxysteroid dehydrogenase-like protein 2

A	Q70MT4_CRAGI	40S ribosomal protein S10
A	K1PQB4_CRAGI	Acyl-CoA dehydrogenase family member 10
A	K1PZI3_CRAGI	SWI/SNF complex subunit SMARCC2
A	K1PNS2_CRAGI	33 kDa inner dynein arm light chain, axonemal
A	K1RG36_CRAGI	Phosphoribosylformylglycinamidine synthase (Fragment)
A	K1QMQ0_CRAGI	Putative exonuclease mut-7-like protein
A	K1QD80_CRAGI	Protein quaking-B
A	K1R0M2_CRAGI	Uncharacterized protein
A	K1QKI4_CRAGI	Lysine--tRNA ligase
A	K1PPH6_CRAGI	Kelch domain-containing protein 8B
A	K1QBE2_CRAGI	Syntaxin-5
A	K1RHP3_CRAGI	Proliferation-associated protein 2G4
A	K1PZU1_CRAGI	Hsc70-interacting protein
A	K1RMW3_CRAGI	Protein kinase C
A	K1R1Q8_CRAGI	Ras-related protein Rab-5C
A	K1PPK1_CRAGI	Actin-related protein 2/3 complex subunit 4
A	K1R8Y9_CRAGI	Translin-associated protein X
A	K1QW41_CRAGI	Leucine-zipper-like transcriptional regulator 1
A	K1Q1G2_CRAGI	Elongator complex protein 1
A	K1RA79_CRAGI	E3 ubiquitin-protein ligase HECTD1
A	K1RZM3_CRAGI	Cartilage acidic protein 1
A	K1QD81_CRAGI	Ubiquitin conjugation factor E4 A
A	K1PMY9_CRAGI	Calmodulin
A	K1RU04_CRAGI	Actin, cytoplasmic
A	K1QND2_CRAGI	Septin-2
A	K1PR25_CRAGI	Regulator of differentiation 1
A	K1QV25_CRAGI	Transcription elongation factor B polypeptide 2
A	K1RJ70_CRAGI	Cytosolic non-specific dipeptidase
A	K1R751_CRAGI	Nuclear pore complex protein Nup88
A	K1QDK0_CRAGI	Engulfment and cell motility protein 2
A	K1PLV6_CRAGI	F-actin-capping protein subunit alpha
A	K1QWN2_CRAGI	Elongation factor 1-delta
A	K1RRP7_CRAGI	Uncharacterized protein
A	K1R6H7_CRAGI	Uncharacterized protein
A	K1REP0_CRAGI	Uncharacterized protein
A	K1R0L4_CRAGI	Sodium/potassium-transporting ATPase subunit alpha
A	K1R0V5_CRAGI	Cell differentiation protein RCD1-like protein
A	K1R2N1_CRAGI	Glutathione reductase
A	K1PRB6_CRAGI	Apolipoprotein D
A	K1QMF1_CRAGI	Isocitrate dehydrogenase [NAD] subunit gamma, mitochondrial
A	K1R5E7_CRAGI	Cathepsin L
A	K1PMI0_CRAGI	Charged multivesicular body protein 4b
A	K1QZN3_CRAGI	Myosin-Id
A	K1S0N3_CRAGI	Glutamate receptor-interacting protein 1
A	K1RDM2_CRAGI	60S ribosomal protein L18a
A	K1R0R7_CRAGI	Putative ATP-dependent RNA helicase DHX36
A	K1QWX0_CRAGI	26S proteasome non-ATPase regulatory subunit 14
A	K1PQA3_CRAGI	Pseudouridylate synthase 7-like protein
A	K1Q7K0_CRAGI	Putative serine carboxypeptidase CPVL
A	K1R7N8_CRAGI	Proteasome endopeptidase complex
A	K1QCL7_CRAGI	Uncharacterized protein
A	K1QQB3_CRAGI	Glycyl-tRNA synthetase
A	K1RFU8_CRAGI	High mobility group protein DSP1
A	K1PJW0_CRAGI	Talin-1
A	K1RBJ3_CRAGI	DnaJ-like protein subfamily C member 13
A	K1PRV2_CRAGI	Threonine synthase-like 1
A	K1R347_CRAGI	Tetratricopeptide repeat protein 38
A	K1S422_CRAGI	Katanin p80 WD40 repeat-containing subunit B1
A	K1QK18_CRAGI	Cytochrome b5
A	K1QJU3_CRAGI	Cell division cycle protein 20-like protein

A	K1QRM9_CRAGI	Acidic leucine-rich nuclear phosphoprotein 32 family member A
A	K1R373_CRAGI	ATP-binding cassette sub-family F member 3
A	K1RE81_CRAGI	Transport protein Sec24B
A	K1QW21_CRAGI	39S ribosomal protein L40, mitochondrial
A	K1PLG1_CRAGI	Putative ribosomal RNA methyltransferase NOP2
A	K1R712_CRAGI	Transforming growth factor-beta receptor-associated protein 1
A	K1Q1K8_CRAGI	Elongation factor 1-beta
A	K1PNK5_CRAGI	Ras GTPase-activating-like protein IQGAP1
A	K1Q1F1_CRAGI	Serine/threonine-protein kinase 31
A	K1QFS4_CRAGI	Actin-related protein 2
A	K1PUK3_CRAGI	Armadillo repeat-containing protein 6
A	K1PI41_CRAGI	Flap endonuclease 1
A	K1QU96_CRAGI	Pre-rRNA-processing protein TSR1-like protein
A	K1QFK8_CRAGI	Target of Myb protein 1
A	K1R4Q3_CRAGI	Spectrin beta chain, brain 1
A	K1QMS7_CRAGI	Malonyl CoA-acyl carrier protein transacylase, mitochondrial
A	K1P8Q1_CRAGI	Putative methyltransferase TARBP1
A	K1RXV8_CRAGI	PAT1-like protein 1
A	K1PXH5_CRAGI	Putative saccharopine dehydrogenase
A	K1QWP1_CRAGI	Nucleoporin seh1
A	K1RDF6_CRAGI	Long-chain specific acyl-CoA dehydrogenase, mitochondrial
A	K1QYH5_CRAGI	Ubiquitin carboxyl-terminal hydrolase 14
A	K1S0J9_CRAGI	Uncharacterized protein
A	K1R247_CRAGI	Condensin complex subunit 1
A	K1QKZ6_CRAGI	Inosine-5'-monophosphate dehydrogenase
A	K1QQ48_CRAGI	Serine/threonine-protein kinase N2
A	K1RIZ3_CRAGI	Bone morphogenetic protein 7
A	K1PVQ8_CRAGI	Eukaryotic translation initiation factor 3 subunit K
A	K1QMQ1_CRAGI	TBC1 domain family member 10B
A	K1QFF0_CRAGI	Vacuolar protein sorting-associated protein 35 (Fragment)
A	K1Q435_CRAGI	Eukaryotic translation initiation factor 2 subunit 1
A	K1QNZ7_CRAGI	Ubiquilin-1
A	K1QYI6_CRAGI	Cullin-3-B
A	K1PFV4_CRAGI	Eukaryotic translation initiation factor 4E
A	K1QVV1_CRAGI	Ribose-5-phosphate isomerase
A	K1RT39_CRAGI	Glutaredoxin-3
A	K1PNG7_CRAGI	Sorting nexin-33
A	K1PYK7_CRAGI	RNA-binding protein 39
A	K1QCP3_CRAGI	Crooked neck-like protein 1
A	K1QSV4_CRAGI	RNA helicase
A	K1R811_CRAGI	Ribonucleoside-diphosphate reductase small chain
A	K1R944_CRAGI	Tetratricopeptide repeat protein 37
A	K1QS07_CRAGI	Proteasome subunit beta type-3
A	K1PZV3_CRAGI	Guanine nucleotide-binding protein-like 3-like protein (Fragment)
A	K1QNU0_CRAGI	Non-specific serine/threonine protein kinase
A	K1R3R4_CRAGI	Cytosolic Fe-S cluster assembly factor NUBP1 homolog
A	K1RJS5_CRAGI	Uncharacterized protein
A	K1RNK8_CRAGI	Rho GTPase-activating protein 17
A	K1RG79_CRAGI	Neuronal acetylcholine receptor subunit alpha-6
A	K1QVF8_CRAGI	Uncharacterized protein in QAH/OAS sulfhydrylase 3'region (Fragment)
A	K1Q4C3_CRAGI	Fumarylacetoacetase
A	K1R7T0_CRAGI	GMP synthase [glutamine-hydrolyzing]
A	K1QX22_CRAGI	4-hydroxyphenylpyruvate dioxygenase
A	K1RIS2_CRAGI	3-oxoacyl-[acyl-carrier-protein] reductase
A	K1Q407_CRAGI	Ras GTPase-activating protein 1
A	K1R9I0_CRAGI	Myosin-VIIa
A	K1Q0N9_CRAGI	Uncharacterized protein
A	K1PUE8_CRAGI	Serine/threonine-protein phosphatase 4 regulatory subunit 3
A	K1PSY2_CRAGI	Fragile X mental retardation syndrome-related protein 1
A	K1RA35_CRAGI	Splicing factor, arginine/serine-rich 7

A	K1QW39_CRAGI	Neurobeachin
A	K1QJI9_CRAGI	Importin-13
A	K1R3M6_CRAGI	Ubiquitin-conjugating enzyme E2-22 kDa
A	K1RCR8_CRAGI	Carbonyl reductase [NADPH] 1
A	K1RJW8_CRAGI	Protein DEK
A	K1R2G9_CRAGI	SEC13-like protein
A	K1PLF8_CRAGI	Diacylglycerol kinase
A	K1PWV7_CRAGI	Uncharacterized protein
A	K1R3W9_CRAGI	Replication protein A 14 kDa subunit
A	K1P8G1_CRAGI	Heterogeneous nuclear ribonucleoprotein H
A	K1R2S2_CRAGI	Peptidylprolyl isomerase
A	K1PNY5_CRAGI	Splicing factor, proline-and glutamine-rich
A	K1P7Q6_CRAGI	40S ribosomal protein S19
A	K1PZN1_CRAGI	Calcium/calmodulin-dependent protein kinase type II delta chain
A	K1PBC0_CRAGI	Non-neuronal cytoplasmic intermediate filament protein
A	K1QNN9_CRAGI	MICOS complex subunit MIC60
A	K1QJ46_CRAGI	Putative methylcrotonoyl-CoA carboxylase beta chain, mitochondrial
A	K1R2G7_CRAGI	Ran-binding protein 3
A	K1RJG6_CRAGI	Heterogeneous nuclear ribonucleoprotein 27C
A	K1QZ58_CRAGI	Splicing factor U2AF 26 kDa subunit
A	K1QCU0_CRAGI	Eukaryotic translation initiation factor 3 subunit G
A	K1PH25_CRAGI	Methionyl-tRNA synthetase, cytoplasmic
A	K1RN97_CRAGI	Hemagglutinin/amebocyte aggregation factor
A	K1Q6M6_CRAGI	6-phosphofructokinase
A	K1PPL6_CRAGI	Malonyl-CoA decarboxylase, mitochondrial
A	K1R9Q4_CRAGI	Uncharacterized protein
A	K1QPX8_CRAGI	Alkyl/aryl-sulfatase BDS1
A	K1PJP2_CRAGI	Putative pre-mRNA-splicing factor ATP-dependent RNA helicase DHX15
A	K1RRZ9_CRAGI	MKI67 FHA domain-interacting nucleolar phosphoprotein-like protein
A	K1S6R2_CRAGI	N-acetyltransferase 11
A	K1PJY4_CRAGI	Calcium-binding protein 39
A	K1Q1G9_CRAGI	Putative ATP-dependent RNA helicase DHX37
A	K1RA95_CRAGI	Filamin-A
A	K1Q865_CRAGI	Trafficking protein particle complex subunit 4
A	K1RFQ4_CRAGI	Tetratricopeptide repeat protein 27
A	K1QRD4_CRAGI	S-formylglutathione hydrolase
A	K1Q9Z4_CRAGI	Aldehyde dehydrogenase
A	K1QB76_CRAGI	Uncharacterized protein
A	K1Q2Y1_CRAGI	40S ribosomal protein S15
A	K1S3Q9_CRAGI	MAK16-like protein (Fragment)
A	K1RAF8_CRAGI	Uncharacterized protein
A	K1QE44_CRAGI	UPF0663 transmembrane protein C17orf28
A	K1PN44_CRAGI	Casein kinase II subunit beta
A	K1PWR4_CRAGI	Signal recognition particle receptor subunit alpha
A	K1QDS1_CRAGI	3-hydroxyacyl-CoA dehydrogenase type-2
A	K1R924_CRAGI	RNA-binding protein 45
A	K1QWZ6_CRAGI	Dolichyl-diphosphooligosaccharide--protein glycosyltransferase subunit 1
A	K1PSH2_CRAGI	28S ribosomal protein S12, mitochondrial
A	K1QKL1_CRAGI	DNA-directed RNA polymerases I, II, and III subunit RPABC3
A	K1RCY7_CRAGI	Eukaryotic peptide chain release factor GTP-binding subunit ERF3B
A	K1Q6U7_CRAGI	78 kDa glucose-regulated protein
A	K1R2E8_CRAGI	Prolyl endopeptidase
A	K1R4M1_CRAGI	Intraflagellar transport protein 52-like protein
A	K1RB91_CRAGI	Neutral alpha-glucosidase AB
A	K1Q056_CRAGI	Calpain-A
A	K1REW8_CRAGI	Ribosomal protein L15
A	K1QQQ5_CRAGI	Replication factor C subunit 5
A	K1QLC6_CRAGI	JmjC domain-containing protein 8
A	K1QFP5_CRAGI	NADH dehydrogenase [ubiquinone] flavoprotein 1, mitochondrial
A	K1Q7H0_CRAGI	ATP-dependent DNA helicase II subunit 2

A	K1PYW7_CRAGI	CDK5 regulatory subunit-associated protein 3
A	K1QVD0_CRAGI	Small nuclear ribonucleoprotein Sm D3
A	K1QAT9_CRAGI	ATP-dependent RNA helicase DDX1
A	K1R920_CRAGI	Eukaryotic translation initiation factor 1A, X-chromosomal
A	K1QQG7_CRAGI	DNA-directed RNA polymerase subunit
A	K1R0T1_CRAGI	V-type proton ATPase subunit G
A	K1PD36_CRAGI	Ubiquitin
A	K1QHI2_CRAGI	Heterogeneous nuclear ribonucleoprotein L
A	K1RED7_CRAGI	Poly(RC)-binding protein 3
A	K1QRE1_CRAGI	COP9 signalosome complex subunit 6
A	K1QHS9_CRAGI	Tubulin polyglutamylase TTLL13
A	K1R6Y8_CRAGI	Uncharacterized protein
A	K1RC37_CRAGI	Uncharacterized protein
A	K1PBG6_CRAGI	Uncharacterized protein
A	K1R150_CRAGI	Ras-related protein Rab-1A
A	K1QVS0_CRAGI	Ras-like GTP-binding protein Rho1
A	K1R716_CRAGI	Putative isovaleryl-CoA dehydrogenase
A	K1Q1I3_CRAGI	Ornithine aminotransferase
A	K1Q151_CRAGI	60S ribosomal protein L32
A	K1QMY8_CRAGI	Dedicator of cytokinesis protein 9
A	K1PR93_CRAGI	3-hydroxyisobutyrate dehydrogenase
A	K1QZX3_CRAGI	Vacuolar protein sorting-associated protein VTA1-like protein
A	K1Q3W3_CRAGI	NADH dehydrogenase [ubiquinone] iron-sulfur protein 3, mitochondrial
A	K1RHA5_CRAGI	Nucleoside diphosphate kinase
A	K1RG61_CRAGI	Cytosolic carboxypeptidase 2
A	K1RSK5_CRAGI	Kelch-like protein 6
A	K1Q105_CRAGI	Ferrochelatase
A	K1QCS7_CRAGI	Leucine-rich repeat-containing protein 16A
A	K1PWR0_CRAGI	Protein SET
A	K1RIA0_CRAGI	Molybdopterin molybdenumtransferase
A	K1RC43_CRAGI	U4/U6 small nuclear ribonucleoprotein Prp31
A	K1S185_CRAGI	Counting factor associated protein D
A	K1PFL3_CRAGI	Dihydropteridine reductase
A	K1QIU2_CRAGI	Putative tRNA (cytidine(32)/guanosine(34)-2'-O)-methyltransferase
A	K1S6H7_CRAGI	Vacuolar protein sorting-associated protein 13C
A	K1QMM4_CRAGI	Leucine zipper transcription factor-like protein 1
A	K1PEX5_CRAGI	Protein hu-li tai shao
A	K1PUM5_CRAGI	Cytoplasmic aconitate hydratase
A	K1QE49_CRAGI	DnaJ-like protein subfamily A member 1
A	K1QGF1_CRAGI	Splicing factor 3B subunit 2
A	K1P8Z2_CRAGI	Histidyl-tRNA synthetase, cytoplasmic
A	K1QFN2_CRAGI	Uncharacterized protein
A	K1QI48_CRAGI	Inositol hexakisphosphate and diphosphoinositol-pentakisphosphate kinase
A	K1PZ93_CRAGI	Dihydropyrimidine dehydrogenase [NADP(+)]
A	K1QN99_CRAGI	Regulator of nonsense transcripts 2
A	K1QXX2_CRAGI	Ubiquitin-conjugating enzyme E2 Q2
A	K1Q6U0_CRAGI	Coatomer subunit zeta-1
A	K1P8F1_CRAGI	Uncharacterized protein
A	K1RTD6_CRAGI	UDP-glucose:glycoprotein glucosyltransferase 1
A	K1RKE5_CRAGI	IQ and AAA domain-containing protein 1
A	K1QKD6_CRAGI	Uncharacterized protein
A	K1QN55_CRAGI	60S acidic ribosomal protein P1
A	K1RGT9_CRAGI	60S ribosomal protein L13a
A	K1PZ23_CRAGI	DnaJ-like protein subfamily C member 3
A	K1PCC8_CRAGI	Serine/threonine-protein kinase 25
A	K1PKD4_CRAGI	40S ribosomal protein S30
A	K1RXA0_CRAGI	cAMP-dependent protein kinase regulatory subunit
A	K1QAL3_CRAGI	RNA-binding protein 28
A	K1Q6J3_CRAGI	Eukaryotic translation initiation factor 2-alpha kinase 4
A	K1S049_CRAGI	Putative RNA-binding protein 16

A	K1RBT3_CRAGI	ATP-dependent RNA helicase SUV3-like protein, mitochondrial
A	K1QFS8_CRAGI	Importin-9
A	K1QVF4_CRAGI	Heterogeneous nuclear ribonucleoprotein L
A	K1PGD2_CRAGI	Putative aminopeptidase NPEPL1
A	K1QUT5_CRAGI	Amine oxidase
A	K1QAG0_CRAGI	Serine-threonine kinase receptor-associated protein
A	K1PHS4_CRAGI	Ribosome-binding protein 1
A	K1RMS0_CRAGI	Translation initiation factor eIF-2B subunit beta
A	K1R604_CRAGI	DCC-interacting protein 13-alpha
A	K1PQE3_CRAGI	RNA-binding protein Raly
A	K1PXH6_CRAGI	Cullin-4A
A	K1PM29_CRAGI	Glucose-6-phosphate 1-dehydrogenase
A	K1QNK4_CRAGI	3-oxoacyl-[acyl-carrier-protein] reductase
A	K1PD41_CRAGI	DNA primase
A	K1PTV5_CRAGI	Programmed cell death protein 10
A	K1PV35_CRAGI	Kyphoscoliosis peptidase
A	K1Q4J3_CRAGI	Nuclear cap-binding protein subunit 1
A	K1RJY3_CRAGI	TRS85-like protein
A	K1QM61_CRAGI	Uncharacterized protein
A	K1PKI9_CRAGI	Uncharacterized protein
A	K1QPB0_CRAGI	U3 small nucleolar RNA-associated protein 6-like protein
A	K1PF70_CRAGI	MON2-like protein (Fragment)
A	K1RFF7_CRAGI	Protein lethal(2)essential for life
A	K1PG60_CRAGI	60S ribosomal protein L17
A	K1Q189_CRAGI	F-box/WD repeat-containing protein 9
A	K1QBM3_CRAGI	Ras-related protein Rab-2
A	K1PNP9_CRAGI	Bullous pemphigoid antigen 1, isoforms 1/2/3/4
A	K1QIJ3_CRAGI	Nuclear pore complex protein Nup85
A	K1QX44_CRAGI	Ras-related protein Rab-11B
A	K1QLD7_CRAGI	Kinetochore protein NDC80-like protein
A	K1QUD7_CRAGI	Conserved oligomeric Golgi complex subunit 3 (Fragment)
A	K1Q9Z5_CRAGI	Peptidyl-prolyl cis-trans isomerase
A	K1RLT0_CRAGI	D-erythrulose reductase
A	K1PG98_CRAGI	rRNA-processing protein FCF1-like protein
A	K1QKQ8_CRAGI	THO complex subunit 4-A
A	K1RB07_CRAGI	60S ribosomal protein L27a
A	K1PEZ6_CRAGI	Kyphoscoliosis peptidase
A	D7EZH1_CRAGI	Cystatin B-like protein
A	K1RJ53_CRAGI	Tetratricopeptide repeat protein 12
A	K1QQH9_CRAGI	DNA (Cytosine-5)-methyltransferase 1 (Fragment)
A	K1PL63_CRAGI	TBC1 domain family member 15
A	K1PG17_CRAGI	60S ribosomal protein L21
A	K1QQ99_CRAGI	Uncharacterized protein
A	K1RG04_CRAGI	ALK tyrosine kinase receptor
A	K1PZP3_CRAGI	Conserved oligomeric Golgi complex subunit 2
A	K1QH68_CRAGI	Syntenin-1
A	K1S4H5_CRAGI	Adenosylhomocysteinase
A	K1R4L8_CRAGI	Electron transfer flavoprotein-ubiquinone oxidoreductase, mitochondrial
A	K1RFD2_CRAGI	Adenylate kinase
A	K1PB87_CRAGI	Uncharacterized protein
A	K1PM74_CRAGI	DNA mismatch repair protein Msh6
A	K1RR99_CRAGI	Rho guanine nucleotide exchange factor 12
A	K1QGQ5_CRAGI	Superoxide dismutase
A	K1PBB1_CRAGI	Stress-induced-phosphoprotein 1
A	K1Q681_CRAGI	Clustered mitochondria protein homolog
A	K1PQR9_CRAGI	Squamous cell carcinoma antigen recognized by T-cells 3
A	K1QSV1_CRAGI	Uncharacterized protein
A	K1QKY7_CRAGI	Uncharacterized protein
A	K1QBJ7_CRAGI	Uncharacterized protein
A	K1S5H7_CRAGI	Cell division cycle 5-related protein

A	K1RHJ9_CRAGI	Suppressor of G2 allele of SKP1-like protein
A	K1R2Z2_CRAGI	Methyltransferase-like protein 13
A	K1QHY6_CRAGI	Rap1 GTPase-GDP dissociation stimulator 1-A
A	K1Q1L1_CRAGI	Kinesin-associated protein 3
A	K1R3Z4_CRAGI	5'-3' exoribonuclease 1
A	K1P951_CRAGI	Fanconi anemia group D2 protein
A	K1PKD7_CRAGI	6-phosphogluconolactonase
A	K1QN54_CRAGI	Brain protein 16
A	K1QYD0_CRAGI	UBX domain-containing protein 1
A	K1QCY6_CRAGI	40S ribosomal protein S28
A	K1QZ29_CRAGI	Uncharacterized protein
A	K1R136_CRAGI	Phosphatidylinositol transfer protein alpha isoform
A	K1R969_CRAGI	Uncharacterized protein
A	K1R1E4_CRAGI	Serine/threonine-protein kinase Chk2
A	K1QVL1_CRAGI	Serine/threonine-protein phosphatase 4 regulatory subunit 4
A	K1QYD8_CRAGI	Trans-1,2-dihydrobenzene-1,2-diol dehydrogenase
A	K1Q927_CRAGI	Neurofibromin
A	K1QAU3_CRAGI	WD repeat-containing protein 63
A	K1Q8P7_CRAGI	Aspartyl aminopeptidase
A	K1QZ64_CRAGI	Nuclear pore complex protein Nup98-Nup96
A	K1PLR8_CRAGI	Chromosome transmission fidelity protein 18-like protein (Fragment)
A	K1P752_CRAGI	UPF0195 protein FAM96B
A	K1QAY3_CRAGI	Dipeptidyl-peptidase 1 (Fragment)
A	K1R669_CRAGI	Uncharacterized protein
A	K1PWS8_CRAGI	Mitotic spindle assembly checkpoint protein MAD2A
A	K1PK87_CRAGI	Putative E3 ubiquitin-protein ligase TRIP12
A	K1QKU6_CRAGI	mRNA export factor
A	K1QQV0_CRAGI	Histone H1.2
A	K1QR54_CRAGI	Zinc finger RNA-binding protein
A	K1PE13_CRAGI	Uncharacterized protein
A	K1QUW5_CRAGI	U2 snRNP auxiliary factor large subunit
A	K1PTH4_CRAGI	ADP-ribosylation factor
A	K1Q3C3_CRAGI	Lambda-crystallin-like protein
A	K1RE82_CRAGI	Uncharacterized protein
A	K1P486_CRAGI	Heat shock 70 kDa protein 12A
A	K1R7A4_CRAGI	Peptidylprolyl isomerase
A	K1PEC8_CRAGI	Actin-related protein 8
A	K1RAR8_CRAGI	Protein FAM49B
A	K1QZD2_CRAGI	Tudor domain-containing protein 7
A	K1QM54_CRAGI	Activator of 90 kDa heat shock protein ATPase-like protein 1
A	K1Q904_CRAGI	PAN2-PAN3 deadenylation complex subunit PAN3
A	K1P6N8_CRAGI	Ubiquitin carboxyl-terminal hydrolase 7
A	K1RBM7_CRAGI	Ubiquitin-conjugating enzyme E2 variant 1
A	K1PV92_CRAGI	Hsp90 co-chaperone Cdc37
A	K1PQU8_CRAGI	Sperm-associated antigen 6
A	K1QUK4_CRAGI	Protein SET
A	K1QJ85_CRAGI	Glutathione S-transferase A
A	K1QJW3_CRAGI	Heat shock 70 kDa protein 12B
A	K1QNW5_CRAGI	MAK10-like protein
A	K1QZ84_CRAGI	Thioredoxin domain-containing protein 3-like protein
A	K1QXH7_CRAGI	DNA replication licensing factor mcm4-B
A	K1Q1L9_CRAGI	Interferon-induced protein 44-like protein
A	K1RGD5_CRAGI	F-box only protein 36
A	K1Q3B4_CRAGI	DNA topoisomerase
A	K1P8Z1_CRAGI	Uncharacterized protein
A	K1PYA2_CRAGI	Host cell factor
A	K1PZR3_CRAGI	U2 small nuclear ribonucleoprotein A
A	K1QB69_CRAGI	Uncharacterized protein
A	K1PI78_CRAGI	Golgi-specific brefeldin A-resistance guanine nucleotide exchange factor 1
A	K1RKK2_CRAGI	Phosphatidylinositol-4-phosphate 5-kinase type-1 alpha

A	K1QLS5_CRAGI	Uncharacterized protein
A	K1QFI3_CRAGI	Apoptosis-inducing factor 3
A	K1QKB1_CRAGI	Tryptophanyl-tRNA synthetase, cytoplasmic
A	K1REU2_CRAGI	WD repeat and HMG-box DNA-binding protein 1
A	K1QUK3_CRAGI	Putative ATP-dependent RNA helicase DDX41
A	K1QBT8_CRAGI	Uncharacterized protein
A	K1QVX4_CRAGI	Glycogen synthase kinase-3 beta
A	K1PF20_CRAGI	Gamma-tubulin complex component
A	K1RFG1_CRAGI	Lipoxygenase-like protein domain-containing protein 1
A	K1PCI8_CRAGI	Cullin-2
A	K1QS27_CRAGI	UBX domain-containing protein 6
A	K1RFF1_CRAGI	Uncharacterized protein
A	K1Q4N9_CRAGI	Uncharacterized protein
A	K1QJN8_CRAGI	AP-3 complex subunit beta
A	K1PXA0_CRAGI	Uncharacterized protein
A	K1QA13_CRAGI	Calcium-transporting ATPase
A	K1QXY4_CRAGI	Kinase
A	K1PBW4_CRAGI	Uncharacterized protein
A	K1PUF0_CRAGI	G-protein coupled receptor moody
A	K1QMY9_CRAGI	Uncharacterized protein
A	K1QZ54_CRAGI	Coiled-coil domain-containing protein 39
A	K1QWU8_CRAGI	Uncharacterized protein
A	K1Q3L1_CRAGI	Kielin/chordin-like protein
A	K1PGR2_CRAGI	G patch domain-containing protein 1
A	K1RXP9_CRAGI	Ventricular zone-expressed PH domain-containing-like protein 1
A	K1PIB2_CRAGI	Uncharacterized protein
A	K1R4U3_CRAGI	Uncharacterized protein

Data S3: Complete list of GO terms of clustered genes of m6A interacting proteins (p-value<0,05)

Cluster	term_ID	description	log10 p-value	Class
cluster1	GO:0006172	ADP biosynthetic process	-2,848	Biological process
cluster1	GO:0006886	intracellular protein transport	-6,1176	Biological process
cluster1	GO:0015031	protein transport	-1,6944	Biological process
cluster1	GO:0006511	ubiquitin-dependent protein catabolic process	-1,8071	Biological process
cluster1	GO:0030833	regulation of actin filament polymerization	-2,5256	Biological process
cluster1	GO:0006563	L-serine metabolic process	-2,3716	Biological process
cluster1	GO:0006544	glycine metabolic process	-2,0706	Biological process
cluster1	GO:0016192	vesicle-mediated transport	-3,119	Biological process
cluster1	GO:0006429	leucyl-tRNA aminoacylation	-2,1763	Biological process
cluster1	GO:0006413	translational initiation	-1,3708	Biological process
cluster1	GO:0006122	mitochondrial electron transport, ubiquinol to cytochrome c	-1,9328	Biological process
cluster1	GO:0048280	vesicle fusion with Golgi apparatus	-2,3699	Biological process
cluster1	GO:0006888	ER to Golgi vesicle-mediated transport	-1,4737	Biological process
cluster1	GO:0030117	membrane coat	-3,0546	Cellular component
cluster1	GO:0030127	COPII vesicle coat	-1,6994	Cellular component
cluster1	GO:0030131	clathrin adaptor complex	-1,5595	Cellular component
cluster1	GO:0005737	cytoplasm	-2,3551	Cellular component
cluster1	GO:0031105	septin complex	-2,0349	Cellular component
cluster1	GO:0005850	eukaryotic translation initiation factor 2 complex	-2,6924	Cellular component
cluster1	GO:0005856	cytoskeleton	-1,6967	Cellular component
cluster1	GO:0005750	mitochondrial respiratory chain complex III	-1,9328	Cellular component
cluster1	GO:0000139	Golgi membrane	-1,4267	Cellular component
cluster1	GO:0003743	translation initiation factor activity	-2,6564	Molecular function
cluster1	GO:0004372	glycine hydroxymethyltransferase activity	-2,3716	Molecular function
cluster1	GO:0005488	binding	-1,66	Molecular function
cluster1	GO:0008565	protein transporter activity	-2,7964	Molecular function
cluster1	GO:0004823	leucine-tRNA ligase activity	-2,1763	Molecular function
cluster1	GO:0008242	omega peptidase activity	-2,0158	Molecular function
cluster1	GO:0008536	Ran GTPase binding	-1,4396	Molecular function
cluster1	GO:0005525	GTP binding	-1,9855	Molecular function
cluster1	GO:0016813	hydrolase activity, acting on carbon-nitrogen (but not peptide) bonds, in linear amidines	-1,9675	Molecular function
cluster1	GO:0002161	aminoacyl-tRNA editing activity	-1,4387	Molecular function
cluster1	GO:0016776	phosphotransferase activity, phosphate group as acceptor	-2,0567	Molecular function
cluster1	GO:0005543	phospholipid binding	-1,3689	Molecular function
cluster1	GO:0004017	adenylate kinase activity	-2,2504	Molecular function
cluster1	GO:0019205	nucleobase-containing compound kinase activity	-1,9387	Molecular function
cluster1	GO:0019904	protein domain specific binding	-1,4245	Molecular function
cluster1	GO:0004843	thiol-dependent ubiquitin-specific protease activity	-1,6596	Molecular function
cluster1	GO:0003779	actin binding	-1,33	Molecular function
cluster 2	GO:0006376	mRNA splice site selection	-2,2802	Biological process
cluster 2	GO:0016192	vesicle-mediated transport	-1,9467	Biological process
cluster 2	GO:0006511	ubiquitin-dependent protein catabolic process	-1,895	Biological process
cluster 2	GO:0051603	proteolysis involved in cellular protein catabolic process	-1,4434	Biological process
cluster 2	GO:0006281	DNA repair	-1,946	Biological process
cluster 2	GO:0006164	purine nucleotide biosynthetic process	-1,9132	Biological process
cluster 2	GO:0006606	protein import into nucleus	-1,6687	Biological process
cluster 2	GO:0006367	transcription initiation from RNA polymerase II promoter	-1,8729	Biological process
cluster 2	GO:0045893	positive regulation of transcription, DNA-templated	-1,8902	Biological process
cluster 2	GO:0051276	chromosome organization	-1,9322	Biological process
cluster 2	GO:0005685	U1 snRNP	-2,0889	Cellular component
cluster 2	GO:0005694	chromosome	-1,6569	Cellular component
cluster 2	GO:0019773	proteasome core complex, alpha-subunit complex	-1,7608	Cellular component
cluster 2	GO:0005839	proteasome core complex	-1,4434	Cellular component
cluster 2	GO:0005643	nuclear pore	-1,5471	Cellular component
cluster 2	GO:0003938	IMP dehydrogenase activity	-2,5964	Molecular function
cluster 2	GO:0005488	binding	-5,6024	Molecular function
cluster 2	GO:0008536	Ran GTPase binding	-3,3815	Molecular function
cluster 2	GO:0008565	protein transporter activity	-1,3099	Molecular function
cluster 2	GO:0017056	structural constituent of nuclear pore	-2,5981	Molecular function
cluster 2	GO:0016844	strictosidine synthase activity	-2,4472	Molecular function
cluster 2	GO:0042578	phosphoric ester hydrolase activity	-2,0068	Molecular function
cluster 2	GO:0008641	small protein activating enzyme activity	-1,8257	Molecular function
cluster 2	GO:0003729	mRNA binding	-1,9507	Molecular function
cluster 2	GO:0000166	nucleotide binding	-1,9175	Molecular function
cluster 2	GO:0030554	adenyl nucleotide binding	-1,4276	Molecular function
cluster 2	GO:0004175	endopeptidase activity	-1,4434	Molecular function
cluster 2	GO:0004298	threonine-type endopeptidase activity	-1,4434	Molecular function
cluster 3	GO:0006184	(obsolete) GTP catabolic process	-1,3497	Biological process
cluster 3	GO:0007156	homophilic cell adhesion via plasma membrane adhesion molecules	-1,6645	Biological process
cluster 3	GO:0008152	metabolic process	-1,9382	Biological process

cluster 3	GO:0015986	ATP synthesis coupled proton transport	-4,8627	Biological process
cluster 3	GO:0006096	glycolytic process	-1,4156	Biological process
cluster 3	GO:0051258	protein polymerization	-2,6757	Biological process
cluster 3	GO:0044262	cellular carbohydrate metabolic process	-2,0966	Biological process
cluster 3	GO:0006388	tRNA splicing, via endonucleolytic cleavage and ligation	-1,523	Biological process
cluster 3	GO:0006879	cellular iron ion homeostasis	-1,4857	Biological process
cluster 3	GO:0007017	microtubule-based process	-2,4915	Biological process
cluster 3	GO:0006412	translation	-2,0331	Biological process
cluster 3	GO:0006122	mitochondrial electron transport, ubiquinol to cytochrome c	-2,0662	Biological process
cluster 3	GO:0000276	mitochondrial proton-transporting ATP synthase complex, coupling factor F(o)	-4,1068	Cellular component
cluster 3	GO:0005750	mitochondrial respiratory chain complex III	-2,0662	Cellular component
cluster 3	GO:0045261	proton-transporting ATP synthase complex, catalytic core F(1)	-2,0025	Cellular component
cluster 3	GO:0005874	microtubule	-2,2282	Cellular component
cluster 3	GO:0005882	intermediate filament	-1,9067	Cellular component
cluster 3	GO:0043231	intracellular membrane-bounded organelle	-2,1492	Cellular component
cluster 3	GO:0005852	eukaryotic translation initiation factor 3 complex	-1,6821	Cellular component
cluster 3	GO:0005737	cytoplasm	-1,9776	Cellular component
cluster 3	GO:0005840	ribosome	-2,0503	Cellular component
cluster 3	GO:0043234	protein complex	-2,6757	Cellular component
cluster 3	GO:0004739	pyruvate dehydrogenase (acetyl-transferring) activity	-2,8179	Molecular function
cluster 3	GO:0016624	oxidoreductase activity, acting on the aldehyde or oxo group of donors, disulfide as acceptor	-2,0554	Molecular function
cluster 3	GO:0005200	structural constituent of cytoskeleton	-2,3865	Molecular function
cluster 3	GO:0005525	GTP binding	-1,9304	Molecular function
cluster 3	GO:0015078	hydrogen ion transmembrane transporter activity	-3,0193	Molecular function
cluster 3	GO:0046961	proton-transporting ATPase activity, rotational mechanism	-1,6263	Molecular function
cluster 3	GO:0046933	proton-transporting ATP synthase activity, rotational mechanism	-1,7326	Molecular function
cluster 3	GO:0004775	succinate-CoA ligase (ADP-forming) activity	-2,3995	Molecular function
cluster 3	GO:0046912	transferase activity, transferring acyl groups, acyl groups converted into alkyl on transfer	-2,3982	Molecular function
cluster 3	GO:0016874	ligase activity	-1,4798	Molecular function
cluster 3	GO:0048037	cofactor binding	-1,6628	Molecular function
cluster 3	GO:0008199	ferric iron binding	-1,4607	Molecular function
cluster 3	GO:0005544	calcium-dependent phospholipid binding	-1,6049	Molecular function
cluster 3	GO:0003878	ATP citrate synthase activity	-2,3995	Molecular function
cluster 3	GO:0003735	structural constituent of ribosome	-1,9881	Molecular function

Table S1: Transitions used for each compound. A: first transition, B: second transition

Nucleoside	Retention time (min)	MRM precursor (m/z)	MRM product (m/z)		Collision Energy (V)	
			A	B	A	B
A	3.07	268.0	135.9	119.0	-30	-12
m^6A	2.12	282.0	150.1	123.1	-17	-46

Table S2: Correspondence between development stages in our study, and the GigaTON database.

Development stages : This Study	Development stages : GigaTON [53]
Oocytes	E (Eggs)
2/8 Cells	TC (Two Cell embryos)
	FC (Four Cell embryos)
	EM (Early Morula)
Morula	M (Morula)
Blastula	B (Blastula)
	RM (Rotary Movement)
Gastrula	FS (Free Swimming)
	EG (Early Gastrula)
	G (Gastrula)
	T (Trochophore) 1
Trochophore	T2
	T3
	T4
	T5
	ED (Early D larvae) 1
D larvae	ED2
	D (D larvae)1
	D2
	D3
	D4
	D5
Spat	S (Spat)
Juvenile	J (Juvenile)